Wnt Signalling and the Regulation of the Axonal Cytoskeleton

Monica Hoyos-Flight

Department of Biological Sciences
Imperial College London

Thesis submitted to the University of London in fulfilment of the requirements for the Doctor of Philosophy degree

2005

ABSTRACT

Wnt proteins are a large family of signalling molecules that have well-established roles in regulating embryonic patterning, cell proliferation and cell fate specification. During the development of the nervous system, Wnts have been found to play a role in the formation of neuronal connections by regulating axon guidance, axonal remodelling, dendritic development and synaptogenesis. Indeed, it has been demonstrated that Wnt7a and Wnt3 have important regulatory effects on neuronal maturation, axonal arborisation and synapse formation in cerebellar granule cells and dorsal root ganglion neurons respectively. Both Wnt7a and Wnt3 induce axonal remodelling, characterised by a decrease in axon length, increase in axonal branching and growth cone size. Analyses of the pattern of expression and the phenotype induced by these Wnts suggest that both Wnt7a and Wnt3 function as retrograde signals to regulate the presynaptic remodelling associated with the modification of an actively advancing growth cone to a presynaptic bouton.

The aim of this work was to characterise the effects of Wnts on axonal behaviour and the underlying changes in axonal microtubules and the actin cytoskeleton. I have used a combination of fluorescence and time-lapse microscopy to elucidate the changes induced by activation of the Wnt signalling pathway.

I found that Wnt3a, like Wnt3, induces axonal remodelling within 2 hours of application in sensory neurons of the mouse dorsal root ganglia. As well as decreasing the speed of growth cone advance, Wnt3a causes an increase in growth cone motility and size. These findings suggest Wnt3a is signalling both to microtubules and the actin cytoskeleton. Indeed, I found that Wnt3a increases microtubule stability as it confers resistance to the microtubule depolymerising drug nocodazole. Wnt3a also affects the organisation of microtubules since growth cones of neurons treated with Wnt3a contain more looped microtubules than controls. In addition, Wnt3a leads to the accumulation of highly dynamic actin filaments in growth cones.

The effect of Wnt3a on axonal remodelling is mimicked by expression of Dvl1, a cytoplasmic protein required for signalling through the three known Wnt pathways, and by inhibition of Gsk-3β, a serine threonine kinase inhibited by the canonical Wnt signalling pathway. Interestingly, Wnt-induced axonal remodelling is achieved through a transcription independent mechanism, suggesting that a divergent canonical Wnt signalling pathway is regulating changes in the axonal cytoskeleton.

In summary, my work is the first detailed characterization of the effect of Wnt signalling on the axonal cytoskeleton. The findings described here provide new insights into how Wnts regulate the behaviour of axons and contributes to the understanding of the mechanisms by which extracellular cues modulate the cytoskeleton to induce changes in axonal behaviour during the initial stages of synaptogenesis.

TABLE OF CONTENTS

	Page
Title page	**1**
Abstract	**2**
Table of Contents	**4**
List of Figures	**8**
Abbreviations	**11**
Chapter 1. Introduction	**13**
1.1 Axon Guidance	14
1.2 Wnt proteins	23
1.3 The Wnt signalling pathways	27
1.4 The axonal cytoskeleton	31
1.4.1 Actin filaments	33
1.4.2 Microtubules	35
1.4.3 Interactions between actin and microtubules	37
1.4.4 Changes in the cytoskeletal organisation underlying axon growth, turning and branching	38
1.4.5 Linking axonal guidance cues to the cytoskeleton	43
1.4.6 The cytoskeleton and synaptogenesis	47
1.5 Wnts and the cytoskeleton	48
1.6 Aims	50
Chapter 2. Materials and Methods	**52**
2.1 Neuronal cultures	52
2.2 Production of Wnt conditioned media	54
2.3 Molecular biology	55
2.4 Cell transfection methods	55
2.5 Western blots	57
2.6 Drug treatments	58
2.7 Immunohistochemistry	58

2.8 Fixation for EM 59
2.9 Imaging and data analyses 60
2.10 Time-lapse 61
2.11 Antibodies 61
2.12 Solutions 62

Chapter 3. Wnts affect the morphology and axonal behaviour of embryonic and neonatal DRGs. 67
3.1 Introduction 67
3.2 Results 68
3.2.1 Wnt3 induces axonal remodelling of embryonic and neonatal DRGs. 68
3.2.2 Axonal remodelling requires overnight exposure to Wnt3 conditioned medium. 71
3.2.3 The effect of Wnt3 on axonal remodelling is correlated to the amount of protein in the conditioned media. 73
3.2.4 Cell density and laminin concentration do not alter the effect of Wnt3 on axonal remodelling. 76
3.2.5 Several Wnts expressed in different cell lines induce axonal remodelling in neonatal and embryonic DRGs. 77
3.2.5.1 Rat1B cell lines 77
3.2.5.2 L-cell cell lines 79
3.2.6 Purified Wnt3a induces axonal remodelling within 2 hours of application. 83
3.3 Discussion 90

Chapter 4. Wnt3a signals through a divergent canonical signalling pathway and induces changes in both the stability and organisation of microtubules. 94
4.1 Introduction 94
4.2 Results 95
4.2.1 Dvl1 expression mimics Wnt3a mediated axonal

remodelling on neonatal DRGs. 95
4.2.2 Wnt3a induced axonal remodelling is mediated through the inhibition of Gsk-3β, but does not require nuclear transcription. 96
4.2.3 Wnt3a affects the organisation of microtubules. 101
4.2.4 Wnt3a confers microtubule stability. 106
4.2.5 Wnt3a alters the directionality of microtubule growth. 107
4.2.6 Dvl1 expression alters the directionality of microtubule growth. 109
4.2.7 Wnt3a does not affect the rate of microtubule growth along axons or in growth cones. 112
4.2.8 Examination of EB1 and APC in Wnt3a and control treated growth cones. 113
4.3 Discussion 115

Chapter 5. Wnt3a affects the organisation and dynamics of actin filaments in growth cones. 121
5.1 Introduction 121
5.2 Results 121
5.2.1 Wnt3a causes an accumulation of F-actin in growth cones. 122
5.2.2 Examination of actin filament organisation in growth cones by electron microscopy. 122
5.2.3 Wnt3a causes actin filaments to depolymerise faster in growth cones. 125
5.2.4 Wnt3a causes actin filaments to polymerise faster in growth cones. 129
5.2.5 Examination of the effect of Wnt3a signalling on the actin cytoskeleton by time-lapse microscopy. 131
5.2.6 Examination of actin regulating proteins that could potentially mediate the effects of Wnt3a on actin dynamics. 133
5.2.7 Examination of the effect of Wnt3a signalling on actin

retrograde flow in growth cones. 135
5.3 Discussion 139

Chapter 6. Discussion **146**

6.1 Summary of results 146
6.2 Wnt3a-induced axonal remodelling 147
6.3 Wnt3a affects microtubules 149
6.4 Wnt3a affects the actin cytoskeleton 153
6.5 Sequence of events 157
6.6 Is Wnt3a a guidance cue? 159
6.7 Wnt3a as a synaptogenic factor 160
6.8 Wnts and neuronal connectivity 161
6.9 Conclusions 162

Acknowledgements **163**

Appendices **164**

Appendix 1. Supplementary figures. 164
Appendix 2. Wnt3 axonal remodelling of neonatal DRGs. 165
Appendix 3. Wnt3a axonal remodelling of neonatal DRGs. 168
Appendix 4. Dvl1 expression and inhibition of Gsk-3β by Lithium mimic the effect of Wnt3a on growth cone size. 170
Appendix 5. The effect of Wnt3a on growth cone size does not require nuclear transcription, but it does require protein translation. 171
Appendix 6. Wnt3a confers resistance to nocodazole. 172
Appendix 7. Wnt3a does not affect the velocity of EB3-GFP excursions. 173
Appendix 8. Wnt3a increases F-actin in growth cones. 173
Appendix 9. F-actin is more susceptible to depolymerisation in the presence of Wnt3a. 174
Appendix 10. F-actin polymerises faster in the presence of Wnt3a. 175
Appendix 11. Wnt3a increases the speed of filopodia and the relative percentage of lamellar perimeter undergoing protrusion. 175
Appendix 12. Inhibition of the actin retrograde flow does not affect the Wnt3a-induced increase in growth cone size or F-actin accumulation in growth cones. 176

Bibliography **177**

Movies (Enclosed CD- requires QuickTime and/or PowerPoint)

Movies Chapter 3- Effect of Wnt3a on axon behaviour
Movies Chapter 4- Effect of Wnt3a on the directionality of microtubules
Movies Chapter 5- Effect of Wnt3a on lamellar protrusion

LIST OF FIGURES

Page

1.1. The four main families of axon guidance molecules. 15

1.2 Wnts as axon guidance molecules. 22

1.3. Wnts induce axonal remodelling and synaptogenesis in the vertebrate cerebellum and spinal cord. 23

1.4. The three main Wnt signalling pathways. 29

1.5. The axonal cytoskeleton. 32

1.6. Summary of how the axonal cytoskeleton is regulated. 42

1.7. Summary of hypotheses tested in this project. 51

2.1. Diagram of the PGK expression vector containing HA-tagged Wnt used to make new Wnt secreting cells lines. 56

2.2. Expression of HA-tagged Wnts in L cells. 56

3.1 Wnt3 induces axonal remodelling in embryonic and neonatal DRG cells. 70

3.2. RT97 stains large caliber DRG neurons. 72

3.3. The effect of Wnt3 on growth cone size requires 18 hours exposure to conditioned medium. 72

3.4. The effect of Wnt3 on growth cone size correlates with the level of protein in the conditioned media. 74

3.5. The Wnt3 mediated increase in growth cone size is not affected by cell density or laminin concentration. 74

3.6. Wnt1 and Wnt6, but not Wnt7b induce axonal remodelling of embryonic and neonatal DRGs. 78

3.7. Wnt3 from L-cells affects L-cell morphology and increases β-catenin levels. 80

3.8. Wnt3 and Wnt3a from L-cell conditioned media induce axonal remodelling in embryonic and neonatal DRGs. 80

3.9. The effect of Wnt3, from L-cell conditioned medium, on growth cone size

requires 22 hours exposure. 82
3.10.The effect of Wnt3 on axonal remodelling is not observed when DRG neurons are grown on L-cell monolayers. 82
3.11 Purified Wnt3a induces axonal remodelling in neonatal DRG cells after 22 hours exposure. 84
3.12 Purified Wnt3a induces axonal remodelling in neonatal DRG cells after 2 hours exposure. 85
3.13. Time-lapse frames of a sensory axon exposed to control media for 120 minutes. 87
3.14. Time-lapse frames of a sensory axon exposed to Wnt3a media for 120 minutes. 88
3.15. Wnt3a decreases the speed of growth cone advance within 20 minutes and increases growth cone size after 80-120 minutes. 89
4.1. The divergent canonical Wnt signalling pathway. 95
4.2. Dvl1 expression induces axonal remodelling. 97
4.3. Inhibition of Gsk-3β by LiCl mimics the effect of Wnt3a on axonal remodelling in DRGs. 98
4.4. The effect of Wnt3a on axonal remodelling does not require nuclear transcription. 100
4.5. The effect of Wnt3a on axonal remodelling requires protein translation. 102
4.6. Wnt3a increases microtubules in growth cones and causes microtubule looping. 104
4.7. Microtubule looping takes place after 60 minutes exposure to Wnt3a. 105
4.8. Dvl1 expression causes microtubule looping in DRG growth cones. 105
4.9. Wnt3a protects microtubules against nocodazole. 108
4.10. EB3-GFP binds to dynamic microtubules. 110
4.11. Wnt3a alters the direction of microtubule growth. 111
4.12. Dvl1 alters the direction of microtubule growth. 111
4.13. Wnt3a does not affect the speed or number of EB3-GFP comets. 114
4.14. Wnt3a does not affect the levels of APC or EB1 in growth cones. 114
5.1. Wnt-3a increases F-actin levels in growth cones. 123

5.2. Wnt3a causes an accumulation of F-actin in growth cones within 15 minutes of application. 124
5.3. Wnt3a induces changes in the organisation of actin filaments in growth cones. 124
5.4. Exposure to cytochalasin D or latrunculin B causes the F-actin area in growth cones to decrease faster in the presence of Wnt3a. 127
5.5. Actin filaments depolymerise faster in the presence of Wnt-3a. 128
5.6. Actin polymerises faster in the presence of Wnt3a. 130
5.7. GFP-β-actin incorporates into native actin filaments in growth cones and is a useful tool for examining actin dynamics in growth cones. 132
5.8. Wnt3a increases lamellar protrusion. 134
5.9. Wnt3a does not affect the levels or localisation of P-PAK-1, p34-Arc or myosin-V. 136
5.10. Inhibition of retrograde flow decreases the percentage of neurons with looped microtubules in growth cones. 138
6.1. Putative mechanisms for the Wnt-induced changes in dynamics and organisation of axonal microtubules. 152
6.2. Potential mechanisms for the Wnt-induced changes in actin dynamics and organisation in growth cones. 155
6.3. The effects of Wnt3a on actin filaments may influence the organisation of microtubules in growth cones. 156
6.4. Sequence of events upon addition of Wnt3a. 158
6.5. Summary of the effects of Wnt3a on the growth cone cytoskeleton. 159
Supplementary figure 1. Wnt3a increases the levels of β-catenin in DRGs. 164
Supplementary figure 2. Microtubules recover within 1 hour of removal of nocodazole. 164

ABBREVIATIONS

ABP	actin binding protein
Ace. Tub.	acetylated tubulin
APC	adenomatous polyposis coli
BDNF	brain derived neurotrophic factor
BME	basal medium Eagle
BMP	bone morphogenetic protein
BSA	bovine serum albumin
C. elegans	*Caenorhabditis elegans*
CAM	cell adhesion molecule
cAMP	cyclic adenosine monophosphate
CLASP	CLIP-associated proteins
CLIP	cytoplasmic linker proteins
CM	conditioned medium
CNS	central nervous system
Comm	commisureless
CRMP-2	collapsin response mediator protein-2
dH_2O	distilled water
DNA	deoxyribonucleic acid
DRG	dorsal root ganglion
Dvl	dishevelled
E	embryonic age
ECM	extracellular matrix
EM	electron microscopy
F-actin	filamentous actin
FGF	fibroblast growth factor
FRAT	fluorescence recovery after photobleaching
FRET	fluorescence resonance energy transfer
GAP	GTP-ase activating protein
GAP-43	growth associated protein 43-KDa

GEF	guanine nucleotide exchange factors
GFP	green fluorescent protein
Gsk-3β	glycogen synthase kinase 3-β
HSPG	heparan sulphate proteoglycan
Ig	immunoglobulin
JNK	jun N-terminal kinase
LEF	lymphocyte enhancer binding factor
LIMK-1	LIM domain containing kinase-1
LRP	low-density lipoprotein (LDL) receptor-related protein
MAP	microtubule associated protein
MBP	microtubule binding protein
mRNA	messenger RNA
MT	microtubule
NGF	nerve growth factor
NMJ	neuromuscular junction
NT-3	neurotrophin-3
P	postnatal age (days)
PAK	p21-activated kinase
PBS	phosphate buffered saline
PDL	poly-D-lysine
PFA	paraformaldehyde
ROCK	Rho associated kinase
RNA	ribonucleic acid
SEM	standard error of the mean
SFM	serum free medium
sFRP	soluble frizzled related protein
Shh	Sonic hedgehog
TCF	T cell factor
+TIP	plus-end-binding protein
Tyr. Tub.	tyrosinated tubulin
Wg	wingless

CHAPTER 1:

Introduction

The formation of a functional nervous system, one of the most amazing feats of development, is completely dependent on the correct positioning of neurons and the establishment of appropriate connections between them. Both the migration of neurons and the extension of neurites require tightly regulated morphological changes in a complex environment. Deciphering how extracellular signalling molecules can affect neuronal morphology is key to understanding how the nervous system is built and functions.

In the mid-1900s, Roger Sperry was the first to prove that axon-target recognition relied on chemical matching, rather than on the functional validation of randomly formed connections as had been proposed by Paul Weiss (Sperry, 1963; Weiss, 1941). Today, it is widely accepted that the formation of precise neural circuits depends not only on molecular matching, but also relies on normal neuronal activity in many parts of the nervous system to form and to stabilise neurite arborisations and synapses.

Thanks to powerful *in vitro* assays, biochemical and genetic studies in both invertebrates and vertebrates, our understanding of the mechanisms underlying axon guidance and synapse formation at the molecular level has improved dramatically. Axons reach their targets in discrete steps (Bate, 1976), encountering positive (attractive) and negative (repulsive) cues along their journey. These cues exist in either diffusible or cell associated forms and are able to regulate both long and short distance pathfinding. The leading edge of the axon, termed growth cone, functions as an exquisite sensor that is able to detect and respond to guidance cues. Growth cones guide axons by transducing extracellular cues into signals that regulate the cytoskeleton thereby determining axonal behaviour. As axons approach their targets, they often cease to extend, and the morphology of the growth cone changes in preparation for branching and/or synapse formation. The signal transduction pathways by which diverse extracellular ligands

influence the axonal cytoskeleton to induce changes in shape and motility, are now beginning to be elucidated.

1.1 Axon guidance.

Axon guidance molecules should satisfy three main criteria: (a) They should be expressed at the right time and in the appropriate region of the nervous system to carry out their repulsive or attractive functions, (b) depletion of the protein or its receptor, by genetic manipulation or other means, should lead to pathfinding errors, and (c) exposure to the factor should elicit attractive or repulsive responses in cultured neurons. Expression pattern profiles, together with the use of mutagenic screens and examination of axonal projections, have enabled the identification of many genes involved in axon guidance. Intermediate targets or decision-making points, are ideal contexts to study defects in axonal trajectories, they include: the projections of retinal ganglion cells to their tectal targets, midline crossing of commissural neurons in the spinal cord, the projections of sensory axons to different levels in of the spinal cord and the navigation of motor neuron axons to specific muscle targets. *In vitro* studies have been most helpful in the determination of how guidance cues exert their effects on the axonal cytoskeleton. Explants or dissociated cultures of embryonic retinal or dorsal root ganglia (DRG) neurons are the models of choice for these studies.

Remarkably, the same genes are required for the correct wiring of the nervous system in *Drosophila*, *C. elegans* and vertebrates. Four highly conserved families of axon guidance molecules: Netrins, semaphorins, Slits and ephrins have been extensively characterised in both vertebrates and invertebrates. Furthermore, these ligand/receptor families of molecules are able to control guidance decisions in more than one location and are capable of inducing different responses depending on the intracellular and extracellular environments.

The first clear evidence for the existence of guidance molecules came from studies by Tessier-Lavigne and colleagues, which identified the vertebrate midline as a source of

chemoattractive signals for commissural axons (Tessier-Lavigne *et al.*, 1988). The attractive factor itself, unc-6/netrin, was discovered in *C. elegans* (Hedgecock *et al.*, 1990). Unc-6 is a secreted ligand able to act simultaneously as an attractive and

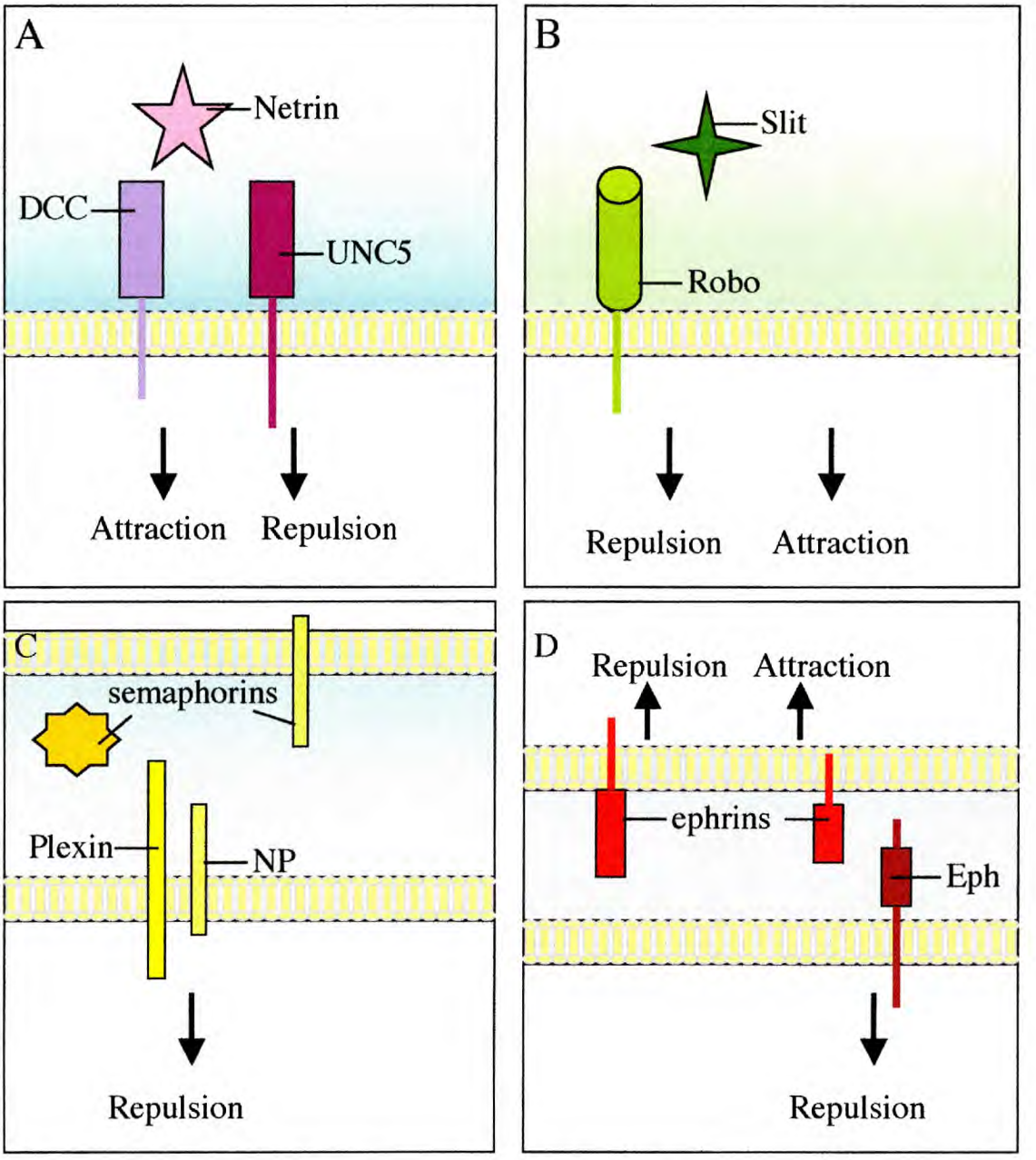


Figure 1.1. The four main families of axon guidance molecules.
(A) Netrins bind DCC and UNC5 receptors to mediate both attractive and repulsive responses. (B) Slits bind Robo receptors and generally induce repulsion. (C) Semaphorins can be soluble or membrane bound, their main receptors are Plexins and Neuropilins. (D) Ephrins, transmembrane or GPI linked, bind transmembrane Eph receptors and trigger bi-directional signalling.

repulsive signal. Both axons growing towards and away from the midline are affected in the *unc-6* mutant (Wadsworth *et al.*, 1996). In vertebrates, netrin-1, the UNC-6 homologue, attracts commissural neurons to the midline (Kennedy *et al.*, 1994; Serafini *et al.*, 1994), but can also have a repulsive effect on retinal axons, aiding their exit from the eye (Deiner *et al.*, 1997), and on trochlear motor neurons, guiding axons away from the ventral midline (Colamarino and Tessier-Lavigne, 1995). There are two main families of netrin receptors, both are single pass transmembrane proteins of the Ig superfamily. Netrin-induced attraction requires the DCC (deleted in colorectal cancer) family of receptors which includes UNC-40 in *C. elegans*, Frazzled in *Drosophila*, and DCC and neurogenin in vertebrates. In contrast, netrin-induced repulsion, is mediated by the UNC-5 family of receptors, including *C. elegans* and *Drosophila* UNC-5 and the three vertebrate homologues (UNC-5H1-3) (Fig.1.1 A, for review see Guthrie, 1997). Regulation of receptor expression and the interactions between these two families of receptors, determines the outcome of the netrin encounter (Keleman and Dickson, 2001). To begin to address the mechanism by which netrin mediates axon guidance responses, *in vitro* studies have analysed netrin-stimulated axon outgrowth, branching and attractive turning in retinal ganglia, cortical and spinal neurons (Del Rio *et al.*, 2004; Dent *et al.*, 2004; Campbell and Holt, 2001; Kennedy *et al.*, 1994).

Slits were also identified in the context of midline crossing. *Drosophila* Slit is a large ECM molecule expressed by midline glia cells and acts as a long-range chemorepellent (Kidd *et al.*, 1999; Zou *et al.*, 2000). Slits signal through the roundabout family of receptors (Robo) and prevent ipsilateral axons from crossing the midline as well as contralateral axons from re-crossing (Battye *et al.*, 1999; Kidd *et al.*, 1998). To overcome Slit repulsion, contralaterally projecting axons prevent Robo from reaching the membrane until the midline has been crossed. This is achieved by the transient expression of Commissureless (Comm) (Keleman *et al.*, 2005; Georgiou and Tear, 2002; Keleman *et al.*, 2002; Tear *et al.*, 1996). Mutations in the *C. elegans* Robo homologue, sax3, also cause axon misrouting at the midline (Zallen *et al.*, 1998). The absence of sax3 gives rise to more severe phenotypes than those observed in the absence of Slt-1 (Hao *et al.*, 2001) suggesting that sax3 may have other ligands in addition to

Slit/Slt-1. This is not the case in *Drosophila*, where axon misrouting in Slit mutants is more severe than in Robo mutants (Kidd *et al.*, 1999). Only when both Robo and Robo2 are mutated a *Slit* phenotype is observed, suggesting both Robo and Robo 2 are required for driving axons away from the midline (Simpson *et al.*, 2000). The repulsive activity of Slits is conserved in vertebrates, where Slits1-3 are expressed by ventral midline cells to repel commissural axons, and by cells surrounding the optic chiasm forming a repulsive corridor to guide all retinal axons through the chiasm (Plump *et al.*, 2002; Erskine *et al.*, 2000; Niclou *et al.*, 2000; Brose *et al.*, 1999). Vertebrate Robo receptors- Robo1-3- are related to *Drosophila* Robo, and the most distantly related Robo3/Rig1 is emerging as a key mediator of Slit repulsion. Unlike wild-type commissural axons that become responsive to Slit after crossing the midline, axons from *Robo3/Rig1* mutants become repulsed before reaching the midline (Sabatier *et al.*, 2004). The premature responsiveness to Slit suggests Robo3 could be regulating the other Robo receptors in a similar way to Comm in *Drosophila* or alternatively may be sequestering Slit before midline crossing (Guthrie, 2004). *In vitro* collagen assays have further established the repulsive action of Slit-2 on retinal axons (Ringstedt *et al.*, 2000), but have also revealed an attractive action of Slit-2 on sensory neurons (Wang *et al.*, 1999), indicating that, like netrins, Slits can exert both positive and negative guidance responses (Fig. 1.1 B).

Semaphorins were first identified on motor neuron axon fascicles in grasshoppers as molecules involved in the defasciculation process that enables motor axons to innervate their individual targets (Kolodkin *et al.*, 1992). Similarly, Semala is expressed in *Drosophila* motor axons acting as a short range repellent to mediate axonal defasciculation (Yu *et al.*, 1998). Semaphorins can be membrane tethered or secreted, and signal through multimeric receptor complexes (Pasterkamp and Kolodkin, 2003; Semaphorin Nomenclature Committee, 1999; Kolodkin *et al.*, 1993). Semaphorin-induced repulsion is exerted by two receptor families, neuropilins and plexins (Fig.1.1 C). While many semaphorins bind directly to plexins to activate signalling cascades (Tamagnone *et al.*, 1999), secreted semaphorins require neuropilins as co-receptors (Takahashi *et al.*, 1999). The homo/hetero dimerisation of these receptors produces receptor complexes with differing semaphorin binding specificities

(for review see Raper, 2000; Tamagnone and Comoglio, 2000). In vertebrates, semaphorins induce repulsion of a subset of sensory neurons from the ventral spinal cord (Messersmith *et al.*, 1995), and of post-crossing commissural axons away from the midline (Zou *et al.*, 2000). The repulsive role of semaphorins at the midline suggests that they can act in concert with Slits to prevent axons from recrossing or lingering at the midline. Purified Sema3A has been a valuable tool for identifying some of the molecules involved in the cytoskeletal rearrangements that take place during repulsive responses *in vitro*, such as growth cone collapse and axonal retraction (Eickholt *et al.*, 2002; Aizawa *et al.*, 2001; Fournier *et al.*, 2000).

Ephrins were first identified as membrane bound ligands required for guiding retinal ganglion neurons to their tectal targets. Ephrins bind to the Eph family of receptor tyrosine kinases and fall into two classes: ephrin-As which are GPI anchored and bind to EphA receptors, and ephrin-Bs, which have a transmembrane domain and bind to EphB receptors (for review see Wilkinson, 2001). Remarkably, an Eph receptor can also act as a ligand, triggering signal transduction cascades in ephrin expressing cells referred to as "reverse signalling" (Bruckner *et al.*, 1997; Holland *et al.*, 1996) (Fig.1.1 D). Topographic mapping of retinal axons along the anterior-posterior axis depends on the graded repulsion between ephrin-A ligands and EphA receptors. Ephrin-A is expressed in a high-to-low gradient along the posterior-to-anterior axis in the tectum, while EphA receptors are expressed in a complementary gradient in the retina. Retinal axons with high Eph levels project to the anterior part of the tectum with lowest levels ephrin-A, while retinal axons with low levels of EphA, the most anterior ones, can tolerate high levels of ephrin-A and project to the posterior part of the tectum (Cheng *et al.*, 1995; Drescher *et al.*, 1995). Ephrins also act as repellents at the spinal cord midline where they prevent corticospinal tract axons from recrossing (Kullander *et al.*, 2001). In contrast, ephrin mediated attraction, is required for dorso-ventral mapping of retinal axons in the tectum (Braisted *et al.*, 1997) and guiding vomeronasal axons to the olfactory bulb (Knoll *et al.*, 2001). There is evidence to suggest that ephrin attraction involves an increase in cellular adhesiveness (Davy *et al.*, 1999; Huynh-Do *et al.*, 1999). Despite playing such important roles in axon guidance in vertebrates, invertebrate ephrin

and Eph mutants do not have dramatic guidance defects (Chin-Sang *et al.*, 1999; George *et al.*, 1998) suggesting ephrins acquired their axon guidance function during vertebrate evolution. The response of axons to ephrins *in vitro*, has been investigated using stripe assays and ephrin clusters. Both ephrin-A2 and ephrin-A5 have been shown to inhibit axon outgrowth and trigger growth cone collapse *in vitro* (Cheng *et al.*, 2003; Gallo *et al.*, 2002; Jurney *et al.*, 2002). Ephrin-induced attraction and regulation of adhesion are less well-characterised.

The fact that only four conserved families of guidance molecules can generate such astonishingly complex and varied patterns of axon behaviour implies that a tight regulation of both guidance cues and their receptors is required. Among the possible mechanisms of regulation are: (a) **temporal and spatial regulation of transcription** which enables axons to make decisions at the right time and place, and to set up opposing ligand and receptor gradients such as the ones required for retino-tectal mapping. Furthermore, alternative splicing of Eph receptors can shift the cellular response from repulsion to adhesion (Holmberg *et al.*, 2000) (b) **post-translational regulation of cues and receptors**, such as axon-segment specific expression of cell surface receptors, which aids midline crossing of commissural axons. EphB1 expression, for example, is restricted to crossed segments of commissural axons by a yet unknown mechanism (Imondi *et al.*, 2000). Interestingly, recent studies on the temporal inactivation of Robo by Comm during midline crossing have supported two potential mechanisms for regulating the spatial segregation of receptors: the clearance model, in which Robo is selectively removed from the plasma membrane in the crossing segment of axon, and the sorting model, in which the delivery of Robo to the plasma membrane is prevented during axon crossing (Keleman *et al.*, 2005; Keleman *et al.*, 2002; Myat *et al.*, 2002). Another example of post-translational modification that regulates axon guidance is the regulation of receptor levels (and hence the sensitivity of an axon to a particular cue) by local adjustments of protein synthesis and degradation (Campbell and Holt, 2001). (c) **receptor interactions** can modulate the outcome of the interaction with a particular ligand, for example, the direct interaction between the cytoplasmic domains of UNC-5 and DCC receptors is required to silence the netrin-DCC attraction and

induce repulsion (Hong *et al.*, 1999). (d) **crosstalk between different families of guidance cues**, recent studies have highlighted interactions between different receptor families that influence the response to guidance cues, for example, the direct interaction between DCC and Robo silences netrin-induced attraction in spinal *Xenopus* neurons (Stein and Tessier-Lavigne, 2001). (e) **intrinsically different signal transduction pathways between cells,** intracellular calcium and cyclic nucleotide levels can play a role in the outcome of guidance decisions, for example low cAMP levels turn netrin-induced attraction to repulsion in *Xenopus* spinal neurons (Ming *et al.*, 1997). Since axons encounter multiple guidance cues simultaneously or in short succession *in vivo*, the integration and outcome of several extracellular signals is also subject of detailed investigation (Dontchev and Letourneau, 2002).

In addition to netrins, Slits, semaphorins and ephrins, short-range contact mediated mechanisms involving cell adhesion molecules (CAMs) and extracellular matrix proteins (ECM) also play critical roles in axonal growth and guidance. Members of the cadherin family form homophilic interactions and mediate Ca^{+2} dependent adhesion. While in *Drosophila* DN-cadherin is required for axon fasciculation (Iwai *et al.*, 1997), in vertebrates N-cadherin is required for retino-tectal guidance (Inoue and Sanes, 1997). N-cadherins also link pre- and post- synaptic membranes (Serafini, 1997), and play critical roles in synaptic assembly (Togashi *et al.*, 2002; Benson and Tanaka, 1998). Ig-like adhesion molecules can form both homophilic and heterophilic interactions. The best-characterised member is NCAM which is also involved in stabilising cell-cell interactions at synaptic sites (Schachner, 1991) and is required for axon fasciculation in *Drosophila* (Fas II) (Lin *et al.*, 1994b). In addition to the roles of CAMs during the development of the nervous system, the defects in learning and memory that result from perturbing cell adhesion function (Cremer *et al.*, 1994) suggest that CAMs are critical in the regulation of synaptic plasticity (Salinas and Price, 2005; Benson *et al.*, 2000).

In vivo, axon navigation takes place among a milieu of ECM proteins. Integrins, are heterotrimeric receptors that can interact with a range of ECM proteins such as laminin, fibronectin and tenascin, to mediate adhesion, and have also emerged as key players in

axon migration and guidance (Hynes, 1992). Cultured neurons can exhibit different responses to well-known guidance cues depending on whether they are grown on fibronectin or laminin coated glass (Hopker *et al.*, 1999) suggesting that the composition of the extracellular matrix can also regulate the formation of axonal connections.

Interestingly, growth factors and other secreted signalling molecules, best known for their roles in early development as morphogens, are emerging as important players in the formation of neuronal circuits (Yoshikawa and Thomas, 2004; Osterfield *et al.*, 2003). BMPs, for instance, are well known for their roles early in development at the roof plate where they are involved in the generation of neural crest cells and determination of cell lineage (Anderson, 1997). However, BMP7 can also act as a repulsive signal to direct commissural axons ventrally (Butler and Dodd, 2003; Augsburger *et al.*, 1999). Conversely, at the floor plate, Shh which is required for ventral spinal cord patterning, can also act at later stages, in concert with netrin 1, as a chemoattractant to draw commissural axons towards the midline (Charron *et al.*, 2003). Furthermore, Shh has been shown to act as a repulsive guidance cue for retinal ganglion cells (Trousse *et al.*, 2001). Similarly, FGFs which play an important role in assigning anterior-posterior identity to spinal motor neurons (Dasen *et al.*, 2003), have also been implicated in the establishment of trochlear motor neuron trajectory (Irving *et al.*, 2002) and in presynaptic differentiation of mossy fibres in the cerebellum (Umemori *et al.*, 2004).

Several members of the Wnt family of proteins have been found to play a role in axon guidance (see Fig. 1.2). Wnt5 in *Drosophila* acts as a repellent to direct axons through the anterior commissure (Yoshikawa *et al.*, 2003), while in vertebrates Wnt4 acts as a chemoattractant to guide postcrossing commissural axons anteriorly towards the brain (Lyuksyutova *et al.*, 2003). Wnt genes are dynamically expressed in the nervous system during synaptogenesis, and roles for Wnt7a and Wnt3 in axonal remodelling and presynaptic differentiation in the cerebellum and the spinal cord have been described (Krylova *et al.*, 2002; Hall *et al.*, 2000). The re-emergence of classic embryonic patterning molecules at later stages of development, to build a functional nervous

system, seems a clever way to exploit complex signalling pathways and established gradients. The ability of these molecules to induce rapid changes at the growth cone as well as transcriptional changes, makes them prime candidates for initiating the formation of synapses and for fine tuning neuronal connections.

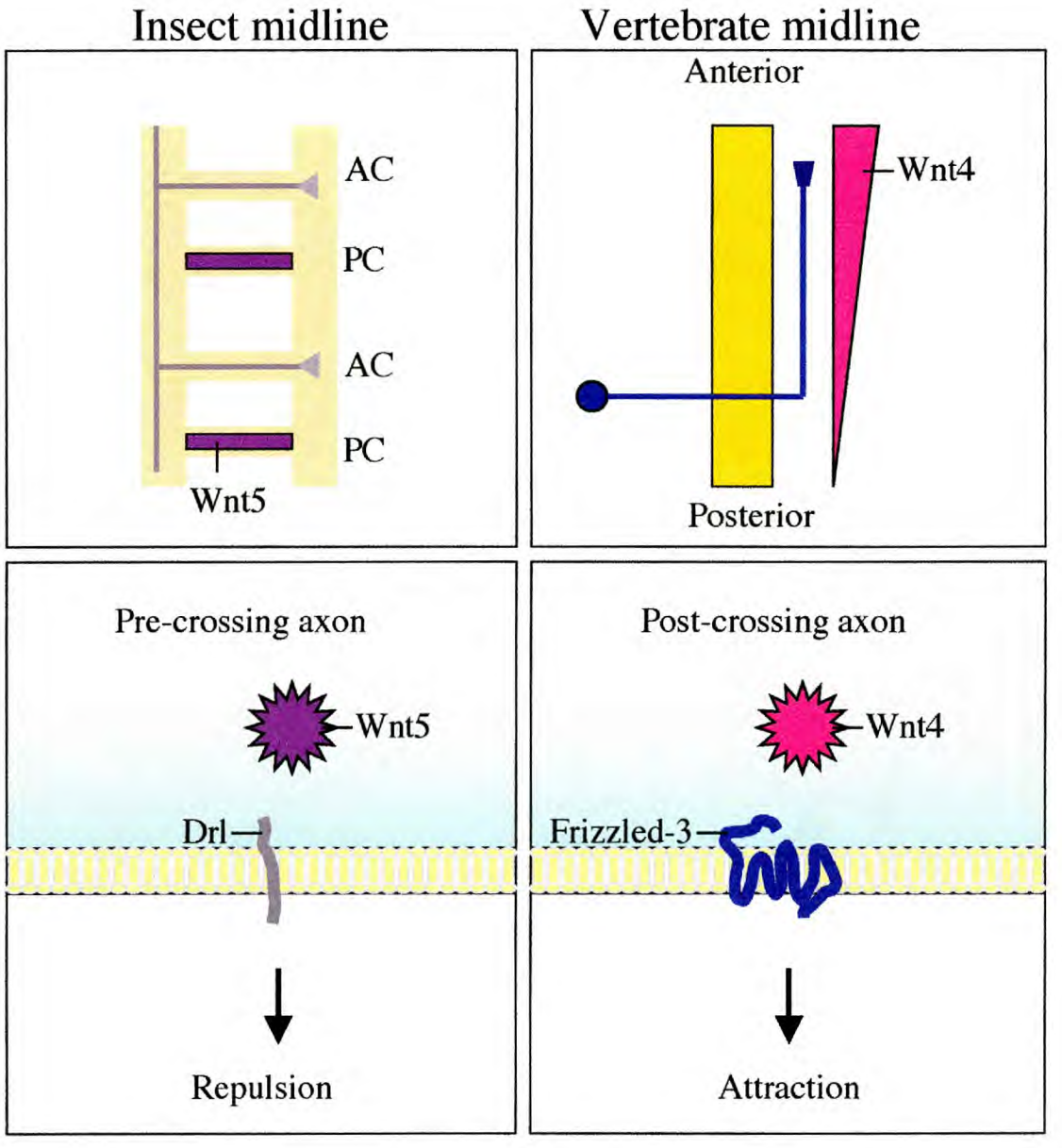


Figure 1.2. Wnts as axon guidance molecules.
In *Drosophila*, Wnt5 and derailed (Drl) receptors mediate repulsion of commissural axons at the midline. In vertebrates however, Wnt4, signalling through Frizzled-3 receptors, acts as an attractive guidance cue for post-crossing commissural axons. AC - anterior commissure, PC - posterior commissure.

1.2 Wnt proteins.

Wnt proteins are a large family of cystein-rich secreted glycoproteins with well-established roles in regulating embryonic patterning, cell proliferation and cell fate specification (Cadigan and Nusse, 1997). The first *Wnt* gene: *int-1* was discovered in 1982 as a protooncogene activated by the integration of mouse mammary tumour virus (Nusse and Varmus, 1982). Only when *wingless* (*Wg*) was identified in *Drosophila* as the *int-1* ortholog, the term *Wnt* was coined as an amalgam of the two (Cabrera *et al.*, 1987; Rijsewijk *et al.*, 1987). Subsequent phenotypic analyses *Wg* mutants provided clear evidence of the involvement of Wnts in many developmental processes. Wg is required in the *Drosophila* embryo for the formation of parasegmental boundaries and maintenance of *engrailed* expression in adjacent cells (Nusslein-Volhard and Wieschaus, 1980). *Wg* mutants are easily identified by their rudimentary segmentation and abnormal cuticle pattern. Instead of displaying denticle belts alternating with naked cuticle, the *Wg* larva is completely covered in denticles. Wg has also been found to be required for the proper development of the head, the midgut, and wing blade among other organs (reviewed in Klingensmith and Nusse, 1994), further demonstrating the importance of Wg in embryonic patterning.

Analysis of the expression of Wnt genes and targeted gene disruptions, have shed light on the range of biological processes that Wnts control during vertebrate development. Roles for Wnts in regulating cell fate and patterning are illustrated by some striking phenotypes, such as the absence of kidneys in *Wnt4* mutants (Stark *et al.*, 1994) and the formation of ventralised limbs as a result of *Wnt7a* inactivation (Parr and McMahon, 1995). More recently, critical roles for Wnt2b in the formation of laminar layers in the retina (Nakagawa *et al.*, 2003), and for Wnt7a in the correct orientation of stereociliary bundles in the inner ear (Dabdoub *et al.*, 2003) highlight the roles of Wnts in tissue organisation and polarity. Wnts also control cell proliferation, which explains the failure of limb buds lacking Wnt5a to grow (Yamaguchi *et al.*, 1999). Interestingly, Wnt genes are expressed in overlapping yet unique patterns in the developing vertebrate nervous system. Their spatial and temporal patterns of expression suggest that Wnt proteins may

play a role not only in the initial induction and early patterning of the nervous system but also at later stages of development, during axon guidance and synapse formation.

Wnts are involved in the induction of neural tissue by inhibiting BMP expression in *Xenopus* embryos (Baker *et al.*, 1999). Wnt6 in particular, is critical for neural crest induction in chick embryos (Garcia-Castro *et al.*, 2002). Wnts are also well-characterised posteriorising signals in the neural tube and forebrain. Kiecker and Niehrs were the first to demonstrate that a Wnt gradient is responsible for anterior-posterior patterning of the neural plate (Kiecker and Niehrs, 2001). Indeed ectopic Wnt expression leads to the aberrant induction of posterior neural markers (Kiecker and Niehrs, 2001), while inhibition of Wnt signalling causes the expansion of forebrain markers (Erter *et al.*, 2001; Glinka *et al.*, 1997). Regulation of Wnt signalling by secreted Wnt antagonists such as Dkk-1, Cerberus, Frzb-1 and Tlc is crucial for the formation of anterior structures in the neural tube and organisation of the forebrain (Houart *et al.*, 2002; Mukhopadhyay *et al.*, 2001; Glinka *et al.*, 1998; Leyns *et al.*, 1997; Bouwmeester *et al.*, 1996). Wnts are also involved in dorso-ventral patterning, inducing dorsal cell fate in the telencephalon (Gunhaga *et al.*, 2003) and in the spinal cord (Muroyama *et al.*, 2002). Interestingly, *Wnt1: Wnt3a* double mutants exhibit defects in the expansion of dorsal precursors (Ikeya *et al.*, 1997), suggesting Wnts regulate cell proliferation as well as cell fate in the spinal cord. Further evidence of the role of Wnts in neurogenesis came from studies of *Wnt3a* mutant mice, which do not develop a hippocampus due to underproliferation of caudomedial cortical progenitors (Lee *et al.*, 2000b). The complex role of Wnts in early stages of nervous system development is best illustrated in hindbrain patterning, where Wnt signalling restricts rhombomere boundaries (Riley *et al.*, 2004) by promoting neurogenesis in non-boundary cells (Amoyel *et al.*, 2005), and modulates programmed cell death of neural crest cells in odd numbered rhombomeres (Ellies *et al.*, 2000).

Wnt expression in defined developing neuronal populations in the brain at the time of neurite extension and synaptogenesis (Lucas and Salinas, 1997; Salinas *et al.*, 1994; Parr *et al.*, 1993) suggests Wnts also participate at later stages in the development of the

nervous system. As mentioned above, Wnts are emerging as important axon guidance molecules able to both repel commissural axons in *Drosophila* (Yoshikawa *et al.*, 2003), and attract post crossing commissural axons anteriorly in mice (Lyuksyutova *et al.*, 2003). Dr Salinas' lab was the first to report the role of Wnts in neuronal maturation, axonal arborisation and synapse formation in the mouse cerebellum (Hall *et al.*, 2000; Lucas and Salinas, 1997) . Wnt7a, secreted by granule cells, plays a critical role in the formation and maturation of glomerular rosettes, multisynaptic structures formed between a mossy fibre axon and dendrites of cerebellar granule cells, *in vivo* (Hall *et al.*, 2000). In addition, *Wnt7a* mutant mice show a delayed accumulation of synapsin I, a protein involved in synapse formation and function, in glomerular rosettes, indicating that Wnt7a acts as a retrograde synaptogenic factor. These results can be reproduced *in vitro*, as mossy fibres or granule cells treated with Wnt7a develop shorter, thicker axons with enlarged growth cones and more synapsin I clusters than controls (Hall *et al.*, 2000; Lucas and Salinas, 1997). More recently, Wnt3 has been found to induce similar morphological changes (decreased axonal length, enlargement of growth cones and increased branching) and stimulate the clustering of presynaptic proteins in embryonic dorsal root ganglion (DRG) neurons (Krylova *et al.*, 2002). Given that Wnt3 is expressed at limb levels by motor neurons at the time when a subset of DRG axons (from proprioceptive sensory neurons) reach the ventral spinal cord, these findings have lead to the proposal that, like Wnt7a in the cerebellum, Wnt3 is a retrograde signal for muscle afferents during the formation of sensory-motor circuits in the spinal cord (Fig.1.3).

Curiously, the effects of Wnt3 and Wnt7a on axon length and growth cone size, cannot be categorized as typical attractive or repulsive responses. However, the fact Wnts are target-derived signals suggests they may serve as stop signals to approaching axons. In addition to indicating that the target is close, Wnts are able to promote synapse formation. Further evidence of a role for Wnts in synaptogenesis has been found at the *Drosophila* neuromuscular junction where Wg coordinates the development of pre- and post- synaptic structures by allowing the presynaptic arbor to expand in correlation with

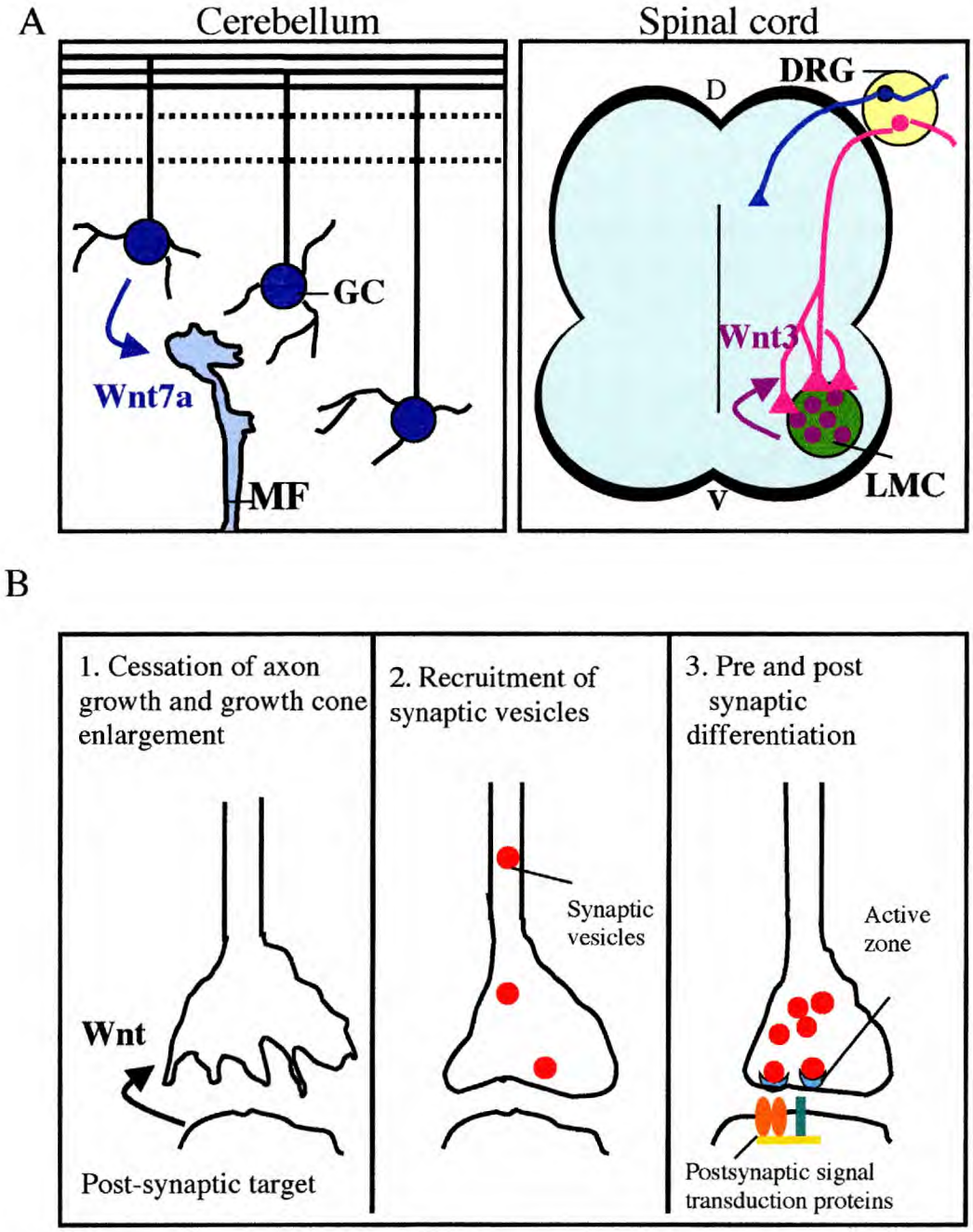


Figure 1.3. Wnts induce axonal remodelling and synaptogenesis in the vertebrate cerebellum and spinal cord.
(A)Wnts induce axonal remodelling of mossy fibres and NT-3 dependent DRGs. The changes in axonal morphology precede the clustering of synaptic vesicles. MF- Mossy fibre, GC- granule cell, D- dorsal, V- ventral, DRG- dorsal root ganglia, LMC- lateral motor column, pink neuron- NT-3 dependent proprioceptive neurons, blue neuron- NGF dependent thermo- and nociceptive neurons. (B) Model of the action of Wnts during synapse formation.

muscle growth (Packard *et al.*, 2002). Furthermore Dishevelled, a crucial transducer of the Wg signal, has been shown to regulate acetylcholine receptor clustering (Luo *et al.*, 2002). Interestingly, Wnts and their receptors are expressed in the murine cerebral cortex postnatally (Shimogori *et al.*, 2004) and in the adult brain (Lucas and Salinas, 1997; Salinas *et al.*, 1994), hinting at the exciting possibility that Wnt signalling could be involved in regulating neuronal plasticity throughout life.

1.3 The Wnt signalling pathways.

The well-characterised Wnt signalling pathways (Fig.1.4) provide a unique opportunity to elucidate the mechanism by which an extracellular signals regulate the axonal cytoskeleton during axon guidance and synaptogenesis. The influence of Wnts in cell fate decisions, cell proliferation and neuronal connectivity begs to question how can Wnts trigger such a variety of cellular responses? The explanation is likely to lie in their tightly regulated signalling system in which the molecular/cellular context is critical for the outcome.

Despite being secreted, Wnt proteins are more hydrophobic than initially predicted from their amino acid sequence. Difficulties in solubilising active Wnt molecules have greatly hindered attempts to purify and characterise them biochemically. However, the discovery of their palmitoylation on a conserved cystein residue which is critical for signalling, has enabled the successful purification of some family members (Willert *et al.*, 2003). The precise function of this posttranslational modification is unknown, but it has been suggested to aid membrane targeting (Nusse, 2003).

Once secreted, Wnts encounter a number of binding partners that can modulate their activity. Heparan sulfate proteoglycans (HSPGs) have been implicated in the transport and stabilisation of Wnts. Absence of *Dally*, a *Drosophila* HSPG, or mutations in genes encoding enzymes that modify HSPGs generate phenotypes similar to *Wg* mutants (Lin and Perrimon, 2000). In addition, Wnts may encounter antagonists such as secreted Frizzled related proteins (sFRPs) or Wnt inhibitory factors (Wifs) able to bind and

sequester Wnts (Uren *et al.*, 2000), or members of the Dickkopf protein family, that interfere with Wnt-receptor/co-receptor binding (Bafico *et al.*, 2001) and can trigger the internalisation of receptors to downregulate Wnt signalling (Mao *et al.*, 2002). The abundant expression of Wnt antagonists in embryos and their abnormal expression patterns in disease states, suggest that they are of vital importance in limiting the range of Wnt activity and refining the Wnt signal (Jones and Jomary, 2002).

The main receptors for Wnt proteins are Frizzleds; seven pass transmembrane receptors with an extracellular cystein-rich Wnt-binding domain (Bhanot *et al.*, 1996; Yang-Snyder *et al.*, 1996). Wnts bind Frizzleds with considerable promiscuity, as any Wnt can bind to more than one Frizzled and vice versa (Wu and Nusse, 2002). Nineteen Wnts and ten Frizzled genes have been identified in the mouse (for latest update see http://www.stanford.edu/~rnusse/wntwindow.html), but much remains to be learnt about the spectrum of Wnt-Frizzled binding interactions. Seven transmembrane receptors usually utilise trimeric G proteins for signalling, but the role of G proteins in Wnt signalling was unclear until a recent report by Katanaev and colleagues, which demonstrates that the G_o subunit acts downstream of Frizzled and is essential for Wnt signalling in *Drosophila* (Katanaev *et al.*, 2005).

The complexity of receptor–ligand specificity is further increased by the existence co–receptors such as LDL-receptor related proteins (LRPs) and the transmembrane tyrosine kinase Ryk. LRPs are single transmembrane proteins required for signalling through the canonical or β-catenin pathway (Pinson *et al.*, 2000; Tamai *et al.*, 2000) and have been shown to form hetero-oligomers with Frizzled receptors upon Wnt binding (Cong *et al.*, 2004). On the other hand, Ryk is emerging as a key mediator of Wnt signalling in the CNS. Ryk is required both for Wnt3a induced neurite outgrowth (Lu *et al.*, 2004) and for DWnt5 repulsion of commissural axons, where it can signal independently of Frizzleds (Yoshikawa *et al.*, 2003).

Interaction of Wnt and Frizzled activates the cytoplasmic protein Dishevelled (Dvl) by a yet unknown mechanism. Dvl has been shown to be recruited to cell membranes

(Yanagawa *et al.*, 1995) where it interacts directly with Frizzleds (Chen *et al.*, 2003; Wong *et al.*, 2003), and to become phosphorylated upon activation of Wnt signalling (Rothbacher *et al.*, 2000; Yanagawa *et al.*, 1995). However, many questions regarding whether Wnt binding to Frizzled receptors regulates Dvl-Frizzled binding, how Dvl phosphorylation is controlled and the roles of phosphorylated Dvl in Wnt signalling remain to be solved. The three main Wnt signalling pathways: canonical, planar cell polarity and the Wnt/Ca^{+2} pathway, diverge downstream of Dvl leaving little doubt that Dvl is a central player in Wnt signalling. How Wnts signal through a particular pathway

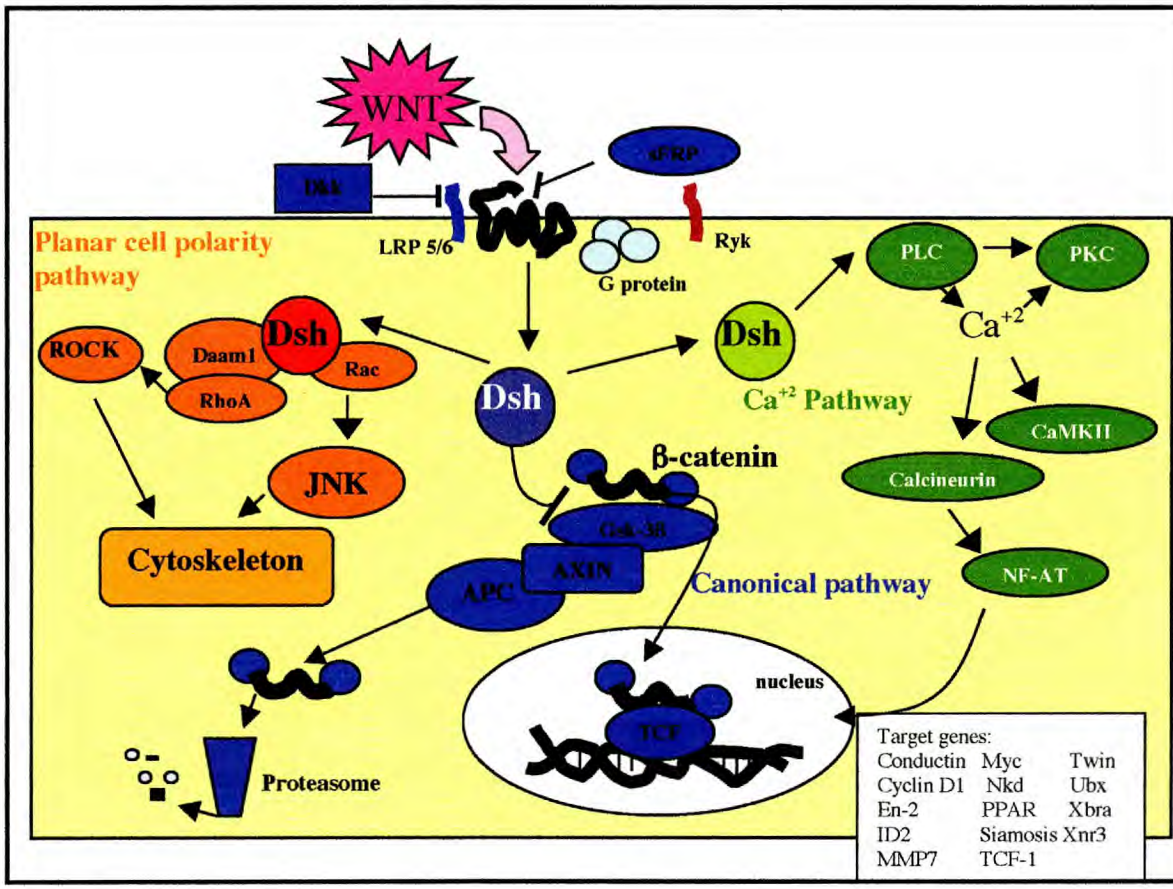


Figure 1.4. The three main Wnt signalling pathways.
The canonical pathway is depicted in blue, planar cell polarity in orange and the Wnt/Calcium pathway in green. T-bars denote inhibition, arrows represent activation. Adapted from Huelsken and Birchmeier, 2001.

is still unknown, though certain Wnt/receptor/co-receptor complexes, the intracellular localisation of Dvl and the availability of Dvl binding partners have been suggested to

play a role in determining the path of signal transduction (Capelluto *et al.*, 2002; Pinson *et al.*, 2000; Tamai *et al.*, 2000; Torres and Nelson, 2000).

In the canonical Wnt pathway (blue one in figure 1.4), Wnts induce β-catenin mediated gene expression. Dvl prevents the degradation of β-catenin by inhibiting the serine/threonine kinase Gsk-3β and disrupting the β-catenin degradation complex. In the absence of Wnt signalling, β-catenin is phosphorylated by Gsk-3β and is subsequently ubiquitinated for proteosomal degradation. Both Axin and APC are part of the β-catenin degradation complex and interact with Dvl (Nakamura *et al.*, 1998; Papkoff *et al.*, 1996). Axin is believed to aid β-catenin degradation by stimulating its phosphorylation by Gsk-3β, but upon Wnt signalling, Axin is found to interact with Dvl and LRP, which could sequester or displace it from the complex (Cong *et al.*, 2004; Wharton, 2003). APC functions as both a positive or negative regulator of Wnt signalling in depending on the cellular context (reviewed in Miller *et al.*, 1999). The activity of Gsk-3β is normally regulated by phosphorylation, and despite the fact that inhibition of the enzyme mimics the effect of Wnt signalling on gene expression, cell fate decisions and axonal morphology (Krylova *et al.*, 2002; Lucas *et al.*, 1998; Lucas and Salinas, 1997; Klein and Melton, 1996), to date there is no evidence that Gsk-3β is post-translationally modified in response to Wnt signalling. As a result of Wnt-induced inhibition of Gsk-3β, β-catenin accumulates in the cytoplasm and is translocated to the nucleus, where it interacts with members of the LEF/TCF family of transcription factors to activate genes involved in different developmental processes (Huelsken and Birchmeier, 2001).

In the Wnt/Ca^{+2} pathway (green in figure 1.4), Wnt signalling results in an increase in intracellular calcium possibly mediated by G proteins (Slusarski *et al.*, 1997). This pathway involves Dvl, phospholipase C, protein kinase C and calmodulin-dependent kinase II (Sheldahl *et al.*, 2003; Kuhl *et al.*, 2000). The Wnt/Ca^{+2} pathway is required for *Xenopus* ventralisation and the regulation of convergent extension movements (Veeman *et al.*, 2003; Saneyoshi *et al.*, 2002). One of the identified targets of this pathway is the calcium sensitive transcription factor NF-AT which is able to suppress canonical Wnt signals during axis formation in *Xenopus* (Saneyoshi *et al.*, 2002).

In the Planar Cell Polarity (PCP) pathway (in orange in figure 1.4) Wnts signal through Dvl to regulate Rho GTPases and activate Jun-terminal kinase (JNK). Wnt-mediated JNK activation is observed during convergent extension movements in vertebrates and during eye and wing development in *Drosophila* (Heisenberg *et al.*, 2000; Mlodzik, 2000; Strutt *et al.*, 1997). In *Drosophila,* the formin homology protein Daam1 mediates Dvl activation of RhoA and its downstream effector, Rho–associated kinase (ROCK), which can in turn regulate actomyosin contractility (Winter *et al.*, 2001). Activation of Rac, upstream or in parallel to RhoA has also been reported in the establishment of planar cell polarity in the *Drosophila* eye (Fanto *et al.*, 2000). Furthermore, Dvl has recently been shown to activate Rac in hippocampal neurons (Rosso *et al.*, 2005). Due to the importance of RhoGTPases in regulating the cytoskeleton, the PCP pathway offers an important line of enquiry into the mechanisms by which Wnts induce axonal remodelling. It is also worth noting that despite the existence of these different pathways, the possibility that Wnts simultaneously signal through more than one of them, thus providing another means to tune the cellular response in different contexts, cannot be ruled out.

1.4 The axonal cytoskeleton.

Neuronal migration, axon extension, axon guidance and synapse formation all rely on changes in the organisation and dynamics of the axonal cytoskeleton. Great insight into the roles of microtubules and actin filament dynamics in axon guidance and motility has been possible thanks to high-resolution imaging of cultured neurons and the use of cytoskeleton-targeted drugs. Biochemical studies and genetic manipulations have begun to shed light on the proteins involved in the regulation of the axonal cytoskeleton, and the signalling cascades triggered by axon guidance cues are beginning to be outlined (for review see Guan and Rao, 2003).

The axonal cytoskeleton is composed of highly dynamic polarised polymers: actin filaments and microtubules. The rapid and continuous assembly and disassembly of

polymers by the tightly regulated addition or removal of monomers, allows cells to respond rapidly to changes in the environment. Neurofilaments are also an important cytoskeletal component during the development of the vertebrate nervous system (Lin and Szaro, 1995), but their function in growth cone motility and guidance remains unknown. Their slow rate of monomer exchange seems inconsistent with them playing a major role in axon growth and motility (Mitchison and Kirschner, 1988).

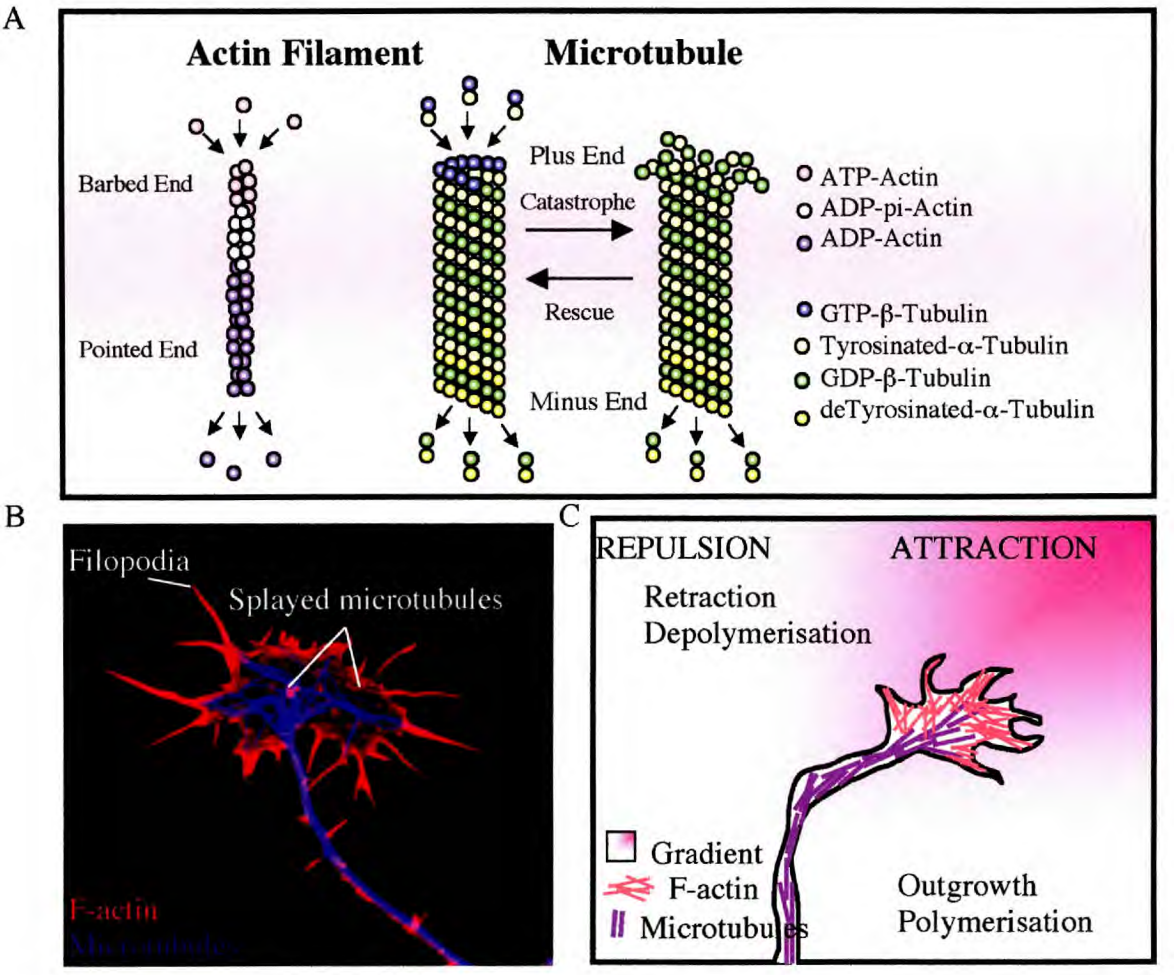


Figure 1.5. The axonal cytoskeleton.
(A) Actin filaments and microtubules are dynamic polarised polymers. While ATP-actin monomers and GTP-tubulin dimmers bind to the barbed or plus end, ADP-actin and GDT-tubulin dissociate from the pointed or minus end (adapted from Dent and Gertler. 2003). (B) Actin filaments are concentrated at the edge of growth cones. Microtubules, which are bundled along the axon, typically splay in the growth cone. (C) Upon encounter with an attractive cue, the polymerisation of both actin filaments and microtubules on the side of the growth cone closest to the attractive cue induce growth cone turning and axon growth towards the attractant.

1.4.1 Actin filaments.

The polymerisation of actin monomers gives rise to helical polymers known as actin filaments or F-actin. Two isotypes of actin: β-actin and γ-actin are found in equal levels in neurons, but whether they have different functions, or whether polymers consist of both or only one isotype is not known. ATP-actin associates preferentially with the barbed end of filaments (generally facing the plasma membrane), while dissociation of ADP-actin is kinetically favoured at the pointed end (Pollard and Borisy, 2003). As the filament "ages", ATP-actin is hydrolysed, first to ADP-p_i-actin and then to ADP-actin.

Actin filaments line the cortex of the axon and are found just beneath the plasma membrane (Fig.1.5). Growth cones contain the highest levels of F-actin. Bundles of actin filaments form filopodia, which are highly motile, slender finger-like projections extending from the growth cone. Filopodia are excellent sensors of guidance cues and have the ability to quickly assemble and disassemble adhesive contacts (Wood and Martin, 2002). F-actin can also adopt a meshwork-like array forming lamellipodia, fan-like protrusions that expand and retract as the growth cone samples the environment. Lamellar protrusion establishes the bulk of the contacts between the growth cone and the extracellular environment, and is required for subsequent axonal outgrowth (Jay, 2000; Tosney and Wessells, 1983). Other actin structures described in neurons include: actin arcs, arranged parallel to the leading edge between the peripheral and central regions of growth cones, where they interact with and influence the organisation of microtubules (Schaefer *et al.*, 2002), and intrapodia, protrusive structures arising from lamellipodia at proximal regions of the growth cone (Rochlin *et al.*, 1999).

Actin filament dynamics are tightly regulated by a large number of actin binding proteins (ABPs). Briefly, they can be classified as proteins that (a) sequester actin monomers (decrease polymerisation), (b) nucleate actin filaments (promote branching of filaments), (c) cap filament ends (inhibiting either polymerisation or depolymerisation), (d) sequester capping proteins, (e) sever actin filaments, (f) bundle or cross-link filaments, (g) anchor filaments to membrane adhesions. Most of these proteins have been found to localise at the growth cone by immunocytochemistry (Endo *et al.*, 2003;

Cohan *et al.*, 2001; Goldberg *et al.*, 2000; Lanier *et al.*, 1999; Tanaka *et al.*, 1993; Letourneau and Shattuck, 1989), but functional and expression studies are yet to be done for many. Rho GTPases are emerging as key regulators of the actin cytoskeleton in neurons. Rho GTPases are found downstream of many extracellular guidance cues and are able to activate several ABPs. Despite the fact their role in neurons is not as well-established as in fibroblasts, there is evidence that Rac1 and Cdc42 are positive regulators of axonal outgrowth and are activated by attractive guidance cues, whereas RhoA is a negative regulator of the axonal outgrowth and is activated in response to repellent cues (for review see Luo, 2000). However, there are some exceptions, Rac1 for instance, has also been found to mediate Sema3A-induced growth cone collapse in sensory and retinal neurons (Jurney *et al.*, 2002; Jin and Strittmatter, 1997).

In addition to filament dynamics, F-actin polymers are transported rearwards from their site of assembly, at the distal part of the growth cone to the central part, by a myosin motor-driven complex in a process known as retrograde actin flow (Lin *et al.*, 1996; Mitchison and Kirschner, 1988). Interestingly, attenuation of retrograde flow, which takes place upon interaction of a growth cone with its target (Suter *et al.*, 2004; Lin and Forscher, 1995), aids actin polymerisation at the leading edge translate into forward motion (Suter *et al.*, 1998; Lin and Forscher, 1995).

A variety of methods have been developed to follow actin dynamics in living cells including photobleaching of fluorescently labelled actin (Wang, 1985) and speckle imaging (Waterman-Storer *et al.*, 1998). In neurons, F-actin retrograde flow has been directly visualised by fluorescent speckle microscopy in growth cones of *Aplysia* neurons injected with fluorescently labelled phalloidin (Schaefer *et al.*, 2002; Zhang *et al.*, 2003). Actin dynamics have also been investigated in dendritic spines of EGFP-actin expressing hippocampal neurons by measuring the recovery of fluorescence after photobleaching (FRAT) (Star *et al.*, 2002). However, the latest strategy to visualise actin dynamics involves fluorescence resonance energy transfer (FRET) between CFP and YFP tagged actin monomers. This technique enables monitoring both the

monomeric and filamentous forms of actin, and has been used to detect shifts in the F-/G-actin ratio in dendritic spines upon tetanic stimulation (Okamoto *et al.*, 2004).

1.4.2 Microtubules

Microtubules are essential for the formation and maintenance of neurites by providing structural support and acting as tracks for the bidirectional transport of proteins and vesicles between the cell body and the axon terminal. Microtubules are composed of 11 to 15 protofilaments arranged in a tubular structure of approximately 25 nm in diameter (Luduena, 1998). Protofilaments are polymers of α/β-tubulin heterodimers. Three α-tubulin genes and five β-tubulin genes are expressed in the brain, but the actual isotypic makeup of individual microtubules is unknown. Interestingly, *in vitro* studies suggest that certain isotypes such as α-βIII-tubulin dimers confer more stability to the polymer than others (Schwarz *et al.*, 1998). Microtubules are polarised structures as α/GTP-β-tubulin subunits associate preferentially to the plus or growing end of the microtubule and α/GDP-β-tubulin dissociates from the minus end (Fig.1.5). In axons, microtubules are bundled and oriented with their minus end pointing towards the cell body and the plus end pointing towards the axon growth cone, however microtubules in dendrites, are found in both orientations (Baas *et al.*, 1989). Post-translational modifications such as detyrosination of the C-terminus on the α subunit after incorporation to the polymer, or acetylation of lysine-40 on α-tubulin, correlate with the age of the microtubule and its degree of stability. Individual microtubules are highly acetylated at their minus ends and highly tyrosinated at their plus ends (Brown *et al.*, 1993; Baas *et al.*, 1993). Labelling microtubules with specific antibodies against tyrosinated and acetylated tubulin, and comparing their distribution makes it possible to determine where the most recently polymerised microtubules are. Tyrosinated microtubules usually splay in the central region of the growth cone and can rapidly extend and retract from the peripheral actin rich region. In contrast, acetylated microtubules tend to remain bundled in the proximal region of the growth cone (Schaefer *et al.*, 2002; Dent and Kalil, 2001; Kabir *et al.*, 2000; Dent *et al.*, 1999).

Like actin filaments, microtubule dynamics are tightly regulated by an ever-increasing number of microtubule binding proteins (MBPs). Microtubules exhibit an intrinsic behaviour characterised by cycles of growth and shrinkage, known as dynamic instability, that allows efficient probing of the extracellular environment. The transitions between the two states are referred to as catastrophe and rescue respectively. MBPs include the structural microtubule associated proteins (MAPs): MAP-1B, MAP-2 and tau, which stabilise microtubules by reducing catastrophe and promoting rescue frequencies (Drewes *et al.*, 1998), and plus-end tracking proteins (+TIPs) which regulate microtubule dynamics at the plus-end and link microtubules with actin associated proteins at the cell surface (Carvalho *et al.*, 2003). Time-lapse recordings of neurons expressing fluorescently labelled tubulin or +TIPs have allowed to directly measure the speed of microtubule growth and shrinkage as well as the frequencies of rescue and collapse (Hasaka *et al.*, 2004; Schaefer *et al.*, 2002; Kabir *et al.*, 2001). The regulatory roles of +TIPs on microtubule dynamics as well as the changes in microtubule dynamics in response to guidance cues are now beginning to be addressed (Dent *et al.*, 2004; Lee *et al.*, 2004; Kalil *et al.*, 2000).

In addition to the dynamics of individual polymers, the microtubule array within an axon and growth cone also depends on the motor-driven transport of pre-assembled polymers (Baas, 2002; Ahmad *et al.*, 1998; Ahmad and Baas, 1995) and their organisation. Changes in the organisation of microtubules such as unbundling, or the formation of microtubule loops, have been found in paused growth cones (Dent and Kalil, 2001; Dent *et al.*, 1999; Tanaka and Kirschner, 1991), in motor axon boutons at the *Drosophila* NMJ (Roos *et al.*, 2000) and in growth cones exposed to Wnt7a (Hall *et al.*, 2000). How microtubule loops form is unclear, though roles for MBPs, such as MAPs and motor proteins, and the retrograde flow of actin filaments have been postulated (Baas and Qiang, 2005; Yu *et al.*, 2001). Equally, whether microtubule looping or unbundling is a cause or consequence of alterations in microtubule dynamics remains to be established. Interestingly, time-lapse imaging of spinal neurons expressing high levels of the microtubule plus end binding protein CLASP-GFP, has revealed a correlation between microtubule looping and a decrease in microtubule growth (Lee *et*

al., 2004). Due to the influence of microtubule organisation on axon behaviour and vesicular transport, future studies may find important links between the organisation of microtubules in neurons and synaptogenesis or axonal degeneration.

1.4.3 Interactions between actin and microtubules

There is accumulating evidence of the close interactions between microtubules and actin filaments and of the importance of their crosstalk for an effective response to guidance cues. Initial findings by Forsher and Smith suggested that actin acts as a barrier for microtubules, as inhibition of actin assembly leads to microtubule invasion of the periphery of growth cones (Forscher and Smith, 1988). The mechanism of restraint could be partially due to actin filaments arranged perpendicularly to the direction of axon growth, and to the actin retrograde flow (Yu *et al.*, 2001). Time-lapse images have shown that microtubules in the periphery of growth cones are often swept backwards at the same rate as the actin retrograde flow (Schaefer *et al.*, 2002). In contrast, interactions of microtubules with actin filopodia favour microtubule advance (Gordon-Weeks, 1991; Letourneau, 1983), indicating that actin bundles can also act as tracts to guide microtubules into the periphery of growth cones. Thus, by serving as tracts or as barriers, actin filaments can influence microtubule advance. However, microtubules can also regulate actin organisation and dynamics. Pharmacological inhibition of microtubule dynamics has revealed a role for microtubules in the regulation and maintenance of lamellar and filopodial structures in growth cones (Gallo, 1998), intrapodia (Rochlin *et al.*, 1999), axon branching (Dent *et al.*, 1999), and in growth cone turning (Buck and Zheng, 2002). Hence, it seems, that the interaction between dynamic actin filaments and microtubules is crucial for axon motility and guidance.

Several proteins are able to mediate signalling between actin filaments and microtubules, these include: (a) MAPs: MAP-1B, MAP-2 and tau have all been to found interact with actin filaments as well as microtubules, depending on their phosphorylation state, though their function on the actin cytoskeleton is yet to be determined (Pedrotti *et al.*, 1996; Correas *et al.*, 1990). (b) Members of the spectraplakins can crosslink actin filaments and microtubules (Roper *et al.*, 2002). Mutations in the *Drosophila* plakin

short-stop lead to defective axon extension (Lee *et al.*, 2000a) and more importantly, *short-stop* requires both microtubule and actin binding motifs to function properly (Lee and Kolodziej, 2002). (c) Finally it is necessary to mention the Rho GTPases, which are emerging as key regulators of both actin and microtubules in migrating cells. One of the mechanisms by which Rac/Cdc42 regulates both actin and microtubules is via the actin crosslinking protein IQGAP-1. IQGAP-1 localises to cortical actin filaments upon Rac activation, where it is able to recruit APC and bind to the microtubule plus end protein CLIP-170. The IQGAP-1/APC/CLIP-170 complex facilitates microtubule targeting and stabilisation at the leading edge allowing directional migration (Watanabe *et al.*, 2004; Fukata et al., 2002a). Conversely, microtubule dynamics have also been shown to modulate Rho GTPases, which in turn can regulate the dynamics of both actin and microtubules. Rapid microtubule growth is able to activate Rac and promote actin polymerisation and leading edge protrusion (Waterman-Storer *et al.*, 1999). In addition, Rac can decrease microtubule catastrophe and promote further microtubule polymerisation by inhibiting the destabilising MAP OP18/Stathmin (Daub *et al.*, 2001), thus forming a positive feedback loop that perpetuates assembly of both actin and microtubules. Furthermore, activation of the guanine nucleotide exchange factor (GEF)-H1 upon microtubule depolymerisation at the trailing end of migrating cells (Krendel *et al.*, 2002), facilitates both Rho mediated contraction of the actin cytoskeleton and microtubule stabilisation via the formin mDia (Palazzo *et al.*, 2001). This negative feedback loop is critical in the control of cell contraction during migration, and highlights once again, the central role of Rho GTPases in the regulation of both actin and microtubules. Unlike migrating cells, little is known about the regulation of actin and microtubules by RhoGTPases in neurons. Only one study implicates Rac in the microtubule-dependent polymerisation of F-actin in laminin-stimulated sympathetic neurons (Grabham *et al.*, 2003).

1.4.4 Changes in the cytoskeletal organisation underlying axon growth, turning and branching

The response of cultured neurons to guidance cues and the use of cytoskeleton-targeted drugs have enabled to study some of the cytoskeletal changes underlying axon growth,

turning and branching. Axon extension takes place during or after cell migration. In the 1970s, Wessells and colleagues were the first to show cessation of axon outgrowth in DRG cultures upon exposure to actin or microtubule depolymerising drugs (Yamada *et al.*, 1971; Yamada *et al.*, 1970). Subsequent experiments have shown that F-actin is required for maintaining growth cone shape, and is essential for correct axon guidance, while microtubules provide rigid support and allow directed axon elongation (Dent and Kalil, 2001). The changes that take place in the cytoskeleton during the establishment of neuronal polarity have been extensively analysed in cultured hippocampal neurons, which extend a single, thin, long axon and multiple thick and comparatively short dendrites. In 1999, Bradke and Dotti showed that pharmacological destabilisation of the actin cytoskeleton stimulates microtubule advance and rapid axonal outgrowth (Bradke and Dotti, 1999). These findings suggest that a decrease in actin stability in one of the immature neurites is sufficient to confer axonal identity. However, recent studies have highlighted the importance of microtubule polymerisation in establishing neuronal polarity. Collapsin response mediator protein-2 (CRMP-2) is preferentially localised in axonal growth cones, and when overexpressed induces the formation of multiple axons (Inagaki *et al.*, 2001). CRMP-2 contributes to axon differentiation by promoting the addition of tubulin subunits to microtubule ends and by regulating the rate of axon growth (Fukata *et al.*, 2002b). Whether the dynamics of microtubules and/or actin themselves are at the heart of establishing neuronal polarity is still a question of debate (Ruthel and Hollenbeck, 2000; Bradke and Dotti, 1999), but there is little doubt that they are key targets in the determination of axonal identity.

Early time-lapse studies of *Aplysia* neurons and rodent cortical and sympathetic neurons growing *in vitro* revealed the main stages of axon growth (Aletta and Greene, 1988; Goldberg and Burmeister, 1986; Kalil and Skene, 1986): (a) protrusion- which consists of the elongation of growth cone filopodia and advance of lamellipodia driven by actin polymerisation (Zheng *et al.*, 1996; Bentley and O'Connor, 1994), (b) engorgement- occurs when microtubules invade the protrusions bringing vesicles and membranous organelles and (c) consolidation- takes place as the proximal part of the growth cone adopts a cylindrical shape to become the new distal axon and probably requires actin

depolymerisation. Similar phases of axon growth have been reported in the developing embryo (Halloran and Kalil, 1994; Harris, 1987). However, since growth *in vivo* is not random and is directed towards a specific synaptic target, it is likely that attractant and repellent gradients simply direct protrusion, engorgement and consolidation in a particular direction by differentially reorganising the cytoskeleton on one side of the growth cone (Fig. 1.5). This has prompted the examination of the cytoskeleton in growth cone turning assays and the outcomes of local application of drugs that affect the cytoskeleton. During growth cone turning, the following changes have been reported: (a) Preferential F-actin protrusion and stabilisation on the turning side of the growth cone. This is achieved by actin polymerisation and an increase in susbstrate adhesion (Suter and Forscher, 2000; Lin *et al.*, 1994a). (b) Preferential polymerisation and/or stabilisation of microtubules on the turning side of the growth cone. Local stabilisation of microtubules by focal uncaging of taxol on one side of the growth cone, leads to growth cone turning towards the side on which microtubules have been stabilised, while local application of the microtubule depolymerising drug nocodazole causes turning towards the opposite side (Buck and Zheng, 2002). This phase may also involve transient microtubule capture at actin rich regions, which renders them less likely to depolymerise (Buck and Zheng, 2002; Dent and Kalil, 2001). (c) Finally, the proximal part of the growth cone has to consolidate into a cylindrical shaft by depolymerising F-actin and bundling microtubules, at present there are not much data regarding this phase of the turning process.

Axon branching enables a single neuron to establish synaptic contacts with multiple targets and is therefore a crucial event in the establishment of neuronal circuits. Axonal branching can occur through bifurcation of the terminal growth cone or by extension of collateral/interstitial branches from the axon shaft. Interestingly, a similar reorganisation of the cytoskeleton is observed in both cases. Points of branch formation are preceded by a pause and enlargement of the growth cone (Kalil *et al.*, 2000). Independently of whether the growth cone bifurcates after pausing or the axon continues to grow and a collateral branch emerges from the point at which the pausing behaviour took place, actin accumulation, local microtubule unbundling and fragmentation have all been

observed to occur prior to branch initiation (Dent and Kalil, 2001; Szebenyi *et al.*, 1998; Yu *et al.*, 1994). It has been postulated that active remnants from the paused growth cone, such as filopodial and lamellar protrusions, are left behind demarcating sites on the axon shaft at which interstitial branches will later emerge (Kalil *et al.*, 2000). The proteins involved in the reorganisation of actin and microtubules during branch formation remain unknown, but the microtubule severing protein katanin has been suggested to play a role in microtubule fragmentation (Ahmad *et al.*, 1999; McNally and Vale, 1993). The first step towards branch formation is the protrusion of filopodia either from the axon shaft or the growth cone. Only filopodia that become invaded by short microtubule fragments will develop into branches (Dent *et al.*, 1999). The anterograde transport of preassembled microtubules, polymerisation, and subsequent stabilisation results in an axonal branch (Dent *et al.*, 1999). Both actin and microtubule dynamics are required to be intact for axon branching to occur (Dent and Kalil, 2001), which emphasizes the importance of actin-microtubule interactions in axon behaviour. Interestingly, FGF-2 and netrin 1 increase branching but have no effect on primary axon outgrowth (Dent *et al.*, 2004), suggesting that axon outgrowth and axon branching may be regulated independently. Since inhibition of microtubule dynamics by drug treatments that decrease axon outgrowth by up to 50% have almost no effect on collateral branch formation (Gallo and Letourneau, 2000), it is possible that branching has a greater dependency on microtubule transport while axon elongation relies more on dynamic instability.

In vivo, the process of axon branching often takes place once an axon has reached its target area and is very closely related to synapse formation. Synaptic activity has been demonstrated to play a role in the axon branch dynamics of tectal neurons in Zebrafish (Niell *et al.*, 2004) and *Xenopus* (Ruthazer *et al.*, 2003). A recent study from the Cline laboratory (Javaherian and Cline, 2005) examined motor neuron branch dynamics and the formation of synaptic contacts in *Xenopus* embryos, and found that branches emerge from presynaptic sites. The authors suggest that Ca^{+2} entry at these sites promotes the necessary reorganisation of the cytoskeleton for branch formation and that synaptogenic

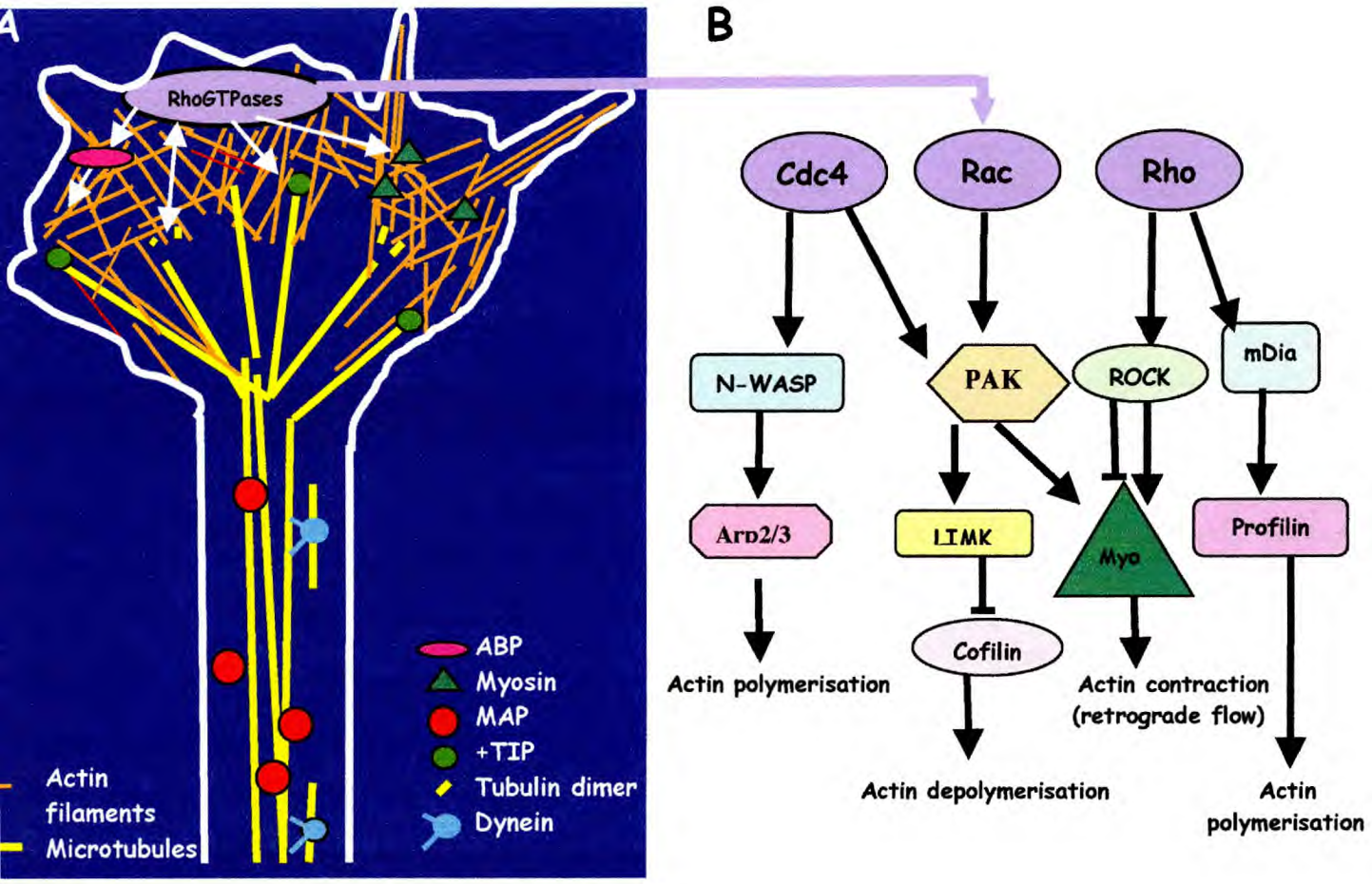


Figure 1.6. Summary of how the axonal cytoskeleton is regulated.
(A) Microtubules grow thanks to the continuous assembly (and disassembly) of tubulin dimers and the incorporation of pre-assembled polymers, which are transported by dynein motors. Microtubule binding proteins such as MAPs and +TIPs have been shown to influence both the dynamics and organisation of microtubules. Actin filaments are also continuously assembled and disassembled, as well as transported rearwards, towards the centre of the growth cone, by myosin-driven retrograde flow. RhoGTPases are key regulators of both actin filaments and microtubules as they are able to modulate microtubule stability and capture at the plasma membrane, as well as influence myosin contractility and other actin binding proteins (ABPs), thus aiding actin filament assembly or disassembly. (B) Diagram of RhoGTPase effectors likely to mediate cytoskeletal changes in neurons (adapted from Luo 2000).

factors, such as candidate plasticity gene (CPG)-15, play a role in the formation of axonal arbors.

1.4.5 Linking axonal guidance cues to the cytoskeleton

Although much is yet to be learnt about how growth cones integrate guidance cues, it is generally believed that activation of cell surface receptors triggers signalling cascades whose final action converges on the axonal cytoskeleton and results in a finite number of cellular responses. Therefore, it should not come as a surprise that attractive and inhibitory guidance cues regulate common cytoskeletal mechanisms to exert opposing effects on the axonal cytoskeleton. The main links between extracellular guidance cues and the axonal cytoskeleton are described below.

Repellent or negative guidance cues cause growth cone collapse or repulsive turning *in vitro*. The cytoskeletal features associated with those responses are: **(a) Actin depolymerisation**, which has been observed to occur within minutes of application of Sema3A, ephrin-A2 and brain-derived collapsing factor (Fan *et al.*, 1993; Jurney *et al.*, 2002). **(b) Inhibition of growth cone motility**. Both lamellar protrusion and filopodial motility are paralysed before Sema3A and brain-derived collapsing factor-induced collapse (Fan *et al.*, 1993; Luo *et al.*, 1993). In addition, axon retraction in response to ephrin-A2 correlates with a decrease in actin turnover (Gallo *et al.*, 2002). These studies suggest that repulsive guidance cues not only decrease the amount of actin filaments in growth cones, but also decrease the dynamics of the remaining ones. **(c) Increase in endocytosis of the growth cone plasma membrane**, which has been shown upon ephrin-A2, ephrin-A5 and Sema3A induced collapse (Jurney *et al.*, 2002; Fournier *et al.*, 2000). Together, these findings suggest that the actin cytoskeleton is the main target for repulsive guidance cues, however, some papers have highlighted the effects of repellent signals on microtubules. Sema3A has been shown to decrease dynamic microtubules (tyrosinated) in growth cones of cortical neurons (Dent *et al.*, 2004) and chick dorsal root ganglia neurons (Fritsche *et al.*, 1999). In addition, it has been postulated that negative guidance cues could induce axonal retraction by regulating the activity of microtubule motors such as dynein (Ahmad *et al.*, 2000). A recent study by Lee and colleagues (Lee *et al.*, 2004) identified Orbit/MAST as a protein that mediates the action of Slit by acting downstream of abelson (Abl) protein tyrosine kinase. Orbit/MAST is a +TIP protein, and analyses of microtubule dynamics in *Xenopus* spinal neurons

expressing the vertebrate Orbit/MAST ortholog, CLASP, suggest that Slit-mediated repulsion involves a decrease in microtubule growth and the formation of microtubule loops which lead to growth cone pausing and eventually to axonal retraction (Kalil and Dent, 2004).

Other intracellular proteins found to mediate negative guidance responses are: (1) Rac 1, though its exact role is controversial. Two research groups (Hu *et al.*, 2001; Shamah *et al.*, 2001) have demonstrated the ability of plexin B and EphA4 to inhibit Rac activity and activate RhoA during chemorepulsion, which would explain the decrease in protrusive activity in collapsing growth cones. However, several other studies have found that Rac activity is required for Sema3A induced collapse (Jin and Strittmatter, 1997) and that it mediates both Sema3A and ephrin-A2 induced endocytosis of the plasma membrane (Jurney *et al.*, 2002). (2) Cofilin, an actin filament depolymerising and severing protein, is transiently inactivated by LIMK downstream of Sema3A signalling causing a decrease in actin dynamics (Endo *et al.*, 2003; Aizawa *et al.*, 2001). (3) Members of the Ena/Vasp family of actin anti-capping proteins, associate with Robo receptors and positively regulate Robo signalling in cortical neurons (Bashaw *et al.*, 2000). The precise mechanism by which Ena/Vasp mediates Slit repulsion remains to be determined. (4) Further upstream in the signalling cascades triggered by negative axon guidance molecules, two highly conserved serine/threonine kinases: Gsk-3β and cdk5 mediate the repulsive responses to Sema3a and ephrin-A5. Gsk-3β, is an enzyme at the heart of glycogen metabolism, apoptosis, cell fate determination and neuronal differentiation signalling pathways (Doble and Woodgett, 2003), and is activated at the leading edge of neuronal growth cones in response to Sema3A (Eickholt *et al.*, 2002). Regulation of the axonal cytoskeleton by Gsk-3β is likely to be mediated by MAP1-B, a major phosphorylation substrate of Gsk-3β in growing axons (Goold *et al.*, 1999). The mechanism by which Gsk-3β activity regulates growth cone collapse is unknown, but interestingly, Gsk-3β inhibition is critical in the response to attractive cues (see below). On the other hand, cdk5, an essential kinase for neuronal migration, is activated by both Sema3A and ephrin-A5 (Cheng *et al.*, 2003; Sasaki *et al.*, 2002), and could mediate

axon repulsion by downregulating the activity of the Rac effector PAK-1 (Rashid *et al.*, 2001).

In contrast to negative cues, positive guidance cues increase the protrusive activity of growth cones, induce attractive turning, axonal outgrowth and branching. An increase in lamellar protrusion, filopodial motility and F-actin in growth cones has been observed within minutes of application of netrin-1, FGF-2 and NGF (Dent *et al.*, 2004; Lebrand *et al.*, 2004; Gibney and Zheng, 2003; Goldberg *et al.*, 2000; Gallo and Letourneau, 1998). Positive guidance cues have been found to target both actin filaments and microtubules.

Netrin 1 mediated attraction requires the activity of Gsk-3β and cdk5 to regulate mode I phosphorylation of MAP-1B (Del Rio *et al.*, 2004). Phosphorylated MAP-1B has been shown to keep actin filaments and microtubules in a dynamic state (Owen and Gordon-Weeks, 2003; Mack *et al.*, 2000; Goold *et al.*, 1999) and hence may be a key mediator of axonal outgrowth. However, the implication of Gsk-3β and cdk5 activity in axon outgrowth is contradictory with their requirement in Sema3A and ephrin-A5 induced collapse and axon retraction (Cheng *et al.*, 2003; Eickholt *et al.*, 2002; Sasaki *et al.*, 2002). These discrepancies may be explained by differences in the mechanism of Gsk-3β activation. Gsk-3β activity is downregulated by phosphorylation of serine 9, and upregulated by phosphorylation of tyrosine 279. While Sema3A activity decreases the phosphorylation of serine 9 (Eickholt *et al.*, 2002), netrin 1 regulates Gsk-3β activity by increasing the phosphorylation of both serines and tyrosines which could result in distinct cellular responses (Del Rio *et al.*, 2004). Interestingly, the NGF signalling cascade leading to axon outgrowth requires inhibition of Gsk-3β, and increases the levels of the tumour suppressor protein APC in growth cones (Zhou *et al.*, 2004). Exactly how APC contributes to axon outgrowth has not been demonstrated, but the authors propose that APC-induced microtubule stability (Zumbrunn *et al.*, 2001) and/or microtubule-APC-actin interactions (Watanabe *et al.*, 2004) favour axon elongation. Further proof of a role for Gsk-3β inhibition in axon outgrowth was found in a recent study by Yoshimura *et al.* (2005) which examines NT-3 and BDNF triggered signalling pathways in hippocampal neurons. NT-3- and BDNF-induced axon outgrowth require

inhibition of Gsk-3β and the subsequent activation of CRMP-2 to promote microtubule assembly (Yoshimura *et al.*, 2005). Together, these studies suggest that Gsk-3β mediates in the response to both attractive and repellent guidance cues, whether the mechanism of activation/inhibition, the stage of axonal development or the availability of downstream targets influence the outcome of Gsk-3β signalling remains to be determined.

Other intracellular signalling proteins mediating positive responses to guidance cues specifically target the actin cytoskeleton. Netrin 1-induced filopodia formation requires activation of PKA, which in turn activates the Ena/Vasp proteins by phosphorylation (Lebrand *et al.*, 2004). Ena/Vasp proteins promote filopodia initiation and elongation presumably by allowing further addition of monomers at the barbed end of actin filaments (Lebrand *et al.*, 2004). Again, this finding contradicts studies showing that Ena/Vasp is required for Slit induced repulsion (Bashaw *et al.*, 2000), and highlights the importance of the tight regulation of cytoskeleton associated proteins for eliciting the appropriate response to guidance cues. Rac activation by netrin mediates the formation of new filopodia (Shekarabi and Kennedy, 2002), whilst inhibition of the actin severing protein cofilin, is required to increase filopodial motility during BDNF-induced attraction (Gehler *et al.*, 2004).

An emerging theme from these *in vitro* studies is that the response to guidance cues is generally fast, within minutes of application, and transcription-independent. Changes in protein synthesis and degradation at the growth cone for example, are sufficient to mediate attractive turning by netrin 1 (Campbell and Holt, 2001). However, netrin and neurotrophin mediated axonal outgrowth have been shown to require NF-AT mediated transcription (Graef *et al.*, 2003). These results suggest that while the rapid initial response to guidance cues may be independent of transcription, subsequent aspects of the response may require new protein synthesis. Further time course experiments employing protein synthesis inhibitors and microarrays, should reveal the extent to which new gene transcription is required and which genes are activated during guidance responses. Despite the identification of many molecules downstream of guidance factors

involved in the regulation of the axonal cytoskeleton, their exact roles are unclear and often contradictory. Furthermore, research has mainly concentrated on the effects of guidance cues on the actin cytoskeleton. Only recently microtubules have been highlighted as direct targets of guidance cues. Many questions remain to be answered, especially regarding the role of microtubule dynamics in attractive and repellent responses.

1.4.6 The cytoskeleton and synaptogenesis

Synapses are asymmetric junctions between neurons that mediate the transmission of information between axons and their target cells. The presynaptic axon terminal is specialised to convert electrical signals into intercellular chemical signals via calcium dependent exocytosis of neurotransmitter filled vesicles. The postsynaptic element specialises in the reception of transmitter and the conversion of the chemical signal back into an electrical one that can be propagated through the cell. Both the pre- and post-synaptic terminals are rich in actin filaments and several studies have highlighted the importance of actin dynamics in synapse formation. For example, inhibition of actin assembly inhibits synapse formation (Zhang and Benson, 2001), and perturbation of molecules that modulate the actin cytoskeleton, such as LIMK-1, lead to synaptogenic defects (Yuste and Bonhoeffer, 2004; Meng *et al.*, 2002)

Interestingly, despite the fact that synapses become largely independent of actin dynamics for their structural preservation as they mature, actin remains enriched at both the pre- and post- synaptic sites (Zhang and Benson, 2001). Varied, and sometimes contradictory, roles have been described for actin filaments at synapses. While in some cases actin depolymerisation leads to an increase in neurotransmitter release, suggesting actin functions as a barrier and is playing an inhibitory role in vesicle mobilisation (Morales *et al.*, 2000; Wang *et al.*, 1996), in other cases actin depolymerisation causes a delay in vesicle recruitment to the active zone (Sakaba and Neher, 2003; Cole *et al.*, 2000), indicating a positive role in vesicle mobilisation. The discrepancies between these studies may be attributed to the extent of actin disruption in different preparations or to intrinsic differences between the types of synapses being examined. Alternatively,

rather than playing an active role in vesicle mobilisation, actin may serve as a scaffold for other important molecules so its disruption may result in a variable dilution of key regulatory molecules that are critical for a particular step in the vesicle cycle (Sankaranarayanan *et al.*, 2003).

In contrast, few studies have addressed the role of microtubules at synapses. However, changes in microtubule organisation and stability are an essential aspect of synapse development at the *Drosophila* NMJ (Ruiz-Canada *et al.*, 2004; Roos *et al.*, 2000). aPKC and the MAP-1B homologue, futsch, stabilise microtubule loops in synaptic boutons, and mutations lead to a decrease in the number of boutons (Ruiz-Canada *et al.*, 2004; Roos *et al.*, 2000). It has been proposed that futsch-dependent protection of microtubule integrity is required during NMJ expansion (Ruiz-Canada *et al.*, 2004). These findings suggest that the regulation of microtubule organisation and stability is important not only for growth cone motility, but also for synaptic growth and plasticity.

1.5 Wnts and the cytoskeleton

Several links between Wnt signalling and cytoskeleton rearrangements have been established in non-neuronal cells. Expression of certain Wnt proteins causes C57MG cells to elongate and become more tightly packed within their colony (Shibamoto *et al.*, 1998; Wong *et al.*, 1994). Analyses of gene expression in Wnt-transformed cells and immunocytochemistry for cytoskeleton related proteins have identified the Wnt-responsive cdc42 homolog (Wrch-1) as a key mediator of Wnt-1 signalling in the regulation of cell morphology (Tao *et al.*, 2001) and revealed a re-distribution of the actin bundling protein Villin, from perinuclear regions to the leading edge of cells, in response to Wnt3a treatment (Shibamoto *et al.*, 1998). Wnt3a also induces changes in CHO cell motility characterised by increased spreading, protrusion and migration in wound healing assays. This effect is mediated by Dvl2, RhoA and ROCK (Endo *et al.*, 2005). In *Drosophila*, Wnt4 facilitates cell movement during ovarian organogenesis through a signalling pathway involving D-Frizzled 2, Dvl and PKC (Cohen *et al.*, 2002). Wnt4 signalling results in the accumulation of the focal adhesion kinase (FAK), which

regulates focal adhesion turnover (Parsons *et al.*, 2000). The finding that Dvl itself binds actin filaments (Capelluto *et al.*, 2002; Torres and Nelson, 2000) suggests it could directly regulate cell shape and movement. However, the fact that the transition from almost complete to partial co-localisation of Dvl and actin correlates with the induction of epithelial cell fate (Torres and Nelson, 2000), and that vesicular rather than actin-bound Dvl is required for canonical Wnt signalling (Capelluto *et al.*, 2002), favours the idea that Dvl localisation may influence commitment to a particular signalling pathway rather than directly influence the cytoskeleton (like a MAP or an ABP). Interestingly, despite detection of strong β-catenin stabilisation in all those reports, the effects of Wnts on cell shape and movement appear to require non-canonical Wnt signalling.

The effects of Wnts on neuronal morphology include both axonal elongation and shortening (Kishida *et al.*, 2004; Lu *et al.*, 2004; Lucas and Salinas, 1997). However, the effects of Wnts on the axonal cytoskeleton are best characterised in Wnt7a-remodelled mossy fibres (Lucas and Salinas, 1997). Wnt7a-induced axonal shortening, thickening and increase in growth cone size requires Gsk-3β inhibition (Lucas and Salinas, 1997), which in turn causes a decrease in the levels of phosphorylated MAP-1B (Lucas *et al.*, 1998). These findings suggest that the canonical Wnt pathway, at least to the level of GSK3-β, is responsible for cytoskeletal changes in neurons (Lucas *et al.*, 1998). Further insight into the signalling pathway by which Wnts regulate the axonal cytoskeleton was gained from analyses of Dvl expressing NB2a cells, which exhibit similar morphologies to Wnt treated neurons (Ciani *et al.*, 2004). Dvl binds microtubules and can locally increase microtubule stability by inhibiting Gsk-3β (Ciani *et al.*, 2004; Krylova *et al.*, 2000). Microtubule stability is achieved through a β-catenin- and TCF-independent mechanism, hence a bifurcation in the canonical signalling pathway downstream of Gsk-3β has been proposed to regulate microtubule dynamics (Ciani *et al.*, 2004). In addition, Wnt treatment, Dvl expression or pharmacological inhibition of Gsk-3β, all cause unbundling of microtubules along axons and looping of microtubules in growth cones (Ciani *et al.*, 2004; Lucas and Salinas, 1997). How this reorganisation occurs and the proteins involved remain unknown.

The effects of Wnts on the neuronal cytoskeleton cannot be only attributed to changes in microtubules, the increase in growth cone size observed in mossy fibres and DRG neurons upon treatment with Wnt7a or Wnt3 (Krylova *et al.*, 2002; Lucas and Salinas, 1997) suggests Wnts also signal to the actin cytoskeleton. This alternative remains largely uninvestigated. Recently, Rosso *et al.* demonstrated that Dvl binds actin filaments in growth cones and activates Rac through a non-canonical signalling pathway in hippocampal neurons (Rosso *et al.*, 2005). However, it remains to be determined whether activation of Rac plays a role in Wnt-induced axonal remodelling of mossy fibres and DRGs. Ultimately, Wnt-induced axonal remodelling could result from signalling through more than one pathway. Moreover, due to the close relationship between actin and microtubule dynamics (Kalil, 2001; Brown, 1999; Dent *et al.*, 1999; Dent and Rochlin *et al.*, 1999), it is possible that Wnts regulate actin dynamics indirectly via their action on microtubules.

1.6 Aims

Little is known about the cytoskeletal changes induced by extracellular factors as axons approach their targets. The fact that Wnt-induced axonal remodelling precedes the formation of synapses offers an interesting context to investigate the changes in the cytoskeleton underlying axonal shortening, branching, growth cone enlargement and ultimately the assembly of the synaptic machinery.

The aims of this thesis were: (a) to characterise the effects of Wnts on axonal behaviour by time-lapse microscopy, (b) to examine in detail the organisation and dynamics of actin filaments and microtubules upon exposure to Wnts, and (c) to address the mechanism by which Wnts signal to the axonal cytoskeleton by examining the effects of Dvl expression, Gsk-3β inhibition and the role of transcription in Wnt-induced axonal remodelling. The localisation and levels of key cytoskeleton binding proteins, which could be potential targets of Wnt signalling, were also investigated.

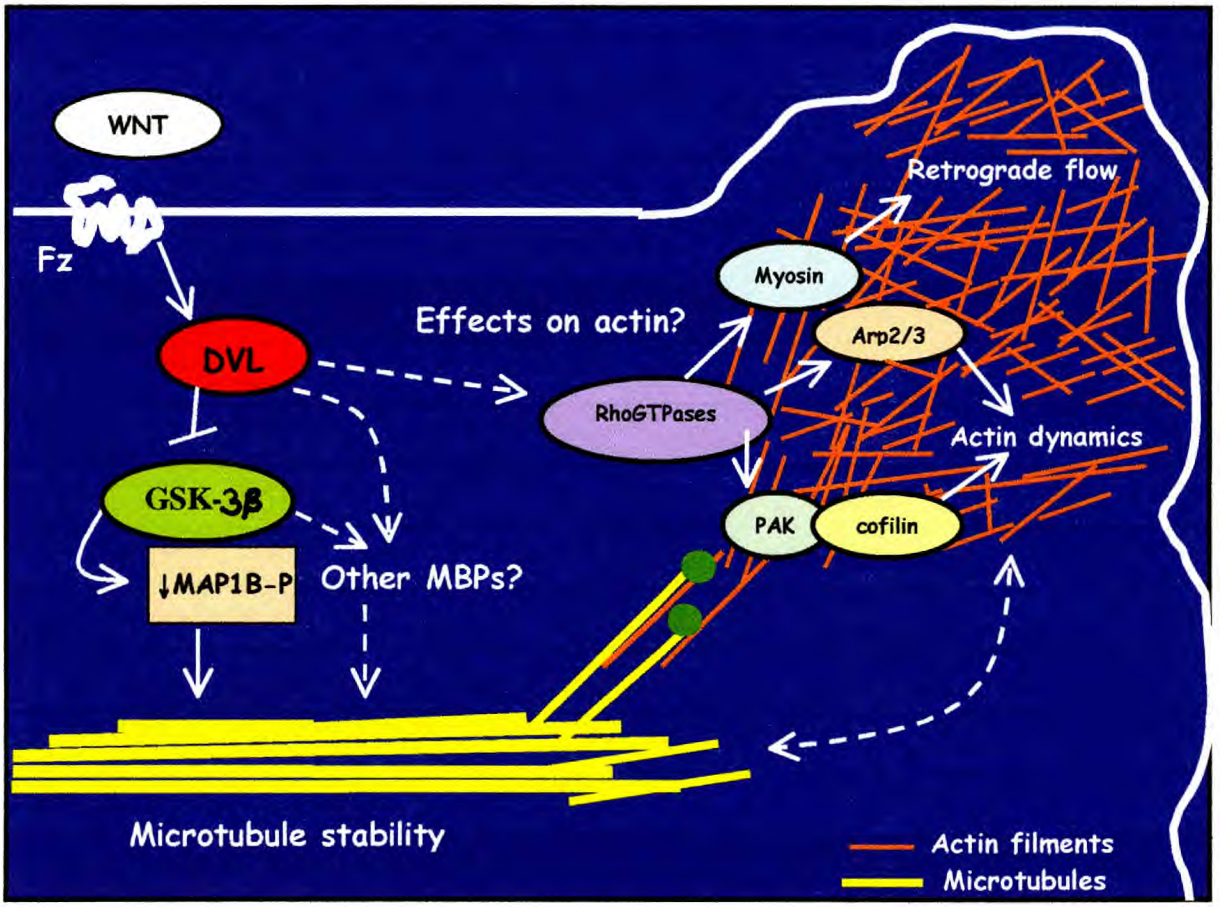


Figure 1.7. Summary of hypotheses tested in this project.
Given that Dvl has previously been shown to increase microtubule stability, we hypothesize that Wnts will also affect microtubule dynamics and possibly influence other microtubule binding proteis (MBPs). Furthermore, given the effects reported on growth cone size and Dvl's ability to activate Rho GTPases, Wnts are likely to affect the actin cytoskeleton. RhoGTPase effectors that influence actin polymerisation and depolymerisation, such as Arp2/3 and cofilin, are likely to be involved. The influence of actin filaments on microtubules and/or vice versa could also underlie Wnt-induced axonal remodelling. Links remaining to be established are represented with dashed arrows.

CHAPTER 2:

Materials and Methods

2.1 Neuronal cultures

Dorsal root ganglia (DRG) cells were the neurons of choice for analysing the effects of Wnt proteins on axonal morphology and the cytoskeleton. This was for several reasons: Wnt proteins have been shown to affect the axonal morphology of embryonic DRGs (Krylova *et al.*, 2002), they are relatively easy to dissect, they are large and extend neurites very rapidly. However, there are some disadvantages to using this type of neuron, the cultures do not give large yields and the neurons are difficult to transfect.

Culture vessels:

Neurons were plated in LabTek chamber slides (Nunc) or coverslips (13 mm or 24 mm diameter from VWR) previously coated with 100 μg/ml poly-D-lysine (PDL) (Sigma). Coating was done overnight at room temperature. The next day, coverslips were washed three times with dH_2O and air-dried inside a sterile hood. Before starting the culture, slides/coverslips were coated with 20 μg/ml laminin (Sigma), unless stated otherwise, and incubated at 37 ℃ for at least two hours.

Embryonic DRGs:

DRG cells were isolated from E 13.5 embryos according to Kleitman *et al.* (1991).

Dissection:

The pregnant mouse was killed using a CO_2 chamber, the uterus was removed from the abdomen and placed in a Petri dish. In the dissection hood, the embryos were released from their sac and placed in Petri dish containing DMEM/Glutamax. They were decapitated using small sharp scissors. The spinal tissue was dissected out and in a separate dish, also containing DMEM/Glutamax, the backbone was gently removed to

expose the spinal cord and DRGs. The ganglia were carefully cut off with a blade holder and the cords discarded.

Cell Harvesting:

The medium in the dish containing the ganglia was removed carefully – not to aspirate the ganglia – and replaced with 1 ml of 1% trypsin/EDTA. The ganglia were incubated with trypsin for 5 minutes at room temperature. 500 µl of Foetal calf serum (FCS) were added to neutralise the trypsin. At this point the ganglia clump together when the dish is swirled. As much medium as possible was removed, and replaced with 1 ml of serum free media (SFM). The ganglia were triturated by passing them through a 23-gauge needle 10-15 times.

Plating:

Cells were counted and plated at a density of 180 cells/mm^2 in wells of LabTek chamber slides. The SFM was supplemented with NT-3 and NGF (50 ng/ml, Alexis biochemicals). Cells were incubated in 5% CO_2 at 37 °C. Typically 8x10^4 cells are obtained per embryo.

Neonatal DRGs:

DRG cells were isolated from postnatal day zero or one day old mice. The entire procedure was carried out under sterile conditions.

Dissection:

Pups were decapitated and with fine sharp scissors, the skin was cut from neck to tail along the spinal cord. A very sharp scalpel was used to cut through muscles, especially thick in the neck region, and the backbone, enabling removal of the spinal cord with fine forceps. DRGs, round and white, are then visible on either side. Excess blood was soaked up with a small piece of tissue. With sharp fine forceps individual DRGS were plucked out and put into a centrifuge tube containing 15 ml DMEM/Glutamax kept on ice.

Cell Harvesting:

The DRGs were centrifuged in a table-top centrifuge for 5 min at 200 g, the medium was aspirated, and 500 µl of 0.25% trypsin in PBS-10% glucose were added. The reaction was stopped after 15 minutes by adding 1 ml of SFM-10% serum. The DRGs

were triturated by passing them 6-8 times through 23-, 21- and 19-gauge needles with increasing force until the cell suspension was free from discernable clumps. The suspension was spun for 10 minutes at 110 g and the trypsin-containing medium was aspirated away. The cells were resuspended in 1 ml of SFM and spun again to wash off any remaining trypsin. The medium was aspirated away, the cells were resuspended in SFM supplemented with 50 ng/ml of NGF, and counted.

Plating:

Cells were plated in 200 µl of SFM-NGF per well or coverslip (in a drop) at the required density. For overnight or longer cultures $1.5x10^4$ cells were plated per well (180 cells/mm^2) in LabTek chamber slides or $2.5x10^4$ cells per coverslip (13 mm diameter). For short-term cultures (fixed on the same day) the cell density was increased, typically $7x10^4$ cells were plated on 13 mm coverslips. If the cells were transfected with Amaxa the density was further increased to aid survival. In these cases, 10^5 cells per 13 mm coverslip were required. Cells were incubated in 5% CO_2 at 37 °C. Typical yields for P0-P1 animals are in the range of 2-2.5x 10^5 cells/pup.

2.2 Production of Wnt conditioned media

Wnt conditioned medium was obtained from Rat1B cells stably transfected with a pLNCX retroviral vector containing HA-tagged Wnt3 or Wnt7b cDNA, or from L-cells expressing either untagged Wnt3a or HA-tagged Wnt3 in a PGK expression vector. Antibiotic resistant non-Wnt expressing cells were used as controls. Both Rat1B and L-cells have been reported to secrete Wnt proteins efficiently (Shibamoto *et al.*, 1998; Kitajewski *et al.*, 1992).

Cells were grown to 70-80% confluence in 6 or 3.5 cm diameter plastic dishes (Corning). Growth media were then removed and replaced with SFM. The cells were allowed to grow for at least 16 hours further to condition the media. A 6 cm dish yields 2 ml of conditioned medium. The conditioned media were collected and centrifuged at 220 g for a couple of minutes, to pellet any cells detached from the monolayers, and added immediately to the cultured neurons. Fresh conditioned media were found to have

a better effect on axonal remodelling than snap-frozen Wnt conditioned media or media concentrated using a Centriprep10 column (Amicon). The levels of Wnt protein in the media were determined by western blotting and by immunostaining the cells with an anti-HA antibody.

Purified Wnt3a was purchased from R and D Systems and used at a concentration of 50 ng/ml, which was sufficient to induce remodelling in DRGs and increase the levels of β-catenin in both DRGs and L-cells (Supplementary figure 1 and Willert *et al.*, 2003).

2.3 Molecular Biology

Due to the variable levels of Wnts obtained from the Rat1B cells, another stable Wnt3-HA secreting cell line was made. HA-tagged Wnt3, Wnt7a and Wnt7b cDNAs were inserted into PGK expression vectors, which are ideally suited for maintaining a constant low level of expression in stably transfected cells (Shibamoto *et al.*, 1998). The Wnt-HA cDNAs were cut out from pCS2 expression vectors using the restriction sites BamH1 and Nsi1, and the inserts were ligated into the PGK PBS$^-$ vector (a kind gift from Dr Brown) at the same sites. A diagram of the construct is shown in figure 2.1. Transient transfections of L-cells were carried out using the Ca^{+2} phosphate method to confirm expression of the constructs (Fig.2.2). In order to obtain stably transfected cell lines, L-cells were co-transfected with the Wnt3-HA or Wnt7a-HA PGK construct and an SV2/neomycin resistant plasmid using Lipofectamine 2000. The cells were allowed to recover for 1 day before the antibiotic selection started. After 10 days, over 150 colonies were picked from each co-transfection and grown. The 5 best Wnt expressing clones were kept along with some antibiotic resistant non-expressors as controls. Western blot analysis confirmed the presence of Wnt in the conditioned media and an increase in β-catenin levels in L-cells exposed to it (see Chapter 3, Fig.3.7 B).

2.4 Cell transfection methods

Cell lines:

Calcium Phosphate transfection method:

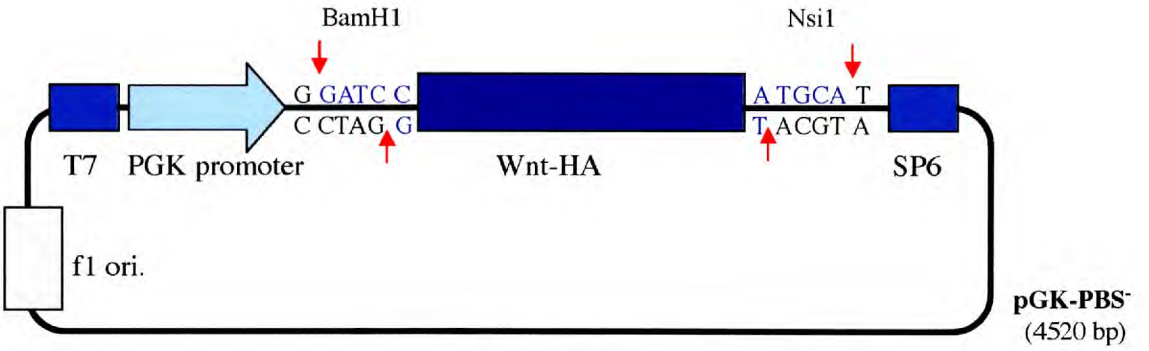


Figure 2.1. Diagram of the PGK expression vector containing HA-tagged Wnt used to make new Wnt secreting cells lines.

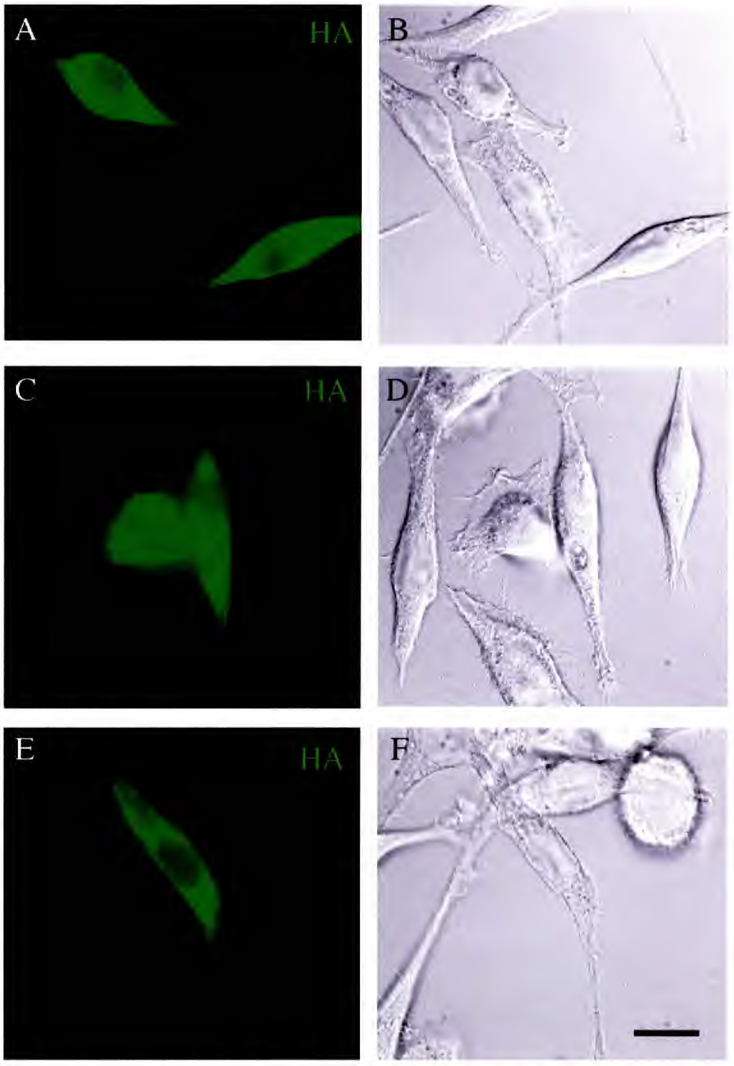


Figure 2.2. Expression of HA-tagged Wnts in L-cells.
A, C and E show transiently transfected L-cells expressing HA-tagged Wnt3a, Wnt7a and Wnt7B respectively. B, D and F are DIC images of the field. Bar, 8μm.

$6x10^5$ cells were plated in a 6 cm dishes the day before transfection. 10 μg of DNA were diluted in 225 μl of dH_2O, and 25 μl of 2.5 M $CaCl_2$ were added dropwise while vortexing gently. The mixture was then added dropwise to a small bijou containing 2 x N,N-bis(2hydroxyethyl)-2-amonoethane sulfonic acid and buffered saline (BBS) and vortexed gently. After leaving the solution at room temperature for 30-60 minutes it was added dropwise to the dish of cells, swirled gently and put back in the incubator. The medium was changed the following day and the cells were allowed to recover for at least 5 hours.

Neurons:

DRG neurons were transfected by electroporation with the mouse neuron nucleofector kit from Amaxa Biosystems. As the transfection takes place while the cells are in suspension, before plating, it is possible to examine the effects of the constructs as neurites are actively extending. Expression was usually detected after 5-6 hours. The protocol was adapted from the manufacturer's instructions for transfecting mouse hippocampal neurons. Dissociated DRGs were centrifuged at 110 g for 5 minutes and resuspended in 100 μl of mouse nucleofector solution. 5 to 10 μgr of DNA were added and mixed with the cell suspension by carefully pipetting up and down. The samples were transferred to an Amaxa cuvette and put into the nucleofector machine. Best efficiency of transfection was achieved using programme 0-05. Once the programme finished, the cells were rapidly added to the desired volume of pre-warmed culture medium and plated at high density to maximise survival. The medium was replaced with fresh medium after 2 hours to remove cellular debris. Using this method, DRG neurons were transfected with Dvl1-HA, EB3-GFP, β-actin-GFP, and GFP alone with an efficiency of ranging between 3 and 15%.

2.5 Western blots

Western blots were performed to determine the amount of Wnt in the conditioned media, or to analyse changes in the levels of proteins such as β-catenin, tubulin or Rac in cells exposed to Wnts. Cells were lysed in 100-50 μl of Laemmli sample buffer, scraped, put in an eppendorf tube and boiled in a heatblock (100 °C) for 3 minutes. To

ensure equal loading of proteins, the total protein levels in the samples were determined using Bio-Rad DC protein assay following the manufacturer's instructions. Up to 40 µl of sample was run on SDS-PAGE (12% or 15% acrylamide) 2 hours at 125 V and transferred to a nitrocellulose membrane (Hybond C, Amersham) overnight at 22 V. Membranes were probed with primary antibodies diluted in 5% milk TBST for an hour at room temperature or overnight at 4 °C. Anti-rabbit or anti-mouse Ig-horseradish-peroxidase (Roche) and chemiluminescence (ECL) solution (Amersham) were used for protein detection. Blots were quantified by measuring the mean density of the bands in NIH image 1.62.

2.6 Drug treatments

To inhibit Gsk-3β, lithium and 6-bromoindirubin (BIO) were used. 1 M LiCl and NaCl stocks were freshly prepared in SFM and diluted to 10-20 mM. BIO (Calbiochem) or DMSO control was used at 1 µM. Drugs were added to the cultures for 2-24 hours prior to fixation. To depolymerise microtubules, nocodazole was added 2-3 hours before fixation. 30 mM stocks of nocodazole solubilized in DMSO were further diluted to 0.1-10 µM in SFM. Actin depolymerising drugs were added to DRG cultures 2-30 minutes prior to fixation, or for 20 minutes prior to the addition of Wnt (recovery experiments). 20 mM stocks of cytochalasin D solubilised in DMSO were used at concentrations ranging from 40 nM to 5 µM. 2.5 mM stocks of latrunculin B solubilised in DMSO were used at concentrations ranging between 100 nM and 5 µM. Actinomycin D was used at 10 µg/ml and was added to the neurons 30 minutes before the Wnt treatment. The protein synthesis inhibitors: anisomycin and cyclohexamide were solubilized in DMSO or ethanol and used at 20 µM and 25 µM respectively. They were added 30 minutes before the Wnt treatment. The myosin inhibitors 2,3-butanedione monoxime (BDM) (Calbiochem) and blebbistatin were solubilized in DMSO and used at 5 mM and 50 µM respectively. Unless stated otherwise, all drugs were purchased from Sigma.

2.7 Immunohistochemistry

Fixation

Primary neuron cultures were fixed with paraformaldehyde (PFA) at room temperature for 25 minutes, or with methanol (-20 °C) for 4 minutes. Depending on the antibodies used, 4% PFA was supplemented with 4% sucrose or detergent. The medium in which the cells were growing was slowly aspirated and the fixative was added very gently to minimise the disruption of the cell morphology. Simultaneous fixation and extraction was carried out following the extraction protocol by Paglini *et al.* (1998). Briefly, cells were incubated for 30 seconds with extraction buffer and 0.02% saponin at 37 °C. Washed once in extraction buffer and fixed with 2% PFA/0.25% gluteraldehyde in extraction buffer for 1 hour. The coverslips were then washed with PBS/0.1 M glycine.

Permeabilisation

After fixation, cells were permeabilised with 0.05% triton in PBS for 3-5 minutes.

Staining

Samples were blocked for 1 hour in PBS-1% BSA. Primary antibodies diluted in the BSA solution were added for 1 hour at room temperature or left overnight at 4 °C. The cells were washed 3 times with PBS over 20-30 minutes. Incubations with fluorescent secondary antibodies (Vector lab or Molecular Probes) were carried out for 1 hour at room temperature in the dark. The cells were washed again 3 times in PBS. Fluorescently conjugated phalloidin (Molecular Probes), a toxin from the deadly *Amanita phalloides* mushroom which binds to F- actin, was diluted in PBS to a final concentration of 66 nM, and added after staining with secondary antibodies for 45 minutes. After the final wash, the coverslips were mounted using a small drop of the anti-fading agent Fluoromount G (Sigma). It is important to press the coverslips down with a tissue to blot out excess mountant, and to allow it to harden. Slides were stored at –20 °C for optimal preservation of the fluorescence.

2.8 Fixation for EM

Cultured neurons were prepared for observation by electron microscopy (EM) following the protocol by Svitkina and Borisy (1995) with the modifications described in Strasser *et al.* (2004). Briefly, cells were washed in PBS and subsequently incubated in extraction solution for 4.5 minutes. The cells were rinsed in cytoskeleton buffer three times and immediately fixed with 2% gluteraldehyde/1% sucrose in 0.1 M Na cacodylate, pH 7.3, for 25 minutes at room temperature. Without washing, the gluteraldehyde was removed and 0.1% aqueous tannic acid was added for 20 minutes. The specimens were rinsed with dH_2O and incubated for 20 minutes in 0.2% uranyl acetate in dH_2O. Mark Turmaine at the EM facility prepared the cytoskeleton for metal coating, by critical point drying with graded ethanols, and made platinum replicas, which were examined on a JEOL1010 electron microscope.

2.9 Imaging and data analyses

Pictures of fixed cultures were taken with a Hamamatsu Orca ER CCD camera on a BX60 Olympus upright microscope or on an Axiovert Zeiss 200. Exposure was controlled by Metamorph software. Pictures were also analysed with this software or NIH 1.62 image programme (available at http://rsb.info.nih.gov/nif-image). Growth cones and axons were traced manually. In DRGs the longest neurite of each cell was considered to be the axon and only growth cones at the end of axons or branches (>20 μm long, containing tyrosinated microtubules) were included in the analyses. Data was logged in to Excel for statistical analysis. Fluorescence intensity was measured in pictures taken with the same exposure time. Exposure time was kept to a minimum to avoid bleaching and saturation. When required, fluorescence thresholds were set per experiment to quantify differences between conditions. In the case of F-actin, the threshold included most of the fine filopodia in control growth cones. When more stringent thresholds were required as in the cytochalasin recovery experiments the threshold was set to include all the staining that remained after treatment with the drug alone, i.e. before starting the recovery in either control or Wnt medium. To quantify the filopodia velocity or EB3 velocity from time-lapse movies the track point or track object function of the Metamorph software were used respectively.

2.10 Time-lapse

Time-lapse experiments were set up on an inverted Axiovert Zeiss 200 microscope with a heated stage and CO_2 chamber. To optimise the stability of the stage and the maintenance of focus, the temperature was switched on at least 4 hours prior to recording. The camera and shutters were controlled by Metamorph software. Growth cones at the end of the longest neurite were recorded. For long term recordings (2-9 hours) frames were captured every 2 minutes. For short recordings, to analyse changes in length of filopodia or EB3 movements frames were taken every 20 and 3 seconds respectively, and over the course of 2 to 3 minutes.

2.11 Antibodies

Primary Antibodies	**Epitope**	**Species**	**Source**	**Dilution**
Acetylated tubulin	Acetylated tubulin	Mouse	Sigma	1:3000
Ac-15	β-actin	Mouse	Sigma	1:2000
APC	APC	Rabbit	Inke Nathke	1:500
β-catenin	β-catenin	Mouse	Affinity	1:500
Dvl1	Dvl1	Rabbit	Upstate	1:500
EB1	EB1	Mouse	BD transduction laboratories	1:100
3F10	HA-tag	Rat	Roche	1:500
GAP-43	Growth associated protein-43	Rabbit	Abcam	1:1000
GFP	GFP	Rabbit	Molecular probes	1:5000
Gsk-3β	Glycogen synthase kinase 3β	Mouse	Transduction Laboratories	1:2000

MAP-1B	MAP-1B phosphorylation independent	Rabbit	Dr Ulloa	1:200
MAP-2	MAP-2 a+b	Mouse	Sigma	1:200
PK-18	Phosphorylated PAK (Thr 212)	Mouse	Sigma	1:500
P34-Arc	p-34-Arc, subunit of the Arp2/3 complex	Rabbit	Upstate	1:100
Rac 1	Rac 1	Rabbit	Santa Cruz	1:200
RT97	Neurofilament	Mouse	B. Andersen	1:80
Y1/2	Tyrosinated tubulin	Rat	Oxford Biotechnology	1:200
32-A	Myosin V	Rabbit	R. Cheney	1:50

Secondary Antibodies	**Conjugate**	**Source**	**Dilution**
Phalloidin	Texas Red	Molecular probes	1:100
Goat Anti Rabbit IgG (H+L)	Alexa 488	Molecular probes	1:600
Donkey Anti Rabbit IgG (H+L)	Alexa 594	Molecular probes	1:600
Donkey Anti Rat IgG (H+L)	Alexa 488	Molecular probes	1:600
Donkey Anti Rat IgG (H+L)	Alexa 594	Molecular probes	1:600
Goat Anti Rat IgG (H+L)	Alexa 350	Molecular probes	1:600
Donkey Anti Mouse IgG (H+L)	Alexa 488	Molecular probes	1:600
Donkey Anti Mouse IgG (H+L)	Alexa 594	Molecular probes	1:600
Donkey Anti Rabbit IgG	HRP	Amersham	1:2000
Sheep Anti Mouse IgG	HRP	Amersham	1:2000

2.12 Solutions

Serum free medium- SFM

Was prepared from a BME Stock solution

BME

	100 ml	50 ml
dH_2O	86 ml	43 ml

Earle's Basal Salt Solution (Gibco)	10 ml	5 ml
BME amino acids (Sigma)	1 ml	0.5 ml
BME vitamins (ICN biomedicals)	1 ml	0.5 ml
1 M $NaHCO_3$	2 ml	1 ml

Serum Free Medium (SFM)

	25 ml	50 ml
BSA (Sigma bovine albumin faction V)	250 mg	500 mg
BME stock (final 1.4 mg/ml HCO_3= 16.7 mM)	23.25 ml	46.5 ml
Glucose 10% (in H_2O)	1.2 ml	2.4 ml
Serum free supplement, Sigma I-1884 (ITS)	0.25 ml	0.5 ml
Penicillin/Streptomycin (final 20 units/ml)	0.1 ml	0.2 ml
L-Glutamine (final 0.29 mg/ml= 2 mM)	0.25 ml	0.5 ml

The solution was gently vortexed until the BSA dissolved, pHed to 7.4, with 1 N NaOH (160 µl per 25 ml of SFM) and filter sterilised.

BBS transfection buffer

50 mM B.E.S. (nn bis 2-(hydroxyethyl)-2-aminoethane sulphonic acid)

280 mM NaCl

1.5 mM Na_2HPO_4, pH to 6.95

Rat 1B media

	50 ml
DMEM-Glutamax	44.5 ml
10% foetal calf serum (FCS)	5 ml
Penicillin/Streptomycin (final 20 units/ml)	500 µl
Geneticin- G418 sulfate (200 mg/ml stock)	80 µl

L-cell media

	50 ml

F12	22.5 ml
DMEM	22.5 ml
10% FCS	5 ml
Penicillin/Streptomycin (final 20 units/ml)	500 µl
Geneticin- G418 sulfate (200 mg/ml stock)	80 µl

4% PFA/4% sucrose

20 ml of H_2O were heated to 60 °C, 2 gr of PFA and 200 µl of 0.1 M NaOH were added. Once dissolved, 2 gr of sucrose and 25 ml of 2xPBS were added. The pH was tested, normally already 7.4, and the volume made up to 50 ml with dH_2O. The solution was filter sterilised and was kept at 4 °C for up to 4 days.

Extraction buffer for immunofluorescence

PIPES 40 mM pH 6.8, $MgCl_2$ 0.5 mM, EGTA 0.5 mM and 15% glycerol

Western Blotting solutions

Gel casting:

<u>10% resolving gel</u> (makes enough for two 0.5 mm mini-gels):

3.3 ml 30% acrylamide

2.5 ml 1.5 M Tris pH 6.8

0.1 ml 10% sodium dodecyl sulphate (SDS)

make up to 10 ml with dH_2O

Just before pouring:

100 µl of fresh ammonium persulfate (APS)

7 µl TEMED

Gel polymerizes in approximately 20 minutes, H_2O was added to the gel before it set to level the surface.

<u>Stacking gel</u>

670 µl 30% acrylamide

1 ml 0.5 M Tris pH 6.8

40 µl 10% SDS

make up to 4 ml dH_2O

when ready to pour add:

40 µl APS

4 µl TEMED

Comb was inserted and the gel polymerised as above.

TBS (Tris Buffered Saline)

10 ml 1 M Tris pH 7.5

30 ml 5 M NaCl

made up to 1 litre with dH_2O

TBST (TBS with 0.1% Tween)

1 ml Tween 20 per litre TBS

1x Cell Lysis Buffer (100 ml)

10 ml 20% SDS (2%)

10 ml glycerol (10%)

16 ml 0.5M Tris pH6.8 (80 mM)

64 ml dH_2O.

Add fresh to 1 ml: 9 µl β-mercaptoethanol

10 µl 2% bromophenol blue

Phosphate buffered saline- PBS

1 litre of 10x PBS

NaCl	80 gr
KCl	2 gr
KH_2PO_4 (anhydrous)	2 gr
Na_2HPO_4 (anhydrous)	11.5 gr

pH a 1x solution to 7.5

Cytoskeleton buffer for EM- PEM buffer:

100 mM PIPES

1 mM $MgCl_2$

1 mM EGTA

supplemented with 1 μM phalloidin, 1 μM taxol and 1% sucrose.

Extraction solution for EM

1% Triton

4% polyetheleneglycol (40,000 mw)

10 μM phalloidin

10 μM taxol

0.2% gluteraldehyde

4.2% sucrose

in PEM buffer

CHAPTER 3:

Wnts affect the morphology and axonal behaviour of embryonic and neonatal DRGs.

3.1 Introduction

Wnt genes are expressed in overlapping yet unique patterns in the developing vertebrate nervous system. Their spatial and temporal patterns of expression suggest that Wnt proteins may play a role not only in the initial induction and early patterning of the nervous system but also at later stages of development, during axon guidance and synapse formation (Rosso *et al.*, 2005; Krylova *et al.*, 2002; Lucas and Salinas, 1997; Parr *et al.*, 1993). Indeed, Wnt4 and DWnt5 are involved commissural axon guidance (Lyuksyutova *et al.*, 2003; Yoshikawa *et al.*, 2003), while Wnt7a and Wnt3 have been shown to play a role in the formation of synapses in the cerebellum and spinal cord, respectively (Krylova *et al.*, 2002; Hall *et al.*, 2000; Lucas and Salinas, 1997).

The expression of Wnt genes in the murine spinal cord has been mainly characterised at early stages of development (Parr *et al.*, 1993). At E9, spinal cord neurons are born and very little differentiation of distinct cell types has occurred. At this stage Wnt1, Wnt3 and Wnt3a are expressed dorsally in the roof plate, while Wnt5a, Wnt7a and Wnt7b are expressed in more ventral areas. Wnt4 is the only Wnt expressed in the floor plate, though it is also expressed in dorsal domains. Parr and colleagues suggest that at this stage Wnts could be playing a role in the expansion of precursor cell populations and/or helping to establish the positional identity of spinal neurons. Indeed, it was later shown that in the absence of Wnt1 and Wnt3a there is a marked reduction in neural crest derivatives in both the hindbrain and spinal cord (Ikeya *et al.*, 1997) implying an important role for Wnts as mitogens or survival factors in the regulation of cell proliferation. Wnts also regulate cell fate in the spinal cord, while Wnt3a induces the expression of dorsal markers in spinal cord explants (Muroyama *et al.*, 2002), Wnt1 is able to instruct neural crest cells to acquire DRG neuron identity (Lee *et al.*, 2004).

Sensory neuron projections from the DRGs come into contact with motor neurons in the ventral part of the spinal cord at E13.5. At this stage, Wnt3 is expressed in the lateral motor columns (LMC) at limb levels (Krylova *et al.*, 2002). Upon addition of exogenous Wnt3, axons of embryonic NT-3 dependent DRGs become shorter and more branched, and growth cones become enlarged. A similar effect is observed upon exposure to conditioned media from cervical and lumbar ventral spinal cord explants, and is blocked by the Wnt antagonist sFRP-1. Together, these results suggest that Wnt3 from motor neurons functions in a retrograde manner to regulate growth and branching of their presynaptic partners: NT-3 dependent DRG cells (Krylova *et al.*, 2002). In addition to inducing axonal remodelling, Wnt3 is able to increase synapsin I clustering, further supporting a role for Wnt3 in the formation of sensory-motor neuron connections in the spinal cord. Since other Wnts, such as Wnt11 and Wnt6, are expressed in discrete domains of the mouse spinal cord at E13.5 (Henriquez and Salinas, unpublished observations), the possibility that other Wnts are mediating the formation of functional spinal connections cannot be ruled out.

In order to study the effects of Wnts on the axonal cytoskeleton in detail, it was necessary to set up an *in vitro* system that would allow the examination of the sequence of events leading to Wnt-induced axonal remodelling. This chapter focuses on the effect of different Wnts and culture conditions on the morphology of neonatal and embryonic DRGs. The most robust and reproducible results on axonal remodelling were obtained with purified Wnt3a. Analyses of both fixed and live DRG neurons, by time-lapse microscopy, show that Wnt3a induces a significant increase in growth cone size, decrease in axon length and increase in branching within 2 hours of application compared to controls.

3.2 Results

3.2.1 Wnt3 induces axonal remodelling of embryonic and neonatal DRGs.

Wnt3 has previously been shown to induce axonal remodelling in embryonic (E 13.5) NT-3-responsive DRG cells. This axonal remodelling is characterised by a decrease in axon length, but an increase in growth cone size and branching (Krylova *et al.*, 2002). To determine whether Wnt3 induces similar remodelling in neonatal DRG cultures, Wnt3 conditioned medium from Rat1B cells was added to embryonic and neonatal DRG cells 2 hours after plating, and cultured for 22 hours. The axonal morphology was examined by staining for GAP-43, a protein present in actively growing neuronal processes (Goslin *et al.*, 1990).

Wnt3 has a similar effect on a subset of embryonic and neonatal DRGs. Wnt3 leads to an increase in growth cone size and branching, but reduces axon length in both embryonic and neonatal DRGs when compared to cells exposed to control conditioned media (Fig.3.1 A-D). Quantification of the effect of Wnt3 on neonatal DRGs shows that Wnt3 induces a 51% increase in growth cone area (control: 25.25 ± 0.82 μm^2, Wnt3: 38.13 ± 1.52 μm^2. Fig.3.1 E). Distribution of growth cone sizes reveals that Wnt3 causes a shift resulting in a decrease of small growth cones and a concomitant increase in the percentage of medium and large growth cones (Fig.3.1 F). Quantification of branching revealed no change in the number of primary branches, but a significant increase the number of secondary, tertiary and quaternary order branches ($p<0.01$ for second and fourth order branches, $p<0.001$ for third order branches Fig.3.1 G). Despite increasing the number of branches, Wnt3 was found to cause a 21% decrease in axon length-measured from the axon hillock to the most distant growth cone along a given neurite (control: 182.02 ± 2.81 μm, Wnt3: 143.32 ± 4.46 μm. Fig.3.1 H). The possibility that Wnt3 is toxic to DRG neurons was discounted as cell survival was comparable to controls (data not shown).

In both embryonic and neonatal DRG cultures only a small proportion of neurons respond to Wnt3. Most of them have large cell bodies and large axon calibre, characteristic of proprioceptive neurons (Snider and Wright, 1996). Since proprioceptive neurons are NT-3 dependent, it was possible to select for this population in embryonic DRG cultures by growing the cells in the presence of NT-3 and absence of NGF. This

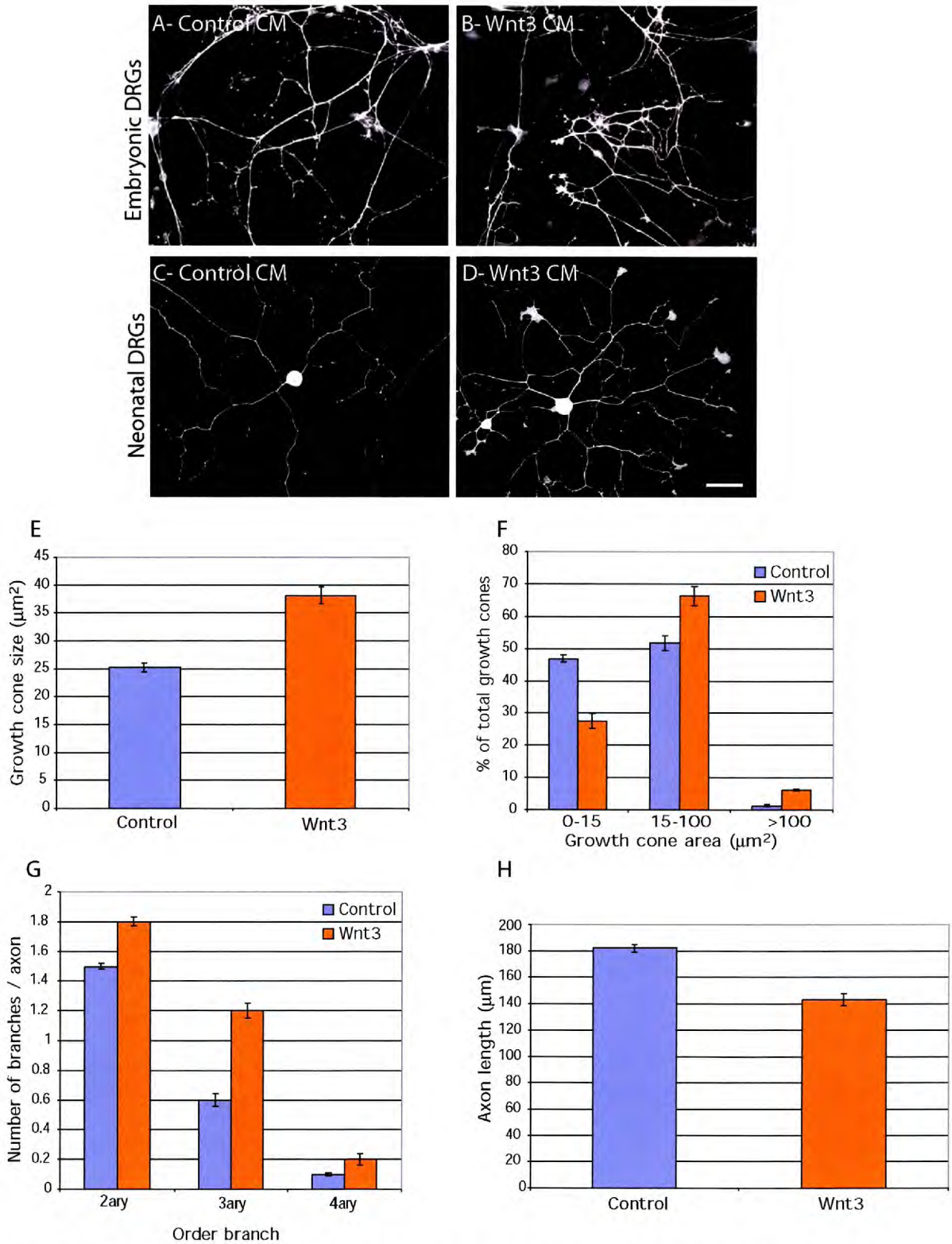


Figure 3.1. Wnt3 induces axonal remodelling in embryonic and neonatal DRG cells.
Wnt3 treated embryonic and neonatal neurons (B,D) have larger growth cones, shorter and more branched axons compared to control treated cells (A,C). Bar, 50µm. (E) Average growth cone size of neonatal DRGs exposed to Wnt3 is larger than controls ($p<0.01$). (F) Wnt3 increases the percentage of large and medium sized growth cones, while decreasing the small ones. (G) Wnt3 causes significant increases in the number of secondary, ($p<0.01$), tertiary ($p<0.001$) and quaternary branches ($p<0.01$). (H) Wnt3 treated neonatal DRGs have shorter axons than controls ($p<0.01$). Values are mean ± SEM from three different experiments (81-164 growth cones and 66-118 axons were measured in each experiment).

method of neurotrophin selection was employed to prove that indeed it is the proprioceptive neurons that respond to Wnt3 and not the thermo/nociceptive (NGF dependent) neurons (Krylova *et al.*, 2002). However, this approach cannot be used for neonatal DRGs due to the downregulation of the NT-3 receptor, TrkC, and the upregulation of the NGF receptor, Trk A, in proprioceptive neurons after E 13.5 (Snider and Wright, 1996; Mu *et al.*, 1993). As a result, in neonatal DRG cultures, both proprioceptive and thermo/nociceptive neurons survive in the presence of only NGF. To distinguish between the two populations, cells were stained with the RT97 antibody that recognises neurofilaments only present in the large diameter proprioceptive neurons (Lawson *et al.*, 1984) (Fig.3.2). This antibody labels less than 5% of small diameter neonatal DRG neurons and approximately 85% of large diameter ones. In neonatal DRG cultures, Wnt3 induces axonal remodelling in 35-45% of this population of cells. The fact that Wnt3 has a similar effect on the morphology of embryonic and neonatal DRGs, suggests that the postulated role for Wnt3 as a stop and branch signal during the formation of sensory-motor connections (Krylova *et al.*, 2002) can be recapitulated in regenerating sensory neurons *in vitro*, upon addition of exogenous Wnt3.

3.2.2 Axonal remodelling requires overnight exposure to Wnt3 conditioned medium.

In order to observe Wnt-induced changes in the cytoskeleton in real time by time-lapse microscopy, it was necessary to determine the time course of action of Wnts on axonal morphology. With this aim in mind, neonatal DRG cells were treated with conditioned media 2 hours after plating and fixed at different time points. The increase in average growth cone size was used as the main criterion for determining the activity of Wnt3. Differences in axonal morphology between control and Wnt3 treated cells were not observed before 18 hours exposure. Indeed, the average growth cone size only becomes significantly different after 18 hours exposure to Wnt3 (control: 27.58 ± 2.04 μm^2, Wnt3: 39.36 ± 3.77 μm^2. Fig.3.3). Interestingly, while the growth cone size in control treated cultures tends to decrease over time (growth cones become 28% smaller in size

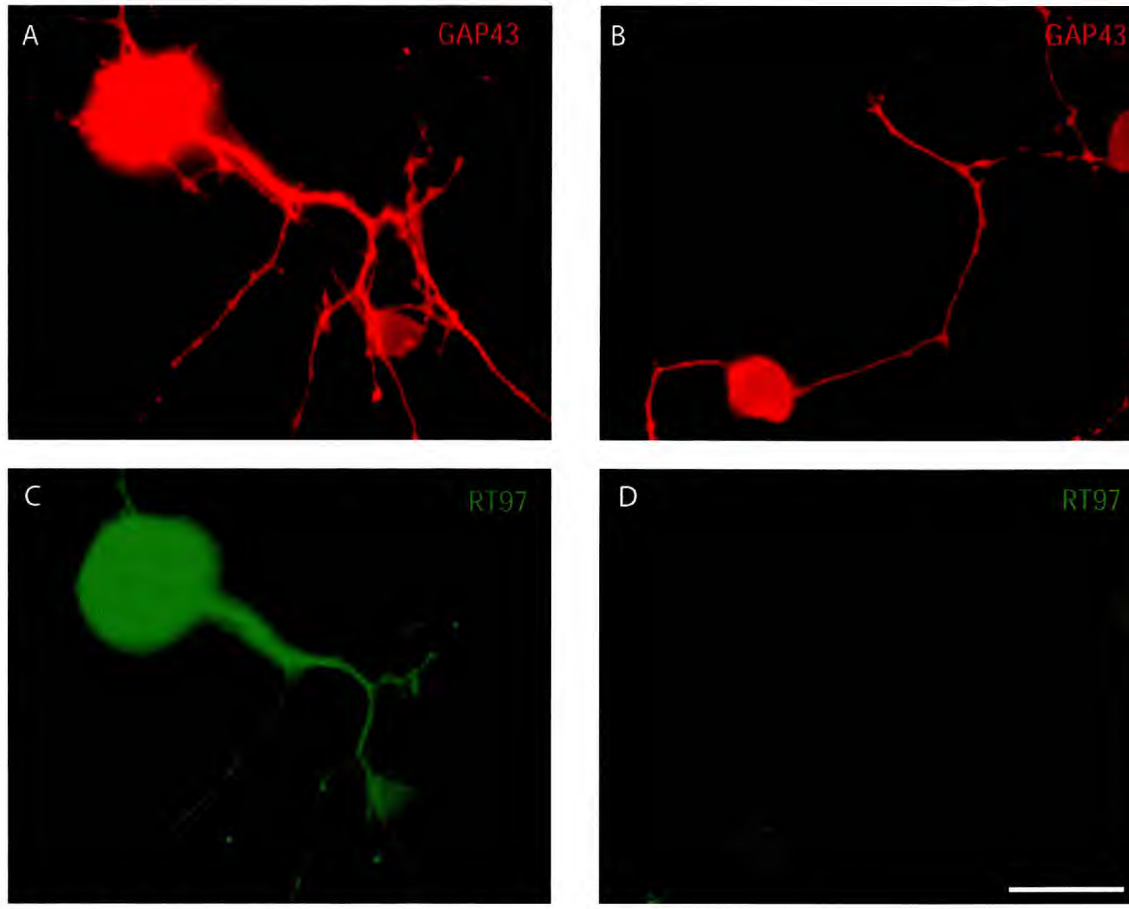


Figure 3.2. RT97 stains large caliber DRG neurons.
GAP-43 labels small and large caliber DRG neurons (A,B). RT97 only labels large caliber DRG neurons, typically the NT-3 responsive ones. Bar, 30µm.

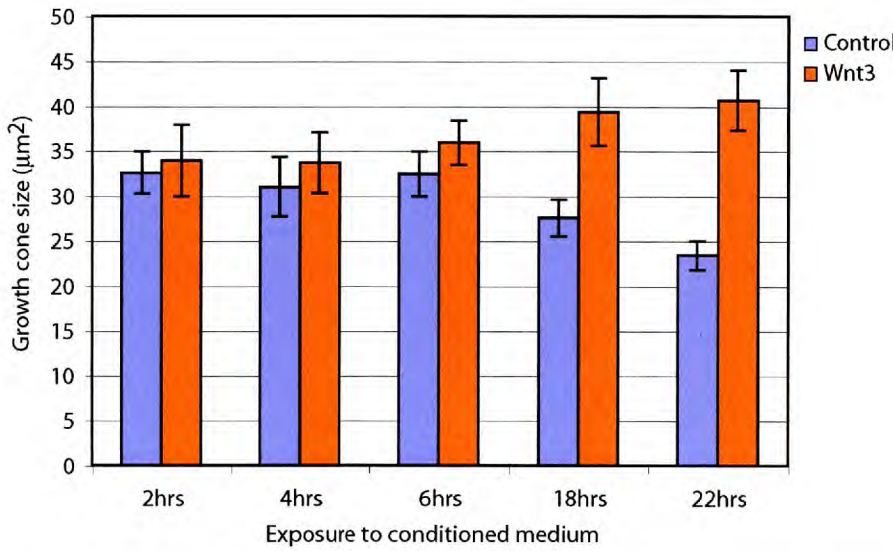


Figure 3.3. The effect of Wnt3 on growth cone size requires 18 hours exposure to conditioned medium.
Graph shows the average growth cone size after different times of exposure to control or Wnt3 conditioned medium. Values are mean ± SEM from three different experiments (at least 30 growth cones were measured in each condition). Differences in growth cone size between control and Wnt3 treated cells only become significant after 18 hours exposure ($p<0.05$, after 22 hours exposure: $p<0.01$).

between 2 and 22 hours), in Wnt3 treated cultures growth cone size increases by 20% between 2 and 22 hours.

In a number of experiments Wnt3 conditioned media did not induce significant changes in axonal morphology when compared to controls. This finding, together with the fact that most extracellular factors that elicit changes in neuronal morphology have an effect on a much shorter time scale (within minutes of application), raised various concerns about the activity of Wnt3 in the conditioned media and the presence of other factors in the conditioned media which could be masking the effect of Wnt3 on axonal remodelling.

3.2.3 The effect of Wnt3 on axonal remodelling correlates to the amount of protein in the conditioned media.

Due to the variability of the effect of Wnt3 on axonal remodelling between experiments, the amount of Wnt3 in the conditioned media was assessed by western blot and the relationship between the levels of Wnt3 in the media and the extent of axonal remodelling was examined. Quantification reveals that high levels of Wnt3 in the conditioned media induce a 50% increase in growth cone size when compared to controls. Conversely, low levels of Wnt3 in the conditioned media only induce a 20% increase in growth cone size compared to controls (Fig.3.4 A-B). The average growth cone size of DRG cells exposed to control conditioned media did not vary significantly between experiments. These results indicate that the level of Wnt3 in the conditioned media directly correlates to the Wnt3 remodelling activity and prompted the assessment of methods to increase the amount of Wnt3 in the conditioned medium.

Despite the fact all Wnt proteins contain signal peptides, required for their entry to the secretory pathway (Burrus and McMahon, 1995), they are inefficiently secreted from most cell types. Overexpression of Wnt genes has been found to result in the accumulation of misfolded protein in the endoplasmic reticulum (Kitajewski *et al.*, 1992), or in the binding of the secreted Wnt protein to the cell surface or extracellular

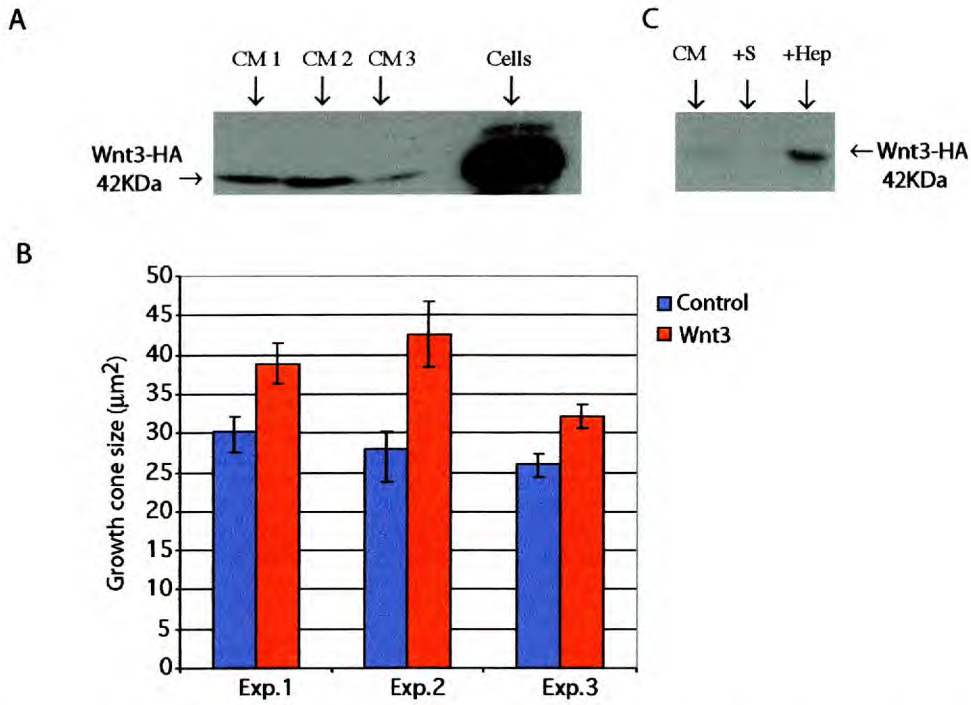


Figure 3.4. The effect of Wnt3 on growth cone size correlates with the level of protein in the conditioned media.

(A) Western blot shows the variable levels of Wnt3 in the conditioned media (CM). Wnt3 is highly expressed in the cells. (B) Average growth cone size in different experiments in which the conditioned media from the blot above were added to neonatal DRG cells. The effect is greatest in experiment 2 in which CM2 was used. (C) Addition of heparin (Hep) to the culture medium increases the levels of Wnt in the conditioned medium yet did not increase the effect on growth cone size. Addition of serum (S) did not improve Wnt3 secretion.

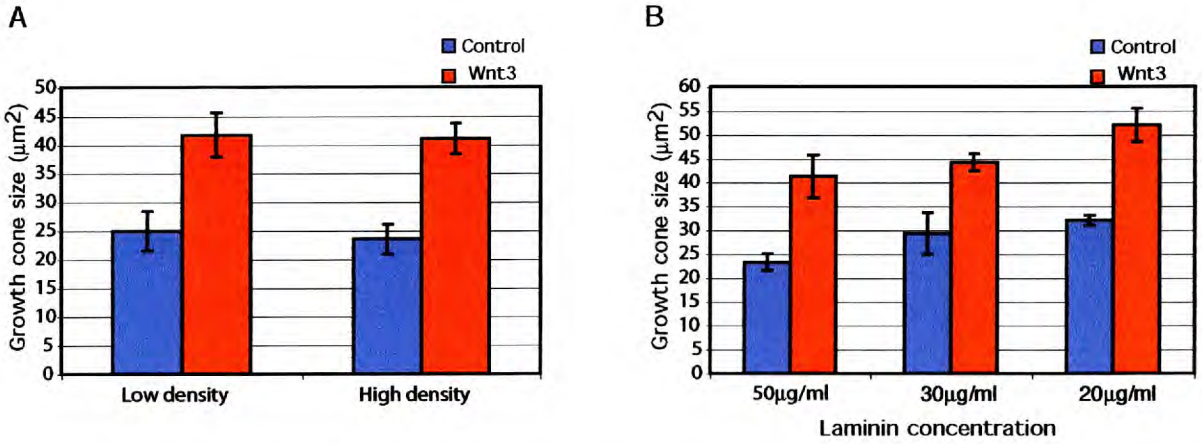


Figure 3.5. The Wnt3 mediated increase in growth cone size is not affected by cell density or laminin concentration.

(A) At both low and high cell density Wnt3 increases growth cone size significantly ($p<0.05$). (B) Wnt3 conditioned medium increases growth cone size of DRG neurons grown on both high and low concentrations of laminin (50µg/ml and 30µg/ml: $p<0.05$; 20µg/ml: $p<0.01$). Values are mean ± SEM from 3 different experiments (at least 25 growth cones were measured per condition).

matrix (ECM) yielding very little soluble protein (Bradley and Brown, 1990; Papkoff and Schryver, 1990). However, in some cell lines, Rat 2 and L-cells chiefly, up to 50% of the total Wnt protein produced is secreted (Bradley and Brown, 1995; Shibamoto *et al.*, 1998). To estimate the percentage of Wnt protein secreted by Rat1B cells expressing epitope-tagged Wnts, samples from conditioned media were analysed by SDS-PAGE and western blots. Rat1Bs were found to secrete between 20-40% of the total Wnt3 protein they produce (Fig.3.4 A).

Interestingly, addition of polyanionic compounds such as heparin to the culture medium has previously been found to increase the amount of soluble Wnt (Bradley and Brown, 1995; Burus and McMahon, 1995). It is possible that heparin competes with heparan sulfate proteoglycans found on the ECM for binding Wnts (Bradley and Brown, 1990; Papkoff and Schryver, 1990), thus effectively releasing the proteins into the medium. Alternatively, it has been proposed that heparin binding to Wnt alters the tertiary structure of the protein in such a way that it protects it from proteolysis as has been found to happen for FGF-1 and FGF-2 (Burrus and McMahon, 1995; Damon *et al.*, 1989). Addition of 50 μg/ml of heparin to the conditioned media did increase the amount of secreted Wnt3 (Fig.3.4 C) 20-fold. Unfortunately, heparin also seems to interfere with the activity of Wnt3 on DRG neurons since the Wnt3 conditioned medium containing heparin did not have remodelling activity (data not shown).

Another simple method to increase the levels of Wnt3 in the conditioned media is by supplementing the serum free culture medium, with 2% foetal calf serum (FCS) to aid Wnt expression and hence secretion. However, these experiments did not lead to an increase in the levels of Wnt3 in the conditioned media (Fig.3.4 C). Moreover, FCS induced axonal remodelling of the control growth cones to an extent that the effect of Wnt3 was no longer detected (data not shown). It should also be noted that the level of Wnt3 in the conditioned media decreases with increasing number of cell passages (cell lines were not passed more than 8-9 times) or if the cells were allowed to reach 100% confluency.

3.2.4 Cell density and laminin concentration do not alter the effect of Wnt3 on axonal remodelling.

In order to investigate whether the culture conditions were optimal for examining the effect of Wnt3 on axonal morphology, the cell density was reduced. In high-density cultures, DRG cells form complex networks in which there are many contacts between processes. If Wnts have an effect on neurons that are actively extending processes, before they reach their synaptic targets, the formation of such contacts could mask the effect of Wnt3. However, plating at 180 cells/mm^2 (low-density) compared to 300 cell/mm^2 (high-density) did not make a significant difference to the effect of Wnt3 on growth cone size after 24 hours (Fig.3.5 A). In both cases Wnt3 induces up to a 60% increase in growth cone size compared to controls. Since the density at which cells were plated did not influence the effect of Wnt3 on axonal morphology, subsequent experiments were done with low-density cultures to facilitate the analyses of the remodelling of single cells and to minimise the number of animals utilised.

Due to the importance of the adhesiveness of neurons to the substrate on which they are cultured, it was necessary to address whether the concentration of laminin used was adequate to maximise the effect of Wnts on axonal morphology. Laminin is a large ECM molecule capable of initiating and sustaining neurite extension in a wide variety of neuronal cell types *in vitro* (For review see Powell and Kleinman, 1997). An even distribution of laminin has been shown to induce multipolar neurite outgrowth in DRGs, while growth on parallel tracks of laminin alternating with non-adhesive tracks, results in a bipolar morphology (Clark *et al.*, 1993). Since coverslips were evenly coated with laminin, this could explain the loss of the typically bipolar morphology in most of the cultured DRG cells. Different substrates do not only alter neuronal growth but can also affect the response to guidance cues, for example, laminin has been shown to cause retinal axons to switch their response to netrin 1 from attraction to repulsion (Hopker *et al.*, 1999). Conversely, L1, a cell adhesion molecule of the immunoglobulin family can switch the response of cortical axons to Sema3A from repulsion to attraction (Castellani *et al.*, 2000). Furthermore, growth cones may loose their ability to respond to a

particular cue, as observed with growth cones of retinal axons which in the presence of L1 can no longer respond to EphB (Suh *et al.*, 2004). Interestingly, while growth cones of retinal ganglia neurons grown on laminin collapse upon exposure to the Wnt antagonist, sFRP, when grown on fibronectin they become spread and greatly enlarged (Rodriguez and Bovolenta, unpublished observations), further highlighting the importance of substrate adhesiveness on Wnt-induced axonal remodelling.

DRG neurons were plated on coverslips coated with 100 μg/ml of PDL and different concentrations of laminin (50, 30 and 20 μg/ml). The effects of the different laminin concentrations on the morphology of DRG neurons exposed to control or Wnt3 conditioned media were examined. The growth cone size of cells exposed to control and Wnt3 was found to increase in inverse proportion to the concentration of laminin (Fig.3.5 B). This result agrees with previous findings showing that neurons plated on PDL and low laminin concentrations have an increased adhesion and reduced motility which is reflected by slower outgrowth and an increase in the number of spread, paused growth cones (Dent *et al.*, 2004). Again, since the extent of the effect of Wnt3 did not change with different concentrations of laminin (Both with 50 and 20 μg/ml the average growth cone size increases by around 50%), all subsequent experiments were done with 20 μg/ml of laminin.

3.2.5 Several Wnts expressed in different cell lines induce axonal remodelling in neonatal and embryonic DRGs.

3.2.5.1 Rat1B cell lines

To establish whether Wnt3 was the best Wnt protein to set up time-lapse experiments with, the effect of other Wnts on axonal morphology was tested. Rat1B cells stably transfected with epitope-tagged Wnt1, Wnt6 and Wnt7b were used to produce conditioned media (expression of Wnts by these cell lines was verified with anti-HA

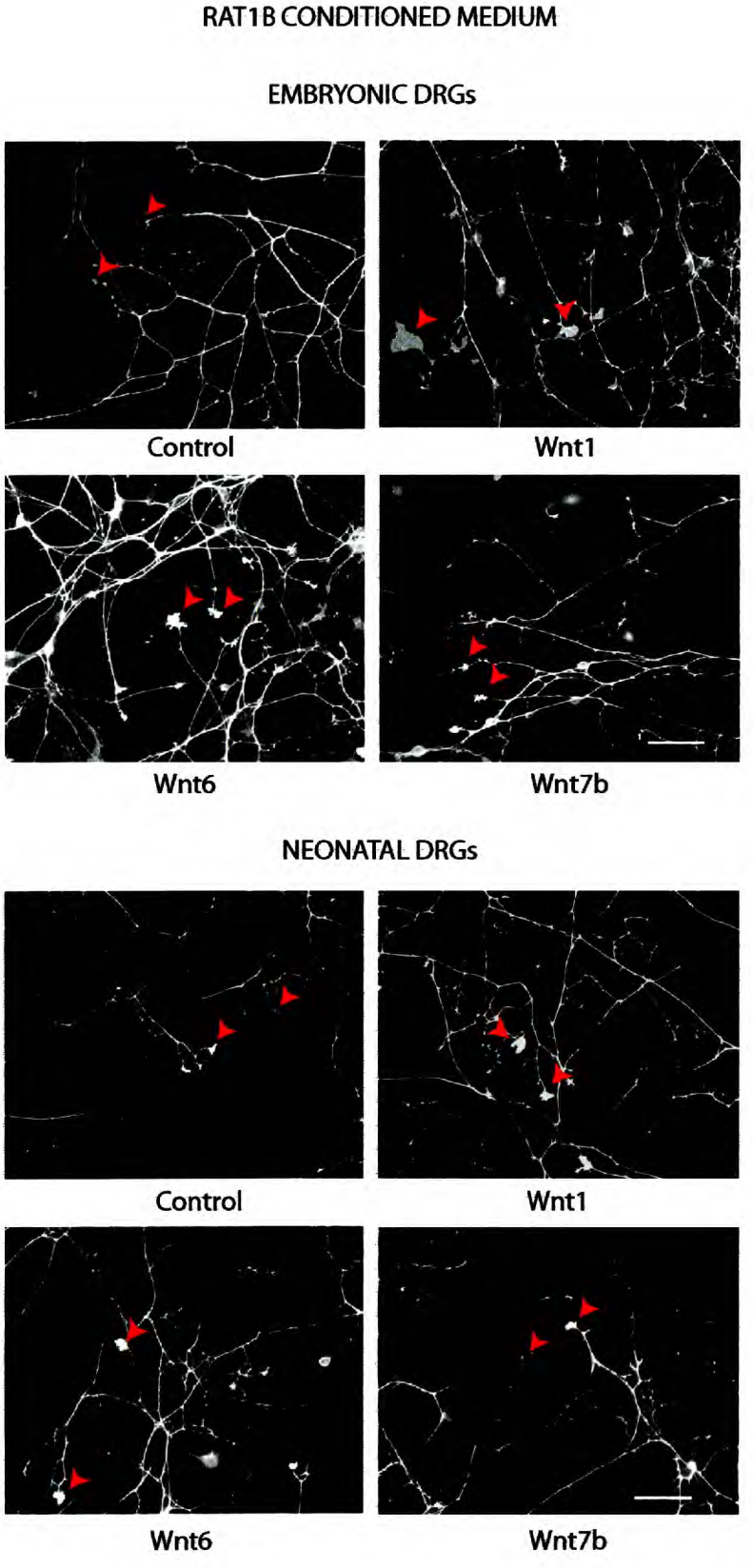


Figure 3.6. Wnt1 and Wnt6, but not Wnt7b induce axonal remodelling of embryonic and neonatal DRGs.
Both embryonic and neonatal DRG neurons exposed to Wnt1 and Wnt6 have larger growth cones (see arrowheads) and more branched axons than those exposed to control or Wnt7b conditioned media. Bar, 50μm.

antibodies). Wnt1 and Wnt6 have similar effects to Wnt3 on both embryonic and neonatal DRG cultures. Wnt6, and to a greater extent Wnt1, induce branching, growth cone spreading and axonal thickening, whereas Wnt7b, has no effect (Fig. 3.6). These results indicate that only certain Wnts are able to induce remodelling in DRG neurons. At present it is not known whether Wnt-induced remodelling is dependent on the combination of Frizzled receptors expressed by the neuron, or on the intrinsic ability of certain Wnts to induce remodelling in particular neuronal populations. Wnt7b for example, does not induce axonal remodelling in DRG neurons, yet is able to induce dendritogenesis in hippocampal neurons (Rosso *et al.*, 2005).

3.2.5.2 L-cell cell lines

Wnt conditioned media from stably transfected L-cells was also tested on the morphology of DRG neurons. L-cell fibroblasts have been shown to be very good secretors of active Wnts (Shibamoto *et al.*, 1998). To improve the levels of Wnt in the conditioned media, three new stably transfected Wnt-secreting cell lines were made with HA-tagged Wnt3, Wnt7a and Wnt7b cDNAs inserted into PGK vectors (see Materials and Methods). However, only Wnt3 was efficiently expressed and secreted.

The activity of the Wnt3 secreted by the new L-cell line was observed on the L-cells themselves (autocrine effect). Wnt3 expressing cells accumulate β-actin at their tips and are more elongated than the control cells (Fig.3.7 A, arrowheads). The fact that surrounding non-Wnt expressing cells have a similar morphology (Fig.3.7 A, arrow), suggests that Wnt3 is secreted and active as a paracrine factor. Interestingly, Wnts have been found to induce similar morphological transformations in C57MG cells. Wnt expression or addition of Wnt conditioned media causes C57MG cells become elongated and more closely packed within their colony compared with controls (Willert *et al.*, 2003; Shibamoto *et al.*, 1998; Bradley and Brown, 1995).

The activity of secreted Wnt3 was further tested by assaying its ability to stabilise β-catenin. Untransfected L-cells were exposed to control, Wnt3 or untagged Wnt3a

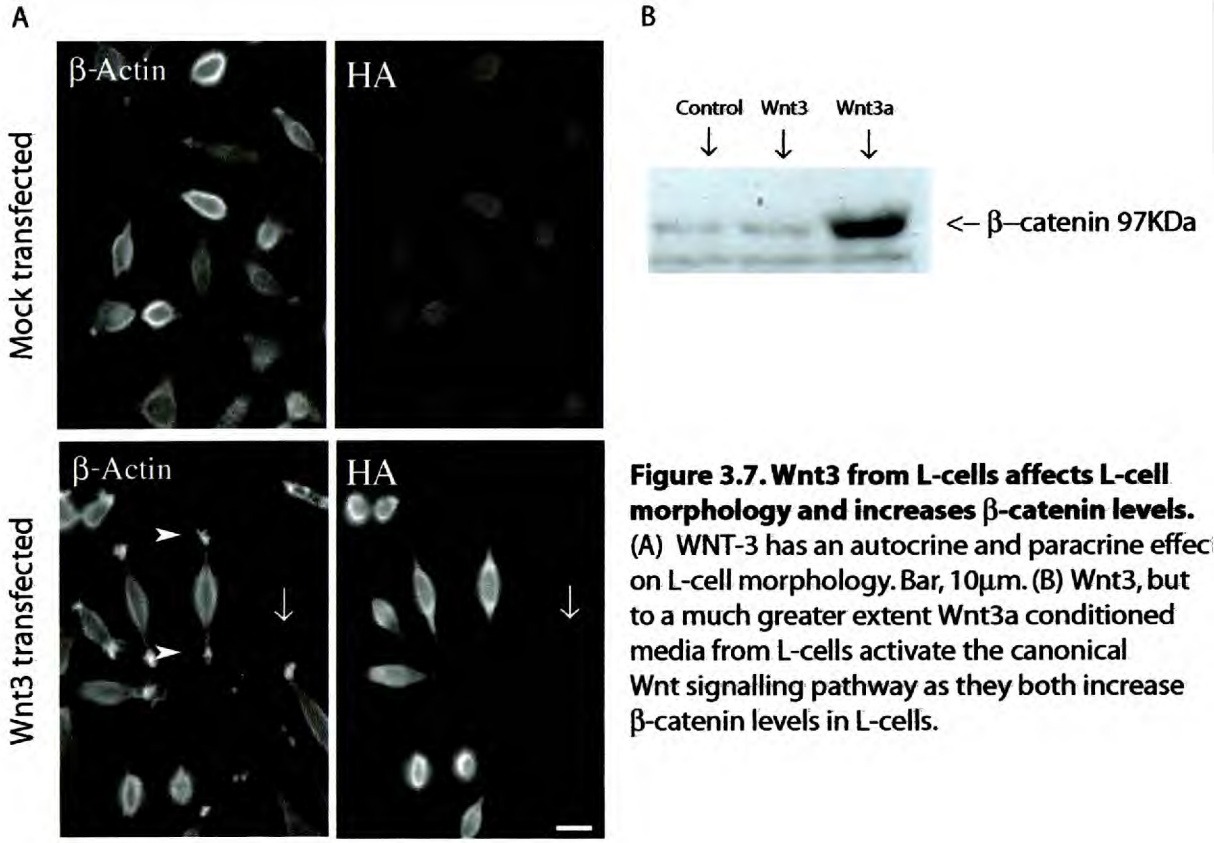


Figure 3.7. Wnt3 from L-cells affects L-cell morphology and increases β-catenin levels. (A) WNT-3 has an autocrine and paracrine effect on L-cell morphology. Bar, 10μm. (B) Wnt3, but to a much greater extent Wnt3a conditioned media from L-cells activate the canonical Wnt signalling pathway as they both increase β-catenin levels in L-cells.

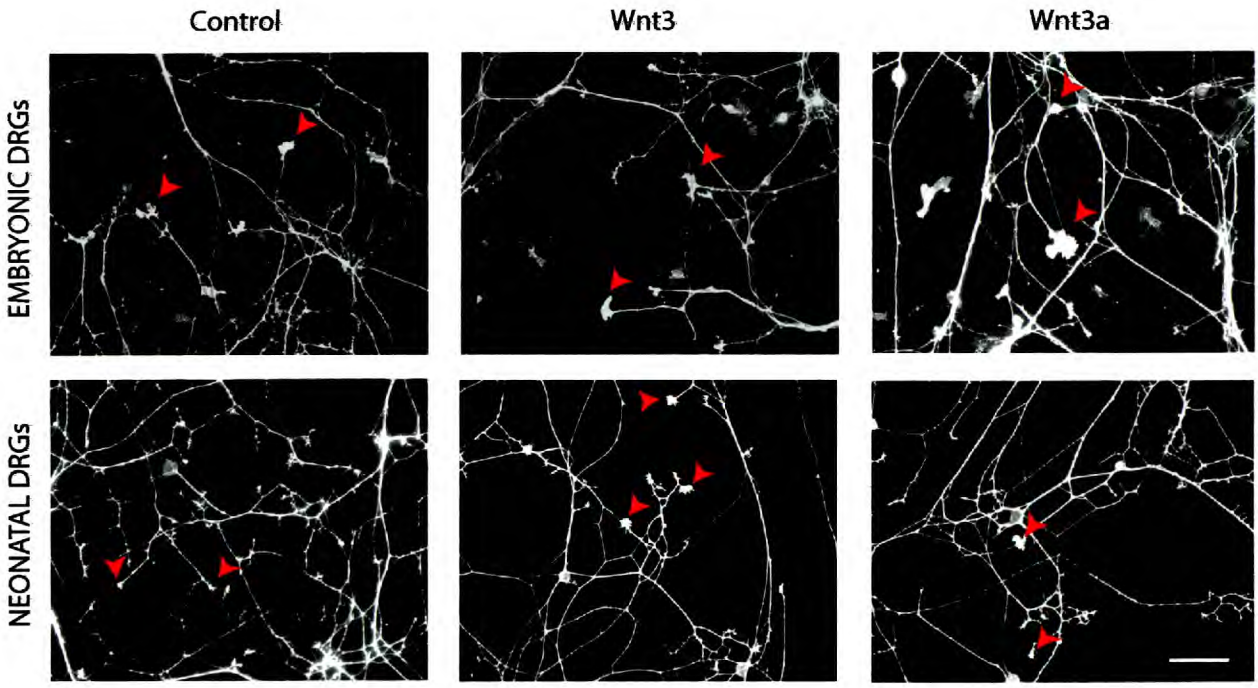


Figure 3.8. Wnt3 and Wnt3a from L-cell conditioned media induce axonal remodelling in embryonic and neonatal DRGs.
Wnt3 and Wnt3a lead to an increase in growth cone size (arrowheads). Unfortunately, L-cell conditioned media also causes some remodelling in control neurons. Bar, 50μm.

(obtained from another L-cell line, kind gift from Dr Willert) conditioned media for 4 hours and the levels of β-catenin examined by western blot (Fig.3.7 B). Wnt3, but to a much greater extent Wnt3a conditioned media, leads to an increase in β-catenin levels compared to control conditioned media. Due to the fact that Wnt3a is untagged, it was not possible to compare the amount of secreted protein in the conditioned medium, but this activity assay does raise the question of whether the HA-tag is hampering Wnt activity. Indeed, it has been recently published that the HA-tag hinders the activity of Wnt7a on the differentiation of cortical neural cells (Hirabayashi *et al.*, 2004). However, both tagged Wnt3 and untagged Wnt3a from L-cell conditioned media induce axonal remodelling in neonatal and embryonic DRG cultures (Fig.3.8). The increase in growth cone size, and branching was more apparent in the Wnt3a treated cells, possibly correlating with the higher level of Wnt activity observed in the β-catenin assay. Unfortunately, L-cell conditioned media also causes greater remodelling in control DRG cells than Rat1B conditioned media (compare controls Fig.3.6 with Fig.3.8). Control growth cones are more spread and axons are more branched, suggesting L-cells are secreting other factors able to induce changes in axonal morphology of DRGs. To further analyse the effects of Wnt3 from L-cell conditioned media on neonatal DRGs, more time course experiments were carried out. These experiments again suggest that Wnt-induced axonal remodelling requires at least overnight exposure to the conditioned medium (Fig.3.9).

Finally, to try to overcome the insolubility of Wnts and potential instability of the protein, DRGs were plated and cultured on monolayers of control or Wnt3 expressing L-cells. However, the morphology of the DRG neurons is greatly affected in both control and Wnt3 conditions. Axons are shorter and thicker and growth cones become greatly enlarged (Fig.3.10 A) masking the Wnt3 effect even after 22 hours exposure. Quantification of growth cone size revealed no significant differences between control and Wnt3 treated cells after 4 or 22 hours exposure (Fig.3.10 B). These experiments indicate that L-cells secrete, or express on their surface, proteins that are able to induce remodelling in DRGs and hence mask the effect of Wnt3.

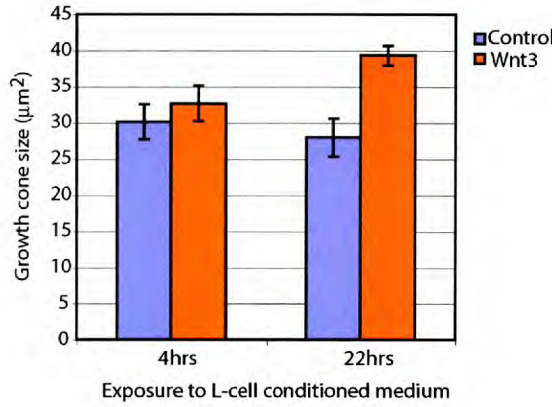


Figure 3.9. The effect of Wnt3, from L-cell conditioned medium, on growth cone size requires 22hrs exposure.
Significant differences in growth cone size between control and Wnt3 treated neonatal DRG neurons are observed after 22 hours exposure to L-cell conditioned media ($p<0.05$). Values are mean ± SEM of 3 independent experiments (at least 29 growth cones were measured per condition).

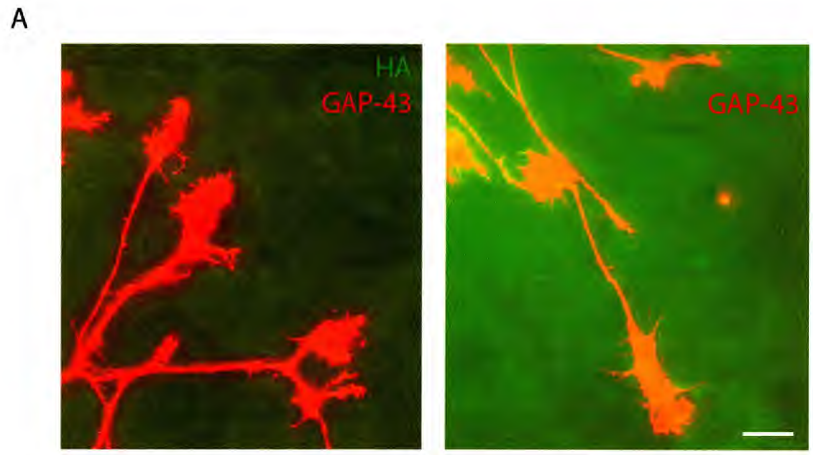


Figure 3.10. The effect of Wnt3 on axonal remodelling is not observed when DRG neurons are grown on L-cell monolayers.
(A) Neonatal DRGs grown on monolayers of control or Wnt3 expressing L-cells have greatly enlarged growth cones and shorter axons. Even after 22 hours exposure the differences in growth cone size are not significant (B). Bar, 10µm.

3.2.6 Purified Wnt3a induces axonal remodelling within 2 hours of application.

To avoid the effects of additional factors that are present in the conditioned media on axonal remodelling, purified Wnt3a was tested on neonatal DRGs. Wnt3a was successfully purified in Roel Nusse's laboratory in 2003 from L-cell conditioned media (Willert *et al.*, 2003). Purified Wnt3a was found to have a similar effect to Wnt3 and Wnt3a conditioned media on axonal remodelling on neonatal DRGs (Fig.3.11 A). Just as Wnt3, Wnt3a causes a significant increase in growth cone size when compared to controls after 22 hours exposure (control: 33.23 ± 2.01 μm^2, Wnt3a: 45.07 ± 2.51 μm^2. $p<0.05$. Fig.3.11 B). Wnt3a also induces a shift in the distribution of growth cone area by increasing the percentage of large growth cones and decreasing the percentage of small and medium ones (Fig.3.11 C). In addition, Wnt3a increases axonal branching while decreasing axon length by 21% compared to controls (control: 176.70 ± 7.9 μm, Wnt3a: 134.66 ± 10.68 μm. Fig.3.11 D-E). More interestingly, the effect of purified Wnt3a can be observed as early as 2 hours after application (Fig.3.12 A). Within 2 hours of Wnt3a addition there is 60% increase in the average growth cone size (control: 35.11 ± 1.78 μm^2, Wnt3a: 56.21 ± 2.46 μm^2) and a greater shift in growth cone size distribution than after 22 hours (over 10% of the total growth cones measured is larger than 100 μm^2, Fig.3.12 B-C). Axons become 33% shorter than controls (control: 128.38 ± 8.88 μm, Wnt3a: 85.88 ± 8.00 μm) and showed a significantly higher number of tertiary and quaternary branches than controls ($p<0.01$ and $p<0.05$ respectively. Fig.3.12 D-E). This is the first demonstration that the effect of Wnts on axonal remodelling can be observed as early as 2 hours after exposure.

To examine in more detail the effect of Wnt3a on axonal remodelling, time-lapse experiments were carried out. DRG neurons were transfected with EGFP before plating by electroporation and cultured for 4-5 hours to allow gene expression. Recordings were started 20-25 minutes prior to the addition of Wnt3a or control media and frames were taken every 2 minutes for a period of up to 9 hours after Wnt3a addition. Control axons

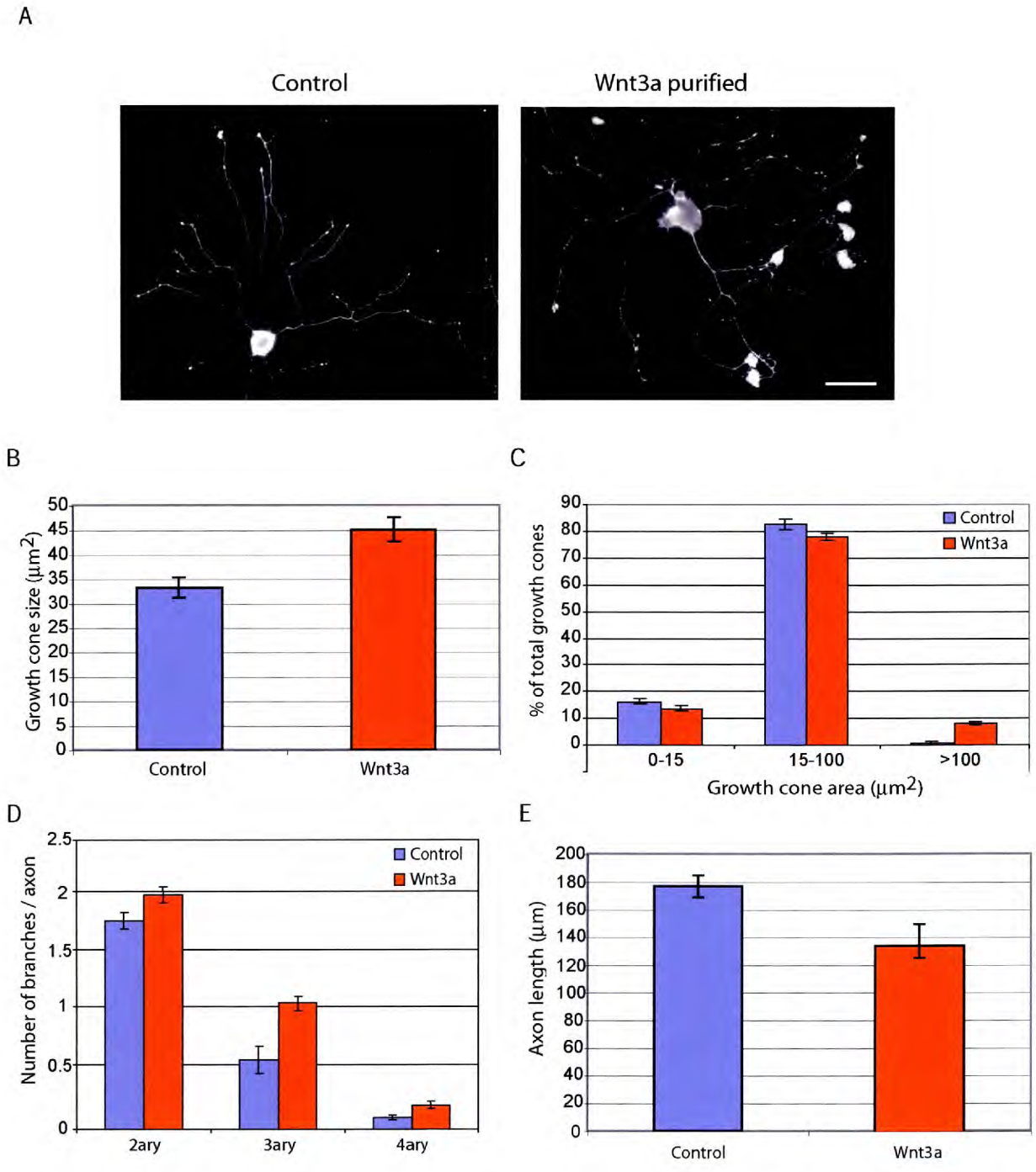


Figure 3.11. Purified Wnt3a induces axonal remodelling in neonatal DRG cells after 22 hours exposure. Wnt3a treated neonatal neurons have larger growth cones, shorter and more branched axons compared to control treated cells (A). Bar, 50µm. (B) Average growth cone size of neonatal DRGs exposed to Wnt3a is larger than controls ($p<0.05$). (C) Wnt3a increases the percentage of large growth cones, while decreasing the number of small ones. (D) Wnt3a causes significant increases in the number of secondary, ($p<0.05$), tertiary ($p<0.001$) and quaternary branches ($p<0.05$). (E) Wnt3a treated neonatal DRGs have shorter axons than controls ($p<0.05$). Values are mean ± SEM from three independent experiments (38-54 growth cones and at least 23 axons were measured in each condition, per experiment).

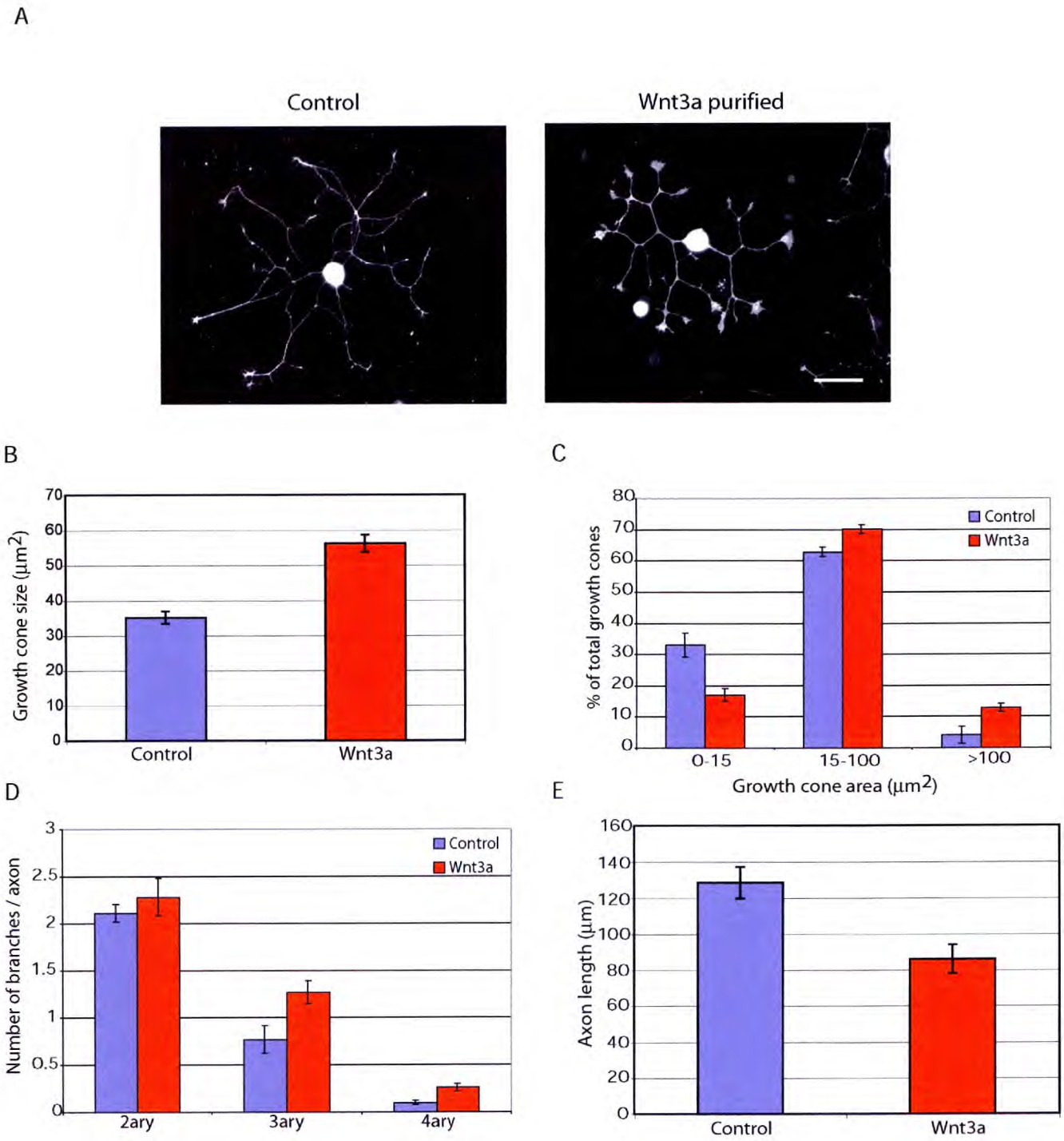


Figure 3.12. Purified Wnt3a induces axonal remodelling in neonatal DRG cells after 2 hours exposure. Wnt3a treated neonatal neurons have larger growth cones, shorter and more branched axons compared to control treated cells (A). Bar, 50µm. (B) Average growth cone size of neonatal DRGs exposed to WNT-3a is larger than controls ($p<0.01$). (C) Wnt3a increases the percentage of medium and large growth cones while decreasing the number of small growth cones. (D) Wnt3a causes significant increases in the number of tertiary ($p<0.01$) and quaternary branches ($p<0.05$). (E) Wnt3a treated neurons have shorter axons than controls ($p<0.05$). Values are mean ± SEM from three different experiments (107-217 growth cones and at least 20 axons were measured in each condition, per experiment).

recorded exhibit steady growth, few branching events and maintain or decrease their growth cone size (Fig.3.13 and see **movies chapter 3**). In contrast, axons recorded during the Wnt3a treatment advance at much slower rates, undergo branching, and exhibit a steady increase in growth cone size (Fig.3.14 and see **movies chapter 3**). In addition, far from being quiescent, Wnt3a treated growth cones exhibit an enhanced motility and membrane activity, behaving as though they were continuously sampling the environment. No differences were observed in the number of growth cones that collapse after addition of control (5/74) or Wnt3a (6/89).

Quantification reveals that Wnt3a reduces the speed of growth cone advance compared to controls. This effect takes place within the first 20 minutes of Wnt3a addition (Average rate of growth cone advance after 20 minutes of addition: control: 0.32 ± 0.1 μm/minute, Wnt3a: 0.07 ± 0.01 μm/minute. Fig.3.15 A). This effect was rarely observed in control neurons. Over time, control growth cones tend to get smaller or maintain their size whereas Wnt3a treated growth cones tend to slowly but steadily increase in size (Fig.3.15 B). After 80 minutes of exposure to Wnt3a the average growth cone size increases by 55% whereas control growth cones decrease in size by 26% on average (Fig.3.15 B). These results are consistent with short time course experiments on fixed cells (Fig.3.15 C), in which there are no significant differences in growth cone size between control and Wnt3a treated cells after 10 or 60 minutes exposure. In these experiments, the differences in growth cone size become significant after 120 minutes exposure to Wnt3a compared to controls (control: 37.18 ± 1.47 μm^2, Wnt3a: 58.36 ± 3.29 μm^2. $p<0.01$. Fig.3.15 C). These findings demonstrate that Wnt3a can induce rapid changes in the rate of axon elongation, within 20 minutes, suggesting that Wnt3a is likely to directly regulate changes in the axonal cytoskeleton. The fact that the large and spread growth cones are only observed at later time points, between 80 and 120 minutes after exposure to Wnt3a suggests that the effect of Wnts on growth cone size may result from the decrease in axonal outgrowth.

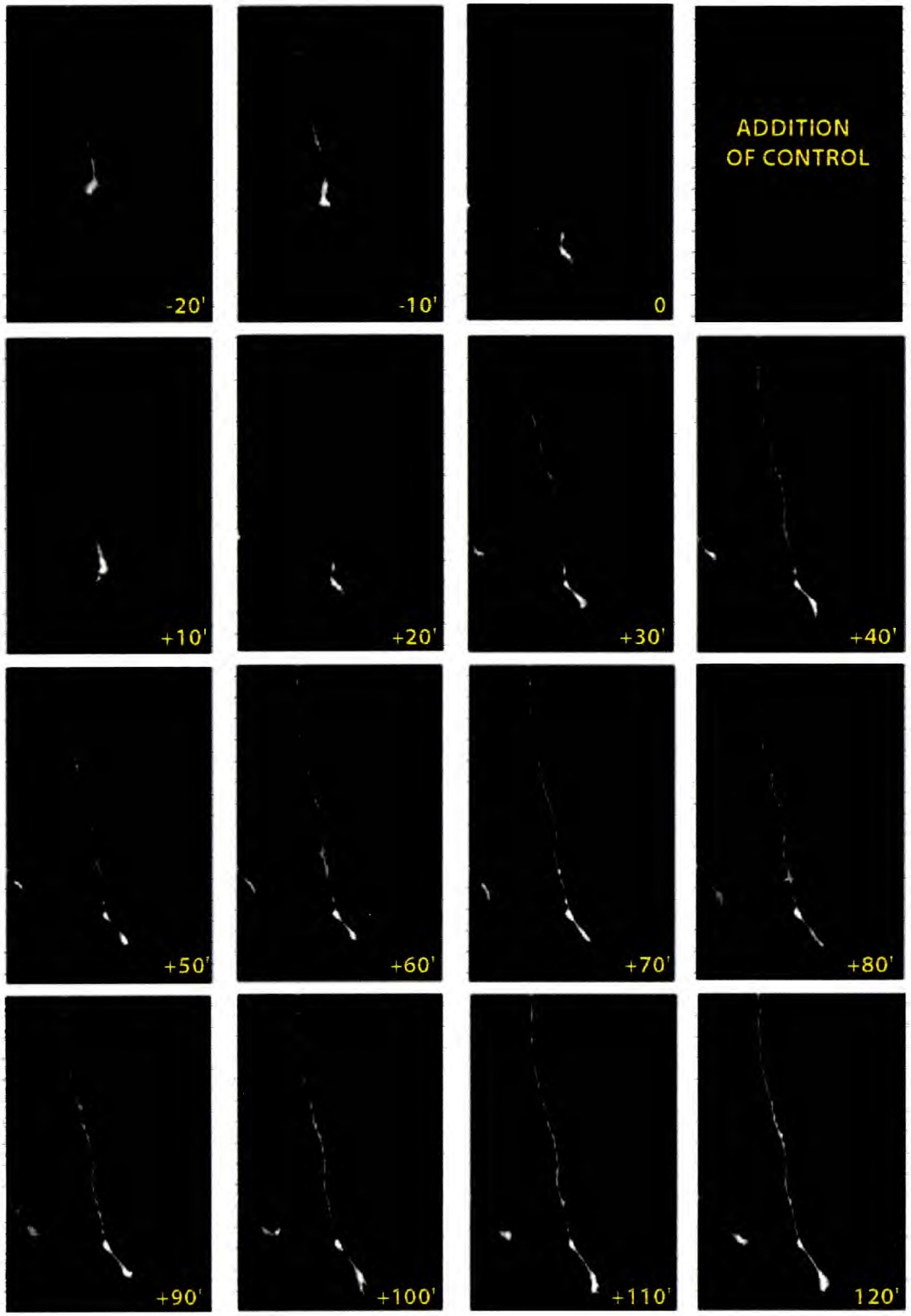


Figure 3.13. Time lapse frames of a sensory axon exposed to control media for 120 minutes. Frames illustrate a typical response of an axon to control media, the axon steadily advances, does not branch and the size of the growth cone does not change significantly.

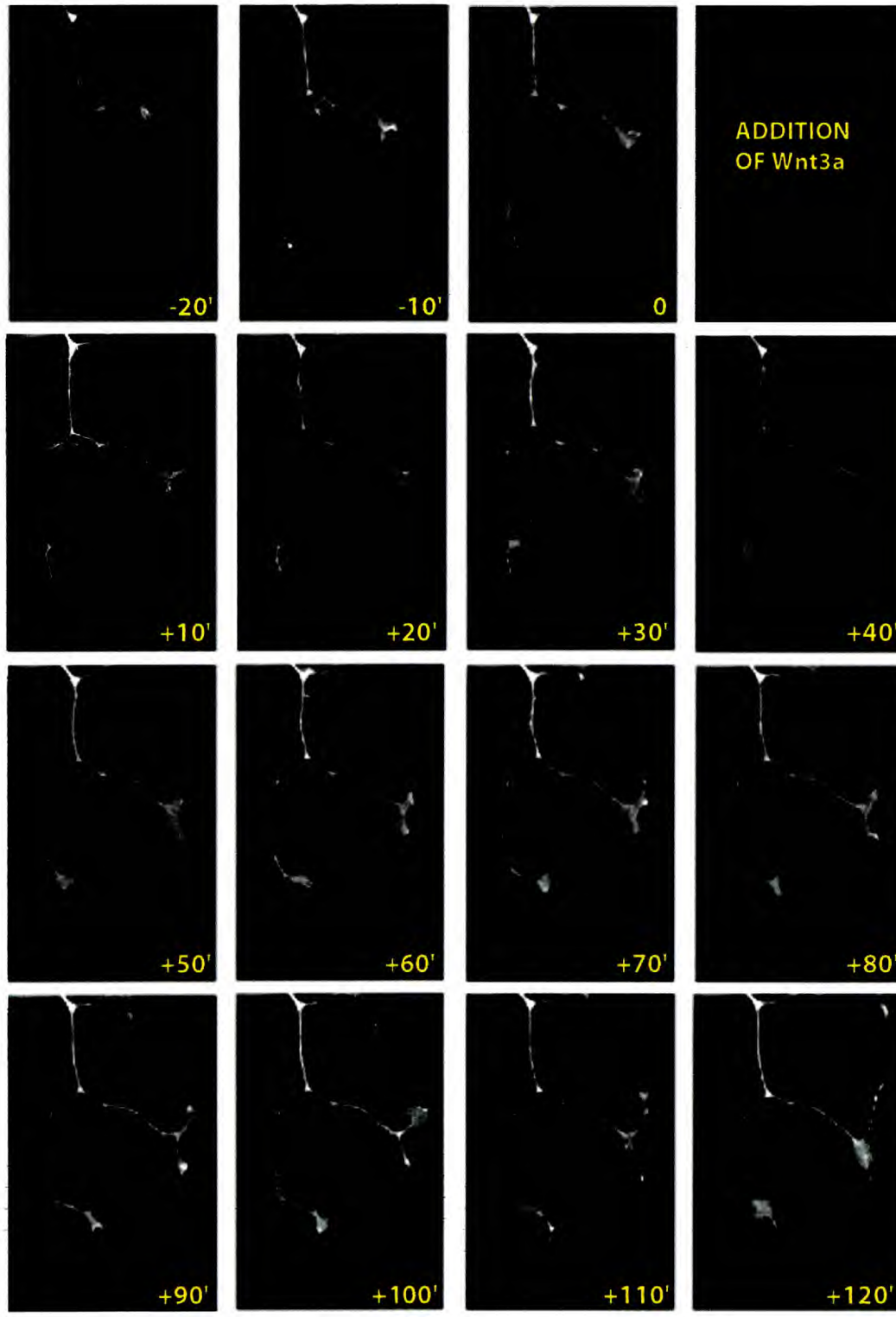


Figure 3.14. Time lapse frames of a sensory axon exposed to Wnt3a media for 120 minutes. Frames illustrate the typical response of a Wnt responding axon, upon addition of the Wnt the axon stops extending, the growth cone on the right attempts to branch and both growth cones become enlarged.

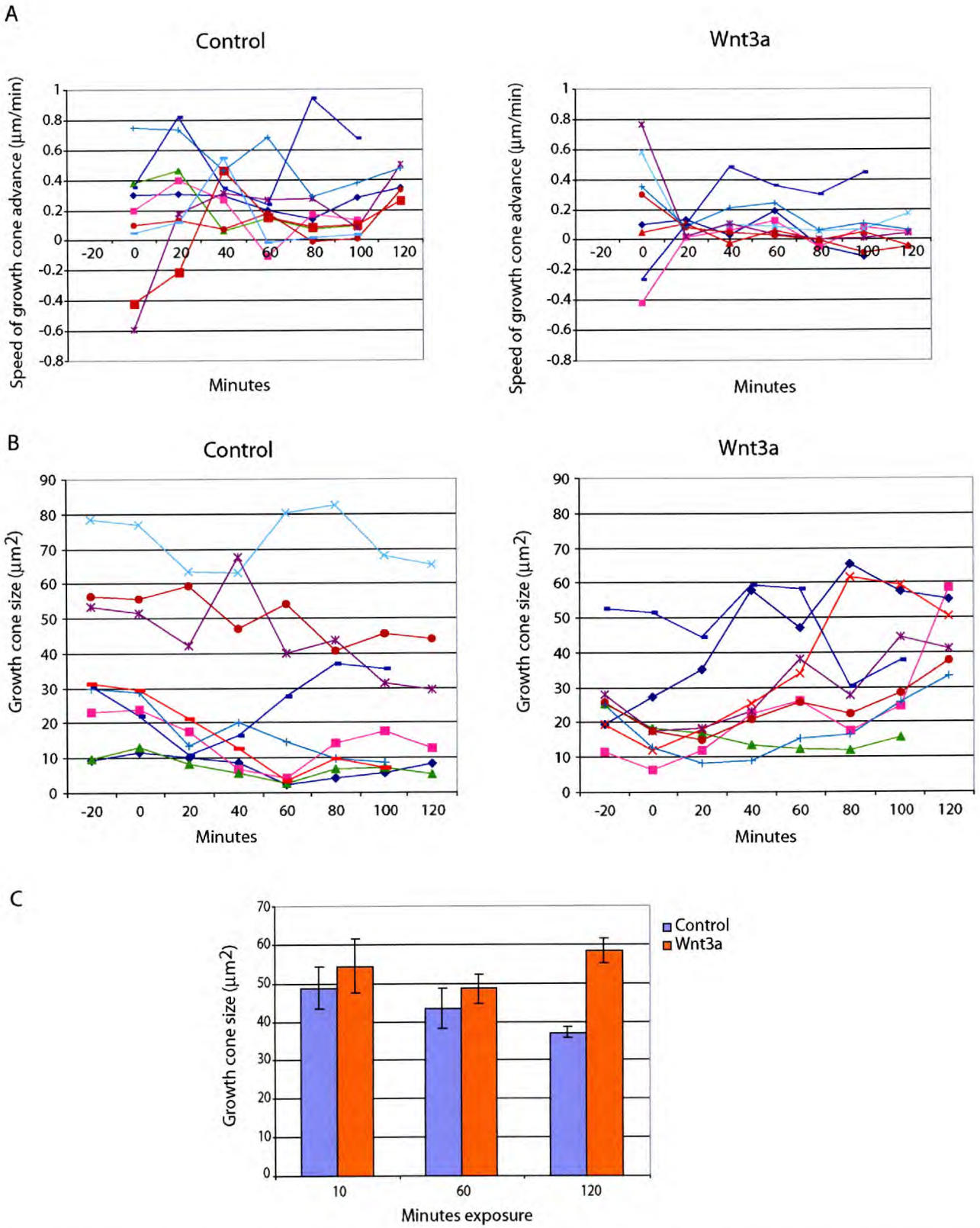


Figure 3.15. Wnt3a decreases the speed of growth cone advance within 20 minutes and increases growth cone size after 80-120 minutes.

(A) Quantification of the speed of growth cone advance from time lapse recordings, 20 minutes after application of Wnt3a the rate of growth cone advance decreases significantly compared to controls. (B) Quantification of growth cone size shows Wnt3a steadily increases growth cone size. Control treated growth cones decrease or maintain their size. (C) Short time courses with fixed cells corroborate the finding that the effect of Wnt3a on growth cone size takes place after the Wnt-induced decrease in growth cone advance.

3.3 Discussion.

Wnt3 has previously been shown to act as a retrograde signal that controls the terminal arborizations of a subset of embryonic DRG neurons, and promotes the formation of sensory-motor conections in the vertebrate spinal cord (Krylova *et al.*, 2002). To shed light on the effects of Wnts on the axonal cytoskeleton underlying Wnt-induced axonal remodelling, the neuronal culture conditions were optimised. In addition to reproducing the effects of Wnt3 on embryonic DRGs, this chapter demonstrates that Wnt3 has the same remodelling effect on a subpopulation of neonatal DRGs. Overnight treatment of either embryonic and neonatal DRGs with Wnt3 leads to shorter, more branched, axons and larger growth cones than controls. Interestingly, a similar effect is observed upon treatment with Wnt1 and Wnt6 conditioned media, but not with Wnt7b. At present it is not known whether only certain Wnts have remodelling activity or whether DRG neurons only recognise particular Wnt proteins due to the set of receptors they express. While Wnt7b does not elicit remodelling of DRG neurons, it does induce dendritogenesis in hippocampal neurons (Rosso *et al.*, 2005), indicating that Wnts are able to elicit distinct responses in different neuronal populations. These differences may be due to the particular growth dynamics of the neuronal cell type and/or to the stage in development at which they encounter the Wnt signal.

The changes in axonal behaviour induced by Wnts in DRGs are similar to those observed in sensory neurons projecting to motor nuclei in the ventral spinal cord *in vivo* (Ozaki and Snider, 1997). Furthermore, transplant experiments have suggested that short-range signals from the ventral spinal cord induce the terminal arborisations of sensory neurons (Sharma and Frank, 1998). The patterns of Wnt expression in the spinal cord and the remodelling effects observed *in vitro*, strongly suggest that Wnts could indeed be one of these signals. Other signalling molecules expressed in the ventral spinal cord that influence the morphology of DRG neurons include Slit2 which induces axonal elongation and branching in small-diameter NGF responsive DRGs (Wang *et al.*, 1999), and Sema3 which inhibits axon growth of the same subpopulation of DRGs (Messersmith *et al.*, 1995). While Slit2 is considered to act as a chemoattractant,

Sema3A functions as a chemorepellent for these neurons. Due to the fact that bath application of Wnt induces branching as well as axonal shortening, makes it difficult to categorise it as an attractive or repulsive guidance cue. Exposing DRGs to a Wnt gradient or a stripe assay would help determine whether Wnts are acting to guide a subset of sensory neurons towards the ventral spinal cord. However, the remodelling effects observed are consistent with Wnts being target-derived signals. Unlike Slit2 or Sema3A, axons may encounter Wnts when they are in close proximity to their targets rather than whilst in transit to them.

There is mounting evidence for a general role for Wnts in the promotion of neuronal connectivity. Wnts have been shown to promote synapse formation in the hippocampus (Rosso *et al.*, 2005), cerebellum (Hall *et al.*, 2000; Lucas and Salinas, 1997) and the spinal cord (Krylova *et al.*, 2002). In particular, the effects of Wnt proteins on DRGs suggest they act as retrograde signals secreted from post-synaptic or intermediate target cells to promote cytoskeletal changes that will aid the formation of synaptic connections. Exactly how Wnts can decrease axon length while increase branch formation is not known, but differences in cytoskeletal dynamics within different parts of the neurite may account for local differences in the response to Wnts. Interestingly, another target derived signal, FGF-2, has also been shown to inhibit axonal extension whilst promoting branch formation in cortical neurons (Szebenyi *et al.*, 2001), suggesting these remodelling effects may commonly occur as axons reach their targets.

The main difficulty encountered using Wnt conditioned media was the variability of the remodelling effect on DRGs. A direct correlation between the amount of Wnt in the conditioned media and the extent of axonal remodelling was observed, but attempts to improve Wnt secretion, using heparin or serum, did not increase the axonal remodelling effect on DRGs. β-catenin assays revealed that media conditioned with untagged Wnt3a induces a greater response than Wnt3-HA conditioned media, suggesting that the HA tag could render Wnts less active. In addition to the levels of active Wnt, the presence of other factors in the conditioned media, which could interfere with the remodelling activity of Wnts, may account for the variability between experiments. Rat1Bs and L-

cells may be producing factors that could either inhibit the effect of Wnts or mimic it, thus reducing the differences in growth cone size, branching and axon length between Wnt treated neurons and controls. The fact that DRGs exhibit axonal remodelling when co-cultured with control L-cells suggests Wnt-mimicking factors are attached to the surface of these cells. In agreement with all these findings, purified and untagged Wnt3a yielded more consistent, robust and faster axonal remodelling in DRGs.

Analysis of fixed DRG neuron cultures indicates that Wnt-induced remodelling can be observed within 2 hours of application of Wnt3a, however, this type of analyses does not allow detection of small changes in axonal behaviour that result in enlarged growth cones, branching and axonal shortening. To understand the sequence of events and observe the effects of Wnt3a on axonal behaviour in real time, time-lapse experiments were carried out. Indeed, time-lapse recordings reveal an effect of Wnt3a on growth cone advance within the first 20 minutes of application. The fact that the increase in growth cone size takes place around 80 minutes after application suggests that in the presence of Wnt, growth cones first stop their advance and then become enlarged. While DRG growth cones have been reported to collapse between 5 and 15 minutes after treatment with Semaphorin and Ephrin-A2 (Aizawa *et al.*, 2001; Fournier *et al.*, 2000; Jurney *et al.*, 2002), the response to positive guidance cues such as Slit2 or NGF requires at least 24 hours (Wang *et al.*, 1999; Zhang *et al.*, 1994). In light of these studies, the effects of Wnt3a on axonal extension and growth cone size are rapid and likely to be mediated by direct regulation the cytoskeleton.

Since microtubules are the main regulators of axon growth, it is likely that Wnts lead to axonal shortening by affecting microtubule dynamics and/or organisation. Indeed, the downstream signalling protein Dvl has been shown to increase microtubule stability (Krylova *et al.*, 2000), and pharmacological inhibition of microtubule dynamics has been reported to decrease axon elongation (Rochlin *et al.*, 1996). On the other hand, growth cone spreading and increased motility is likely to be due to an effect of Wnt on the actin cytoskeleton. It remains to be determined whether Wnt signalling can directly

regulate the actin cytoskeleton or whether any effect on actin is an indirect consequence of the effect of Wnts on microtubules.

To summarise, this chapter has described the development of a reliable *in vitro* system to study the effects of Wnts on axonal behaviour in real time. Having demonstrated the effects of Wnt3a on growth cone advance and size in DRG neurons, the next step is to characterise the cytoskeletal changes taking place in response to Wnt3a in developing axons and to outline the signalling pathway/s involved.

CHAPTER 4:

Wnt3a signals through a transcription independent pathway and induces changes in both the stability and organisation of microtubules.

4.1 Introduction.

The well-characterised Wnt signalling pathways provide a unique opportunity to unravel the mechanism by which Wnts regulate axonal behaviour. The fact that the three main Wnt signalling pathways: canonical, planar cell polarity and the Wnt-Ca^{+2} pathway, require the cytoplasmic scaffolding protein Dishevelled (Dvl), stongly suggests it is a mediator of Wnt-induced axonal remodelling. There are 3 ubiquitously expressed Dvl proteins in mice, Dvl1, -2 and –3 (for review see Wodarz and Nusse, 1998). *Dvl1* knockout mice exhibit abnormal social behaviour, but the fact that they do not have any obvious anatomical defects (Lijam *et al.*, 1997), indicates that there is some redundancy between them. Indeed, Dvl1 expression has previously been shown to induce similar morphological changes to those observed with Wnts in differentiated neuroblastoma cells (NB2a). Dvl1 expression decreases axonal length, increases axon diameter and growth cone size mimicking the effect of Wnts in developing axons (Ciani *et al.*, 2004). The effect of Dvl1 on axonal morphology can be largely attributed to the effects of Dvl1 on microtubules. Dvl1 is associated to the most stable pool of microtubules in neurons and has been shown to confer microtubule stability by inhibiting Gsk-3β (Krylova *et al.*, 2000). It was recently shown that Dvl stabilises microtubules locally through a β-catenin- and TCF-independent mechanism (Ciani *et al.*, 2004) indicating a diversion of the canonical Wnt signalling pathway (see figure 4.1). Whether Wnt-induced axonal remodelling in DRGs involves microtubule stabilisation via the same signalling pathway remains to be proved. The finding that Wnt3a can decrease axonal extension within 20 minutes of application (Chapter 3) does suggest that microtubules are key targets of Wnt signalling during axonal remodelling.

This chapter addresses the mechanism by which Wnt3a induces axonal remodelling in DRG neurons. The effect of Dvl1 gain of function and Gsk-3β inhibition on neonatal DRG neurons will be described as well as the effects of protein transcription and translation drugs in Wnt-mediated axonal remodelling. Finally the effect of Wnt3a on microtubules and the extent to which Wnt3a mimics the effect of Dvl1 expression on microtubule organisation and dynamics will be analysed.

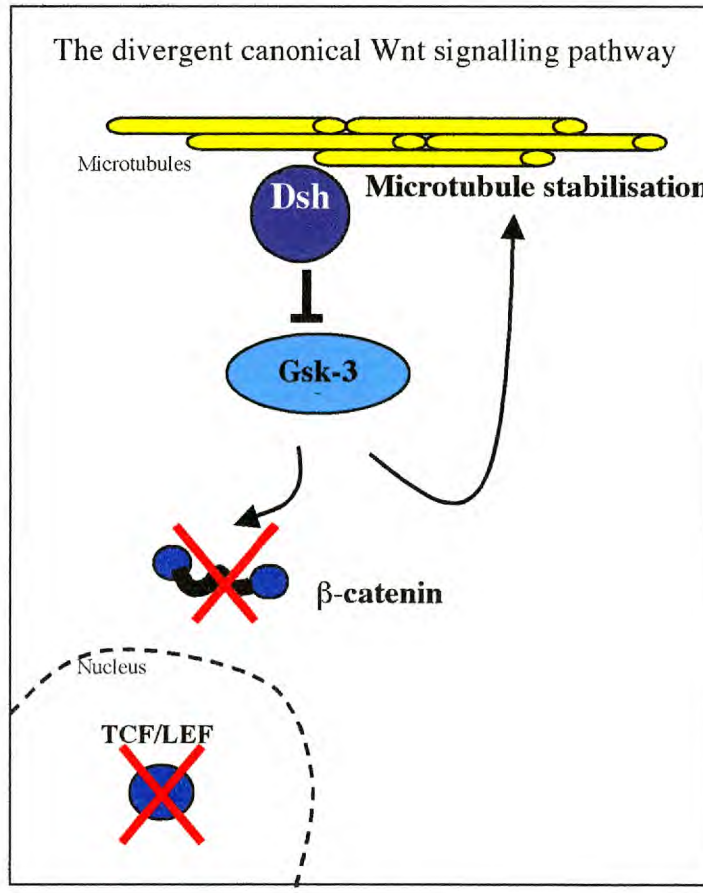


Figure 4.1. The divergent canonical Wnt signalling pathway.
Dvl binds to microtubules and confers microtubule stability by inhibition of Gsk-3β, but through a β-catenin- and TCF-independent mechanism (Ciani *et al.*, 2004)

4.2 Results

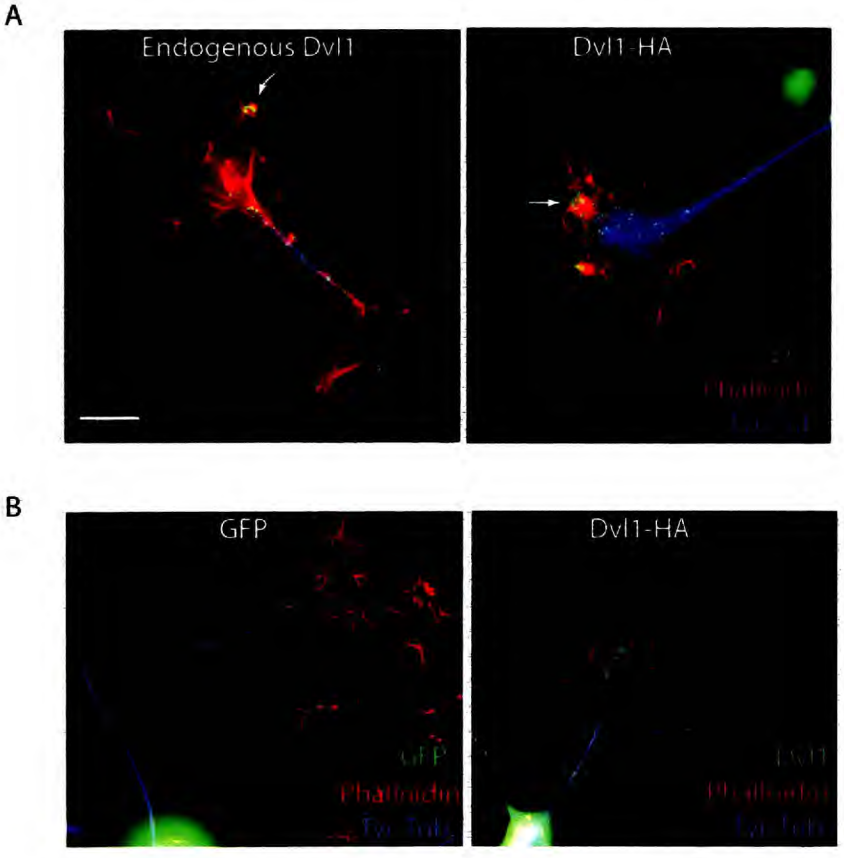
4.2.1 Dvl1 expression mimics Wnt3a mediated axonal remodelling on neonatal DRGs.

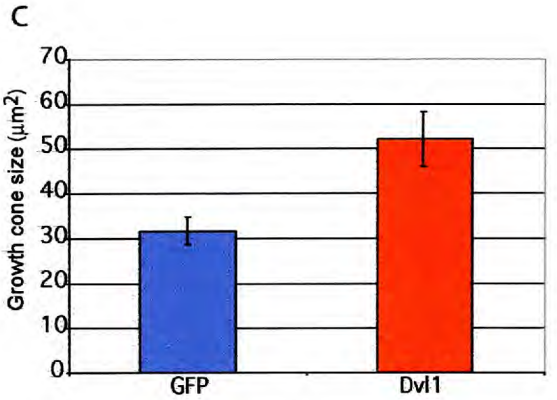
To examine the effects of Dvl on neuronal morphology Dvl1-HA was expressed in neonatal DRGs. To ensure Dvl1-HA adopts a similar localisation pattern to the endogenous Dvl1, the localisation of the two proteins was examined by immunofluorescence. Endogenous Dvl1 is found in cell bodies and neurites of cultured DRG neurons. Dvl1 has a punctate distribution along axons and is found in growth cones. Dvl1 puncta are mainly associated with microtubules, but are also detected in the actin rich periphery of growth cones (Fig.4.2 A arrow). When Dvl1-HA is expressed in DRG neurons a similar pattern to endogenous Dvl1 is observed (Fig.4.2 A). Dvl1-HA is found in a punctate distribution along axons, is especially abundant in growth cones, and is associated with microtubules and actin filaments (Fig.4.2 A).

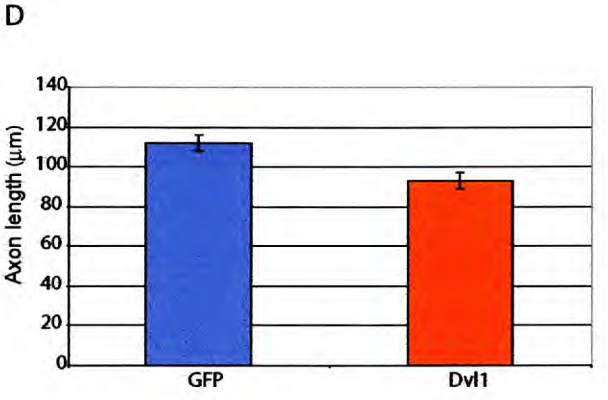
More importantly, Dvl1-HA causes significant changes in the axonal morphology of DRG neurons. Axons become shorter and growth cones greatly enlarged compared to GFP transfected cells (Fig.4.2 B). Quantification revealed that Dvl1 increases growth cone size by 60% compared to GFP-expressing control DRG neurons (GFP: 31.66 ± 3.07 μm^2, Dvl1: 52.12 ± 6.14 μm^2. Fig.4.2 C). In addition, Dvl1 decreases axonal length by 17% (GFP: 112 ± 4.04 μm, Dvl1: 93 ± 4.04 μm. Fig.4.2 D) and significantly increases quaternary branching compared to GFP controls ($p<0.05$. Fig.4.2 E). However, no significant differences in the number of primary, secondary or tertiary order branches were found. These results demonstrate that Dvl1 expression mimics the effects of Wnt3a on DRG neurons suggesting that Dvl1 mediates the effect of Wnt3a on axonal remodelling.

4.2.2 Wnt3a induced axonal remodelling is mediated through the inhibition of Gsk-3β, but does not require nuclear transcription.

Wnt-mediated axonal remodelling in mossy fibres and granule cells has been previously shown to depend on the inhibition of Gsk-3β (Hall *et al.*, 2000; Lucas *et al.*, 1998; Lucas and Salinas, 1997). Lithium, a well-known direct Gsk-3β inhibitor, is able to







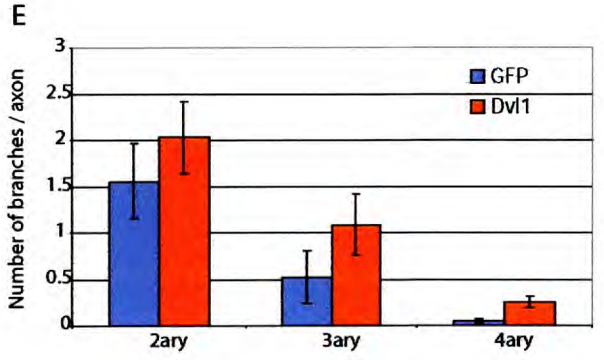


Figure 4.2. Dvl1 expression induces axonal remodelling.
(A) Endogenous Dvl1 is localised along axons and in growth cones. Dvl1-HA shows similar localisation. (B) Dvl1 overexpression mimics the effect of Wnt3a on axonal morphology. (C) Dvl1 expression causes a significant increase in growth cone size compared to GFP transfected controls. ($p<0.05$). (D) Axon length decreases significantly in Dvl1 expressing cells ($p<0.05$). (E) Dvl1 increases quaternary branch formation ($p<0.05$). Values are mean ± SEM from 4 independent experiments (at least 24 growth cones and 15 axons were measured in each). Bar, 12µm A, 30µm B.

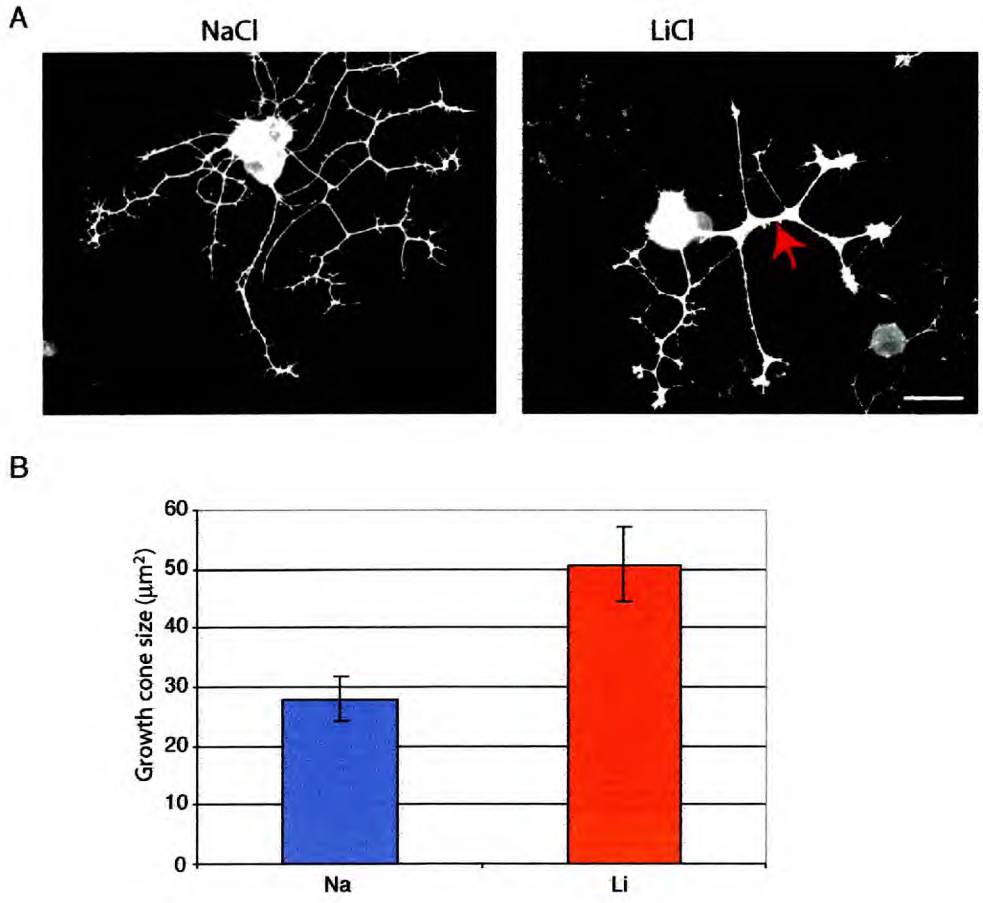


Figure 4.3. Inhibition of GSK-3β by LiCl mimics the effect of Wnt3a on axonal remodelling in DRGs. (A) 10mM lithium induces growth cone enlargement, axonal shortening and thickening (arrow) in DRGs. Bar, 30mm. (B) Average growth cone size is significantly larger in DRGs exposed to lithium compared to sodium controls ($p<0.05$). Values are mean ± SEM of three independent experiments (at least 43 growth cones were measured per condition).

mimic Wnt induced axonal remodelling in mossy fibres and granule cells. To address whether the effect of Wnt3a on DRG neurons also involves inhibition of Gsk-3β, cells were treated with lithium for 2 hours. Lithium can also inhibit inositol monophosphatase and inositol polyphosphate phosphatase, resulting in inositol depletion (Berridge *et al.*, 1989). Exogenous *myo*-inositol has been shown to rescue the effect of lithium on the inositol pathway by restoring the inositol pool (Atack *et al.*, 1995). To eliminate the possibility that the effect of lithium on axonal remodelling is due to inositol depletion, cultures were supplemented with 10 mM *myo*-inositol. Treatment with 10 mM LiCl and 10 mM *myo*-inositol can mimic the effect of Wnt3a on growth cone size when compared to neurons exposed to 10 mM NaCl and 10 mM *myo*-inositol (NaCl: 27.93 ± 3.97 μm^2, LiCl: 50.73 ± 6.21 μm^2 Fig.4.3 A-B). Exposure to lithium also causes a decrease in axonal length while increasing axonal thickening (Fig.4.3 A, arrow). These results suggest that inhibition of Gsk-3β is mediating Wnt3a induced axonal remodelling in DRGs.

In the canonical Wnt signalling pathway, Gsk-3β inhibition leads to an increase in the levels of β-catenin and subsequent activation of transcription through β-catenin binding to LEF/TCF transcription factors (Wodarz and Nusse, 1998). Indeed Wnt3a treatment increases the levels of β-catenin in DRGs (see supplementary figure 1), but to determine whether Wnt3a-induced axonal remodelling requires signalling to the nucleus and the activation of gene trancription, neurons were treated with 10 μg/ml actinomycin D. Actinomycin D inhibits RNA polymerase by binding to double-helical DNA and preventing it from being an effective template for RNA synthesis (Perry and Kelley, 1970). To test that 10 μg/ml actinomycin D blocks transcription, the expression of EGFP in transfected COS cells was examined. Indeed, at this concentration, EGFP is undetectable in the cells (Dr Ciani's observation). DRG cells were treated with 10 μg/ml actinomycin D for 30 minutes before addition of Wnt3a or control media to block all transcriptional activity. Neurons were fixed after 2 hours and their morphology examined. Despite the presence of actinomycin D, Wnt3a is able to induce axonal remodelling (Fig.4.4 A). The average growth cone size is significantly larger in Wnt3a treated cultures than controls (control: 33.14 ± 2.81 μm^2, Wnt3a: 46.82 ± 0.76 μm^2.

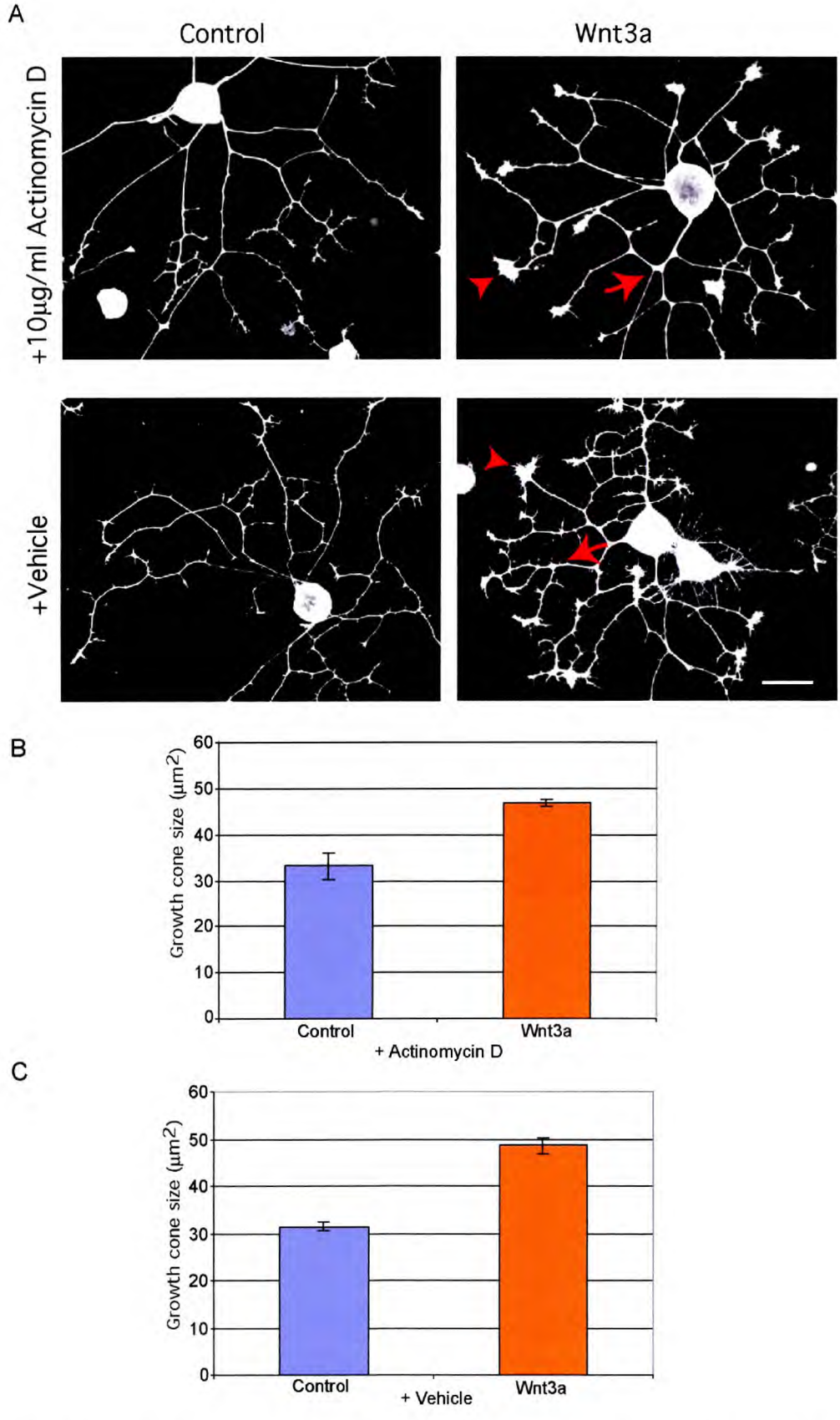


Figure 4.4. The effect of Wnt3a on axonal remodelling does not require nuclear transcription. (A) Wnt3a induces axonal remodelling in the presence of actinomycin D. Growth cones are larger (arrowheads) and axons shorter and more branched (arrows) than controls. Bar, 30µm. (B) Average growth cone size is significantly larger in DRGs exposed to Wnt3a and actinomycin D ($p<0.01$). (C) Average growth cone size is significantly larger in DRGs exposed to Wnt3a and DMSO, the drug vehicle ($p<0.01$). Values are mean ± SEM of three independent experiments (at least 48 growth cones were measured per condition).

$p<0.01$. Fig.4.4 B), while axons are shorter and more branched than controls (Fig.4.4 A-arrow). Treatment with the drug vehicle alone (DMSO) did not influence the effect of Wnt3a on axonal morphology and growth cone size (Fig.4.4 A and C). In the presence of DMSO, the growth cones of Wnt3a treated cells are significantly larger than controls (control: $31.47 \pm 0.50\ \mu m^2$, Wnt3a: $48.54 \pm 0.92\ \mu m^2$. $p<0.001$. Fig.4.4 C). These results indicate that gene transcription is not required for the Wnt3a mediated axonal remodelling.

The independence of transcription suggests that Wnt3a could induce axonal remodelling through changes in protein synthesis, post-translational changes, or both. To begin to address this, the consequences of blocking protein synthesis on the Wnt3a effect were examined. Interestingly, Wnt3a-mediated axonal remodelling is completely abolished when neurons are treated with non-toxic concentrations of the protein translation inhibitors: anisomycin (20 μM) or cyclohexamide (25 μM) (Zhang and Poo, 2002; Campbell and Holt, 2001) (Fig.4.5 A-B). In the presence of anisomycin or cyclohexamide, axons become shorter, and growth cones become smaller in both control and Wnt3a treated neurons (control + anisomycin: $20.43 \pm 1.86\ \mu m^2$, Wnt3a + anisomycin: $21.32 \pm 0.69\ \mu m^2$. Fig.4.5 A and C). These experiments indicate that Wnt3a mediated axonal remodelling requires new protein synthesis but not transcription.

4.2.3 Wnt3a affects the organisation of microtubules.

To begin to understand the cytoskeletal changes underlying axonal remodelling by Wnt3a, the distribution and organisation of microtubules were examined. Previous studies have shown that Wnt7a induces unbundling of microtubules in mossy fibre growth cones (Hall *et al.*, 2000) and that Dvl1 expression increases the amount of stable microtubules along axons and induces microtubule looping in growth cones of differentiated neuroblastoma cells (Ciani *et al.*, 2004).

Microtubules are subject to various post-translational modifications (reviewed in Luduena, 1998), and specific antibodies can be used to examine different populations of

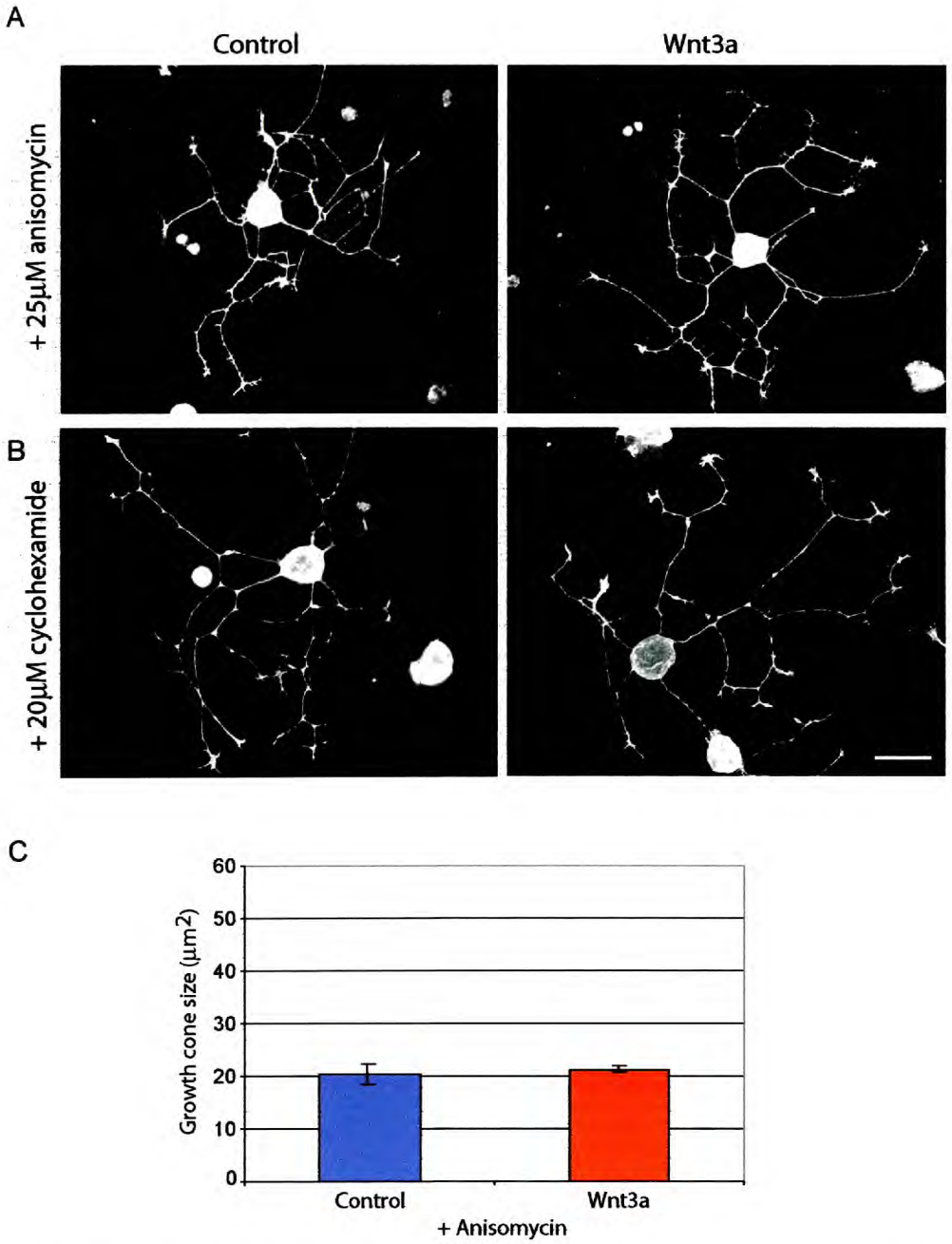


Figure 4.5. The effect of Wnt3a on axonal remodelling requires protein translation.
(A) Wnt3a does not induce axonal remodelling in the presence of anisomycin. (B) Wnt3a does not induce axonal remodelling in the presence of cyclohexamide. Bar, 30µm. (C) There are no differences in growth cone size between neurons exposed to Wnt3a or control media in the presence of anisomycin. Values are mean ± SEM of three independent experiments (at least 48 growth cones were measured per condition).

microtubules. Antibodies against tyrosinated tubulin, which label the most dynamic microtubules, and against acetylated tubulin, which label older, typically more stable microtubules, were used to examine the organisation and distribution of microtubules in Wnt3a or control treated DRG neurons. Dynamic (tyrosinated) microtubules are normally found to splay in the central region of the growth cone and occasionally invade the peripheral domain, whereas stable (acetylated) microtubules remain bundled in the proximal region of the growth cone. Control treated growth cones exhibit this typical distribution of dynamic and stable microtubules (Fig.4.6 A and C). Wnt3a increases the amount of tyrosinated and acetylated microtubules along axons and in growth cones compared to control neurons (Fig.4.6 B and D). The differences in microtubule density between control and Wnt3a treated neurons become apparent in pseudocoloured images of acetylated microtubules, which reflect the differences in fluorescence intensity (Fig.4.6 E-F). The fluorescence intensity of acetylated microtubules in Wnt3a treated neurons is much higher along axons and in growth cones (red and white colours) compared to the controls. The differences in microtubule content between control and Wnt3a treated cells cannot be detected by western blot of the total lysate of DRG neurons (Fig.4.6 G). However, this method is unlikely to be sensitive enough to detect changes in microtubule populations that only occur in a subpopulation of cells (the Wnt3a-responsive proprioceptive neurons), which could explain this negative result.

In addition to increasing the amount of microtubules along axons and in growth cones, Wnt3a affects the organisation of microtubules in growth cones. Wnt3a treatment increases the proportion of growth cones containing looped microtubules compared to controls (Fig.4.6 B and D). Both tyrosinated and acetylated microtubules adopt this looped morphology. When quantified, the number of growth cones with looped microtubules was up to 8 times higher in Wnt3a treated cultures compared to controls (Fig.4.6 H). Microtubule loops have been described in pausing growth cones (Kalil *et al.*, 2000; Dent *et al.*, 1999) and in mossy fibres exposed to Wnt7a (Hall *et al.*, 2000). Since Wnt3a slows down axonal extension (Fig.3.15 A), it is likely that these looped microtubules are indeed found in pausing growth cones. In order to dissect the sequence of events, DRGs exposed to control or Wnt3a were fixed at different time points and the

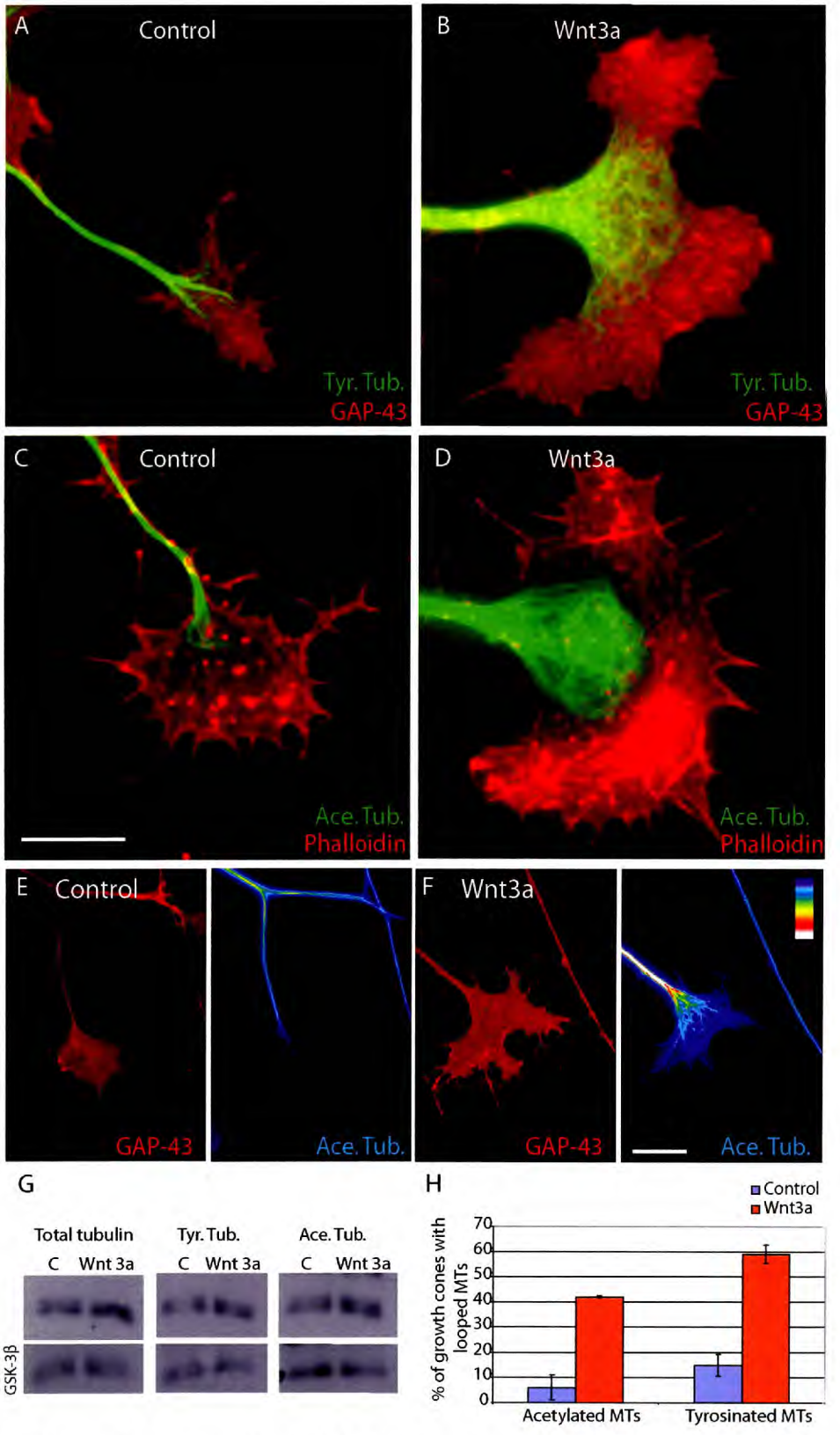


Figure 4.6. Wnt3a increases microtubules in growth cones and causes microtubule looping.
(A-D) Growth cones exposed to Wnt3a have looped tyrosinated and acetylated microtubules. Bar, 10μm. (E-F) Pseudocoloured acetylated microtubules higlight the differences in fluorescence intensity between control and Wnt3a treated growth cones. Bar, 10μm. (G) Western blot of DRG cell lysates. No differences were found in the total levels of tubulin, tyrosinated tubulin or acetylated tubulin between control and Wnt 3a treated cells. Total GSK-3β was used as loading control. (H) The percentage of growth cones with looped microtubules is 8 times higher in Wnt3a treated neurons. Values are mean ± SEM of three independent experiments (at least 200 growth cones were counted per condition).

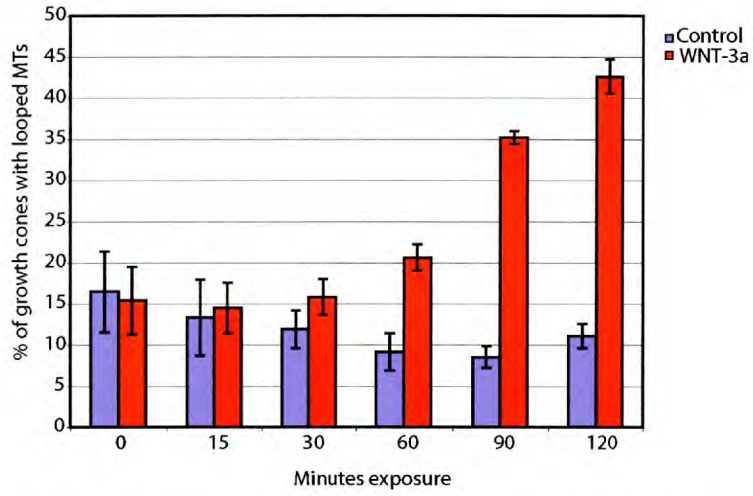


Figure 4.7. Microtubule looping is observed after 60 minutes exposure to Wnt3a. The percentage of growth cones with looped microtubules is significantly higher in Wnt3a treated DRGs after 60 minutes of exposure ($p<0.05$). Values are mean ± SEM from three independent experiments (at least 150 growth cones were counted in each).

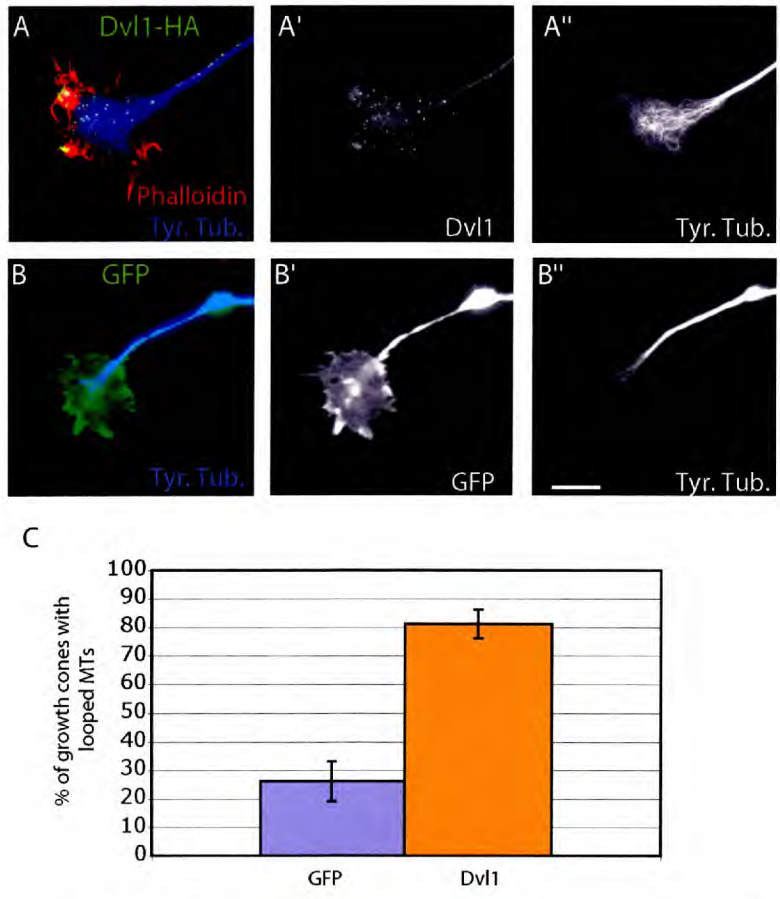


Figure 4.8. Dvl1 expression causes microtubule looping in DRG growth cones. (A) Microtubules in Dvl1 expressing neurons adopt a similar looped organisation to those in Wnt3a treated growth cones. (B) Microtubules in GFP expressing growth cones adopt the typical splayed distribution. Bar, 12µm. (C) The percentage of growth cones containing looped tyrosinated microtubules is significantly higher in Dvl1 expressing cells ($p<0.01$).

percentage of growth cones containing looped microtubules was determined (Fig.4.7). Differences between Wnt3a and control treated growth cones become apparent 60 minutes after exposure, hence it would seem that microtubule looping takes place after the decrease in growth cone advance, but before the Wnt-induced increase in growth cone size.

Interestingly, microtubule looping was also observed in growth cones of DRG neurons expressing Dvl1 when compared to GFP-expressing controls (Fig.4.8 A-B). Quantification revealed the percentage of growth cones with looped tyrosinated microtubules is significantly higher in Dvl1-expressing neurons than GFP-expressing ones. This finding further supports the notion that microtubules are downstream targets of Wnt3a-Dvl signalling in DRGs.

To summarise, Wnt3a increases the amount of microtubules along axons and in growth cones, and induces microtubule looping in DRG neurons. These effects are similar to those described in mossy fibres upon exposure to Wnt7a (Hall *et al.*, 2000), in neuroblastoma cells and DRGs expressing Dvl1 (Ciani *et al.*, 2004; and Fig.4.8), strongly suggesting that Wnts signal through Dvl to induce changes in microtubule organisation and axonal remodeling. Another novel finding is that Wnt3a affects both acetylated and tyrosinated microtubules. Both populations of microtubules are found in higher quantities and to form loops in growth cones compared to controls.

4.2.4 Wnt3a confers microtubule stability.

Since Wnt3a increases the amount of microtubules along axons and in growth cones, and expression of Dvl1 has been previously shown to induce microtubule stability in dividing cells, differentiated neuroblastoma cells and cerebellar granule neurons (Ciani *et al.*, 2004; Krylova *et al.*, 2000), the effect of Wnt3a on microtubule dynamics was investigated. To determine if Wnt3a could increase microtubule stability, DRG neurons were exposed to the microtubule depolymerising drug nocodazole. Exposure to 15 μM nocodazole for 2 hours depletes control cells of tyrosinated microtubules, the staining

appears diffuse as polymers are broken down (Fig.4.9 A). In addition, the amount of acetylated microtubules is greatly reduced. Axons appear bent and retracted (Fig.4.9 A). Full recovery of the microtubule polymers and axon morphology was observed 1 hour after removal of the drug, confirming that the drug was not causing irreversible damage to the cells (supplementary figure 2). Interestingly, in the presence of Wnt3a, acetylated microtubules remain intact and axonal length is not affected. To quantify these differences, the percentage of total axon length containing acetylated microtubules was measured. While in control treated cells, addition of nocodazole causes a significant decrease in the percentage of axon labelled with acetylated tubulin ($p<0.05$), Wnt3a treated neurons are not affected (Fig.4.9 B). These results suggest that Wnt3a stabilises microtubules along axons.

To investigate the effect of Wnt3a on microtubule stability in growth cones, lower concentrations of nocodazole were used. 1 μM nocodazole depolymerises tyrosinated microtubules in growth cones of DRG neurons, yet it does not interfere with growth cone morphology or size. Interestingly, application of 1 μM nocodazole for 1 hour causes the loss of acetylated microtubules from growth cones exposed to control media but not in those exposed to Wnt3a (Fig.4.9 C-D). Quantification reveals a 78% decrease in the percentage of growth cones containing acetylated microtubules in control treated neurons, whereas in Wnt3a treated neurons exposed to nocodazole there is only a 43% decrease (Fig.4.9 C). Indeed, growth cones exposed to Wnt3a are still invaded by acetylated microtubules in the presence of nocodazole (Fig.4.9 D), suggesting that Wnt3a is stabilising microtubules in growth cones as well as along the axon shaft.

4.2.5 Wnt3a alters the directionality of microtubule growth.

The presence of looped microtubules in growth cones of Wnt3a treated neurons could be due to the continuous polymerisation of microtubules in non-advancing growth cones which become forced to bend as they encounter the leading edge. Alternatively, Wnt3a may influence the direction of microtubule growth, which may then lead to a decrease in growth cone advance. To begin to distinguish between these two possibilities, the

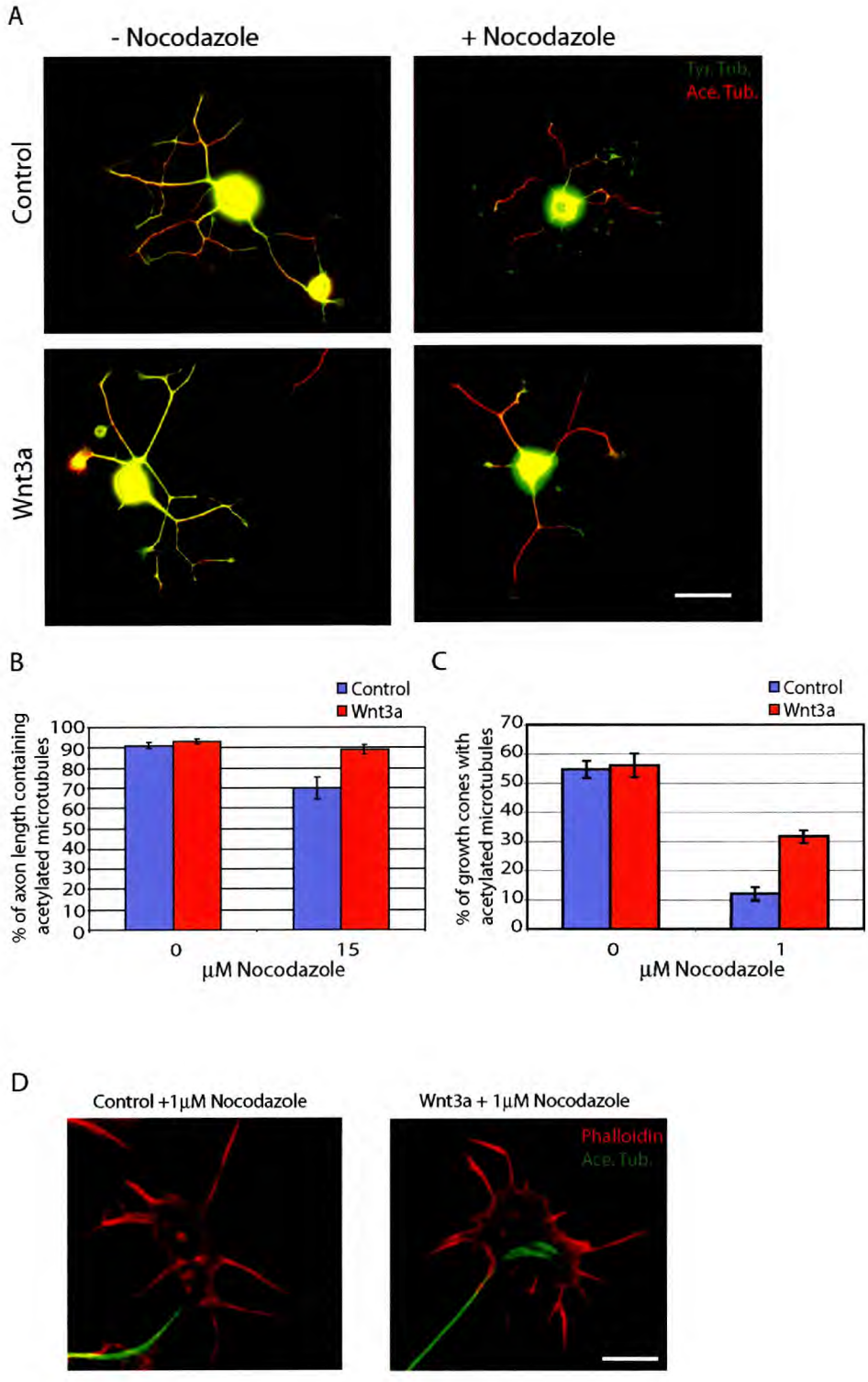


Figure 4.9. Wnt3a protects microtubules against nocodazole.
(A) Nocodazole depolymerises microtubules of DRG neurons treated with control media, but Wnt3a treated neurons are able to mantain their acetylated microtubules intact. Bar, 30µm. (B) Nocodazole treatment decreases the percentage of total axon length containing acetylated microtubules in controls, but not in Wnt-3a treated neurons. (C) Nocodazole decreases the percentage of growth cones with acetylated microtubules in controls but not in Wnt3a treated neurons. Values are mean ± SEM of three independent experiments (at least 23 axons and 95 growth cones were analysed per condition). (C) 1µM nocodazole depolymerises acetylated microtubules in growth cones of control treated cells but not of Wnt3a treated cells. Bar, 12µm.

plus-end of microtubules was labelled with EB3-GFP and time-lapse experiments performed. EB3 is a microtubule plus-end binding protein that is highly enriched in the nervous system (Nakagawa *et al.*, 2000). Several recent studies have used EB3-GFP to examine the dynamic behaviour of microtubules in neurons (Hasaka *et al.*, 2004; Stepanova *et al.*, 2003). Low expression of EB3-GFP does not alter the behaviour of microtubules in neurons since the microtubule growth rates measured with EB3-GFP are similar to the values obtained after injection of fluorescently labelled tubulin (Stepanova *et al.*, 2003). Thus, EB3-GFP appears to be an excellent tool not only for labelling polymerising microtubules, but also for studying microtubule growth dynamics.

EB3-GFP was expressed in DRG neurons by electroporation before plating. Time-lapse recordings reveal that EB3-GFP forms comet-like dashes along axons and in growth cones (**see movies chapter 4**). The EB3-GFP dashes rapidly disappear upon addition of nocodazole (Fig.4.10 A) and staining of fixed DRG neurons shows that EB3-GFP mainly colocalises with tyrosinated microtubules (Fig.4.10 B), indicating that EB3-GFP is indeed binding to dynamic, actively growing, microtubules. To examine the effect of Wnt3a on the growth of plus-end labelled microtubules, DRG neurons were exposed to Wnt3a or control media for 16 hours before time-lapse recordings were made. Frames were captured every 3 seconds over a period of 30-90 seconds. EB3-GFP recordings enabled the visualisation of the direction of microtubule growth. In control growth cones, 77% of the EB3-GFP comets grow outwards – towards the leading edge of the growth cones, 19% of them grow inwards – away from the leading edge, and a small proportion, 4%, move across the growth cone (Fig. 4.11 A-B). In contrast, in DRG neurons exposed to Wnt3a, a significantly larger percentage of EB3-GFP comets were found to move across the growth cone (18%, $p<0.05$). No significant differences were found in the percentage moving outwards or inwards compared to controls (68% and 14% respectively, Fig.4.11 A-B, **see movies chapter 4**). These findings show that Wnt3a alters the directionality of microtubule growth and are consistent with the observation of microtubule loops in Wnt3a treated growth cones.

4.2.6 Dvl1 expression alters the directionality of microtubule growth.

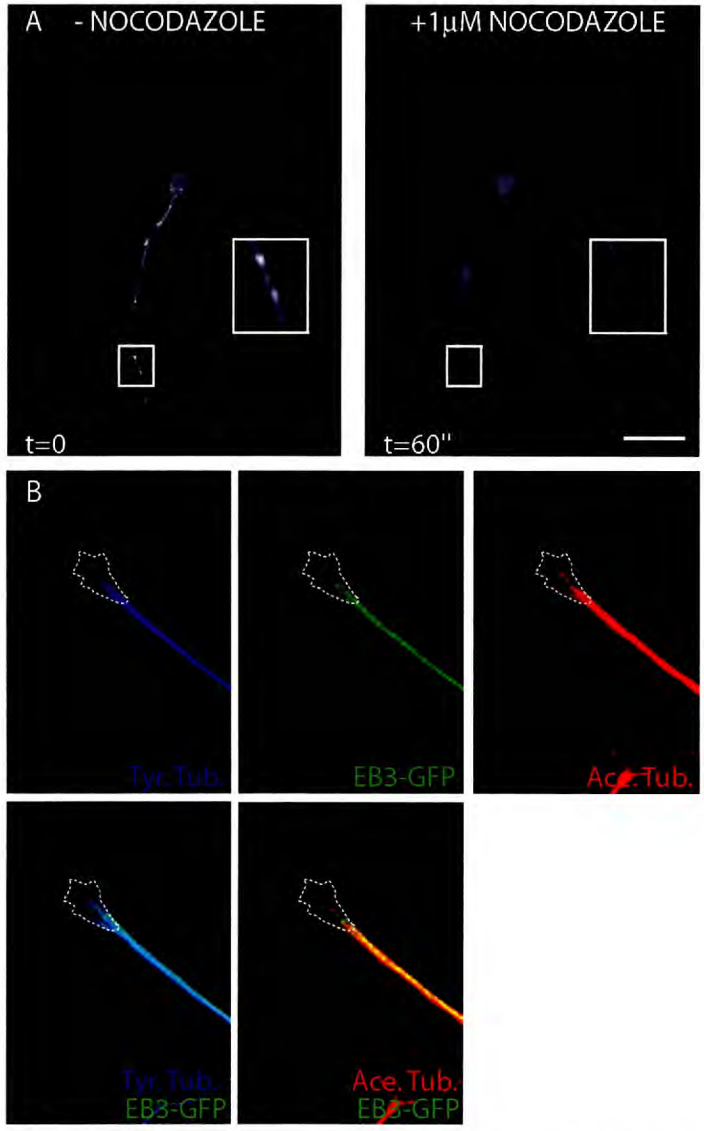
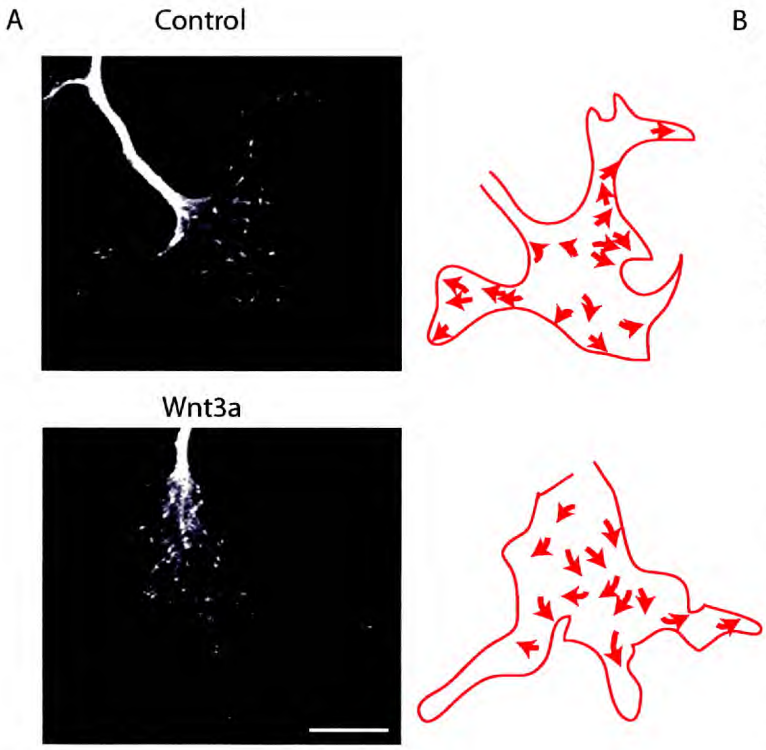


Figure 4.10. EB3-GFP binds to dynamic microtubules.
(A) EB3-GFP comets disappear within 60 seconds of addition of 1μM nocodazole. (B) EB3-GFP dashes mainly colocalise with tyrosinated microtubules, especially at the periphery of the growth cone. Bar, 10μm.



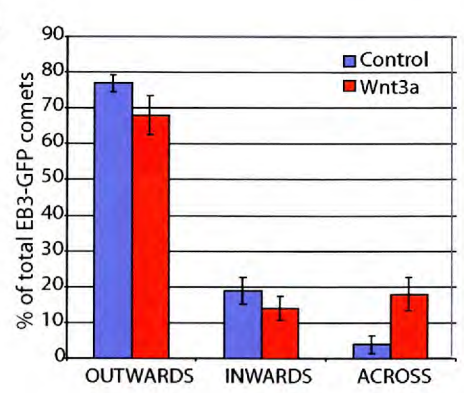
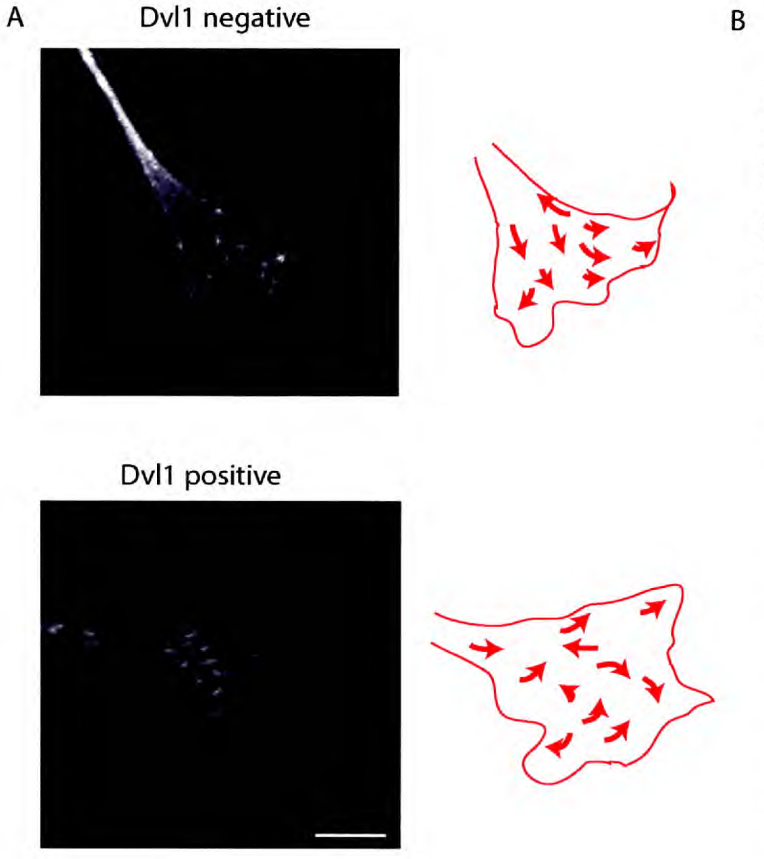


Figure 4.11. Wnt3a alters the direction of microtubule growth.
(A) Still frames from EB3-GFP time-lapse recordings with arrows indicating the direction of the EB3-GFP comet growth. Bar, 15µm. (B) Quantification shows that Wnt3a significantly increases the number of comets moving across growth cones ($p<0.05$). The direction of EB3-GFP comets from at least 12 growth cones were analysed per condition in four independent experiments.



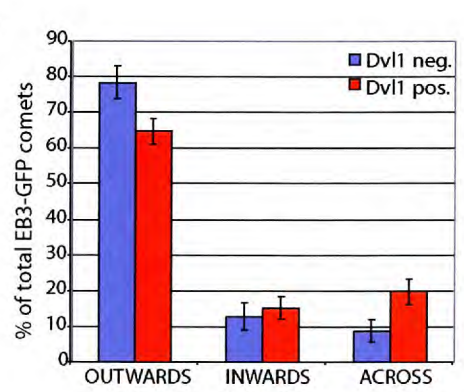


Figure 4.12. Dvl1 alters the direction of microtubule growth.
(A) Still frames from an EB3-GFP time-lapse recordings with arrows indicating the direction of the EB3-GFP comet growth. Bar, 15µm. (B) Quantification shows that Dvl1 significantly increases the number of comets moving across growth cones ($p<0.05$) while decreasing the number moving outwards, towards the leading edge ($p<0.05$). The direction of EB3-GFP comets from at least 10 growth cones were analysed per condition in four independent experiments.

To examine whether the direction of microtubule growth is also affected in Dvl1 expressing neurons, time-lapse recordings of DRG growth cones co-expressing EB3-GFP and Dvl1 were made. Interestingly, a similar loss of microtubule directionality to that induced by Wnt3a was observed. Nearly 20% of EB3-GFP comets move across the growth cone compared to 8% in cells that only express EB3-GFP (Fig.4.12 A-B, **see movies chapter 4**). Expression of Dvl1 also causes a significant decrease in the number of comets moving outwards ($p<0.05$). While 79% of EB3-GFP comets move towards the edge of the growth cone in control neurons expressing EB3-GFP, only 65% of comets move outwards in neurons co-expressing EB3-GFP and Dvl1. Dvl1 expression was confirmed by fixing and staining the cells after the time-lapse recordings. Typically 60% of the neurons were co-transfected with Dvl1 and EB3-GFP. The fact that Dvl1 expression can mimic the effect of Wnt3a on the direction of microtubule growth suggests Dvl1 is mediating this effect.

4.2.7 Wnt3a does not affect the rate of microtubule growth along axons or in growth cones.

To investigate whether Wnt3a can influence microtubule growth in DRG neurons, the movement of EB3-GFP comets was tracked. The speed of movement of EB3-GFP was calculated from consecutive frames, but only dashes that could be followed clearly over three frames or more were included in the analyses ("Trackable EB3-GFP comets"). The average speed of EB3-GFP movement in DRG neurons treated with control media was 0.14 ± 0.04 μm/sec along the axon shaft, and 0.13 ± 0.02 μm/sec in growth cones, hence it would seem that the EB3-GFP speeds do not vary between these two neuronal compartments (Fig.4.13 A). There were no significant differences in the speed of movement of EB3-GFP comets in the presence of Wnt3a (0.12 ± 0.02 μm/sec along axons and 0.11 ± 0.01 μm/sec in growth cones) compared to controls (0.14 ± 0.04 μm/sec along axons and 0.13 ± 0.02 μm/sec in growth cones), suggesting that Wnt3a does not affect the rate of microtubule polymerisation.

Due to the lack of a commercially available EB3 antibody it was not possible to examine endogenous EB3 in the cultures. Hence, at present, the possibility that EB3 itself is a target of Wnt3a signalling cannot be ruled out. To begin to examine potential differences between Wnt3a treated or Dvl1 expressing neurons and controls, the number of trackable EB3-GFP comets per growth cone were counted. There were no significant differences in the number of EB3-GFP comets in Dvl1 expressing neurons compared to those only expressing EB3-GFP ($p=0.056$), nor between control and Wnt3a treated cells ($p=0.57$) (Fig.4.13 B). However, due to variable levels of EB3-GFP expression and the fact that not all comets can be resolved with widefield microscopy, it is still possible that Wnt3a or Dvl1 may affect the levels of EB3 in growth cones and alter microtubule growth.

4.2.8 Examination of EB1 and APC in Wnt3a and control treated growth cones.

In order to identify proteins downstream of Wnt-Dvl, which could be mediating the effects on microtubule stability and organisation, the localisation and levels of the canonical Wnt signalling component APC and of the plus-end binding protein EB1, were examined by immunofluorescence. APC is a well characterised tumour suppressor protein that mediates Wnt-induced β-catenin degradation (for review see Bienz, 2002). APC can directly bind microtubules, induce microtubule stability (Zumbrunn *et al.*, 2001), and can mediate NGF stimulated axon outgrowth (Zhou *et al.*, 2004). Since phosphorylation of APC by Gsk-3β inhibits APC-microtubule interactions (Zumbrunn *et al.*, 2001), treatment with Wnt3a, which inhibits Gsk-3β, could increase the amount of APC bound to microtubules. However, no significant differences were found in the levels or localisation of APC in growth cones after exposure to Wnt3a or control media for two hours (Fig. 4.14 A-B). In DRG neurons, APC is found not only bound to microtubules but also at the periphery of growth cones where it may associate with actin filaments or the plasma membrane (Fig. 4.14 A).

EB1, was first identified as an APC binding protein (Su *et al.*, 1995). EB1 also associates with microtubules where it can promote microtubule polymerisation

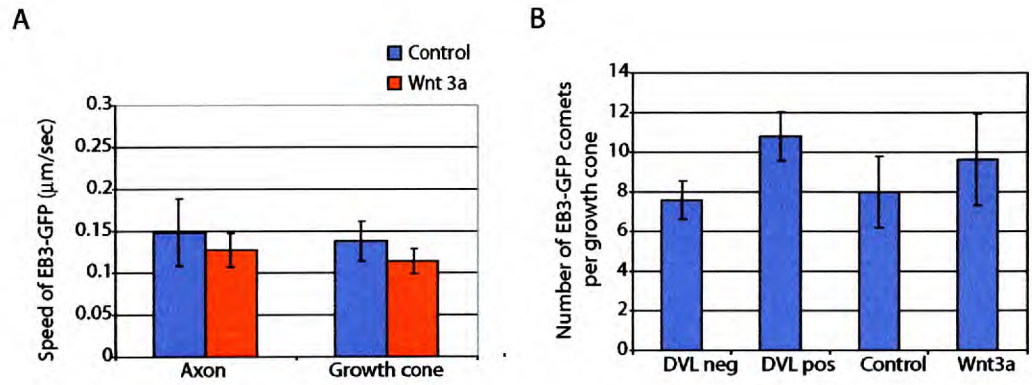


Figure 4.13. Wnt3a does not affect the speed or number of EB3-GFP comets.
(A) There are no differences between control and Wnt3a treatment on the speed of EB3-GFP comets along axons or in growth cones. (B) There are no significant differences in the number of trackable EB3-GFP comets in growth cones between Dvl1 expressing neurons and those only expressing EB3-GFP (p=0.056), or between control and Wnt3a treated neurons (p=0.57). Values are mean of 3 independent experiments ± SEM (EB3 comets from at least 10 growth cones were tracked per condition per experiment).

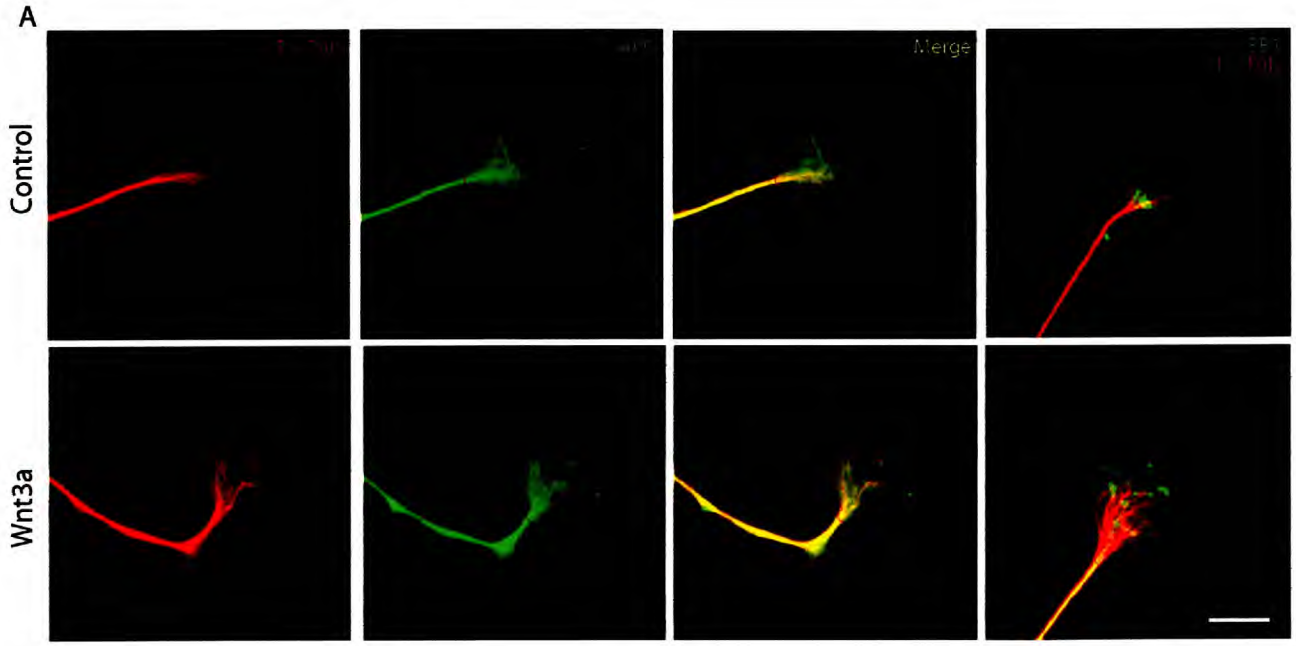
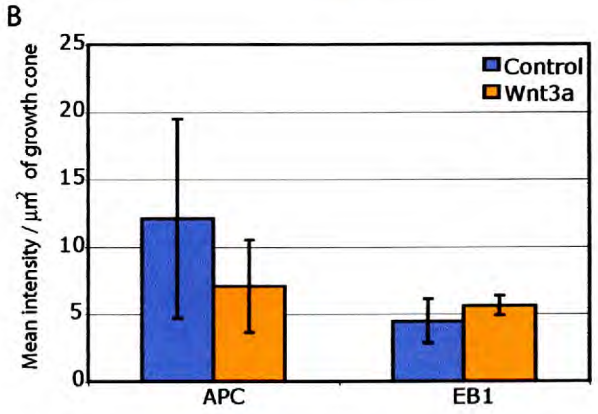


Figure 4.14. Wnt3a does not affect the levels of APC or EB1 in growth cones.
(A) Immunofluorescence stainings of APC and EB1 in growth cones of DRGs. Bar, 10µm. (B) Quantification of the mean fluorescence intensity in growth cones reveals there are no differences between Wnt3a and control treated growth cones. Values are mean ± SEM from three independent experiments, at least 12 growth cones were measured per experiment, per condition.



(Nakamura *et al.*, 2001) and recruit APC to the plus-end (Askham *et al.*, 2000). In a similar way to the CLIP170-APC-IQGAP, the EB1-APC complex may also regulate the interaction between the plus-ends of dynamic microtubules and actin filaments (Watanabe *et al.*, 2004). No changes in the levels of EB1 in growth cones treated with Wnt3a or control media were detected (Fig. 4.14 A-B). In DRG growth cones, EB1 localises to the tip of a subpopulation of tyrosinated microtubules. Interestingly, microtubules with EB1 at their plus-end were found at the neck and central regions of control growth cones, whereas EB1-tipped microtubules were found in the peripheral regions of Wnt3a treated growth cones. Despite finding no differences in the average levels of EB1 fluorescence in growth cones, more EB1 staining was observed along Wnt3a treated axons compared with controls. However, these differences may be due to the Wnt-induced increase in microtubule content, rather than a direct effect of Wnt3a on EB1.

4.3 Discussion

Expression of Dvl1 in DRG neurons mimics the effect of Wnt3a on axonal remodelling, suggesting that Dvl is a key transducer of the Wnt signal to the cytoskeleton. Two findings suggest Wnt3a-Dvl signalling activates the canonical Wnt signalling pathway: Firstly, pharmacological inhibition of Gsk-3β mimics the effect of Wnt3a and Dvl1 on the morphology of DRGs. Consistent these findings, a 50% increase in growth cone size and a 60% decrease in growth cone advance was found in chick DRGs exposed to either lithium or another direct Gsk-3β inhibitor: SB-216763 (Owen and Gordon-Weeks, 2003). Furthermore, Gsk-3β inhibition has been shown to mimic the effect of Wnt7a on granule cells and mossy fibres (Hall *et al.*, 2000; Lucas and Salinas, 1997). Secondly, an increase in β-catenin is observed in DRG neurons after Wnt3a treatment (Supplementary figure 1). However, blocking all transcriptional activity with actinomycin D does not inhibit Wnt-induced axonal remodelling, suggesting that the activation of Wnt target genes through β-catenin and TCF/LEF is not required. These data are consistent with previous findings showing that Dvl regulates microtubule stability through a divergent canonical signalling pathway that branches downstream of

Gsk-3β (Ciani *et al.*, 2004) and support the notion that Wnt signalling through a divergent canonical signalling pathway induces axonal remodelling.

The fact that both anisomycin and cyclohexamide block Wnt-induced remodelling indicates that protein translation is required. Similarly, the responses of retinal growth cones to Sema3A and netrin 1 have also been shown to be transcription independent and require protein translation (Campbell and Holt, 2001). Clusters of polyribosomes were first spotted in growth cones in 1970 (Tennyson, 1970) but it was not until mRNAs were detected in dendrites and axons (Bassell *et al.*, 1998; Kleiman *et al.*, 1994) that local protein synthesis was considered to be involved in axon growth and guidance. A potential candidate translated in response to guidance cues is β-actin mRNA, since it is localised to growth cones (Campbell and Holt, 2001; Zhang *et al.*, 1999). As has been found for netrin 1 and Sema3A, rapid and local changes in protein levels appear to underlie the effects of Wnts on axonal morphology.

To begin to address the effects of Wnt3a on the axonal cytoskeleton, the organisation and dynamics of microtubules were examined. The effects of Dvl1 on microtubules have been well documented (Ciani *et al.*, 2004; Krylova *et al.*, 2000). Dvl1 binds to the most stable pool of microtubules and confers microtubule stability (Krylova *et al.*, 2000). Examination of microtubules in DRGs exposed to Wnt3a revealed an increase in the amount of microtubules along axons and in growth cones compared to controls. Pseudocoloured images show that Wnt3a treated growth cones contain a higher microtubule density than controls. Since similar effects have been reported in neurons treated with Gsk-3β inhibitors (Zhou *et al.*, 2004; Goold *et al.*, 1999), the effect of Wnt3a on microtubule density is likely to be achieved through the inhibition of Gsk-3β. Inhibition of Gsk-3β could regulate axonal microtubule levels by promoting microtubule assembly or stabilisation (Yoshimura *et al.*, 2005; Zhou *et al.*, 2004) independently of gene transcription, as nuclear involvement has been ruled out in the remodelling effect of Wnt3a. Interestingly, Wnt3a increases both acetylated and tyrosinated microtubules rather than just the acetylated ones as has been reported in DRGs treated with Gsk-3β

inhibitors (Goold *et al.*, 1999), hence the increase in acetylated microtubules does not appear to be at the expense of the tyrosinated ones.

More striking is the effect of Wnt3a on microtubule organisation. Compared to the typical splayed distribution observed in most control growth cones, Wnt3a treated growth cones often contain looped microtubules. Examination of EB3-GFP comets in DRG neurons further confirmed the presence of looped microtubules in Wnt3a treated growth cones as the percentage of EB3-GFP comets moving across growth cones, rather than towards the leading edge, is significantly higher than controls. These time-lapse sequences prove that Wnt3a is able to alter the directionality of microtubule growth.

Microtubule looping was first reported by Tsui and colleagues in growth cones of spinal cord neurons examined by EM (Tsui *et al.*, 1984), and has subsequently been observed in living neurons (Schaefer *et al.*, 2002; Dent and Kalil, 2001; Dent *et al.*, 1999; Tanaka and Kirschner, 1991). Microtubule loops are found in pausing growth cones (Kalil *et al.*, 2000), but how they form is still unknown. It is possible that as microtubules polymerise in a non-advancing growth cone they bend to accommodate their increase in length. Another possibility is that interactions with actin filaments flowing retrogradely force microtubules to buckle. Simultaneous recordings of fluorescently labelled tubulin and actin may shed some light on this issue. In dividing cells, motor proteins have also been found to play a role in microtubule organisation thanks to their ability to zipper or splay microtubules (Sharp *et al.*, 2000). Functionally, microtubule looping may affect intrinsic binding properties of microtubules and may regulate the direction or amount of axonal transport. Alternatively, it has been suggested that microtubule loops control the localisation of vesicles, as large membranous organelles have been observed encaged within microtubule loops (Tsui *et al.*, 1984). Due to the reported effects of Wnts on presynaptic differentiation and the presence of microtubule loops in boutons at the *Drosophila* NMJ, it will be interesting to examine the role of microtubule loops during synaptogenesis.

In addition to Wnt3a, Wnt7a and FGF-2 have also been found to induce microtubule looping in enlarged growth cones (Dent *et al.*, 2004; Hall *et al.*, 2000). Since Wnt3a and FGF-2 decrease the rate of growth cone advance and Wnt3a and Wnt7a cause axonal shortening (Chapter 3, Dent *et al.*, 2004; Lucas and Salinas, 1997), it is likely that microtubule loops are indeed present in pausing growth cones. Data presented here suggests that the formation of microtubule loops (60 minutes after Wnt3a treatment) follows the decrease in axon advance (observed 20 minutes after Wnt3a treatment) rather than vice versa, and favour the idea that in the presence of Wnt, microtubule loops arise as microtubules continue to polymerise in a non-advancing growth cone. However, the EB3-GFP time-lapse recordings of DRG growth cones exposed to Wnt3a overnight would dispute this hypothesis as microtubules are seen to loose their directionality before they reach the leading edge (**see movies chapter 4**). Longer time-lapse recordings of the EB3-GFP excursions taken immediately after addition of Wnt3a should shed light on this matter. Such experiments would have to be carried out after one day *in vitro*, when axons have greatly reduced their outgrowth and the response to Wnt is not as well characterised, to allow for the expression of EB3-GFP.

To assess whether Wnt3a can mimic the effect of Dvl on microtubule dynamics, DRGs were exposed to nocodazole. Wnt3a confers resistance to nocodazole both along axons and in growth cones. Microtubule stability has been shown to decrease axon elongation in superior cervical ganglia neurons (Rochlin *et al.*, 1996; Tanaka *et al.*, 1995), but since it does not decrease the rate of axoplasm production (Rochlin *et al.*, 1996), microtubule stability can lead to an increase in growth cone size. These effects are consistent the finding that Wnt3a decreases the rate of axon elongation before inducing an increase in growth cone size (Fig.3.15). Unfortunately, due to the fact that Wnt induces axonal remodelling within two hours and the current method employed to assess microtubule stability requires at least two hours exposure to nocodazole, it was not possible to determine the exact time point in the sequence of events leading to axonal remodelling when Wnt-induced microtubule stabilisation takes place.

Microtubule stabilisation has been observed following the capture of the plus-end of dynamically unstable microtubules by cortical actin particles and appears to be necessary for the acquisition of cell polarity (Goode *et al.*, 2000). A growing number of proteins have been shown to locate to the plus-end of microtubules, and there is increasing evidence of their importance in mediating interactions between microtubule ends and cortical actin (for review see Howard and Hyman, 2003). Examination of the levels of two plus-end binding proteins, EB1 and APC, in growth cones, revealed no significant differences between control and Wnt3a treated neurons. It is possible that Wnts induce small, local and/or temporary changes in the levels or binding affinities of these proteins, which cannot be readily detected in the experiments described. Interestingly, more EB1 was found along axons and on microtubules projecting to peripheral regions of growth cones in Wnt3a treated neurons than controls. These findings hint at the possibility that Wnt3a can alter directly or indirectly (due to the effects on microtubule content) the localisation of EB1. The levels and localisation of EB1 and two other plus-end binding proteins, which are also Gsk-3β targets, CLIP-170 and CLASP-2 (Akhmanova *et al.*, 2001), in response to Wnt treatment and Dvl1 expression, are currently being examined in detail.

MAPs have also been shown to induce microtubule stability (Drewes *et al.*, 1998). Indeed, it has been previously shown that MAP-1B is a Wnt-signalling target in primary neurons. Inhibition of Gsk-3β, with drugs, by Wnt7a treatment or Dvl1 expression, leads to a decrease in the phosphorylation of MAP-1B (Ciani *et al.* 2004; Goold *et al.*, 1999; Lucas *et al.*, 1998). MAP-1B protects microtubules against nocodazole depolymerisation, but phosphorylation of MAP-1B by Gsk-3β abolishes this protective effect (Goold *et al.*, 1999). Expression of high levels of MAP-1B-P results in a decrease of dynamic microtubules, whereas expression of low levels of MAP-1B-P leads to an increase in stable microtubules (Goold *et al.*, 1999). Goold and colleagues suggest that Gsk-3β-mediated phosphorylation of MAP-1B interferes with post-translational modifications of tubulin. Hence, it is possible that in the presence of Wnt, microtubules are more easily acetylated and detyrosinated becoming more stable than in controls. Unfortunately due to the fact antibodies against MAP-1B-P also recognise

neurofilaments present in DRGs, it was not possible to examine changes in the levels of MAP-1B-P in response to Wnt3a by immunofluorescence.

Curiously, analyses of the rate of EB3-GFP comet movement, which reflects microtubule growth, revealed no differences between Wnt3a and control treatments. The rate of EB3-GFP comet movement in DRGs are slightly lower than those reported for microtubule growth in other cell types. The average velocity of EB3-GFP has been reported to be 0.21 ± 0.08 μm/sec in hippocampus cell axons, and 0.21 ± 0.04 μm/sec in purkinje cell axons (Stepanova *et al.*, 2003). These differences may be due to the rate of axon outgrowth. From the moment they are plated, DRGs extend neurites extremely quickly, but after 16 hours in culture, when the rates of EB3-GFP movement were analysed, axons have practically ceased to extend further. Hippocampal and cortical neurons on the other hand, continue to rapidly extend processes after 3-4 days in culture. This suggestion would imply a direct correlation between the rate of microtubule growth and axon outgrowth, but there is little evidence of this in the literature. Analyses of the mean duration of EB3-GFP excursions (which reflects microtubule growth lifetime) or of the transport of microtubule polymer may reveal a yet undiscovered effect of Wnts on microtubule growth.

To summarise, Wnt3a-induced axonal remodelling in DRGs is mimicked by Dvl1 expression and Gsk-3β inhibition. Interestingly, the remodelling activity of Wnt3a does not require gene transcription but does involve translation. Together, these findings suggest that Wnt3a signals through a divergent canonical pathway to trigger changes in axonal morphology. Wnt3a affects both microtubule organisation and dynamics in DRGs. Wnt3a increases the amount of microtubules along axons and in growth cones, increases microtubule stability and induces the formation of microtubule loops. However, Wnt3a does not affect the rate of microtubule growth. The mechanisms through which Wnts and Dvl induce microtubule stability and looping in DRG neurons are likely to involve a decrease in MAP-1B-P as has been shown in mossy fibres exposed to Wnt7a (Lucas *et al.*, 1998), and changes in the levels or localisation of microtubule plus-end binding proteins.

CHAPTER 5:

Wnt3a affects the organisation and dynamics of actin filaments in growth cones.

5.1 Introduction

The findings described so far have shown that Wnt3a affects axonal behaviour and the dynamics and organisation of microtubules in DRG neurons. However, some of the effects of Wnts on axonal morphology such as the increase in growth cone size, and changes in growth cone motility, suggest that Wnts could be inducing changes in the actin cytoskeleton as well. The Wnt signalling pathways offer several potential links to actin regulating proteins. For example, the canonical Wnt signalling pathway leads to an increase in β-catenin (Wodarz and Nusse, 1998) which has been shown to affect the actin cytoskeleton through cadherins, thus altering the adhesive properties of cells (Barth *et al.*, 1997). Activation of the Wnt-Ca^{+2} pathway could also lead to changes in the actin cytoskeleton, as calcium transients can regulate growth cone advance (Tang *et al.*, 2003; Gomez and Spitzer, 1999). In addition, Dishevelled has been shown to colocalise with actin filaments and is able to activate both Rac and Rho in non-neuronal cells through the planar cell polarity pathway (Habas *et al.*, 2003; Capelluto *et al.*, 2002; Winter *et al.*, 2001; Fanto *et al.*, 2000). In neurons, Dishevelled has been shown to bind actin filaments in growth cones and to activate Rac in hippocampal neurons (Rosso *et al.*, 2005). However, it remains to be determined whether activation of Rac and changes in the actin cytoskeleton underlie some of the effects of Wnt-induced axonal remodelling.

This chapter will focus on the effects of Wnt3a on the actin cytoskeleton of DRG neurons. A pharmacological approach combined with time-lapse microscopy was used to demonstrate for the first time that Wnts affect the dynamics and organisation of the actin cytoskeleton in growth cones.

5.2 Results

5.2.1 Wnt3a causes an accumulation of F-actin in growth cones.

To examine actin filaments, DRG neurons were stained with rhodamine conjugated phalloidin, a toxin from the *Amanita phalloides* mushroom that binds polymerised actin filaments (Wulf *et al.*, 1979). F-actin is concentrated in growth cones, particularly at the leading edge, and in filopodia (Letourneau, 1983). Examination of F-actin in growth cones exposed to Wnt3a or control media for two hours reveals that the fluorescence intensity of F-actin is higher in Wnt3a treated growth cones compared with controls (Fig.5.1 A). This effect becomes clearer in the pseudocoloured images. The growth cone area with the brightest levels of F-actin was measured (white and red area in pseudocoloured images) and was found to be significantly larger in Wnt3a treated growth cones compared to controls (control: 13.13 ± 1.85 μm^2, Wnt3a: 43.98 ± 3.05 μm^2, $p<0.001$. Fig.5.1 B). To ensure the differences were not just due to the Wnt3a-induced increase in growth cone size, growth cones of similar sizes were compared (Fig.5.1 A) and the percentage of total growth cone area with high F-actin levels was measured (Fig.5.1 C). In control neurons 33% of the total growth cone area contains high levels of F-actin, whereas in Wnt3a treated neurons 44% of the total growth cone area contains high levels of F-actin ($p<0.05$). This result suggests that Wnt3a increases F-actin in growth cones irrespective of their size.

To determine the time required for Wnt3a to increase F-actin levels in growth cones time course experiments were carried out. DRG neurons were treated with Wnt3a or control media for different lengths of time. Quantification of the F-actin area in growth cones reveals that Wnt3a induces an accumulation of F-actin in growth cones within 15 minutes of application (Fig.5.2). These experiments suggest that changes in F-actin not only precede the Wnt-induced changes in axonal remodelling (Fig.3.12), but also changes in microtubule organisation (Fig.4.7).

5.2.2 Examination of actin filament organisation in growth cones by electron microscopy.

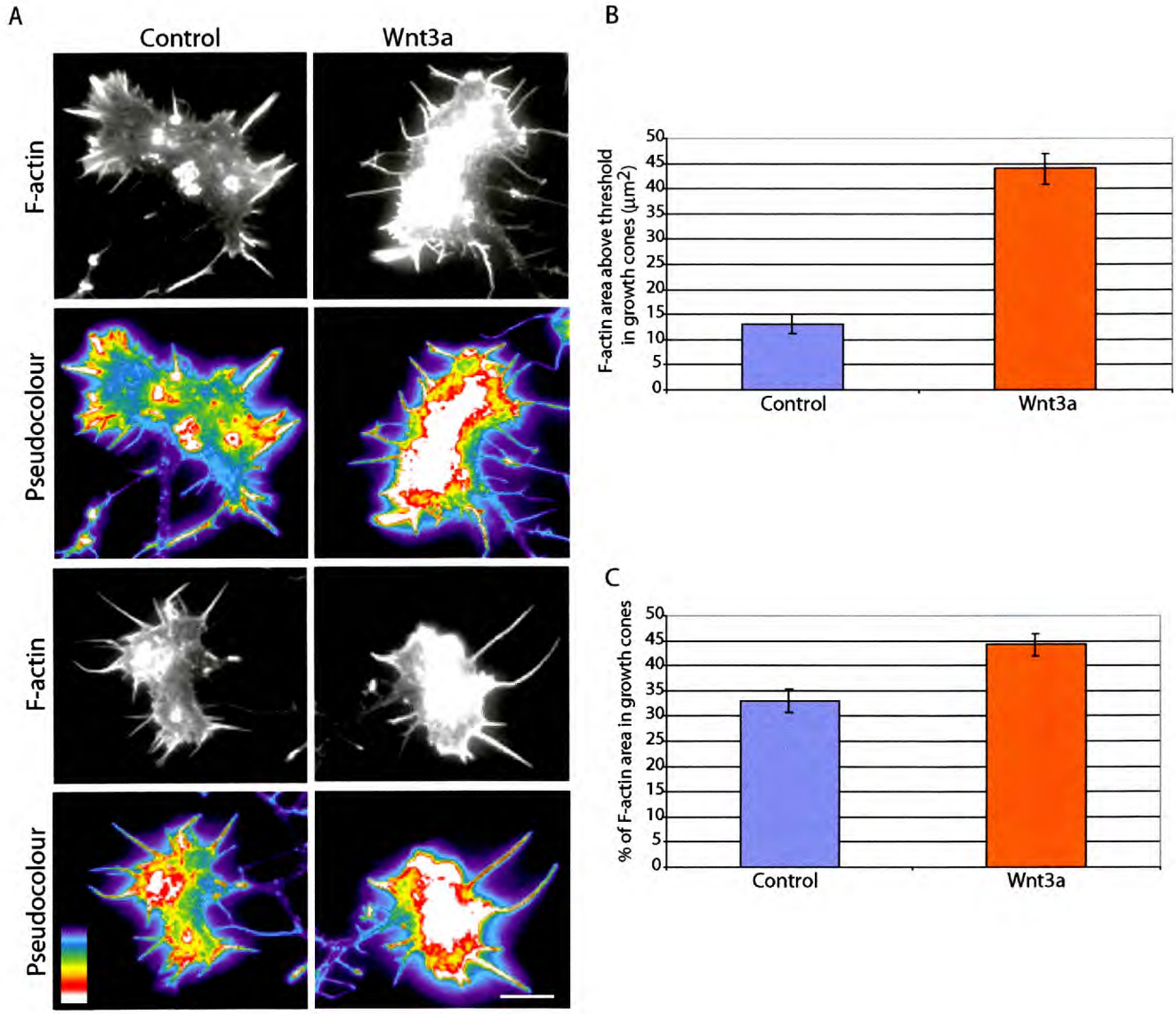


Figure 5.1. Wnt3a increases F-actin levels in growth cones.
(A) Pseudocouloured images of growth cones labelled with rhodamine phalloidin highlight the differences in F-actin levels between Wnt3a and control treated cells. Bar, 10µm.(B) The area of growth cones with bright F-actin staining (red and white in pseudocoloured images) is larger in Wnt3a treated growth cones than controls ($p<0.001$). To ensure this effect is not due to the fact that Wnt3a treated growth cones are larger in size, the percentage of total growth cone area with bright F-actin fluorescence was measured (C). A larger percentage of growth cone area contains bright levels of F-actin in Wnt3a treated cells than controls ($p< 0.05$). Values are mean ± SEM from 3 independent experiments (at least 48 growth cones were analysed per condition).

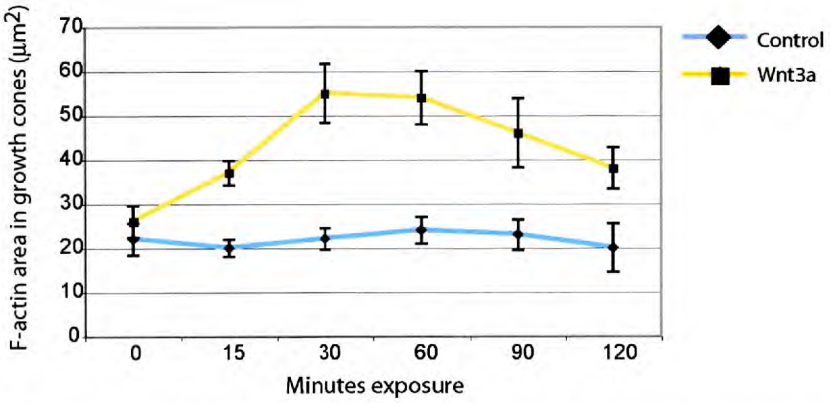


Figure 5.2. Wnt3a causes an accumulation of F-actin in growth cones within 15 minutes of application.
The F-actin area in Wnt3a treated growth cones increases significantly 15 minutes after application ($p<0.01$). Values are mean ± SEM from three independent experiments (at least 35 growth cones were measured per condition).

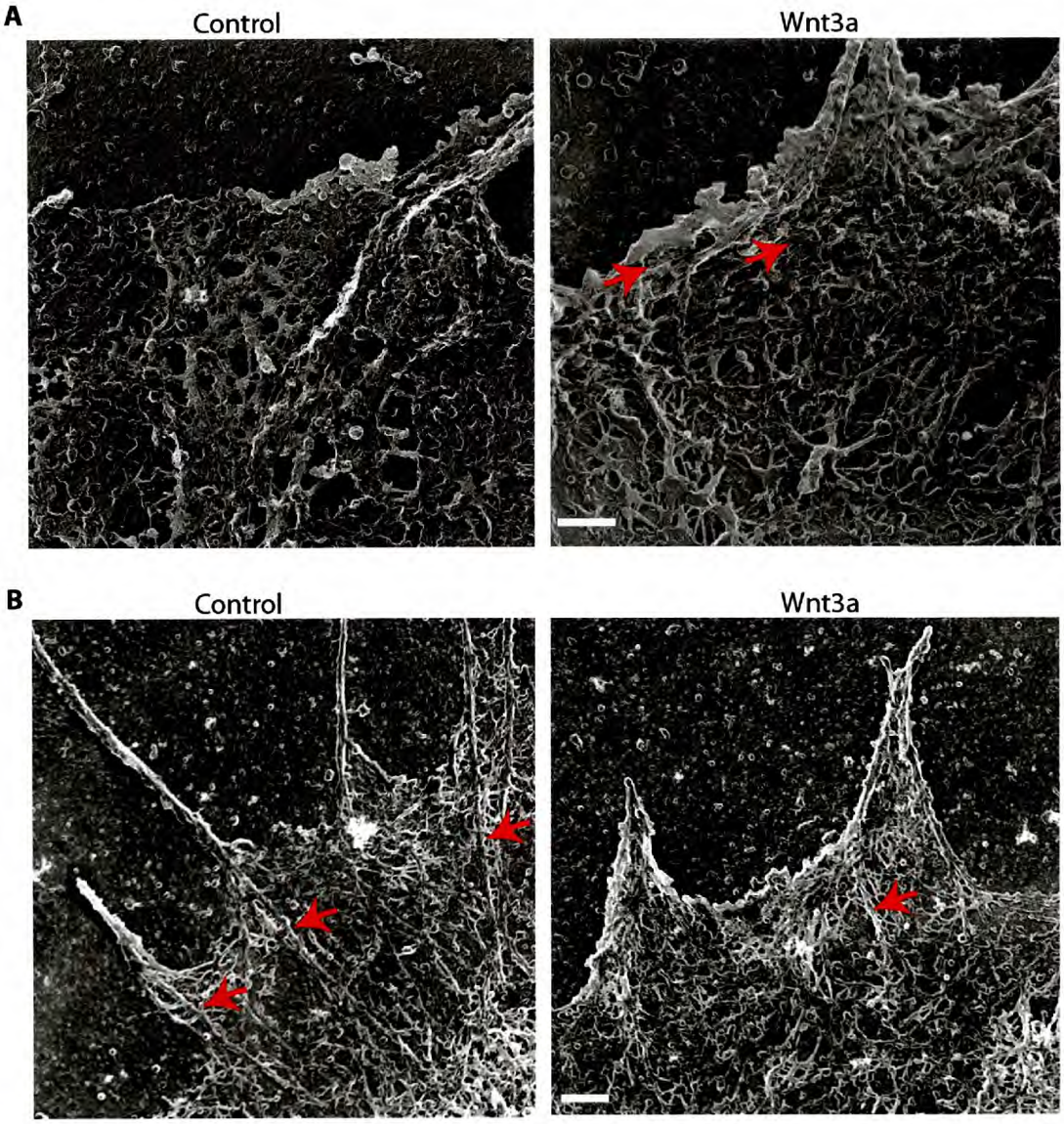


Figure 5.3. Wnt3a induces changes in the organisation of actin filaments in growth cones.
(A) The actin meshwork is more densely packed in lamellas of Wnt3a treated growth cones and more filaments appear to align parallel to the leading edge (arrows). (B) There are fewer radial actin filament bundles in Wnt3a treated growth cones (see arrows). Bar, 200nm.

Due to the influence of the organisation of actin filaments on growth cone morphology and the organisation of microtubules (Zhou *et al.*, 2002; Zhou and Cohan, 2001; Fan *et al.*, 1993), the organisation of actin filaments in Wnt3a treated growth cones was examined by electron microscopy. Growth cone lamellas contain dense meshworks of actin filaments, while filopodia are composed of straight radially projecting bundles of filaments (Fig.5.3). In Wnt3a treated growth cones, spread lamellas contain a higher density, or tighter mesh, of actin filaments than controls, which is consistent with previous observations of a higher actin content. In addition, Wnt3a causes more actin filaments to align parallel to the leading edge than in controls (Fig.5.3 A arrows). No significant differences in filament length or branching were observed. Since radial actin bundles act as tracks for microtubules, causing them to splay and allowing them to reach the periphery of growth cones (Zhou and Cohan, 2004; Gordon-Weeks, 1991), the effect of Wnt3a on actin bundles was examined. Interestingly, fewer radial actin bundles are found in the large spread Wnt3a treated growth cones than controls (Fig.5.3 B arrows). Thus, the presence of fewer radial actin bundles, could explain why fewer microtubules project to the periphery, and are therefore unable to drive growth cone advance, in the presence of Wnt3a.

5.2.3 Wnt3a causes actin filaments to depolymerise faster in growth cones.

To determine whether Wnt3a is altering actin dynamics in growth cones, neurons were exposed to different concentrations of the actin depolymerising drugs cytochalasin D and latrunculin B, and the decrease in F-actin area in growth cones was measured. Both drugs are widely used to disrupt the actin cytoskeleton in neurons (Lalli *et al.*, 2003; Zhou *et al.*, 2002; Dent and Kalil, 2001; Bradke and Dotti, 1999; Forscher and Smith, 1988). Cytochalasin D inhibits subunit assembly and disassembly at barbed ends (Brenner and Korn, 1980), while latrunculin inhibits actin polymerisation by sequestering actin monomers (Spector *et al.*, 1989). For these experiments, DRG neurons were treated with Wnt3a for two hours and the depolymerising drugs were

added 30 minutes prior to fixation. In the presence of cytochalasin D or latrunculin B, the effect of Wnt3a on actin accumulation is abolished (Fig.5.4 B-C). However, Wnt3a is still able to induce an increase in growth cone size (Fig.5.4 A).

Surprisingly, treatment with cytochalasin D or latrunculin B leads to a much more rapid decrease in F-actin area in Wnt3a treated growth cones than in controls (Fig.5.4 B-C). Treatment with cytochalasin D results in a significant decrease in the F-actin area in both control and Wnt3a treated growth cones. In controls the F-actin area in growth cones decreases from 13.9 ± 0.98 μm^2 in the absence of drug to 7.54 ± 0.97 μm^2 in the presence of 2 μM cytochalasin D, this represents a 45.7% decrease. In Wnt3a treated growth cones the F-actin area decreases from 38.10 ± 5.02 μm^2 in the absence of drug to 16.20 ± 1.93 μm^2 in the presence of 2 μM cytochalasin D, which represents a 57.4% decrease (Fig.5.4 A). Similarly, treatment with 5 μM cytochalasin D results in a 52% decrease of F-actin area in control growth cones, whereas in Wnt3a treated growth cones the F-actin area decreases 72% (Fig.5.4 B). Latrunculin B was found to have a stronger effect on actin depolymerisation. Treatment with 0.5 μM latrunculin for 30 minutes causes a significant decrease in F-actin area in growth cones of both control and Wnt3a treated neurons (Fig.5.4 C), however, there is a sharper decrease in Wnt3a treated growth cones. Despite there being 2.6 times more F-actin area in Wnt3a treated growth cones, after treatment with 0.5 μM latrunculin B the F-actin area is similar to that found in control growth cones exposed to the drug. Together, these findings show that Wnt3a makes the actin cytoskeleton more susceptible to depolymerisation in growth cones, and suggest that actin is more dynamic in the presence of Wnt3a.

To further examine the effect of Wnt3a on actin dynamics, short time courses with lower concentrations of cytochalasin D and latrunculin B were performed (Fig.5.5 A-C). 1 μM cytochalasin D and 0.1 μM latrunculin B were used as they do not cause significant changes in the F-actin area in control growth cones over the course of 6 minutes. However, filopodia do start to disappear and F-actin aggregates begin to form (Fig.5.5 A), proving that the drugs are working (Forscher and Smith, 1988). In contrast to controls, the F-actin area in Wnt3a treated growth cones decreases significantly 2

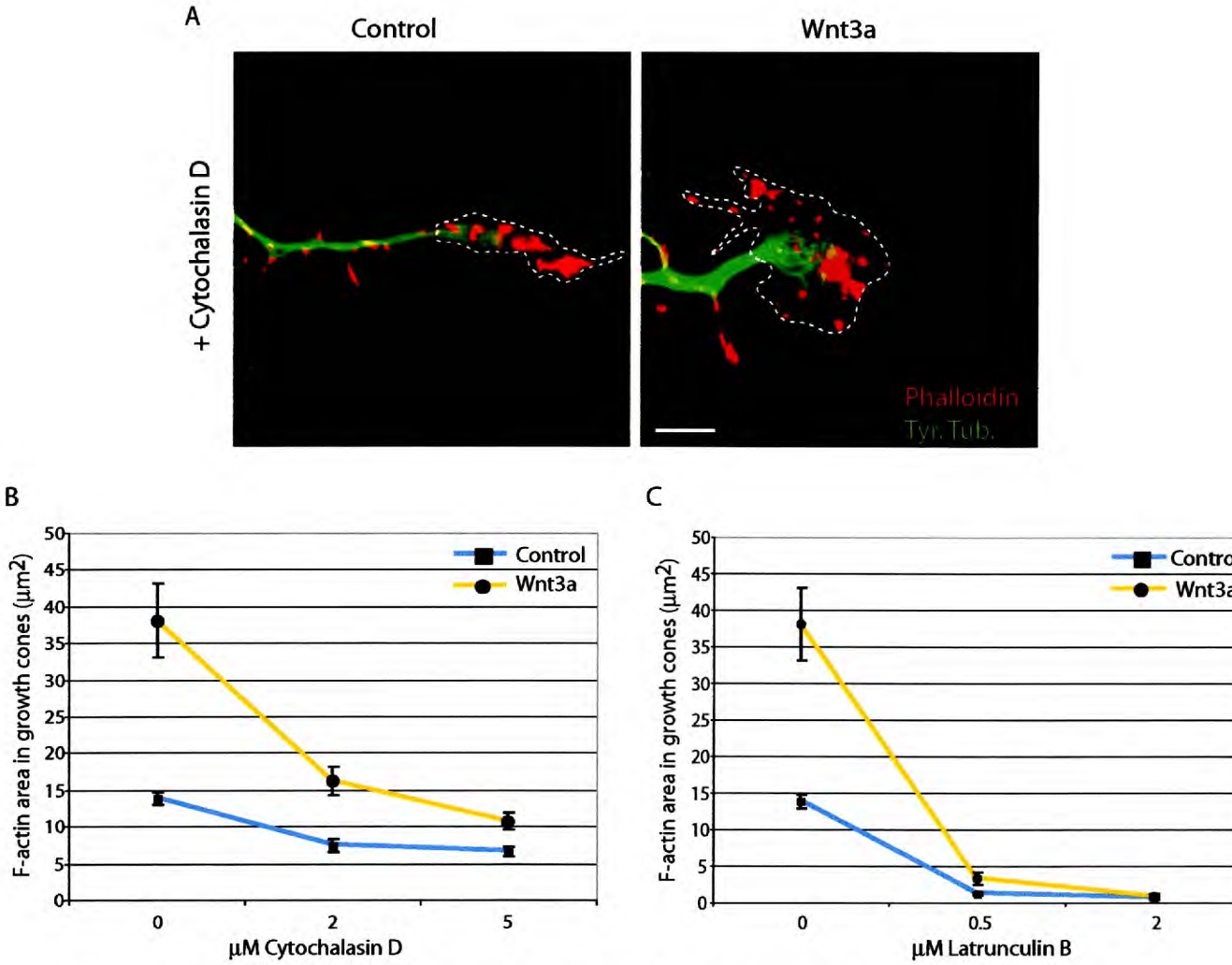


Figure 5.4. Exposure to cytochalasin D or latrunculin B causes the F-actin area in growth cones to decrease faster in the presence of Wnt3a.

(A) Despite the presence of cytochalasin D, Wnt3a treated growth cones remain enlarged. Bar, 10µm. However, cytochalasin D causes a greater decrease in F-actin area in growth cones of Wnt3a treated neurons than controls (B). Latrunculin B also causes a sharper decrease in F-actin area in Wnt3a treated growth cones than controls (C). Values are mean ± SEM from three independent experiments (the F-actin fluorescence in at least 43 growth cones was measured per condition).

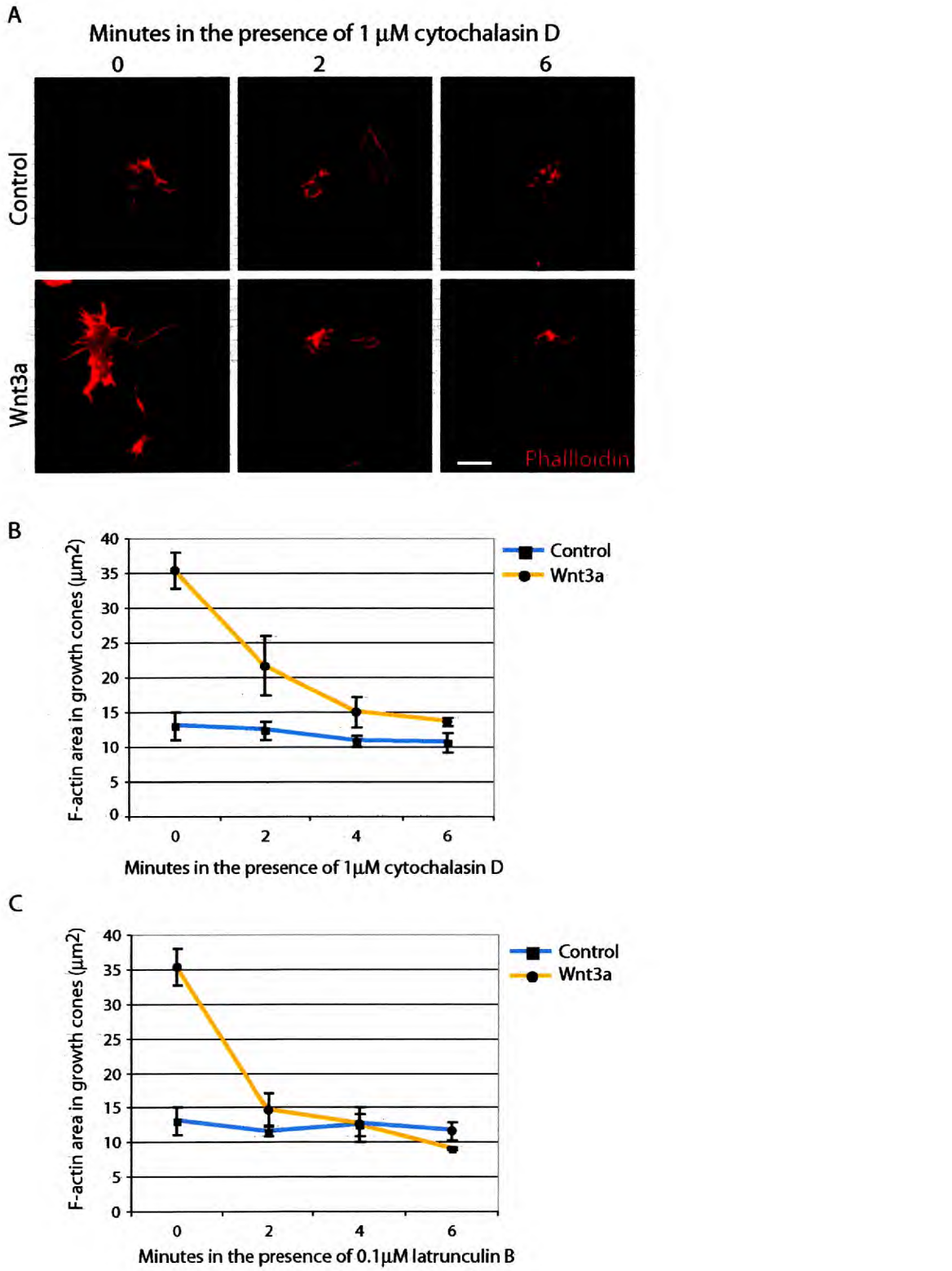


Figure 5.5. Actin filaments depolymerise faster in the presence of Wnt3a.
(A) Short exposure to 1µM cytochalasin D causes the loss of filopodia and the formation of F-actin aggregates in growth cones. However, while the F-actin fluorescence in control growth cones does not decrease, there is a marked reduction in F-actin fluorescence in Wnt3a treated growth cones. Bar, 10µm. (B) Quantification indicates exposure to 1µM cytochalasin D for just 2 minutes causes a significant reduction in F-actin area in Wnt3a treated growth cones ($p<0.05$), but not in controls. (C) Equally, exposure to 0.1µM latrunculin B for only 2 minutes causes a significant decrease in F-actin area in Wnt3a treated growth cones ($p<0.01$) but not in controls. Values are mean ± SEM from three independent experiments (the F-actin area in at least 30 growth cones was measured per condition per experiment).

minutes after addition of either drug. In the presence of cytochalasin D or latrunculin B, the F-actin area in Wnt3a treated growth cones decreased by 38.8% and 58.3% respectively, whereas in controls there is only a 5.8 and 12% decrease (Fig.5.5 B-C). These results further demonstrate that in the presence of Wnt3a the F-actin depolymerises faster than in control growth cones suggesting that Wnt3a induces actin instability.

5.2.4 Wnt3a causes actin filaments to polymerise faster in growth cones.

Although Wnt3a increases actin instability, Wnt3a also increases the amount of F-actin in growth cones. These results suggest that Wnt3a might affect the rate of actin polymerisation. To investigate whether Wnt3a increases actin polymerisation in DRG neurons, recovery experiments were set up adapting a protocol from Grabham *et al.* (2003). Four hours after plating, neurons were treated with concentrations of cytochalasin D that deplete actin filaments from the peripheral region of growth cones for 20 minutes. The neurons were then allowed to recover in the presence of control or Wnt3a media for 30 minutes. Due to variability in the depolymerisation and recovery of F-actin levels between experiments, the results of three independent experiments were normalised. When growth cones are allowed to recover from cytochalasin D treatment in the presence of Wnt3a, there is a 3-fold increase in the accumulation of F-actin (measured as F-actin area) compared to controls (Fig.5.6 A-B). In controls, the extent of F-actin recovery appears to be dependent on the concentration of cytochalasin D, as a greater recovery was achieved with the lowest concentration of the drug (500 nM). The effect of Wnt3a on F-actin recovery was best observed after treatment with 1000 nM cytochalasin D (Fig.5.6 A-B). At this concentration, there is very little, if any, recovery of F-actin fluorescence in controls, yet the levels of F-actin in growth cones treated with Wnt3a for 30 minutes are greatly increased. These results suggest that Wnt3a increases the polymerisation of actin in growth cones within 30 minutes of application. Together with the previous finding that Wnt3a increases actin depolymerisation in growth cones, these results suggest that Wnt3a increases actin dynamics.

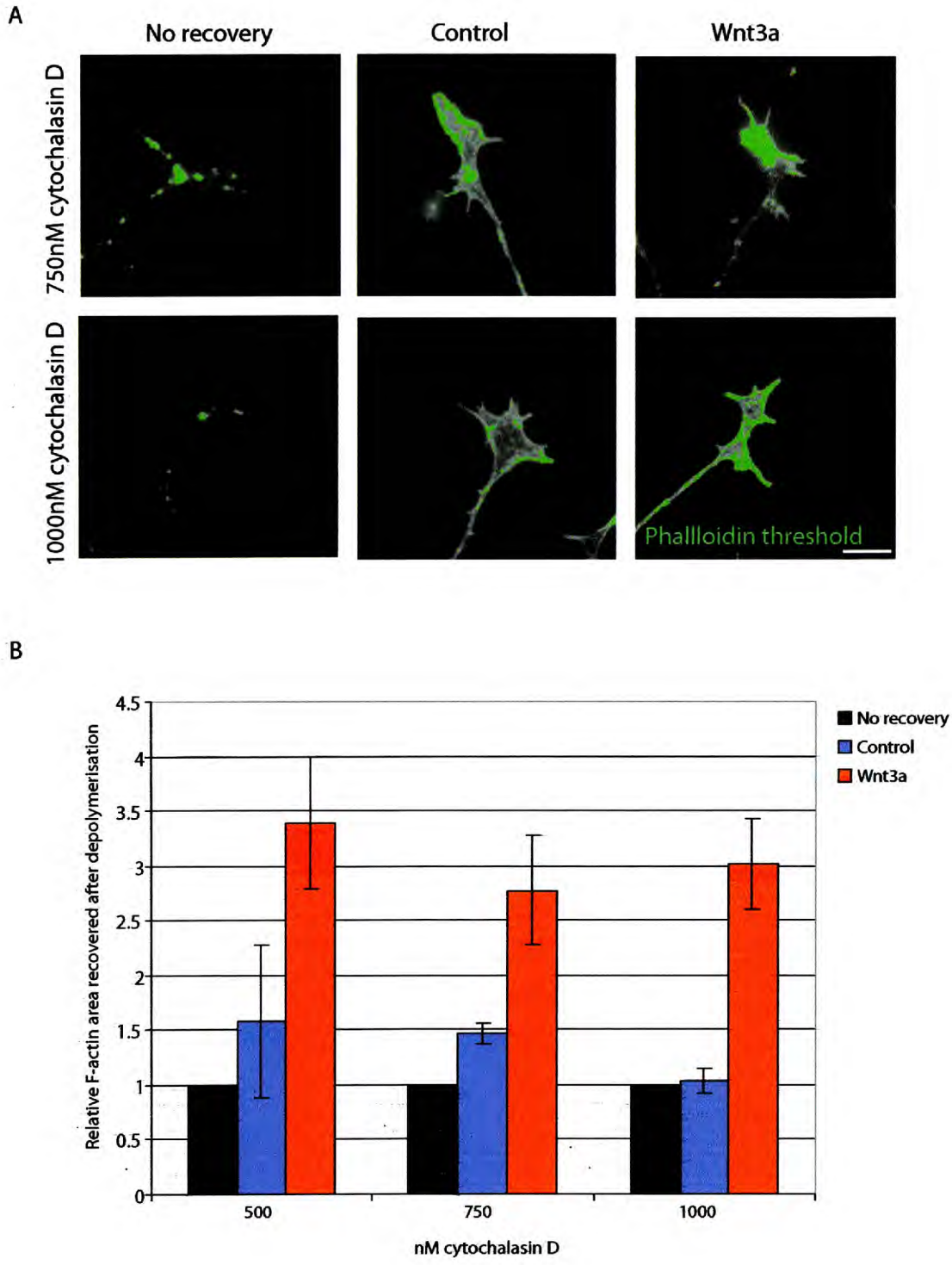


Figure 5.6. Actin polymerises faster in the presence of Wnt3a.
(A) After treatment with cytochalasin D, the F-actin area in growth cones is recovered faster in the presence of Wnt3a than control media. Bar, 10µm. (B) Quantification of the recovery of F-actin fluorescence after treatment with cytochalasin D in the presence of Wnt3a compared to controls (after 1000nM cytochalasin $p<0.05$). Values are relative to F-actin area in growth cones fixed after treatment with cytochalasin D from three independent experiments (at least 27 growth cones were analysed per condition).

5.2.5 Examination of the effect of Wnt3a signalling on the actin cytoskeleton by time-lapse microscopy.

To gain further insight into the effects of Wnt3a on the actin cytoskeleton, DRG neurons were transfected with fluorescently labelled actin. The GFP-β-actin fusion protein can incorporate into native actin filaments and therefore is a valuable tool to study actin dynamics in living cells (Ballestrem *et al.*, 1998). *In vitro* experiments have shown that GFP-β-actin expression does not interfere with cell motility when the levels of fusion protein do not exceed 30% of the native actin (Westphal *et al.*, 1997). In order to avoid this deleterious effect, the β-actin promoter itself is commonly used to control the transcription rates (Ballestrem *et al.*, 1998). Several laboratories have successfully monitored actin dynamics in living neurons with a similar GFP-β-actin construct (Okamoto *et al.*, 2004; Fischer *et al.*, 1998).

To ensure that GFP-β-actin is being incorporated into actin filaments, DRG neurons expressing GFP-β-actin were counter-stained with rhodamine phalloidin. The high degree of co-localisation indicates that GFP-β-actin is being incorporated to native actin filaments (Fig.5.7 A). Furthermore, neuronal morphology was not affected by GFP-β-actin expression (data not shown). DRG neurons were electroporated with GFP-β-actin before plating and exposed to control or Wnt3a media two hours later. Time-lapse recordings were carried out the following day to allow for the expression of the construct. Filopodia velocity and lamellar protrusion were examined. The speed of growth cone filopodia was measured by tracking their tips over consecutive frames. Recordings were three to five minutes long with frames captured every 20 seconds. Interestingly, the speed of filopodia is significantly higher in neurons exposed to Wnt3a compared to controls (control: 0.031 ± 0.001 μm/sec, Wnt3a: 0.057 ± 0.008 μm/sec. $p<0.05$. Fig.5.7 B). No significant differences in the number of filopodia per growth cone were found between control and Wnt3 treatments (control: 7.15 ± 2.08, Wnt3a: 7.70 ± 1.24).

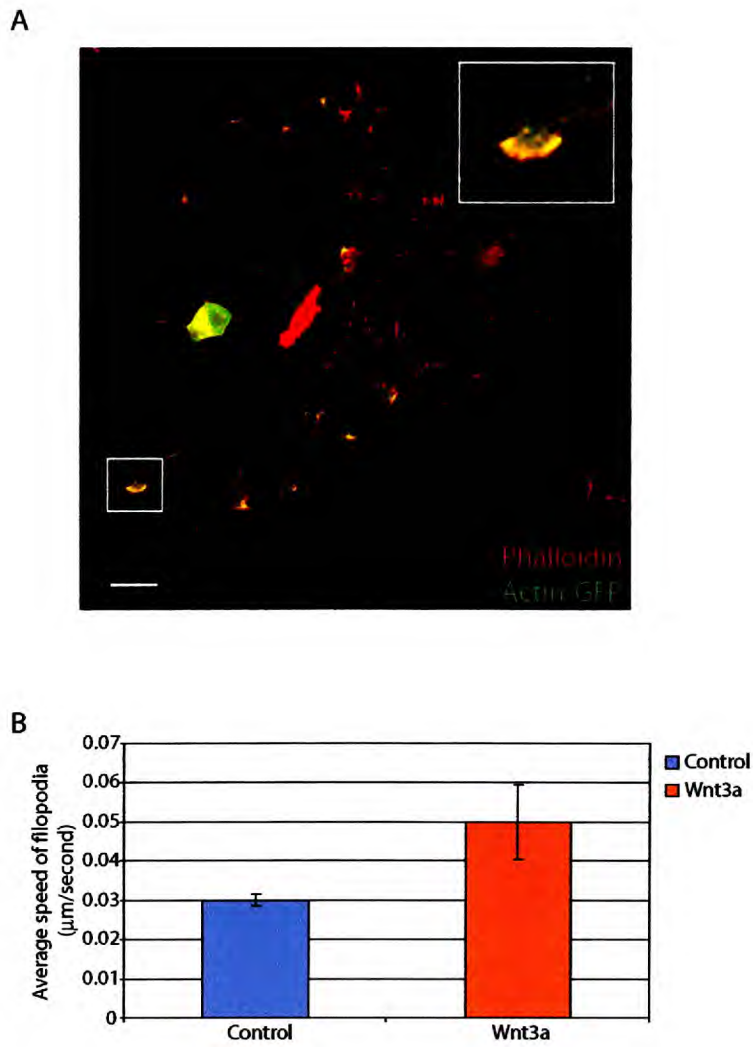


Figure 5.7. GFP-β-actin incorporates into native actin filaments in growth cones and is a useful tool for examining actin dynamics in growth cones.
(A) DRG neuron expressing GFP-β-actin fixed and stained with phalloidin. GFP-β-actin colocalises with native actin filaments, see inset. Bar, 30μm. (B) Wnt3a significantly increases the speed of filopodia movement ($p<0.05$). Values are mean ± SEM of data gathered from 3 independent experiments (the speed of at least 142 filopodia were measured per condition).

Another characteristic frequently observed in Wnt3a treated growth cones is the protrusion of lamella (Fig.5.8 A and **see movies chapter 5**). The relative percentage of lamellar perimeter undergoing protrusion was quantified from time-lapse frames captured 60 seconds apart. Indeed, Wnt3a significantly increases the percentage of lamellar perimeter undergoing protrusion compared to controls (control: 19.58 ± 2.99%, Wnt3a: 32.77 ± 1.15%, $p<0.05$. Fig.5.8 B). The Wnt3a-induced increase in both lamellar protrusion and speed of filopodia is consistent with previous findings showing Wnt3a increases actin dynamics and growth cone motility (Fig. 5.5, 5.6, **movies chapter 3**).

5.2.6 Examination of actin regulating proteins that could potentially mediate the effects of Wnt3a on actin dynamics.

To begin to identify proteins that mediate the effect of Wnt3a on actin dynamics, the localisation and levels of actin regulating proteins were examined by immunofluorescence. Since Wnt7b increases the activity of Rac in hippocampal neurons (Rosso *et al.*, 2005) and Rac1 is a positive regulator of lamellar protrusion (Luo, 2000; Nobes and Hall, 1995), phosphorylated p21-activated kinase (P-PAK) was examined in Wnt3a treated neurons. PAK, is a Rac effector which becomes active upon phosphorylation (Manser *et al.*, 1994), thus P-PAK can be used as a read-out of Rac activity. P-PAK activates LIM domain-containing kinase (LIMK) leading to the downregulation of cofilin activity and inhibition of actin depolymerisation (Luo, 2002). In DRG neurons, P–PAK is localised mainly in the centre of growth cones and to a lesser extent in the periphery of the lamellas (Fig. 5.9). However, when neurons were treated with Wnt3a for two hours, no differences in the localisation or levels of P-PAK were found with respect to control growth cones.

The effects of Wnt3a on actin dynamics suggest Wnt3a increases actin polymerisation. The Arp2/3 complex is able to induce the polymerisation of new filaments as well as branching of existing ones in fibroblasts (Pollard and Beltzner, 2002). Interestingly, Arp2/3 in growth cones negatively regulates growth cone translocation (Strasser *et al.*, 2004). The localisation and levels of p34-Arc, a subunit of the Arp2/3 complex was

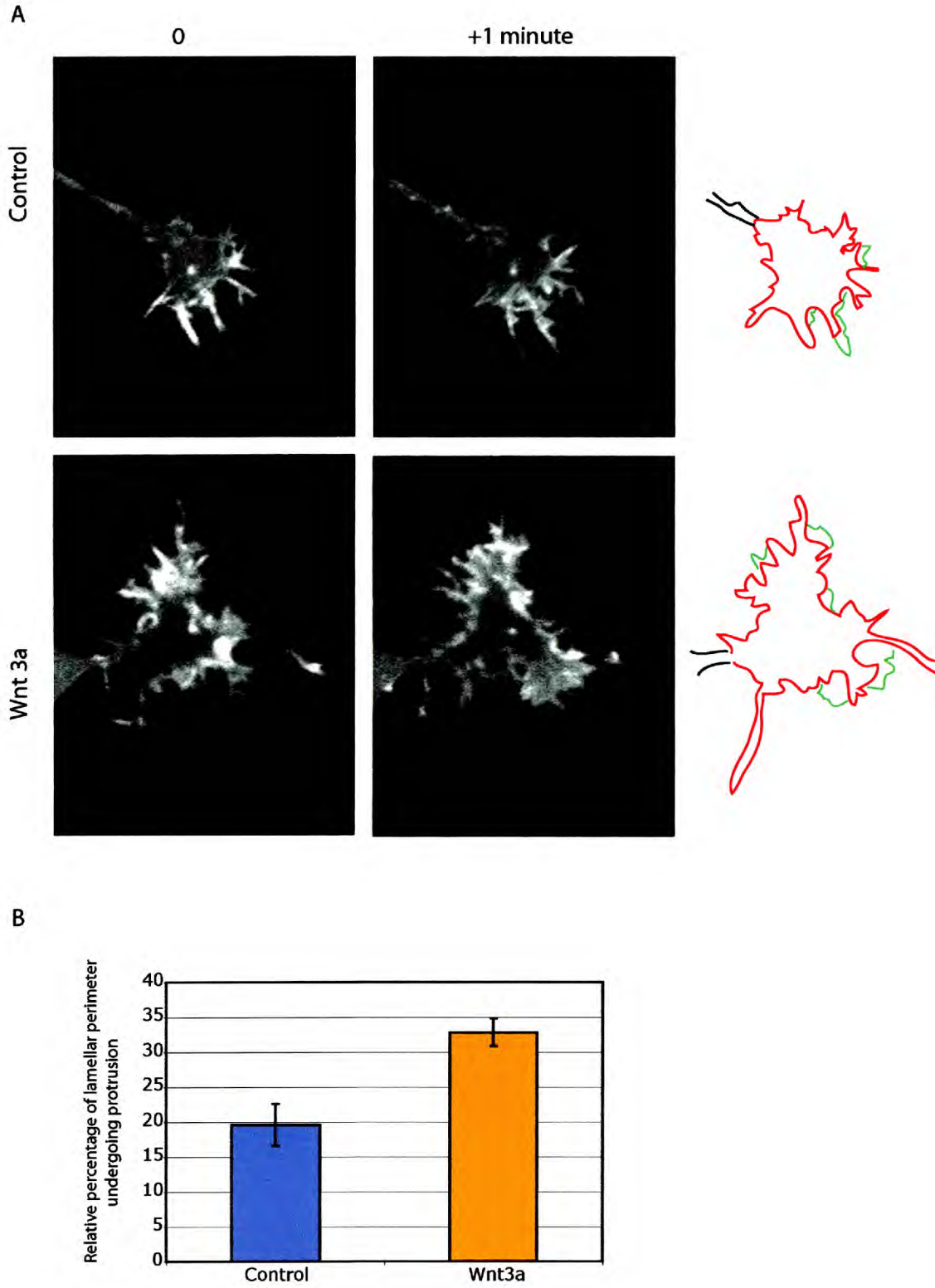


Figure 5.8. Wnt3a increases lamellar protrusion.
(A) Still frames from time-lapse recordings of GFP-β-actin expressing neurons exposed to control or Wnt3a and tracings of perimeter (protruded perimeter depicted in green). (B) Quantification shows Wnt3a significantly increases the percentage of lamellar perimeter undergoing protrusion ($p<0.05$). Values are mean ± SEM from 3 independent experiments, at least 12 growth cones were analysed per condition.

examined in Wnt3a treated growth cones (Fig.5.9). As previously reported (Strasser *et al.*, 2004), p34-Arc is enriched in the neurite shafts and the central region of growth cones rather than the periphery (Fig.5.9). However, no differences in the level or distribution of p34-Arc were found between Wnt3a and control treated growth cones.

Finally, since Wnt3a induces lamellar protrusion and growth cone spreading, which requires the incorporation of plasmalemmal precursor vesicles into the cell surface (Pfenninger *et al.*, 2003), a protein involved in vesicle transport: myosin-V (Espreafico *et al.*, 1992), was examined. Myosin-V is the primary actin-based motor responsible for short-range transport in neuronal cells (Tabb *et al.*, 1998), and forms a heteromotor complex with kinesin (Stafford *et al.*, 2000), which suggests it could be involved in the transition of vesicles between microtubules and actin. Myosin-V co-localised with F-actin at the periphery of growth cones, but is also found in the centre of the growth cones and in neurite shafts (Fig. 5.9). Again, no significant differences in the levels or localisation of myosin-V were found between control and Wnt3a treated growth cones.

5.2.7 Examination of the effect of Wnt3a signalling on actin retrograde flow in growth cones of DRG neurons.

Back in the 1970s, Bray, one of the pioneers in the study of growth cone motility, observed that inert particles placed on the surface of the growth cone would move in a retrograde direction, suggesting that there is a centripetal flux of membrane or actin filaments (Bray, 1970). Since then, the study of this retrograde flow has greatly advanced thanks to the analysis of actin dynamics in Aplysia growth cones (Schaefer *et al.*, 2002; Suter *et al.*, 1998; Lin *et al.*, 1996; Lin and Forscher, 1995). Work from the Forscher lab has demonstrated that the retrograde flux is actually due to the assembly of actin filaments at the leading edge or growth cone periphery, followed by retrograde translocation and filament disassembly at the centre of the growth cone (Forscher *et al.*, 1992). This process has been observed in a wide variety of motile cells and appears to be fundamental for directed cell motility (Cramer *et al.*, 1994; Bray and White, 1988).

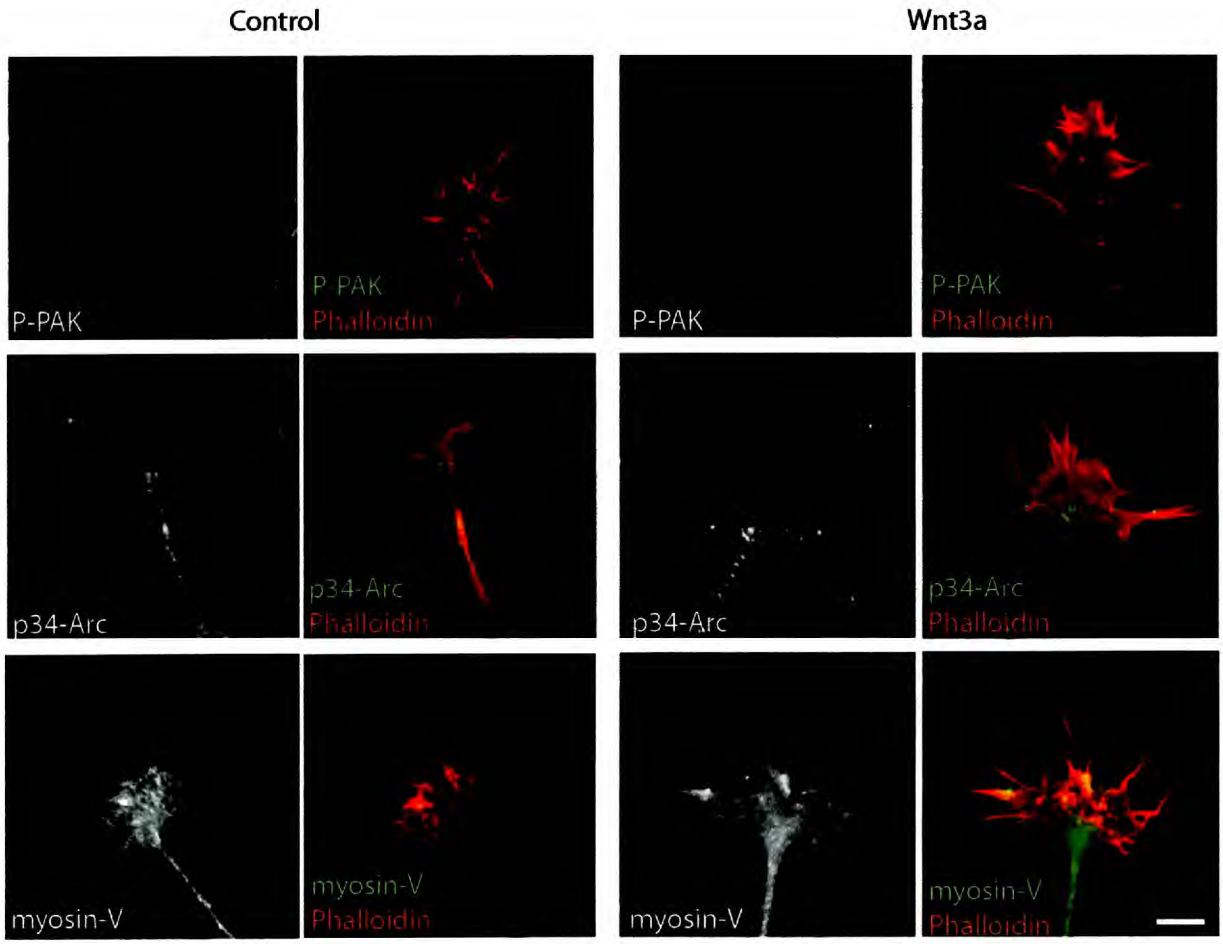


Figure 5.9. Wnt3a does not affect the levels or localisation of P-PAK, p-34-Arc or myosin-V. P-PAK-1 and p-34-Arc are enriched in the central domain of growth cones, myosin-V was also found in the peripheral regions of growth cones. Bar, 10μm.

In addition to actin filament assembly, retrograde actin flow also requires myosin motors (Lin *et al.*, 1996). Inhibition of myosin ATPase activity with 2,3-butanedione monoxime (BDM) causes a dose dependent attenuation of F-actin retrograde flow, while increasing filopodia and leading edge extension (Lin *et al.*, 1996). Interestingly, the rate of growth cone advance is inversely proportional to the actin retrograde flow (Lin and Forscher, 1995) and retrograde actin flow influences the organisation of microtubules by inhibiting microtubule advance (Suter *et al.*, 2004; Zhang *et al.*, 2003). As an increase in the retrograde flow could explain some of the effects of Wnt3a in growth cones such as the lower rate of growth cone advance and the formation of looped microtubules, one could speculate that Wnt3a affects the retrograde actin flow. To test this hypothesis DRGs were treated with two different myosin inhibitors: BDM, a general myosin inhibitor, and blebbistatin, a specific inhibitor of myosin II. Whilst in the presence of control or Wnt3a, DRG neurons were exposed to the drugs for 30 minutes prior to fixation. The effect of Wnt3a on growth cone size and actin accumulation was not affected by BDM or blebbistatin, as Wnt3a still causes a significant increase in growth cone area (Fig.5.10 A) and in the accumulation of F-actin (Fig.5.10 B). However, treatment with the myosin inhibitors led to an increase in filopodial length and number (Fig.5.10 D). This effect has been previously observed and it is attributed to the continuous polymerisation of F-actin at the leading edge (Lin *et al.*, 1996). These results suggest that the Wnt-induced increase in growth cone size and accumulation of F-actin do not depend on myosin motors.

Importantly, treatment with myosin inhibitors led to a decrease in the percentage of growth cones with looped microtubules (Fig.5.10 C-D). BDM and blebbistatin cause a decrease in the percentage of growth cones with looped microtubules when compared with DMSO controls. The decrease in microtubule looping is observed both in control and Wnt3a treated growth cones (control+BDM: 43.6% decrease, Wnt3a+BDM: 64.9% decrease, control+blebbistatin: 68.9% decrease and Wnt3a+blebbistatin: 82.4% decrease). These results highlight the influence of retrograde actin flow on the organisation of microtubules in growth cones and suggest that Wnt3a-induced microtubule looping could result from an increase in the retrograde actin flow. Whether

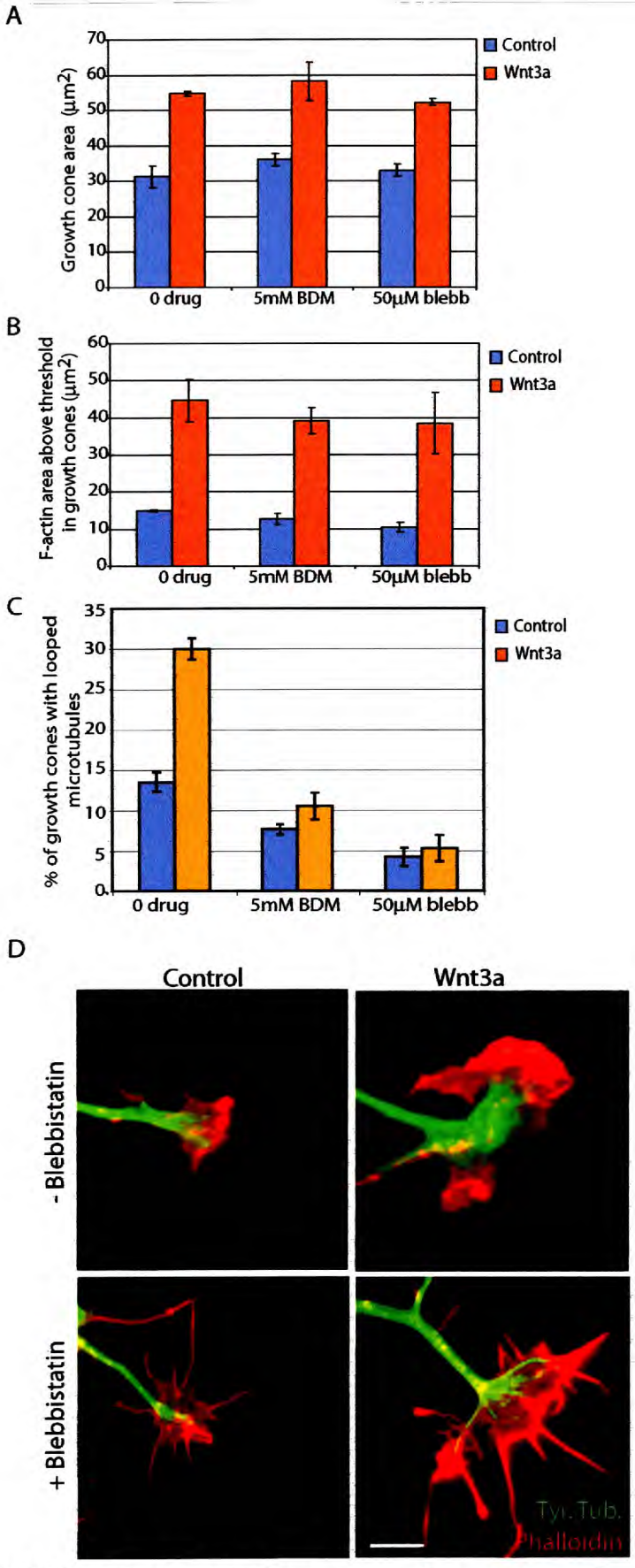


Figure 5.10. Inhibition of retrograde flow decreases the percentage of neurons with looped microtubules in growth cones.

(A) Neither BDM nor blebbistatin influence the effect of Wnt3a on growth cone size. (B) Neither BDM nor blebbistatin influence the Wnt3a-induced increase of F-actin in growth cones. (C) BDM and blebbistatin significantly decrease the percentage of cells with looped microtubules in growth cones. (D) Representative growth cones of neurons exposed to blebbistatin. Bar, 12µm.

an increase in retrograde actin flow is a cause or a consequence of the higher actin content and dynamics induced by Wnt3a is unknown. To ultimately resolve the hypothesis that Wnt3a increases actin retrograde flow, the rate of retrograde actin flow in growth cones should be measured with membrane-bound flow-coupled beads (Lin and Forscher, 1995).

5.3 Discussion

Wnt3a induced axonal remodelling of DRG neurons is not only mediated by changes in the organisation and dynamics of microtubules, but also involves changes in the actin cytoskeleton. Wnt3a induces an accumulation of F-actin in growth cones within 15 minutes of application. Since gene transcription is not required for Wnt3a induced remodelling (Fig.4.4), this finding suggests that Wnt3a could locally stimulate the translation of actin-mRNA and/or actin polymerisation (by activating ABPs that regulate actin dynamics) without nuclear involvement. Monitoring both the monomeric and filamentous forms of actin by FRET (Okamoto *et al.*, 2004), would allow to determine whether Wnt3a causes a shift in the F-/G-actin ratio in growth cones. The short time required to see an effect on actin accumulation suggests Wnt3a is signalling directly to the actin cytoskeleton rather than indirectly, via its action on microtubules (the earliest effect detected is microtubule looping after 60 minutes exposure to Wnt3a). The accumulation of F-actin probably contributes to the effect of Wnt3a on growth cone spreading, though microtubule looping is also likely to mediate this effect (see Fig.5.4 A).

Examination of the organisation of actin filaments in Wnt3a treated growth cones by EM revealed an effect of Wnt3a on both the actin meshwork and actin bundles. In the presence of Wnt3a actin filaments form a more compact mesh, which would be consistent with the higher concentration of F-actin in Wnt3a treated growth cones. In addition, there are fewer radially projecting actin bundles in growth cones exposed to Wnt3a compared to controls. Interestingly, a similar effect was observed upon depletion

of Ena/Vasp in growth cones, which not only increased growth cone area and lamella formation, but also induced a reduction in long actin bundles and an increase in the density of short actin filament networks near the leading edge (Lebrand *et al.*, 2004). Thus, the effect of Wnt3a on actin could involve the downregulation of Ena/Vasp activity in growth cones. Alternatively, the Wnt3a-induced decrease in actin bundles could be due to the inactivation of actin bundling proteins such as villin or fascin (Cohan *et al.*, 2001; Shibamoto *et al.*, 1998). Interestingly, no significant changes in the number of filopodia per growth cone were observed between control and Wnt3a treated neurons, suggesting that Wnt3a does not prevent filopodia formation. However, examination by EM reveals that unlike control treated growth cones, the actin bundles which give rise to filopodia in Wnt3a treated growth cones do not project from central regions, but are found at the periphery or edge of them (see figure 5.3).

Many attractive guidance cues have been shown to increase the levels of F-actin in growth cones. Consistent with the observations made in Wnt3a treated growth cones, NGF, BDNF, FGF-2 and netrin 1 have also been found to increase actin levels within 5 to 15 minutes of application, as well as stimulate the polymerisation of actin filaments (Dent *et al.*, 2004; Avwenagha *et al.*, 2003; Gallo and Letourneau, 2000; Goldberg *et al.*, 2000). Conversely, repellent guidance cues have the opposite effect, as loss of F-actin precedes Sema3A and ephrin-A2-induced growth cone collapse (Jurney *et al.*, 2002; Fritsche *et al.*, 1999; Fan *et al.*, 1993). These results suggest that actin polymerisation and depolymerisation are common responses to attractive and repulsive guidance cues respectively. Indeed, in addition to increasing F-actin in growth cones, Wnt3a affects actin dynamics. Growth cones exposed to Wnt3a and cytochalasin D or latrunculin B are able to remain enlarged, possibly due to the presence of unbundled and looped microtubules at growth cones, but the effect of Wnt3a on actin accumulation is abolished. More interestingly, Wnt3a increases the susceptibility of F-actin to the drugs, suggesting that F-actin filaments are less stable and hence depolymerise faster than in controls. A similar approach was used by Gallo *et al.* to determine the effect of ephrin-A2 on actin dynamics. Interestingly, ephrin-A2 causes slower depolymerisation of actin in growth cones upon addition of latrunculin, suggesting repulsive cues may inhibit

actin dynamics (Gallo *et al.*, 2002). In light of these findings, the changes taking place in the actin cytoskeleton upon exposure to Wnt3a are similar to those elicited by attractive axon guidance molecules.

Wnt3a also promotes the polymerisation of actin filaments in growth cones. Cytochalasin recovery experiments reveal that within 30 minutes, Wnt3a induces the assembly of more actin filaments than in controls. These experiments show that actin polymerises faster in the presence of Wnt3a and further demonstrate that Wnt3a increases actin dynamics. Analyses of time-lapse recordings of DRG neurons expressing GFP-β-actin revealed that Wnt3a increases filopodial velocity as well as growth cone protrusion. Both the speed of filopodia and lamellar protrusion have been previously shown to depend on the assembly and disassembly of actin filaments (Cramer, 1999; Mallavarapu and Mitchison, 1999), hence these effects are in agreement with an increase in actin dynamics. Due to the requirement of actin depolymerising drugs to reveal the effect of Wnt3a on actin polymerisation, it was not possible to resolve whether the accumulation of F-actin (observed within 15 minutes of Wnt3a treatment) precedes the effect on dynamics or is a result from an increase in filament assembly.

An increase actin dynamics, also referred to as actin instability, has been associated with axon formation and outgrowth in hippocampal neurons (Bradke and Dotti, 1999), though more recently has also been implicated in dendrite growth and branching (Jones *et al.*, 2004). It has been suggested that the decrease in actin stability allows microtubules to polymerise faster and hence promotes neurite outgrowth (Bradke and Dotti, 1999). This hypothesis would not fit with the effect of Wnt3a, as Wnt3a decreases both axon length and slows down growth cone advance (Fig.3.12 and 3.15). However, it is possible that the effects of Wnt3a on microtubule organisation and dynamics inhibit axonal extension despite favourable actin dynamics. Another possibility is that in DRG neurons, actin instability plays a role in Wnt3a-induced branch formation rather than axonal extension (Fig.3.12), by favouring growth cone bifurcation or the microtubule invasion of axonal filopodia to give rise to collateral branches. Other molecules that can induce branching but do not affect primary axon outgrowth are FGF-2 and netrin 1

(Dent *et al.*, 2004), further suggesting that axon outgrowth and axon branching may be regulated independently.

The effect of Wnt3a on actin dynamics is consistent with the wandering behaviour of growth cones and increased membrane activity observed in the GFP recordings (**chapter 3 movies**). A Wnt-induced decrease in growth cone adhesion, which would prevent the stabilisation of protrusions, could also explain the increase in lamellar protrusions and the decrease in forward advance observed in Wnt3a treated growth cones. The effect of Wnt3a on the adhesion of DRGs is yet to be addressed. Curiously, pharmacological inhibition of Gsk-3β in DRG neurons was found to decrease the movement of filopodia, implying an increase in actin stability (Owen and Gordon-Weeks, 2003), this finding hints at the possibility that Wnt3a signalling to the actin cytoskeleton might not involve inhibition of Gsk-3β. In hippocampal neurons, Wnt7b and Dvl1 induce dendritogenesis through a non-canonical Wnt signalling pathway involving Rac and Jun-terminal kinase (JNK) (Rosso *et al.*, 2005). It will be interesting to examine whether a non-canonical Wnt signalling pathway mediates the effects of Wnt on the actin cytoskeleton in DRG neurons.

The effect of Wnt3a on lamellar protrusion suggests a possible role for Rac. Rac regulates the formation of lamellipodia in fibroblasts (Nobes and Hall, 1995) and stimulates actin polymerisation (Luo, 2000). Unfortunately, Rac assays performed from DRG lysates did not provide consistent results (data not shown). The levels and localisation of the active Rac effector: P-PAK remain unchanged by Wnt3a. However, due to the numerous Rac effectors and the cyclic mode of action of RhoGTPases (Luo, 2000), an effect of Wnt3a on Rac activity in DRGs cannot be ruled out. Another potential mediator of the effect of Wnt3a on actin dynamics is p34-Arc, a subunit of the Arp2/3 complex involved in the polymerisation and branching of actin filaments, but no differences in levels or localisation were observed after treatment with Wnt3a for 2 hours. Finally, since lamellar protrusion requires the sustained transport and fusion of plasmalemmal precursor vesicles (Pfenninger *et al.*, 2003), the distribution and levels of the vesicle transport protein myosin-V were examined, but again no significant

differences were found in Wnt3a treated growth cones when compared to controls. Despite these negative results, it remains possible that Wnt3a does affect the localisation and activity of these molecules but that it is inducing changes that are too small and/or temporary to be detected by immunofluorescence in fixed cells.

A growing number of actin regulating proteins are being identified downstream of guidance molecules, but their roles can be contradictory. Activation of Rac for example, has been shown downstream of both attractive and repulsive guidance cues (Grabham *et al.*, 2003; Jurney *et al.*, 2002; Shekarabi and Kennedy, 2002; Jin and Strittmatter, 1997). Similarly, Arp2/3 was reported to play a positive role in NGF-induced neurite outgrowth as it is recruited to sites of actin polymerisation in growth cones upon exposure to NGF (Goldberg *et al.*, 2000), yet another group found Arp2/3 to play a negative role in growth cone advance (Strasser *et al.*, 2004). A possible explanation for these apparent discrepancies could lie in the tightly regulated localisation and cyclic mode of action of these proteins (cells may have to constantly switch them on and off). Other ABPs that could potentially mediate the effects of Wnt3a on the actin cytoskeleton are: the actin depolymerising protein cofilin, which has been shown to increase actin dynamics in response to BDNF (Fass *et al.*, 2004), and N-WASP, which activates Arp2/3 downstream of ephrin signalling in dendritic spines (Irie and Yamaguchi, 2004). To determine whether the effect of Wnt3a on lamellar protrusion is due to an increase in vesicle transport, it would be interesting to examine the dynamics of plasmalemmal precursor vesicle fusion (Pfenninger *et al.*, 2003).

Actin filaments can act as a barrier or as a guide for microtubules depending on the dynamics of the retrograde actin flow and the organisation of filaments into bundles or meshwork (reviewed in Zhou and Cohan, 2004). Inhibition of retrograde flow leads to extensive microtubule protrusion into the periphery of growth cones despite the presence of dense actin meshwork (Zhou *et al.*, 2002). In addition, actin arcs – filaments oriented parallel to the leading edge – can also act as a physical barrier for microtubules, limiting protrusion and affecting their organisation in growth cones (Schaefer *et al.*, 2002). Interestingly, when the retrograde flow of actin filaments is inhibited the effect of

Wnt3a on microtubule looping is abolished. Despite the fact Wnt3a is still able to induce an increase in F-actin and growth cone size, there is a significant decrease in the percentage of growth cones with looped microtubules. These findings suggest that Wnt3a may affect the organisation of microtubules by increasing the rate of retrograde flow. The Wnt3a-induced accumulation of actin and increased dynamics may be responsible for an increase in rate and bulk of retrograde actin flow. Curiously, the accumulation of F-actin in Wnt3a treated growth cones often occurs in the central region of growth cones, as well as at the leading edge (Fig. 5.1), further suggesting that Wnt3a influences actin retrograde flow. Although, LPA has recently been found to regulate actin retrograde flow in migrating cells to reposition the nucleus and initiate cell polarisation (Gomes *et al.*, 2005), at present, there are no reports of axon guidance molecules able to impinge on actin retrograde flow.

As mentioned above, the organisation of actin filaments is important for the distribution of microtubules in growth cones. Microtubules splay out to the periphery as they track along radial actin bundles (Zhou and Cohan, 2004). Loss of actin bundles after treatment with cytochalasin leads to microtubule looping at the periphery of growth cones (Zhou *et al.*, 2002; Forscher and Smith, 1988). Indeed, fewer radial actin bundles were found in Wnt3a treated growth cones. Two findings support the notion that Wnt3a induces microtubule looping through changes in the actin cytoskeleton. Firstly, at the EM level, fewer actin bundles are observed in Wnt3a treated growth cones. Secondly, experiments with myosin inhibitors suggest Wnt3a increases actin retrograde flow. It is plausible that by inhibiting the formation of actin bundles and increasing the retrograde flow of actin filaments, Wnt3a could affect the splaying behaviour of microtubules in the periphery of growth cones and induce the formation of microtubule loops. The identity of the molecules and the mechanisms by which Wnt3a regulates the organisation of actin filaments, their retrograde flow and dynamics are yet to be determined.

In summary, this chapter has shown that: Wnt3a induces both an accumulation of actin in growth cones and increases actin dynamics, since the depolymerisation and polymerisation of filaments is enhanced in the presence of Wnt3a. These processes

probably underlie the effects of Wnt3a on growth cone size and motility. Furthermore, investigation of the retrograde actin flow and the organisation of actin filaments in growth cones suggest that the effects of Wnt3a on actin organisation and dynamics could influence the organisation of microtubules. The combination of an increase in retrograde flow and the lack of radial actin bundles could prevent microtubules from reaching the periphery of growth cones, forcing them to bend back and form loops, and prevent growth cone advance.

CHAPTER 6:

Discussion

6.1 Summary of results

The effects of Wnt proteins on axonal morphology and the cytoskeleton were characterised in detail using Wnt3a and DRG neurons as a model system. Application of Wnt3a to developing axons causes a decrease in axonal length, an increase in branching and growth cone enlargement. These effects can be observed within two hours of treatment. Further time-lapse analysis revealed that Wnt3a is able to significantly decrease growth cone advance within 20 minutes. The effects of Wnt3a on axonal morphology are mediated by the intracellular scaffolding protein, Dvl1, and through inhibition of Gsk-3β. Protein translation, but not gene transcription, is required for Wnt3a-induced remodelling. As Wnts have previously been shown to regulate the phosphorylation of MAPs (Lucas *et al.*, 1998), these findings indicate that Wnts can induce changes in the the axonal cytoskeleton not only by directly affecting the phosphorylation and activity of cytoskeleton regulating proteins but also by influencing their translation.

Examination of the axonal cytoskeleton reveals Wnt3a induces changes in the organisation and dynamics of both microtubules and actin filaments. Wnt3a increases the amount of microtubules in axons and growth cones and affects the direction of microtubule growth. In the presence of Wnt3a, microtubules tend to grow across growth cones and form loops rather than splay out to the periphery as in controls. Furthermore, Wnt3a is able to increase microtubule stability. Wnt3a induces an accumulation of actin in growth cones within 15 minutes of application and increases both the depolymerisation and polymerisation of actin filaments. The increase in filopodia motility and lamellar protrusion observed in the presence of Wnt3a are consistent with these findings. Finally, investigation of the effects of Wnt3a on retrograde actin flow and the organisation of actin filaments by EM suggest that the effects of Wnt3a on microtubules may result from a Wnt3a-induced increase in retrograde flow and decrease of radially projecting actin bundles. The results presented in this thesis highlight the

influence of microtubule and actin polymers on each other, and shed new light on the cytoskeletal changes elicited by extracellular cues during the formation of neuronal connections.

6.2 Wnt3a-induced axonal remodelling

The correct navigation of axons to their targets requires the appropriate response to extracellular guidance cues. However, very little is known about the underlying changes taking place in the axonal cytoskeleton and the signaling pathways involved in mediating axon attraction or repulsion. Wnts are dynamically expressed in the developing nervous system (Lucas and Salinas, 1997; Salinas *et al.*, 1994; Parr *et al.*, 1993), and have been found to play important roles during axon guidance (Lyuksyutova *et al.*, 2003; Yoshikawa *et al.*, 2003), dendritogenesis (Rosso *et al.*, 2005), synapse formation and maturation (Hall *et al.*, 2000; Lucas and Salinas, 1997). Both Wnt7a, expressed by granule cells, and Wnt3, expressed by motor neurons of the lateral motor columns, have been shown to induce axonal remodelling of their presynaptic partners, mossy fibres and a subset of DRG neurons, respectively (Krylova *et al.*, 2002; Hall *et al.*, 2000). Wnt-induced axonal remodelling is characterised by short axons and enlarged growth cones, though Wnt3 can also induce branching in DRGs (Krylova *et al.*, 2002). Interestingly, these effects take place prior to synaptogenesis. Both Wnt3 and Wnt7a induce an accumulation of synapsin 1 and induce synaptic vesicle clustering (Krylova *et al.*, 2002; Hall *et al.*, 2000). Together, these findings have lead to the proposal that Wnts are target-derived retrograde signals able to remodel axon terminals and induce synapse formation (Krylova *et al.*, 2002; Hall *et al.*, 2000).

To characterise the cytoskeletal changes underlying Wnt-induced axonal remodelling, neonatal DRGs were treated with various Wnt-conditioned media. However, variations in the amount of Wnt in the medium and the presence of other cell secreted factors, often hampered the Wnt remodelling effect. These problems were overcome using purified Wnt3a. The protein sequence of Wnt3a is 90% identical to that of Wnt3 (Roelink and Nusse, 1991). Wnt3a has a similar effect to Wnt3 on axonal remodelling of

neonatal DRGs, but more importantly, Wnt3a has a faster, more consistent and robust remodelling activity. Within two hours of application, neurons exposed to Wnt3a have significantly larger growth cones and shorter, more branched, axons than controls. Large growth cones have been associated with pausing axonal behaviours (Kalil *et al.*, 2000). Consistent with these findings, time-lapse recordings revealed that Wnt3a is indeed able to cause axon stalling – growth cone advance decreases significantly in the first 20 minutes of Wnt3a application – and that this effect precedes growth cone enlargement, which takes place after 80 minutes of exposure. FGF-2, FGF-22, FGF-7 and FGF-10 also induce growth cone enlargement and branching while inhibiting axon outgrowth (Umemori *et al.*, 2004; Szebenyi *et al.*, 2001). Interestingly, like Wnt7a, FGF-22 is expressed in the developing cerebellum and has been found to act as a target-derived factor able to induce presynaptic differentiation in mossy fibres (Umemori *et al.*, 2004). These findings suggest that growth cone stalling and axon branching may be common responses of neurons approaching their synaptic targets.

The receptor for Wnt3a in DRGs remains to be identified, but roles for both Frizzleds and Ryk have been ascribed (Lu *et al.*, 2004). Since Wnt3a induces axonal remodelling in a subpopulation of DRGs, and not all Wnts induce remodelling, it will be interesting to determine whether different DRG populations express distinct subsets of Wnt receptors enabling them to respond to some Wnts and not others. Wnt3a signals through Dvl1 and GSK-β to induce axonal remodelling. Both expression of Dvl1 and inhibition of Gsk-3β, with lithium, mimic the effects of Wnt3a on neuronal morphology. Despite increasing the levels of β-catenin, the transcription of Wnt target genes through β-catenin and TCF/LEF is not required for Wnt3a-induced axonal remodelling. Blocking all transcriptional activity with actinomycin does not abolish the Wnt effect. The ability of Wnt3a to induce remodelling independently of transcription suggests Wnts can elicit rapid and local changes in the cytoskeleton, allowing axons to navigate efficiently in an ever-changing extracellular environment. However, Wnt3a-induced remodelling does not result merely from the relocalisation of existing proteins, as it requires protein translation. Blocking protein synthesis with anisomycin or cyclohexamide completely abolishes Wnt3a induced remodelling. Together, these

results suggest that Wnts may modulate axonal morphology through a divergent canonical signalling pathway. A Wnt signalling pathway that branches downstream of Gsk-3β has been shown to mediate the effects of Dvl on microtubule stabilisation (Ciani *et al.*, 2004), hence it is possible that Wnts activate the same pathway to induce axonal remodelling. The potential role of β-catenin in the regulation of growth cone adhesion remains to be investigated. However, Wnts may also signal to the axonal cytoskeleton, in particular to the actin cytoskeleton, through other pathways. Both the planar cell polarity pathway, by regulating Rac and Rho, and the Wnt/Ca^{+2} pathway, through the regulation of Ca^{+2} transients, could modulate axon behaviour and morphology (Tang *et al.*, 2003; Huelsken and Birchmeier, 2001; Luo, 2000; Gomez and Spitzer, 1999).

In addition to the effects of Wnt3a on axon outgrowth, time-lapse recordings reveal an interesting wandering behaviour of growth cones. Far from remaining static, the non-advancing Wnt3a growth cones are highly motile, and behave as though they were continuously sampling the environment. While axon outgrowth is commonly attributed to changes in microtubules (Rochlin *et al.*, 1996; Tanaka *et al.*, 1995), growth cone motility relies on the dynamics of actin filaments (Luo, 2002; Jay, 2000; Forscher *et al.*, 1992). The effects observed upon addition of Wnt3a suggest that Wnt3a can influence both microtubules and actin filaments in neurons.

6.3 Wnt3a affects microtubules

Examination of microtubules in Wnt3a treated neurons revealed that Wnt3a increases the amount of microtubules along axons and growth cones. This effect could be achieved by an increase in tubulin synthesis, polymerisation or stability. Quantification of the rate of microtubule growth using EB3-GFP revealed no differences between control and Wnt3a treated neurons suggesting that Wnts do not affect the rate microtubule polymerisation. However, Wnt3a does affect microtubule stability since microtubules in Wnt3a treated neurons are more resistant to the effects of nocodazole. Similar results have been reported upon expression of Dvl1 in neuroblastoma and granule cells (Ciani *et al.*, 2004), which suggests that Wnt-induced microtubule stability

is mediated by Dvl1. Preliminary work, done in collaboration with Dr Ciani, indicates that microtubules in cerebellar granule cells, DRGs and cortical neurons from *Dvl1* knockout mice are less stable than in wild type neurons as microtubules of *Dvl1* knockout neurons depolymerise faster in the presence of nocodazole than microtubules of wild-type neurons. These results suggest that Dvl1 is required for microtubule stability *in vivo*. Microtubule stabilisation has previously been shown to cause axonal shortening (Rochlin *et al.*, 1996; Tanaka *et al.*, 1995), hence it is possible that the effect of Wnt3a on axonal outgrowth is achieved by stabilising microtubules. Unfortunately due to the time required to reveal the effect of Wnt3a on microtubule stability (at least two hours exposure to nocodazole), it was not possible to determine how long after exposure to Wnt3a the stabilisation takes place. Time course experiments and careful analyses of the most stable population of microtubules- acetylated or detyrosinated- by immunofluorescence may reveal the exposure time required to see differences between control and Wnt3a treated neurons and overcome the need to challenge the cells with nocodazole.

One of the downstream proteins mediating the effect of Wnts on microtubule dynamics is the Gsk-3β substrate: MAP-1B. Gsk-3β-mediated MAP-1B phosphorylation decreases microtubule stability (Goold *et al.*, 1999), which suggests that the decrease in MAP-1B-P observed following pharmacological inhibition of Gsk-3β, exposure to Wnt7a or Dvl1 expression in cerebellar granule cells (Ciani *et al.*, 2004; Goold *et al.*, 1999; Lucas *et al.*, 1998) is responsible for the increase in microtubule stability. Surprisingly, axin, a negative regulator of the canonical Wnt signalling pathway (Huelsken and Birchmeier, 2001), has also been shown to function upstream of Dvl to decrease MAP-1B-P and regulate microtubule stability (Ciani *et al.*, 2004). The different functions of axin may correlate with its intracellular localisation. By bringing Gsk-3β and β-catenin together in the cytoplasm, axin favours the destruction of βcatenin, whereas on microtubules, axin could be promoting the interaction between Gsk-3β and Dvl thus favouring Gsk-3β inhibition. Other microtubule regulating proteins which could be mediating the effect of Wnt-Dvl on microtubule dynamics are APC and tau. APC can regulate both Wnt signalling and increase microtubule stability (Zumbrunn *et*

al., 2001; Papkoff *et al.*, 1996), however, with the antibodies available to us, no differences in levels or localisation were observed between Wnt3a and control treated growth cones by immunofluorescence. The amount of APC bound to microtubules of brain lysates from *Dvl1* knockout and wild type mice are currently being examined by immunoprecipitation experiments (Dr Ciani, unpublished work). Tau is also a target of Gsk-3β that dissociates from microtubules upon phosphorylation (Wagner *et al.*, 1996), however the effects of tau on microtubule dynamics appear to be more dependent on the levels of tau than on its phosphorylation state (Nuydens *et al.*, 2002; Baas *et al.*, 1994). The effects of Wnt treatment and Dvl expression on the levels and localisation of tau in neurons, remains to be investigated.

Wnt3a affects the organisation of microtubules in growth cones, rather that splaying out to the periphery, as is typically observed in control growth cones, in the presence of Wnt3a microtubules bend backwards and form loops. Time-lapse recordings with EB3-GFP reveal that Wnt3a influences the direction of microtubule growth in axon terminals as a higher percentage of microtubules grow across growth cones rather than outwards, towards the leading edge. Microtubule loops have been observed in pausing growth cones (Kalil *et al.*, 2000; Dent *et al.*, 1999) and time course experiments suggest that in the presence of Wnt3a, growth cones first cease to advance before microtubule loops form. The effect of Wnts on microtubule looping could be mediated by changes in microtubule plus end proteins that regulate interactions between microtubules and actin filaments (Howard and Hyman, 2003) or, as has recently been reported, between the plus ends and the sides of microtubules (Reilein and Nelson, 2005). It is possible that Wnts induce changes in plus end proteins that render microtubules unable to bind and track along actin bundles and/or be captured under the plasma membrane causing them to adopt a looped rather than splayed organisation. Examination of endogenous CLIP-170 and CLASP, or the effects induced by their overexpression may shed some light on the effect of Wnts on the plus end of microtubules. Alternatively, the effects of Wnts on the actin filaments could influence the organisation of microtubules in growth cones (see below).

Since Wnt3a induces microtubule stability but does not affect the rate of microtubule polymerisation, how can Wnt3a promote axon branching, which requires dynamic microtubules? A possible explanation lies in the timing of events, Wnts may promote branch initiation by first destabilising the actin cytoskeleton, which promotes microtubule advance, and subsequently stabilise newly formed branches by promoting the stabilisation of microtubules (Dent and Kalil, 2001; Kalil *et al.*, 2000). Alternatively, differential regulation of microtubule transport in branches and the main axon may account for this effect.

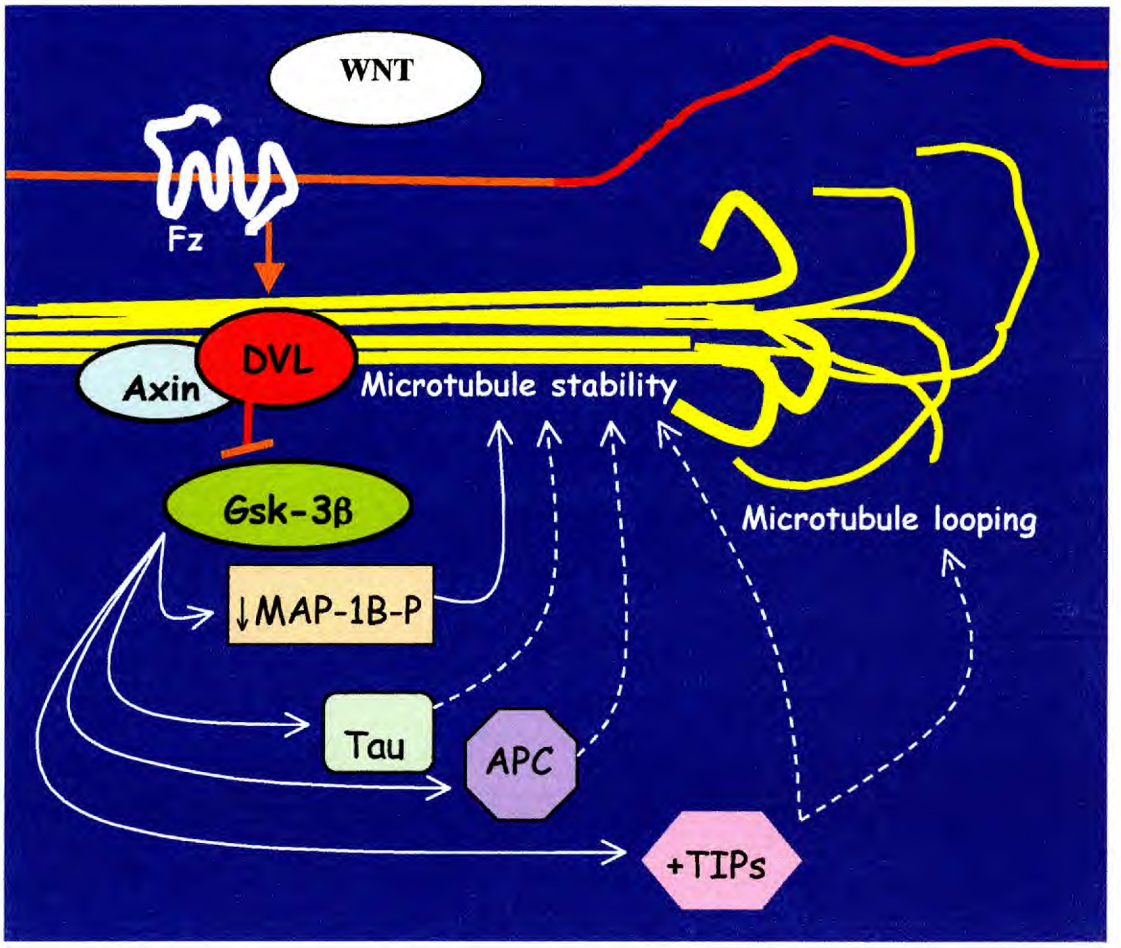


Figure 6.1. Putative mechanisms for the Wnt-induced changes in dynamics and organisation of axonal microtubules.
Wnt3a-Dvl induced Gsk3β inhibition decreases the phosphorylation of MAP-1B which contributes to the stabilisation of microtubules. Gsk3β also affects the localisation of tau and APC which can influence microtubule dynamics. Finally, plus end binding proteins, which can also be regulated by Gsk3β, could modulate both microtubule stability and induce microtubule looping. Links remaining to be established are represented with dashed lines.

6.4 Wnt3a affects the actin cytoskeleton

Wnt3a causes an accumulation of F-actin in growth cones within 15 minutes of exposure. Examination of actin dynamics in growth cones revealed that Wnt3a increases actin dynamics. Actin filaments not only depolymerise faster than controls when cytochalasin D or latrunculin B are added , but also polymerise faster upon removal of the drugs. Further evidence of the effect of Wnt3a on actin dynamics was obtained from time-lapse recordings of GFP-β-actin-expressing DRGs. Both filopodial motility and growth cone protrusion increase after overnight exposure to Wnt3a. As Wnt3a has an effect on the actin cytoskeleton within minutes, it is possible that these effects are even greater if measured upon addition of Wnt3a on the day of plating. These experiments would have to be done using DIC microscopy or by injecting fluorescently labelled actin or phalloidin, as the expression of GFP-β-actin is too weak on the day of plating.

The ability of Dvl1 to activate Rac in hippocampal neurons (Rosso *et al.*, 2005) suggests that the effects of Wnt3a on actin dynamics in DRG growth cones could be mediated by Rac and its effectors. Rac activity assays did not reveal consistent differences between control and Wnt3a treated DRG cultures, however, as only a subpopulation of DRGs respond to Wnt3a, and Rac may only be activated in growth cones, these assays are probably not sensitive enough to detect changes. To overcome these difficulties, the levels and localisation patterns of the Rac effector P-PAK were examined in growth cones. Unfortunately, no differences between control and Wnt3a treated growth cones were found. Other potential Wnt3a targets which could mediate the effects of Wnt3a on actin dynamics are the Arp2/3 actin polymerising complex, and myosin-V, which could be playing a role in bringing vesicles to the plasma membrane to sustain growth cone spreading and lamellar protrusions. Immunofluorescence studies showed no differences in either. Other potential candidates worth examining in the future are cofilin, which has been shown to increase actin dynamics (Fass *et al.*, 2004) and the activator of Arp2/3: N-WASP (Irie and Yamaguchi, 2004). Interestingly, vinculin stabilises lamellipodial protrusions during integrin-mediated adhesion (Varnum-Finney and Reichardt, 1994),

hence the effect of Wnt3a on maintaining constantly protruding lamellas may be achieved by downregulating vinculin.

In addition to regulating actin dynamics, Wnt3a affects the organisation of actin filaments in growth cones. EM studies reveal a more densely packed lamella at the edge of Wnt3a treated growth cones, but more strikingly a decrease in the number of radially projecting actin bundles. Possible mediators of the effect of Wnt3a on actin filament organisation are Ena/Vasp proteins or actin bundling proteins such as fascin (Cohan *et al.*, 2001). Ena/Vasp promotes actin filament elongation by antagonising capping proteins, and decreases the density of actin filament branching (Lebrand *et al.*, 2004). Conversely, inactivation of Ena/Vasp in growth cones, leads to a similar organisation of actin to that observed in Wnt3a treated growth cones: less straight actin bundles and a more densely packed meshwork (Lebrand *et al.*, 2004). Alternatively, Wnts could regulate the phosphorylation of fascin, which decreases its affinity for actin filaments and leads to the loss of actin bundles (Cohan *et al.*, 2001), or the localisation of Villin, another actin bundling protein which becomes redistributed in fibroblasts in response to Wnt3a (Shibamoto *et al.*, 1998). Interestingly, endogenous Dvl1 localises to actin bundles in hippocampal growth cones (Rosso *et al.*, 2005), and in non-neuronal cells, Dvl is recruited to the plasma membrane upon activation of Wg signalling (Yanagawa *et al.*, 1995). These findings hint at the possibility that Dvl1 itself could mediate the effect of Wnt3a on actin filament organisation. If Dvl1 has an actin bundling activity, re-localisation upon Wnt3a addition would explain the Wnt3a-induced loss of actin bundles. Close examination of the localisation of endogenous Dvl1 before and after Wnt3a addition, and of the organisation of actin filaments in neurons of Dvl1 mutant mice will help clarify this hypothesis.

Actin retrograde flow has been shown to play an important role in preventing both growth cone advance and microtubule invasion to the periphery of growth cones (Schaefer *et al.*, 2002; Zhou *et al.*, 2002; Lin and Forscher, 1995). Despite the presence of drugs that inhibit the retrograde flow of actin filaments, Wnt3a is able to induce

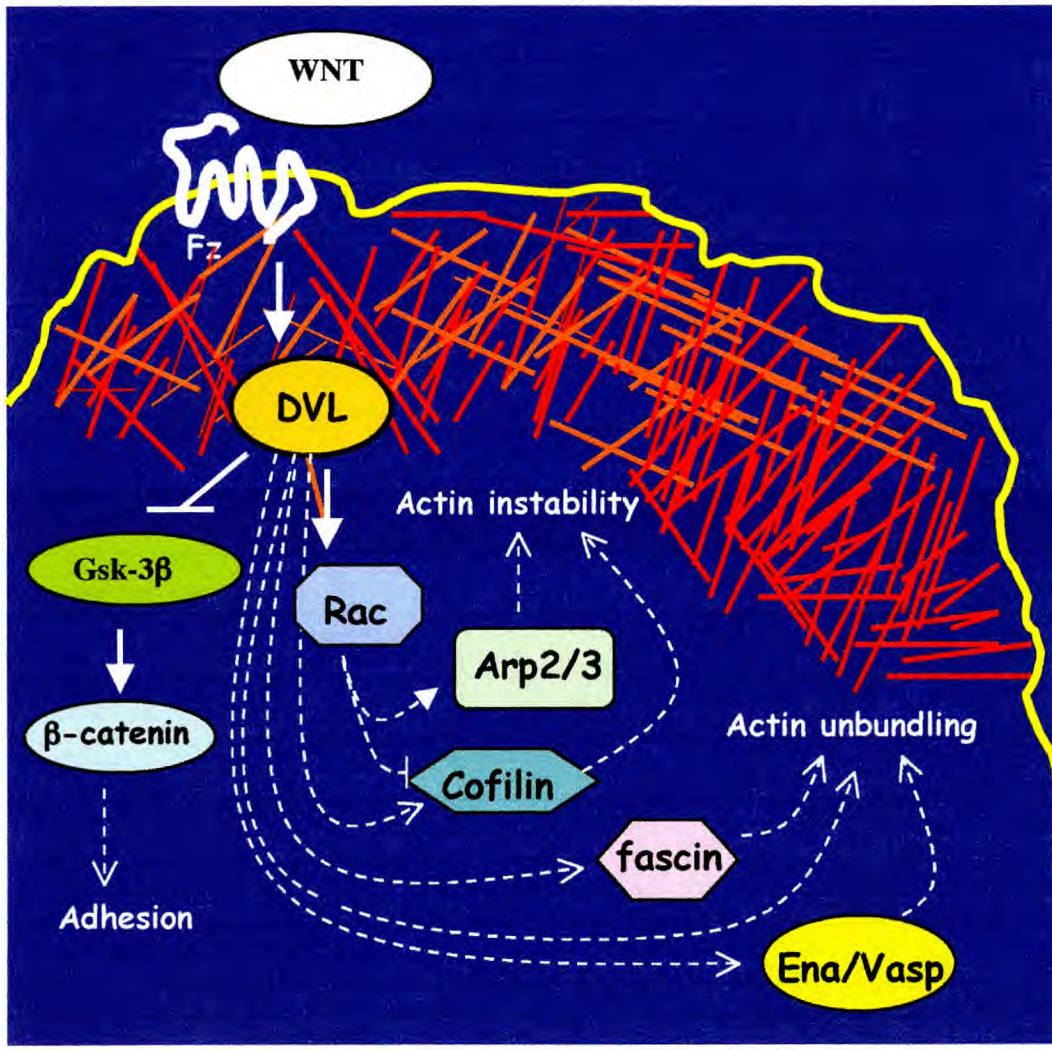


Figure 6.2. Potential mechanisms for the Wnt-induced changes in actin dynamics and organisation in growth cones.
Links remaining to be established represented with dashed arrows.

growth cone enlargement and actin accumulation, but more interestingly the effect of Wnt3a on microtubule looping is abolished. This finding highlights the importance of the retrograde flow of actin filaments on microtubule organisation and has lead to the hypothesis that Wnt3a induces microtubule looping, at least in part, by increasing the rate of retrograde flow. The Wnt3a-induced accumulation of F-actin and increase in actin dynamics may account for an increase in both the bulk and rate of the flow, which in turn could cause microtubules to be swept back and loop. Further evidence for the influence of the actin cytoskeleton on microtubules comes from the examination of actin filaments in growth cones at the EM level. Wnt3a causes a decrease in the number of

radially projecting actin bundles. Since actin bundles serve as microtubule tracks to guide them towards the periphery (Gordon-Weeks, 1991), this effect of Wnt3a on the organisation of actin filaments could also help explain the lack of microtubule splaying to the periphery in Wnt3a treated neurons. Loss of actin bundles has been associated with repulsive growth cone turning and collapse (Zhou *et al.*, 2002; Zhou and Cohan, 2001), which begs to question how can Wnt3a treated growth cones remain spread despite the lack of actin bundles? The Wnt3a-induced accumulation of actin, increased protrusion and microtubule unbundling may explain this effect.

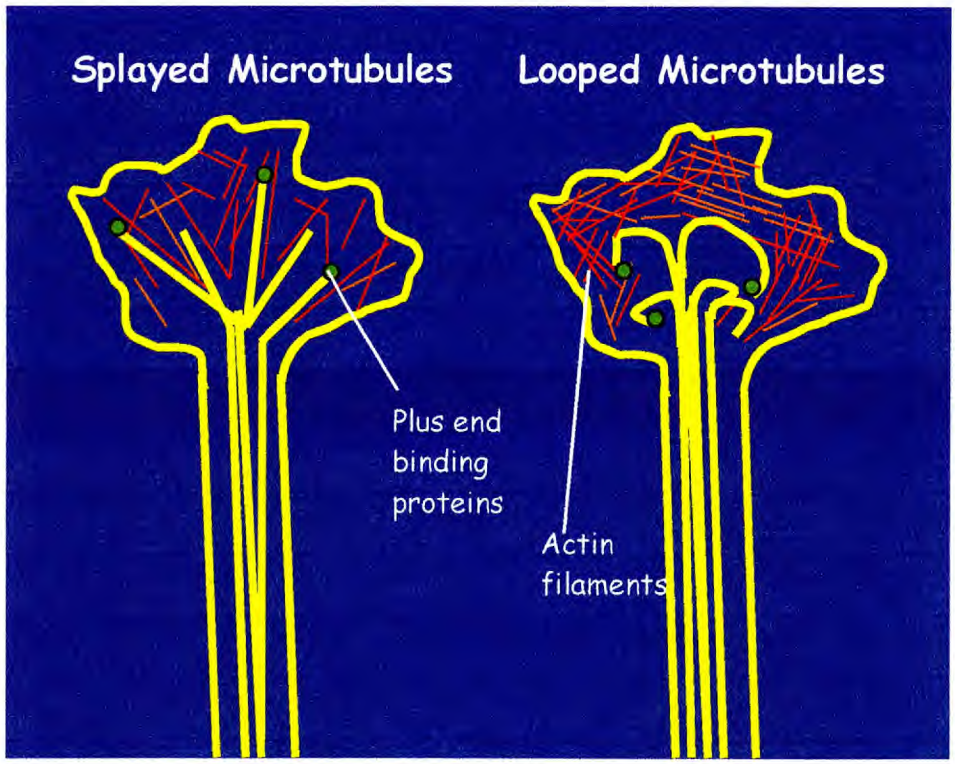


Figure 6.3. The effects of Wnt3a on actin may influence the organisation of microtubules in growth cones.
Wnt-induced accumulation of actin, loss of radially projecting actin bundles and increase in retrograde flow could explain the formation of microtubule loops in growth cones.

Myosin motors are the main candidates likely to mediate the effect of Wnt3a on retrograde flow. Examination of the retrograde flow in neurons from myosin knockout mice, or in neurons in which specific myosins are inactivated by chromophore assisted laser inactivation (CALI), have revealed distinct roles for different myosins (Brown and Bridgman, 2003; Diefenbach *et al.*, 2002). While inactivation of myosin-Ic decreases

actin retrograde flow in growth cones (Diefenbach *et al.*, 2002), neurons from myosin-IIb knockout mice exhibit an increased rate of retrograde flow and decreased axonal outgrowth. This finding suggests that retrograde actin flow, possibly through its compressive forces on microtubules, can play a role in the inhibition of axonal extension. Since the polymerisation of actin filaments is regulated independently from actin retrograde flow (Mallavarapu and Mitchison, 1999), growth cone size and motility need not be affected by changes in the retrograde flow. Finally, it is worth mentioning that the rate of retrograde actin flow is also regulated by adhesion (Suter and Forscher, 2000), hence the effect of Wnt on the retrograde flow may be related to changes in growth cone adhesion.

6.5 Sequence of events

Experiments described in this thesis suggest that Wnt induces changes in the organisation and dynamics of both actin and microtubules. Wnt-Dvl1 signalling has been shown increase microtubule stability by inhibiting Gsk-3β and regulating MAP-1B (Lucas *et al.*, 1998). While Wnt3a may signal independently to actin and microtubules to regulate their dynamics, the effect of Wnt3a on the organisation of microtubules may also result from Wnt3a-induced effects on actin organisation and dynamics. Since Gsk-3β inhibition and Dvl expression in DRGs mimic the effect of Wnt3a on growth cone size it is possible that they may also mediate the effect of Wnt3a on actin. Time-lapse studies of DRGs expressing Dvl1 or exposed to Gsk-3β inhibitors would corroborate this hypothesis. Two findings suggest that Dvl1, but not inhibition of Gsk-3β, mediate the effects of Wnt3a on actin. Firstly, Gsk-3β inhibition has been shown to actually decrease filopodial dynamics in growth cones (Owen and Gordon-Weeks, 2003). Secondly, Dvl1 activation of Rac, a strong candidate to mediate the effects of Wnts on the actin cytoskeleton, does not require Gsk-3β inhibition in hippocampal neurons (Rosso *et al.*, 2005). As microtubules form loops and grow across growth cones, rather than outwards, in Dvl-expressing DRGs, if indeed the effects of Wnt signalling on actin are responsible for microtubule looping, this finding would imply that Dvl1 mediates the effects of Wnt3a on actin as well as on microtubule stability.

The sequence of events taking place upon addition of Wnt3a to DRG neurons can begin to be elucidated from the time-lapse and time-course experiments (Fig. 6.4). The first detectable change is the accumulation of F-actin in growth cones 15 minutes after exposure to Wnt3a (Fig.5.2), this is closely followed by the decrease in growth cone advance after 20 minutes (Fig. 3.15). Microtubule looping is observed after 60 minutes exposure (Fig. 4.7), yet growth cone size does not become significantly larger than controls until after 80 minutes exposure to Wnt3a (Fig. 3.15). The full effect of Wnt3a on axonal remodelling, that is on growth cone size, axonal length and branching is found after 2 hours exposure. Unfortunately, for technical reasons, it is only possible to speculate when the changes in actin and microtubule dynamics are taking place. If the increase in actin dynamics indeed influences the organisation of microtubules, it should be taking place before the microtubule looping occurs. Similarly, if microtubule stabilisation is responsible for a decrease in axonal outgrowth it should be taking place in the first 20 minutes after addition of the Wnt. Experiments with low doses of actin or microtubule depolymerising drugs, to freeze their dynamics, may enable to determine which cytoskeletal element is affected first. However, due to the influence of the dynamics of microtubules on actin dynamics and vice versa, these experiments are not easy to interpret.

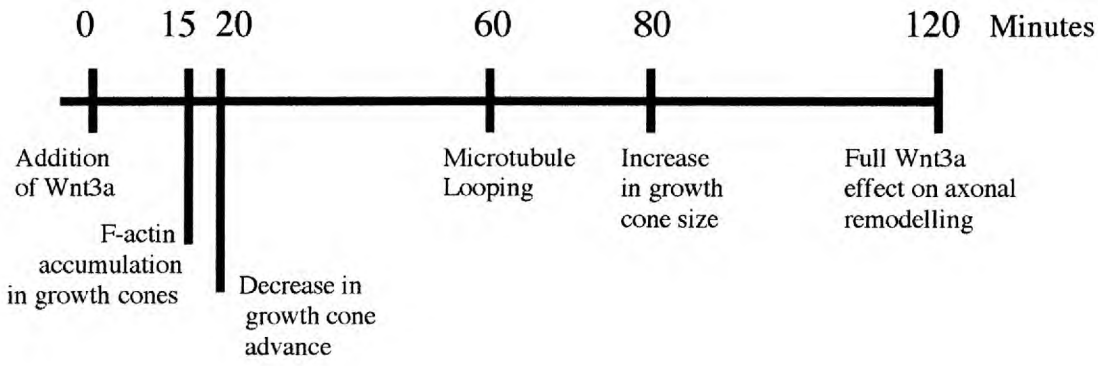


Figure 6.4. Sequence of events upon addition of Wnt3a.
Time line of changes taking place in neuronal morphology and the cytoskeleton upon addition of Wnt3a.

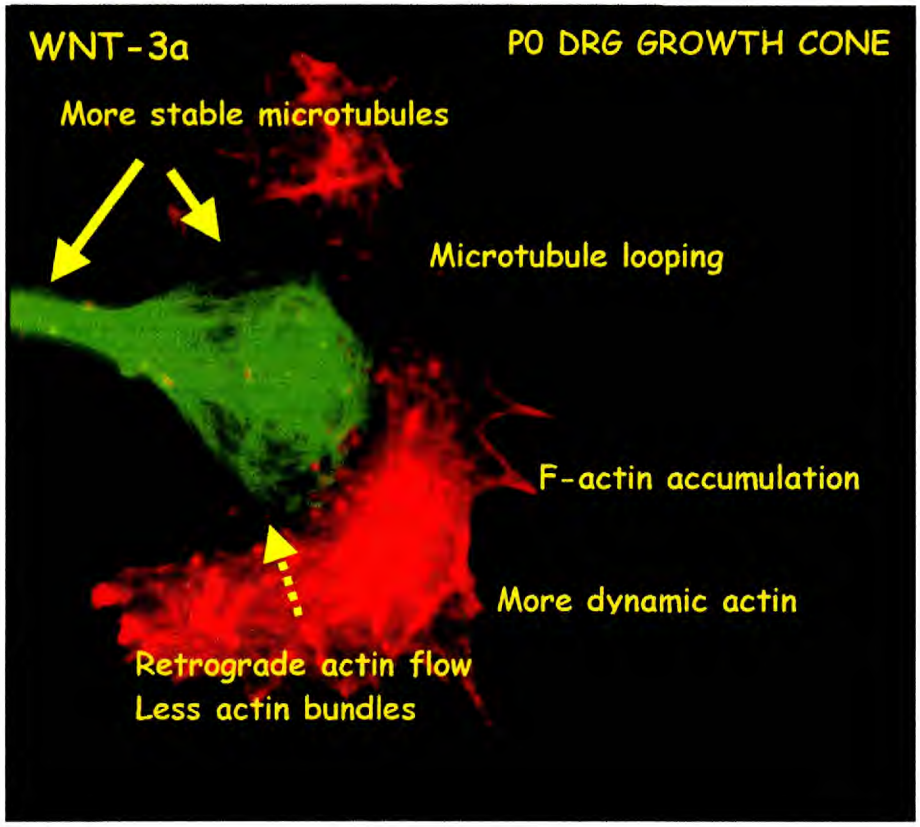


Figure 6.5. Summary of the effects of Wnt3a on the growth cone cytoskeleton.

6.6 Is Wnt3a a guidance cue?

The effects of Wnt3a on axonal remodelling and on the cytoskeleton raise the question of whether Wnt3a is acting as a guidance molecule. Typically positive guidance cues induce axonal extension and branching, and promote the dynamics of both actin and microtubules, whilst negative cues inhibit axonal extension and induce growth cone collapse by decreasing the cytoskeletal dynamics (Dent *et al.*, 2004; Kalil *et al.*, 2000). Since Wnt3a inhibits axonal extension but promotes branching and growth cone enlargement, and can increase microtubule stability yet at the same time stimulate actin dynamics, it does not fit either category. To ultimately determine the role of Wnt3a as a guidance cue it will be necessary to set up experiments where DRGs are exposed to a local source of Wnt3a. Giving growth cones a choice, in a turning assay or a stripe assay will help determine whether they are attracted or repelled by Wnt3a. It will also be interesting to test the effects of different concentrations of Wnt3a, since it is possible that DRGs encounter a gradient of Wnts as they project into the spinal cord. Very low concentrations of Wnt3a may actually enhance axonal outgrowth whereas once axons

are close to their targets, higher concentrations of Wnt3a, cause axons to come to halt and start assembling the synaptic machinery. Interestingly, other guidance molecules such as netrin 1 and Sema3A can induce attractive or repulsive responses depending on their concentration (Holt, C. unpublished observations) and may explain why Lu *et al.* observe axon outgrowth in DRG explants, rather than axonal shortening, upon addition of Wnt3a conditioned media (Lu *et al.*, 2004). Finally, the examination of neuronal projections in conditional Wnt mutants, to bypass the early requirement of Wnts during early embryonic patterning, may shed some light on the roles of Wnts in axon guidance.

The localisation and timing of Wnt gene expression, support the idea that Wnt3a is not acting as a guidance cue in the spinal cord, but as a target-derived synaptogenic factor that regulates the terminal arborisations of a subset of approaching axons. By inhibiting axonal extension and promoting branching, Wnt3a prevents axons from overshooting their targets and favours target innervation. In this context, the dampening of microtubule dynamics would stop axonal extension, while the upregulation of actin dynamics would allow growth cones to actively search for their post-synaptic targets in the near vicinity.

6.7 Wnt3a as a synaptogenic factor

Wnts are emerging as evolutionarily conserved synaptogenic factors. In addition to the roles of Wnt7a and Wnt3 in axonal remodelling and synapse formation in the cerebellum and spinal cord (Krylova *et al.*, 2002; Hall *et al.*, 2000), Wg has been shown to be required for the normal growth and maturation of the NMJ in *Drosophila* (Packard *et al.*, 2002). Interestingly, Wg induces changes in the microtubule organisation at pre-synaptic terminals by regulating the MAP-1B homologue, futsch (Packard *et al.*, 2002). Both Wg^{ts} and *futsch* mutants exhibit a decrease in the number of synaptic boutons and active zones, a phenotype that has been associated to a more dynamic cytoskeleton. These findings are consistent with the studies on Wnts and MAP-1B in mice (Lucas *et al.*, 1998) and highlight a role for microtubule dynamics in synapse formation.

If the effects of Wnt3a on the cytoskeleton of developing DRG axons are maintained during synaptogenesis, they could be contributing to the effect of Wnts on synaptic differentiation. Interactions between growth cone filopodia or neuronal processes, and the subsequent stabilisation of a subset of the resulting contacts are central features of synaptogenesis. As mentioned above, the effects of Wnt3a on the dynamics of actin and microtubules would facilitate target recognition. Interestingly actin accumulation at presynaptic terminals and a dynamic turnover of actin filaments are required for the formation of functional synapses (Colicos *et al.*, 2001; Zhang and Benson, 2001). Consistent with a potential role in synaptogenesis, Wnt3a induces both an accumulation of actin in growth cones and promotes actin dynamics. Depolymerisation of actin dynamics has been found to cause both the dispersal of synaptic vesicles and transiently increase neurotransmitter release (Sankaranarayanan *et al.*, 2003; Morales *et al.*, 2000). These findings point towards roles for actin filaments as both a scaffold, to keep synaptic vesicles clustered, and as negative regulators of vesicle fusion. Whilst the clustering of synaptic vesicles may be dependent on the organisation of actin filaments, it is likely that the dynamics of filaments play a role in the endo- and exo-cytosis of vesicles (Shupliakov *et al.*, 2002). The tightly packed meshwork of actin filaments at the leading edge of Wnt3a treated growth cones could facilitate vesicle clustering. The effects of Wnts on synaptic vesicle recycling are currently being examined, but in light of the effect of Wnt3a on actin dynamics it is possible that Wnts increase vesicle fusion and recycling. The contribution of the Wnt3a-induced microtubule loops to synapse formation are not known, but roles in both the regulation of axonal transport and vesicle localisation (Tsui *et al.*, 1984) are plausible.

6.8 Wnts and neuronal connectivity

In addition to the roles of Wnt3 and Wnt7a in axonal remodelling and synaptogenesis (Hall *et al.*, 2000; Krylova *et al.*, 2002), Wnt7b has recently been shown to be a key player in dendrite morphogenesis (Rosso *et al.*, 2005). Wnt7b is expressed in the hippocampus and increases both dendritic length and branching of hippocampal neurons. These effects are mediated by Dvl1 and a non canonical Wnt signalling pathway involving Rac and JNK (Rosso *et al.*, 2005). The different effects of Wnts on

different cells types could be due to the specific time points during development when they encounter the Wnt signal or to intrinsic differences in the axonal cytoskeleton. However, they are also likely to be achieved through different signalling pathways. These findings highlight the versatility of Wnt signalling on the axonal cytoskeleton and suggest a general function for Wnts in regulating the morphology of axons during the formation of neuronal connections.

Since different Wnt family members have distinct effects on neuronal morphology, are expressed by distinct neuronal cell types and act on particular subpopulations of neurons (Rosso *et al.*, 2005; Krylova *et al.*, 2002; Lucas and Salinas, 1997), Wnts may not only be involved in synaptic differentiation but also in the specificity with which particular inputs synapse on particular targets. Whether Wnts can also modulate synaptic function is currently being investigated, but the maintenance of Wnt expression in the adult nervous system (Lucas and Salinas, 1997; Salinas *et al.*, 1994) hints at a potential role in the regulation of synaptic plasticity throughout life.

6.9 Conclusions

This thesis has characterised the effects of Wnt3a on axon behaviour as well as the underlying changes taking place in the cytoskeleton. Wnt3a decreases axonal outgrowth, while promoting branching and growth cone enlargement in DRGs. These effects can be attributed to locally induced changes in the organisation and dynamics of both microtubules and actin filaments. Due to the roles of Wnts as guidance cues and synaptogenic factors, the effects described could be important for axon pathfinding and synapse formation. The well-characterised Wnt signalling pathways, will enable further elucidation of the mechanisms by which Wnts regulate the cytoskeleton, axon behaviour and synaptic differentiation as axons approach their synaptic targets.

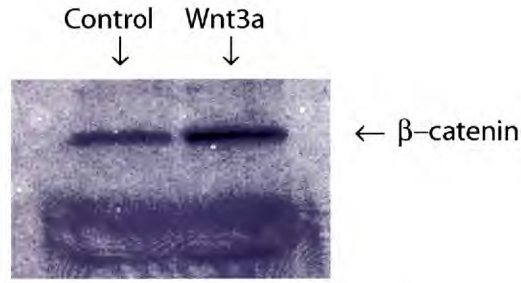
Acknowledgements.

I would like to thank my supervisor, Patricia Salinas, for her help and enthusiasm throughout my project, as well as past and present members of the group for their technical advice and friendship.

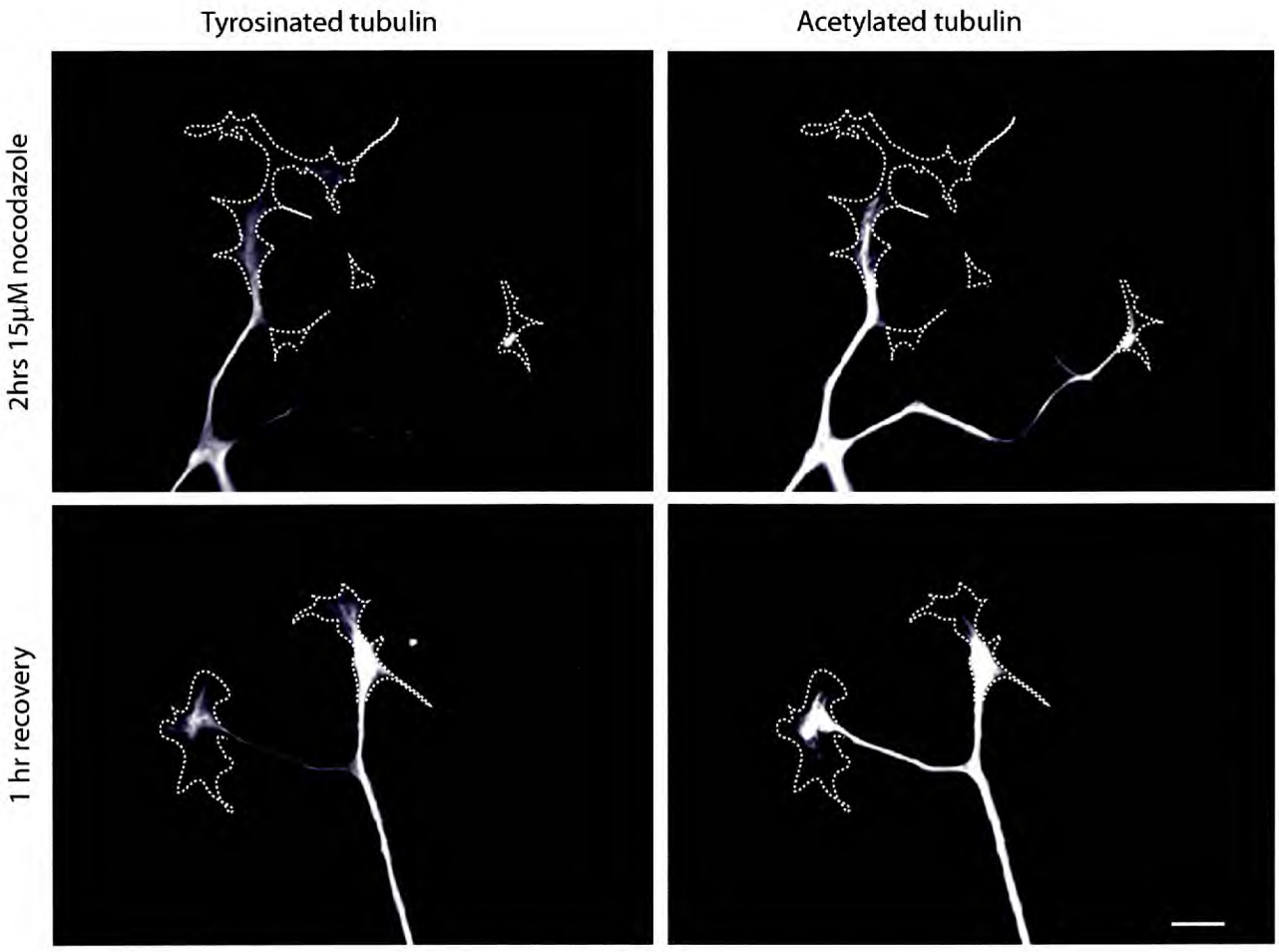
Thank you to John and the rest of my family for their constant encouragement and emotional support.

Finally, I would also like to thank the BBSRC (Biotechnology and Biological Sciences Research Council) for the funding that facilitated my completion of this project.

Appendix 1. Supplementary figures.



Supplemetary figure 1. Wnt3a increases the levels of β-catenin in DRGs.
Western blot of DRGs treated with control or Wnt3a media for 2 hours.



Supplementary figure 2. Microtubules recover within 1 hour of removal of nocodazole.
Two hours exposure to 15μM nocodazole causes depolymerisation of tyrosinated microtubules and retraction of acetylated microtubules. Within an hour of removing the drug, tyrosinated tubulin polymers are rebuilt and acetylated microtubules can be found in growth cones indicating that the health of the neurons is not being jeopardised by the nocodazole treatment. Bar, 10μm.

Appendix 2. Wnt3 axonal remodelling of neonatal DRGs.

Average growth cone size (μm^2)	**Control**	**Wnt3**
Experiment 1	25.28 (n=137)	36.29 (n=81)
Experiment 2	26.66 (n=152)	36.94 (n=164)
Experiment 3	23.81 (n=134)	41.16 (n=154)
MEAN	25.25	38.13
STD DEV	1.42	2.64
STD ERROR	0.82	1.52
Student t test	p=0.0017	
Average axon length (μm)	**Control**	**Wnt3**
Experiment 1	183.3 (n=78)	134.4 (n=78)
Experiment 2	186.12 (n=76)	148.14 (n=76)
Experiment 3	176.64 (n=66)	147.42 (n=118)
MEAN	182.02	143.32
STD DEV	4.86	7.73
STD ERROR	2.81	4.46
Student t test	p=0.0018	

Wnt3 time course.
n>30

Average growth cone size (μm^2)	**2 hrs Con.**	**2 hrs Wnt3**	**4 hrs Con.**	**4 hrs Wnt3**	**6 hrs Con.**	**6 hrs Wnt3**	**18 hrs Con.**	**18 hrs Wnt3**	**22 hrs Con.**	**22 hrs Wnt3**
Exp 1	35.67	26.29	37.47	37.67	27.53	31.38	24.78	37.41	20.87	41.01
Exp 2	27.96	35.86	26.19	36.63	35.86	39.96	26.44	46.65	22.89	46.32
Exp 3	34.09	39.72	29.35	27.03	33.98	36.46	31.54	34.02	26.42	34.69
MEAN	32.57	33.95	31.00	33.77	32.45	35.92	27.58	39.36	23.39	40.68
STD DEV	4.07	6.91	5.81	5.86	4.36	4.31	3.52	6.53	2.8	5.82
STD ERROR	2.35	3.99	3.35	3.38	2.52	2.49	2.04	3.77	1.61	3.36
Student t test	p=0.78		p=0.59		p=0.38		p=0.049		p=0.009	

Wnt3 mediated increase in growth cone size is not affected by cell density or laminin concentration.

Average growth cone size (μm^2)	Control Low density	Wnt3 Low density	Control High density	Wnt3 High density
Exp 1	27.00 (n=40)	49.21 (n=42)	15.68 (n=38)	36.47 (n=42)
Exp 2	18.33 (n=43)	36.22 (n=58)	30.97 (n=44)	45.75 (n=43)
Exp 3	29.58 (n=55)	39.73 (n=67)	23.97 (n=49)	40.92 (n=39)
MEAN	24.97	41.72	23.54	41.04
STD DEV	5.89	6.71	7.65	4.64
STD ERROR	3.4	3.88	4.42	2.68
Student t test	p=0.031		p=0.027	

Average growth cone size (μm^2)	50µg/ml laminin Control	50µg/ml laminin Wnt3	30µg/ml laminin Control	30µg/ml laminin Wnt3	20µg/ml laminin Control	20µg/ml laminin Wnt3
Exp 1	26.51(n=23)	49.39(n=27)	28.00(n=25)	44.10(n=29)	29.90(n=30)	54.34(n=32)
Exp 2	23.08(n=26)	33.55(n=45)	37.41(n=69)	41.24(n=48)	33.38(n=53)	56.60(n=46)
Exp 3	20.44(n=28)	41.01(n=75)	22.55(n=54)	47.38(n=41)	32.84(n=46)	45.13(n=30)
MEAN	23.34	41.31	29.32	44.24	32.04	52.02
STD DEV	3.04	7.92	7.51	3.07	1.87	6.07
STD ERROR	1.75	4.58	4.34	1.77	1.08	3.51
Student t test	p=0.021		p=0.032		p=0.005	

The effect of Wnt3, from L-cell conditioned medium, on growth cone size requires 22 hours exposure.

Average growth cone size (μm^2)	4 hours Control	4 hours Wnt3	22 hours Control	22 hours Wnt3
Exp 1	26.78(n=36)	29.45(n=39)	24.73(n=28)	38.61(n=35)
Exp 2	34.89(n=37)	37.51(n=29)	33.21(n=41)	41.94(n=43)
Exp 3	28.71(n=29)	31.05(n=38)	25.97(n=32)	37.42(n=31)
MEAN	30.12	32.67	27.97	39.32
STD DEV	4.23	4.26	4.58	2.34
STD ERROR	2.44	2.46	2.64	1.35
Student t test	p=0.504		p=0.018	

The effect of Wnt3 on axonal remodelling is not observed when DRG neurons are grown on L-cell monolayers.

Average growth cone size (μm^2)	**4 hours Control**	**4 hours Wnt3**	**22 hours Control**	**22 hours Wnt3**
Exp 1	39.03(n=27)	42.33(n=26)	33.92(n=31)	36.51(n=29)
Exp 2	45.81(n=25)	47.89(n=27)	39.28(n=28)	44.36(n=30)
Exp 3	41.23(n=31)	43.96(n=33)	36.63(n=32)	39.89(n=27)
MEAN	42.02	44.72	36.61	40.25
STD DEV	3.45	2.85	2.68	3.93
STD ERROR	1.99	1.65	1.54	2.27
Student t test	p=0.355		p=0.255	

Appendix 3. Wnt3a axonal remodelling of neonatal DRGs.

Purified Wnt3a induces axonal remodelling in DRGs after 22 hours exposure.

Average growth cone size (μm^2)	**Control**	**Wnt3a**
Experiment 1	35.92 (n=38)	48.36 (n=40)
Experiment 2	34.48 (n=44)	46.73 (n=39)
Experiment 3	29.30 (n=52)	40.13 (n=54)
MEAN	33.23	45.07
STD DEV	3.48	4.35
STD ERROR	2.01	2.51
Student t test	p=0.021	
Average axon length (μm)	**Control**	**Wnt3a**
Experiment 1	187.92 (n=35)	114.29 (n=32)
Experiment 2	161.43 (n=20)	150.93 (n=28)
Experiment 3	180.76 (n=22)	150.78 (n=23)
MEAN	176.70	134.66
STD DEV	13.7	18.47
STD ERROR	7.9	10.68
Student t test	p=0.032	

Purified Wnt3a induces axonal remodelling in DRGs after 2 hours exposure.

Average growth cone size (μm^2)	**Control**	**Wnt3a**
Experiment 1	36.25 (n=107)	61.03 (n=127)
Experiment 2	31.63 (n=184)	54.70 (n=217)
Experiment 3	37.47 (n=141)	52.91 (n=167)
MEAN	35.11	56.21
STD DEV	3.08	4.27
STD ERROR	1.78	2.46
Student t test	p=0.0022	
Average axon length (μm)	**Control**	**Wnt3a**
Experiment 1	146.02 (n=28)	70.52(n=20)
Experiment 2	121.31 (n=20)	89.74 (n=25)
Experiment 3	117.82 (n=21)	97.39 (n=23)
MEAN	128.38	85.88
STD DEV	15.37	13.84
STD ERROR	8.88	8.00
Student t test	p=0.023	

Wnt3a time course.

Average growth cone size (μm^2)	**10 minutes Control**	**10 minutes Wnt3a**	**60 minutes Control**	**60 minutes Wnt3a**	**120 minutes Control**	**120 minutes Wnt3a**
Exp 1	59.13(n=124)	64.90(n=108)	34.34(n=92)	41.28(n=129)	35.86(n=103)	52.20(n=119)
Exp 2	41.19(n=109)	41.05(n=100)	52.51(n=78)	53.76(n=116)	35.55(n=106)	59.46(n=102)
Exp 3	46.30(n=124)	57.18(n=109)	43.50(n=94)	50.80(n=129)	40.13(n=66)	63.44(n=132)
MEAN	48.87	54.37	43.45	48.61	37.18	58.36
STD DEV	9.24	12.16	9.08	6.52	2.55	5.69
STD ERROR	5.33	7.02	5.24	3.76	1.47	3.29
Student t test	p=0.56		p=0.46		p=0.004	

Appendix 4. Dvl1 expression and inhibition of Gsk-3β by lithium mimic the effect of Wnt3a on growth cone size.

Average growth cone size (μm^2)	**GFP**	**Dvl1**
Experiment 1	27.38 (n=64)	37.14 (n=54)
Experiment 2	34.79 (n=29)	50.38 (n=42)
Experiment 3	38.75 (n=24)	67.10 (n=26)
Experiment 4	25.75 (n=58)	53.96 (n=34)
MEAN	31.66	52.12
STD DEV	6.14	12.28
STD ERROR	3.07	6.14
Student t test	p=0.02	

Inhibition of Gsk-3β by Lithium mimics the effect of Wnt3a on growth cone size.

Average growth cone size (μm^2)	**NaCl**	**LiCl**
Experiment 1	21.88 (n=51)	62.91 (n=44)
Experiment 2	26.49 (n=43)	42.47 (n=46)
Experiment 3	35.43 (n=65)	46.81 (n=69)
MEAN	27.93	50.73
STD DEV	6.88	10.7
STD ERROR	3.97	6.21
Student t test	p=0.03	

Appendix 5. The effect of Wnt3a on growth cone size does not require nuclear transcription, but it does require protein translation.

n>48

Average growth cone size (μm^2)	Vehicle Control	Vehicle Wnt3a	Actinomycin Control	Actinomycin Wnt3a	Anisomycin Control	Anisomycin Wnt3a
Exp 1	31.03	47.58	38.66	46.09	16.93	20.85
Exp 2	32.40	50.40	31.31	46.02	21.09	22.69
Exp 3	30.90	47.66	29.45	48.35	23.29	26.47
MEAN	31.47	48.54	33.14	46.82	20.43	21.32
STD DEV	0.88	1.60	4.87	1.32	3.22	1.20
STD ERROR	0.50	0.92	2.81	0.76	1.86	0.69
Student t test	$p=8x10^{-5}$		p=0.009		p=0.67	

Appendix 6. Wnt3a confers resistance to nocodazole.

n>23

% of axon length containing Ace. Tub.	Control	Wnt3a	Nocodazole Control	Nocodazole Wnt3a
Exp 1	89	91	59	87
Exp 2	92	95	75	87
Exp 3	94	95	76	94
MEAN	91.66	93.66	70	89.33
STD DEV	2.51	2.30	9.53	4.04
STD ERROR	1.45	1.33	5.50	2.33

n>95

% of growth cones with Ace. Tub. In growth cones	Control	Wnt3a	Nocodazole Control	Nocodazole Wnt3a
Exp 1	59	61	16	36
Exp 2	56	59	8	29
Exp 3	49	48	12	30
MEAN	54.66	56	12	31.66
STD DEV	5.13	7	4	3.78
STD ERROR	2.96	4.04	2.31	2.18

Appendix 7. Wnt3a does not affect the velocity of EB3-GFP excursions.

The speed of EB3-GFP comets in at least 10 growth cones was measured per experiment.

Speed of EB3-GFP (μm/sec)	**Axon Control**	**Axon Wnt3a**	**Growth cone Control**	**Growth cone Wnt3a**
Exp 1	0.077	0.074	0.096	0.088
Exp 2	0.148	0.152	0.140	0.116
Exp 3	0.220	0.156	0.181	0.140
MEAN	0.148	0.127	0.138	0.114
STD DEV	0.071	0.046	0.042	0.026
STD ERROR	0.041	0.026	0.022	0.015
Student t test	p=0.69		p=0.44	

Appendix 8. Wnt3a increases F-actin in growth cones.

n>48

F-actin area in growth cones (μm^2)	**Control**	**Wnt3a**	**% of F-actin area in growth cones**	**Control**	**Wnt3a**
Exp 1	9.64	46.21	Exp 1	32.13	42.43
Exp 2	13.79	37.95	Exp 2	40.21	51.36
Exp 3	15.96	47.8	Exp 3	27.29	40.26
MEAN	13.13	43.98	MEAN	33.21	44.69
STD DEV	3.21	5.28	STD DEV	6.52	5.87
STD ERROR	1.85	3.05	STD ERROR	3.77	3.39
Student t test	p=0.0009		Student t test	p=0.043	

Appendix 9. F-actin is more susceptible to depolymerisation in the presence of Wnt3a.

n>43

F-actin area (μm^2)	0 drug Control	0 drug Wnt3a	2μM Cyt. D Control	2μM Cyt. D Wnt3a	0.5μM Lat. B Control	0.5μM Lat. B Wnt3a
Exp 1	13.0	31.1	9.41	17.27	1.61	4.74
Exp 2	15.9	47.8	7.12	12.44	1.05	3.34
Exp 3	12.9	35.4	6.10	18.91	0.87	2.05
MEAN	13.9	38.1	7.54	16.20	1.17	3.37
STD DEV	1.70	8.71	1.69	3.35	0.38	1.34
STD ERROR	0.98	5.02	0.97	1.93	0.22	0.77
Student t test	p=0.009		p=0.01		p=0.052	

1μM Cytochalasin D (n>36).

F-actin area (μm^2)	0 min. Control	0 min. Wnt3a	2 min. Control	2 min. Wnt3a	4 min. Control	4 min. Wnt3a	6 min. Control	6 min. Wnt3a
Exp 1	10.4	30.1	13.6	24.8	9.9	18.2	8.4	14.6
Exp 2	11.8	37.8	13.6	27.1	12.4	15.8	13.2	13.6
Exp 3	17.1	38.3	9.8	13.0	9.9	10.7	10.4	12.7
MEAN	13.10	35.40	12.33	21.66	10.77	14.92	10.67	13.64
STD DEV	3.47	4.62	2.19	7.54	1.46	3.82	2.41	0.94
STD ERROR	2.01	2.66	1.26	4.35	0.84	2.21	1.39	0.54

0.1μM Latrunculin B (n>30).

F-actin area (μm^2)	0 min. Control	0 min. Wnt3a	2 min. Control	2 min. Wnt3a	4 min. Control	4 min. Wnt3a	6 min. Control	6 min. Wnt3a
Exp 1	10.4	30.1	12.1	12.0	15.8	8.3	8.8	10.5
Exp 2	11.8	37.8	10.1	19.2	10.5	17.2	9.4	14.3
Exp 3	17.1	38.3	12.2	13.1	11.2	12.2	9.1	9.9
MEAN	13.10	35.40	11.50	14.76	12.5	12.58	9.09	11.60
STD DEV	3.47	4.62	1.18	3.87	2.88	4.47	0.30	2.37
STD ERROR	2.01	2.66	0.68	2.23	1.66	2.58	0.17	1.36

Appendix 10. F-actin polymerises faster in the presence of Wnt3a.
n>27

Relative recovery of F-actin	500nM Cyt. D Control	500nM Cyt. D Wnt3a	750nM Cyt. D Control	750nM Cyt. D Wnt3a	1000nM Cyt. D Control	1000nM Cyt. D Wnt3a
Exp 1	3.06	2.84	1.46	2.83	0.87	3.84
Exp 2	1.27	4.60	1.65	3.62	1.00	2.52
Exp 3	0.41	2.74	1.30	1.86	1.25	2.68
MEAN	1.58	3.39	1.47	2.77	1.04	3.01
STD DEV	1.35	1.04	0.17	0.88	0.19	0.72
STD ERROR	0.78	0.60	0.10	0.50	0.11	0.41

Appendix 11. Wnt3a increases the speed of filopodia and the relative percentage of lamellar perimeter undergoing protrusion.

n>142 filopodia

Average speed of filopodia (μm/sec)	Control	Wnt3a
Exp 1	0.030	0.074
Exp 2	0.029	0.043
Exp 3	0.034	0.044
MEAN	0.031	0.057
STD DEV	0.002	0.015
STD ERROR	0.001	0.008
Student t test	p=0.04	

n>12 growth cones

Relative % of perimeter protruding	Control	Wnt3a
Exp 1	25.10	34.81
Exp 2	18.80	30.81
Exp 3	14.84	32.71
MEAN	19.58	32.77
STD DEV	5.17	2.00
STD ERROR	2.99	1.15
Student t test	p=0.014	

Appendix 12. Inhibition of the actin retrograde flow does not affect the Wnt3a-induced increase in growth cone size or F-actin accumulation in growth cones.

n>36

Average growth cone size (μm^2)	**0 drug Control**	**0 drug Wnt3a**	**5mM BDM Control**	**5mM BDM Wnt3a**	**50μM blebb. Control**	**50μM blebb. Wnt3a**
Exp 1	35.76	55.35	34.11	59.02	30.00	50.42
Exp 2	32.79	55.61	39.62	67.18	33.59	53.37
Exp 3	25.44	53.24	34.53	48.42	35.78	52.83
MEAN	31.33	54.73	36.08	58.20	33.12	52.20
STD DEV	5.31	1.22	3.06	9.40	2.91	1.57
STD ERROR	3.07	0.75	1.77	5.43	1.68	0.90
Student t test	p=0.0017		p=0.017		p=0.0005	

n>36

F-actin area in growth cones (μm^2)	**0 drug Control**	**0 drug Wnt3a**	**5mM BDM Control**	**5mM BDM Wnt3a**	**50μM blebb. Control**	**50μM blebb. Wnt3a**
Exp 1	15.41	54.56	9.92	44.80	8.13	44.74
Exp 2	15.00	44.86	14.94	40.39	12.17	48.57
Exp 3	14.64	34.47	13.35	32.52	11.08	22.23
MEAN	15.01	44.63	12.73	39.23	10.46	38.51
STD DEV	0.38	10.04	2.56	6.22	2.09	14.23
STD ERROR	0.22	5.80	1.48	3.59	1.20	8.22
Student t test	p=0.006		p=0.002		p=0.027	

Bibliography

Ahmad, F. J. and Baas, P. W. (1995). Microtubules released from the neuronal centrosome are transported into the axon. *J Cell Sci* **108 (Pt 8)**, 2761-9.

Ahmad, F. J., Echeverri, C. J., Vallee, R. B. and Baas, P. W. (1998). Cytoplasmic dynein and dynactin are required for the transport of microtubules into the axon. *J Cell Biol* **140**, 391-401.

Ahmad, F. J., Hughey, J., Wittmann, T., Hyman, A., Greaser, M. and Baas, P. W. (2000). Motor proteins regulate force interactions between microtubules and microfilaments in the axon. *Nat Cell Biol* **2**, 276-80.

Ahmad, F. J., Yu, W., McNally, F. J. and Baas, P. W. (1999). An essential role for katanin in severing microtubules in the neuron. *J Cell Biol* **145**, 305-15.

Aizawa, H., Wakatsuki, S., Ishii, A., Moriyama, K., Sasaki, Y., Ohashi, K., Sekine-Aizawa, Y., Sehara-Fujisawa, A., Mizuno, K., Goshima, Y. *et al.* (2001). Phosphorylation of cofilin by LIM-kinase is necessary for semaphorin 3A-induced growth cone collapse. *Nat Neurosci* **4**, 367-73.

Akhmanova, A., Hoogenraad, C. C., Drabek, K., Stepanova, T., Dortland, B., Verkerk, T., Vermeulen, W., Burgering, B. M., De Zeeuw, C. I., Grosveld, F. *et al.* (2001). Clasps are CLIP-115 and -170 associating proteins involved in the regional regulation of microtubule dynamics in motile fibroblasts. *Cell* **104**, 923-35.

Aletta, J. M. and Greene, L. A. (1988). Growth cone configuration and advance: a time-lapse study using video-enhanced differential interference contrast microscopy. *J Neurosci* **8**, 1425-35.

Amoyel, M., Cheng, Y. C., Jiang, Y. J. and Wilkinson, D. G. (2005). Wnt1 regulates neurogenesis and mediates lateral inhibition of boundary cell specification in the zebrafish hindbrain. *Development* **132**, 775-85.

Anderson, D. J. (1997). Cellular and molecular biology of neural crest cell lineage determination. *Trends Genet* **13**, 276-80.

Akhmanova, A.,Hoogenraad, C. C., Drabek, K., Stepanova, T., Dortland, B., Verkerk, T., Vermeulen, W., Burgering, B. M., De Zeeuw, C. I., Grosveld, F. *et al.* (2001). Clasps are CLIP-115 and -170 associating proteins involved in the regional regulation of microtubule dynamics in motile fibroblasts. *Cell* **104**, 923-35.

Atack, J. R., Broughton, H. B. and Pollack, S. J. (1995). Inositol monophosphatase--a putative target for Li+ in the treatment of bipolar disorder. *Trends Neurosci* **18**, 343-9

Augsburger, A., Schuchardt, A., Hoskins, S., Dodd, J. and Butler, S. (1999). BMPs as mediators of roof plate repulsion of commissural neurons. *Neuron* **24**, 127-41.

Avwenagha, O., Campbell, G. and Bird, M. M. (2003). Distribution of GAP-43, beta-III tubulin and F-actin in developing and regenerating axons and their growth cones in vitro, following neurotrophin treatment. *J Neurocytol* **32**, 1077-89.

Baas, P. W. (2002). Microtubule transport in the axon. *Int Rev Cytol* **212**, 41-62.

Baas, P. W., Ahmad, F. J., Pienkowski, T. P., Brown, A. and Black, M. M. (1993). Sites of microtubule stabilization for the axon. *J Neurosci* **13**, 2177-85.

Baas, P. W., Black, M. M. and Banker, G. A. (1989). Changes in microtubule polarity orientation during the development of hippocampal neurons in culture. *J Cell Biol* **109**, 3085-94.

Baas, P. W., Pienkowski, T. P., Cimbalnik, K. A., Toyama, K., Bakalis, S., Ahmad, F. J. and Kosik, K. S. (1994). Tau confers drug stability but not cold stability to microtubules in living cells. *J Cell Sci* **107 (Pt 1)**, 135-43

Baas, P. W. and Qiang, L. (2005). Neuronal microtubules: when the MAP is the roadblock. *Trends Cell Biol* **15**, 183-7.

Bafico, A., Liu, G., Yaniv, A., Gazit, A. and Aaronson, S. A. (2001). Novel mechanism of Wnt signalling inhibition mediated by Dickkopf-1 interaction with LRP6/Arrow. *Nat Cell Biol* **3**, 683-6.

Baker, J. C., Beddington, R. S. and Harland, R. M. (1999). Wnt signaling in Xenopus embryos inhibits bmp4 expression and activates neural development. *Genes Dev* **13**, 3149-59.

Ballestrem, C., Wehrle-Haller, B. and Imhof, B. A. (1998). Actin dynamics in living mammalian cells. *J Cell Sci* **111 (Pt 12)**, 1649-58.

Barth, A. I., Nathke, I. S. and Nelson, W. J. (1997). Cadherins, catenins and APC protein: interplay between cytoskeletal complexes and signaling pathways. *Curr Opin Cell Biol* **9**, 683-90.

Bashaw, G. J., Kidd, T., Murray, D., Pawson, T. and Goodman, C. S. (2000). Repulsive axon guidance: Abelson and Enabled play opposing roles downstream of the roundabout receptor. *Cell* **101**, 703-15.

Bassell, G. J., Zhang, H., Byrd, A. L., Femino, A. M., Singer, R. H., Taneja, K. L., Lifshitz, L. M., Herman, I. M. and Kosik, K. S. (1998). Sorting of beta-actin mRNA and protein to neurites and growth cones in culture. *J Neurosci* **18**, 251-65.

Bate, M. (1976). Pioneer neurons in an insect embryo. *Nature*, 54-56.

Battye, R., Stevens, A. and Jacobs, J. R. (1999). Axon repulsion from the midline of the Drosophila CNS requires slit function. *Development* **126**, 2475-81.

Benson, D.L., Schnapp, L. M., Shapiro, L. and Huntley, G. W. (2000). Making memories stick: cell adhesion molecules in synaptic plasticity. *Trends Cell Biol* **10**, 473-82.

Benson, D. L. and Tanaka, H. (1998). N-cadherin redistribution during synaptogenesis in hippocampal neurons. *J Neurosci* **18**, 6892-904.

Bentley, D. and O'Connor, T. P. (1994). Cytoskeletal events in growth cone steering. *Curr Opin Neurobiol* **4**, 43-8.

Berridge, M. J., Downes, C. P. and Hanley, M. R. (1989). Neural and developmental actions of lithium: a unifying hypothesis. *Cell* **59**, 411-9.

Bhanot, P., Brink, M., Samos, C. H., Hsieh, J. C., Wang, Y., Macke, J. P., Andrew, D., Nathans, J. and Nusse, R. (1996). A new member of the frizzled family from Drosophila functions as a Wingless receptor. *Nature* **382**, 225-30.

Bienz, M. (2002). The subcellular destinations of APC proteins. *Nat Rev Mol Cell Biol* **3**, 328-38.

Bouwmeester, T., Kim, S., Sasai, Y., Lu, B. and De Robertis, E. M. (1996). Cerberus is a head-inducing secreted factor expressed in the anterior endoderm of Spemann's organizer. *Nature* **382**, 595-601.

Bradke, F. and Dotti, C. G. (1999). The role of local actin instability in axon formation. *Science* **283**, 1931-4.

Bradley, R. S. and Brown, A. M. (1995). A soluble form of Wnt-1 protein with mitogenic activity on mammary epithelial cells. *Mol Cell Biol* **15**, 4616-22.

Bradley, R. S. and Brown, A. M. (1990). The proto-oncogene int-1 encodes a secreted protein associated with the extracellular matrix. *Embo J* **9**, 1569-75.
Braisted, J. E., McLaughlin, T., Wang, H. U., Friedman, G. C., Anderson, D. J. and O'Leary D, D. (1997). Graded and lamina-specific distributions of ligands of EphB receptor tyrosine kinases in the developing retinotectal system. *Dev Biol* **191**, 14-28.
Bray, D. (1970). Surface movements during the growth of single explanted neurons. *Proc Natl Acad Sci U S A* **65**, 905-10.
Bray, D. and White, J. G. (1988). Cortical flow in animal cells. *Science* **239**, 883-8.
Brenner, S. L. and Korn, E. D. (1980). The effects of cytochalasins on actin polymerization and actin ATPase provide insights into the mechanism of polymerization. *J Biol Chem* **255**, 841-4.
Brose, K., Bland, K. S., Wang, K. H., Arnott, D., Henzel, W., Goodman, C. S., Tessier-Lavigne, M. and Kidd, T. (1999). Slit proteins bind Robo receptors and have an evolutionarily conserved role in repulsive axon guidance. *Cell* **96**, 795-806.
Brown, A., Li, Y., Slaughter, T. and Black, M. M. (1993). Composite microtubules of the axon: quantitative analysis of tyrosinated and acetylated tubulin along individual axonal microtubules. *J Cell Sci* **104 (Pt 2)**, 339-52.
Brown, M. E. and Bridgman, P. C. (2003). Retrograde flow rate is increased in growth cones from myosin IIB knockout mice. *J Cell Sci* **116**, 1087-94
Brown, S. S. (1999). Cooperation between microtubule- and actin-based motor proteins. *Annu Rev Cell Dev Biol* **15**, 63-80.
Bruckner, K., Pasquale, E. B. and Klein, R. (1997). Tyrosine phosphorylation of transmembrane ligands for Eph receptors. *Science* **275**, 1640-3.
Buck, K. B. and Zheng, J. Q. (2002). Growth cone turning induced by direct local modification of microtubule dynamics. *J Neurosci* **22**, 9358-67.
Burrus, L. W. and McMahon, A. P. (1995). Biochemical analysis of murine Wnt proteins reveals both shared and distinct properties. *Exp Cell Res* **220**, 363-73.
Butler, S. J. and Dodd, J. (2003). A role for BMP heterodimers in roof plate-mediated repulsion of commissural axons. *Neuron* **38**, 389-401.
Cabrera, C. V., Alonso, M. C., Johnston, P., Phillips, R. G. and Lawrence, P. A. (1987). Phenocopies induced with antisense RNA identify the wingless gene. *Cell* **50**, 659-63.
Cadigan, K. M. and Nusse, R. (1997). Wnt signaling: a common theme in animal development. *Genes Dev* **11**, 3286-305.
Campbell, D. S. and Holt, C. E. (2001). Chemotropic responses of retinal growth cones mediated by rapid local protein synthesis and degradation. *Neuron* **32**, 1013-26.
Capelluto, D. G., Kutateladze, T. G., Habas, R., Finkielstein, C. V., He, X. and Overduin, M. (2002). The DIX domain targets dishevelled to actin stress fibres and vesicular membranes. *Nature* **419**, 726-9.
Carvalho, P., Tirnauer, J. S. and Pellman, D. (2003). Surfing on microtubule ends. *Trends Cell Biol* **13**, 229-37.
Castellani, V., Chedotal, A., Schachner, M., Faivre-Sarrailh, C. and Rougon, G. (2000). Analysis of the L1-deficient mouse phenotype reveals cross-talk between Sema3A and L1 signaling pathways in axonal guidance. *Neuron* **27**, 237-49.

Charron, F., Stein, E., Jeong, J., McMahon, A. P. and Tessier-Lavigne, M. (2003). The morphogen sonic hedgehog is an axonal chemoattractant that collaborates with netrin-1 in midline axon guidance. *Cell* **113**, 11-23.
Chen, W., ten Berge, D., Brown, J., Ahn, S., Hu, L. A., Miller, W. E., Caron, M. G., Barak, L. S., Nusse, R. and Lefkowitz, R. J. (2003). Dishevelled 2 recruits beta-arrestin 2 to mediate Wnt5A-stimulated endocytosis of Frizzled 4. *Science* **301**, 1391-4.
Cheng, H. J., Nakamoto, M., Bergemann, A. D. and Flanagan, J. G. (1995). Complementary gradients in expression and binding of ELF-1 and Mek4 in development of the topographic retinotectal projection map. *Cell* **82**, 371-81.
Cheng, Q., Sasaki, Y., Shoji, M., Sugiyama, Y., Tanaka, H., Nakayama, T., Mizuki, N., Nakamura, F., Takei, K. and Goshima, Y. (2003). Cdk5/p35 and Rho-kinase mediate ephrin-A5-induced signaling in retinal ganglion cells. *Mol Cell Neurosci* **24**, 632-45.
Chin-Sang, I. D., George, S. E., Ding, M., Moseley, S. L., Lynch, A. S. and Chisholm, A. D. (1999). The ephrin VAB-2/EFN-1 functions in neuronal signaling to regulate epidermal morphogenesis in C. elegans. *Cell* **99**, 781-90.
Ciani, L., Krylova, O., Smalley, M. J., Dale, T. C. and Salinas, P. C. (2004). A divergent canonical WNT-signaling pathway regulates microtubule dynamics: dishevelled signals locally to stabilize microtubules. *J Cell Biol* **164**, 243-53.
Clark, P., Britland, S. and Connolly, P. (1993). Growth cone guidance and neuron morphology on micropatterned laminin surfaces. *J Cell Sci* **105 (Pt 1)**, 203-12.
Cohan, C. S., Welnhofer, E. A., Zhao, L., Matsumura, F. and Yamashiro, S. (2001). Role of the actin bundling protein fascin in growth cone morphogenesis: localization in filopodia and lamellipodia. *Cell Motil Cytoskeleton* **48**, 109-20.
Cohen, E. D., Mariol, M. C., Wallace, R. M., Weyers, J., Kamberov, Y. G., Pradel, J. and Wilder, E. L. (2002). DWnt4 regulates cell movement and focal adhesion kinase during Drosophila ovarian morphogenesis. *Dev Cell* **2**, 437-48.
Colamarino, S. A. and Tessier-Lavigne, M. (1995). The axonal chemoattractant netrin-1 is also a chemorepellent for trochlear motor axons. *Cell* **81**, 621-9.
Cole, J. C., Villa, B. R. and Wilkinson, R. S. (2000). Disruption of actin impedes transmitter release in snake motor terminals. *J Physiol* **525 Pt 3**, 579-86.
Colicos, M. A., Collins, B. E., Sailor, M. J. and Goda, Y. (2001). Remodeling of synaptic actin induced by photoconductive stimulation. *Cell* **107**, 605-16.
Cong, F., Schweizer, L. and Varmus, H. (2004). Wnt signals across the plasma membrane to activate the beta-catenin pathway by forming oligomers containing its receptors, Frizzled and LRP. *Development* **131**, 5103-15.
Correas, I., Padilla, R. and Avila, J. (1990). The tubulin-binding sequence of brain microtubule-associated proteins, tau and MAP-2, is also involved in actin binding. *Biochem J* **269**, 61-4.
Cramer, L. P. (1999). Role of actin-filament disassembly in lamellipodium protrusion in motile cells revealed using the drug jasplakinolide. *Curr Biol* **9**, 1095-105.
Cramer, L. P., Mitchison, T. J. and Theriot, J. A. (1994). Actin-dependent motile forces and cell motility. *Curr Opin Cell Biol* **6**, 82-6.
Cremer, H., Lange, R., Christoph, A., Plomann, M., Vopper, G., Roes, J., Brown, R., Baldwin, S., Kraemer, P., Scheff, S. *et al.* (1994). Inactivation of the N-CAM gene

in mice results in size reduction of the olfactory bulb and deficits in spatial learning. *Nature* **367**, 455-9.

Dabdoub, A., Donohue, M. J., Brennan, A., Wolf, V., Montcouquiol, M., Sassoon, D. A., Hseih, J. C., Rubin, J. S., Salinas, P. C. and Kelley, M. W. (2003). Wnt signaling mediates reorientation of outer hair cell stereociliary bundles in the mammalian cochlea. *Development* **130**, 2375-84.

Damon, D. H., Lobb, R. R., D'Amore, P. A. and Wagner, J. A. (1989). Heparin potentiates the action of acidic fibroblast growth factor by prolonging its biological half-life. *J Cell Physiol* **138**, 221-6.

Dasen, J. S., Liu, J. P. and Jessell, T. M. (2003). Motor neuron columnar fate imposed by sequential phases of Hox-c activity. *Nature* **425**, 926-33.

Daub, H., Gevaert, K., Vandekerckhove, J., Sobel, A. and Hall, A. (2001). Rac/Cdc42 and p65PAK regulate the microtubule-destabilizing protein stathmin through phosphorylation at serine 16. *J Biol Chem* **276**, 1677-80.

Davy, A., Gale, N. W., Murray, E. W., Klinghoffer, R. A., Soriano, P., Feuerstein, C. and Robbins, S. M. (1999). Compartmentalized signaling by GPI-anchored ephrin-A5 requires the Fyn tyrosine kinase to regulate cellular adhesion. *Genes Dev* **13**, 3125-35.

Deiner, M. S., Kennedy, T. E., Fazeli, A., Serafini, T., Tessier-Lavigne, M. and Sretavan, D. W. (1997). Netrin-1 and DCC mediate axon guidance locally at the optic disc: loss of function leads to optic nerve hypoplasia. *Neuron* **19**, 575-89.

Del Rio, J. A., Gonzalez-Billault, C., Urena, J. M., Jimenez, E. M., Barallobre, M. J., Pascual, M., Pujadas, L., Simo, S., La Torre, A., Wandosell, F. *et al.* (2004). MAP1B is required for Netrin 1 signaling in neuronal migration and axonal guidance. *Curr Biol* **14**, 840-50.

Dent, E. W., Barnes, A. M., Tang, F. and Kalil, K. (2004). Netrin-1 and semaphorin 3A promote or inhibit cortical axon branching, respectively, by reorganization of the cytoskeleton. *J Neurosci* **24**, 3002-12.

Dent, E. W., Callaway, J. L., Szebenyi, G., Baas, P. W. and Kalil, K. (1999). Reorganization and movement of microtubules in axonal growth cones and developing interstitial branches. *J Neurosci* **19**, 8894-908.

Dent, E. W. and Gertler, F. B. (2003). Cytoskeletal dynamics and transport in growth cone motility and axon guidance. *Neuron* **40**, 209-27.

Dent, E. W. and Kalil, K. (2001). Axon branching requires interactions between dynamic microtubules and actin filaments. *J Neurosci* **21**, 9757-69.

Diefenbach, T. J., Latham, V. M., Yimlamai, D., Liu, C. A., Herman, I. M. and Jay, D. G. (2002). Myosin 1c and myosin IIB serve opposing roles in lamellipodial dynamics of the neuronal growth cone. *J Cell Biol* **158**, 1207-17.

Doble, B. W. and Woodgett, J. R. (2003). Gsk-3: tricks of the trade for a multi-tasking kinase. *J Cell Sci* **116**, 1175-86.

Dontchev, V. D. and Letourneau, P. C. (2002). Nerve growth factor and semaphorin 3A signaling pathways interact in regulating sensory neuronal growth cone motility. *J Neurosci* **22**, 6659-69.

Drescher, U., Kremoser, C., Handwerker, C., Loschinger, J., Noda, M. and Bonhoeffer, F. (1995). In vitro guidance of retinal ganglion cell axons by RAGS, a 25 kDa tectal protein related to ligands for Eph receptor tyrosine kinases. *Cell* **82**, 359-70.

Drewes, G., Ebneth, A. and Mandelkow, E. M. (1998). MAPs, MARKs and microtubule dynamics. *Trends Biochem Sci* **23**, 307-11.
Eickholt, B. J., Walsh, F. S. and Doherty, P. (2002). An inactive pool of Gsk-3 at the leading edge of growth cones is implicated in Semaphorin 3A signaling. *J Cell Biol* **157**, 211-7.
Ellies, D. L., Church, V., Francis-West, P. and Lumsden, A. (2000). The WNT antagonist csFRP2 modulates programmed cell death in the developing hindbrain. *Development* **127**, 5285-95.
Endo, M., Ohashi, K., Sasaki, Y., Goshima, Y., Niwa, R., Uemura, T. and Mizuno, K. (2003). Control of growth cone motility and morphology by LIM kinase and Slingshot via phosphorylation and dephosphorylation of cofilin. *J Neurosci* **23**, 2527-37.
Endo, Y., Wolf, V., Muraiso, K., Kamijo, K., Soon, L., Uren, A., Barshishat-Kupper, M. and Rubin, J. S. (2005). Wnt-3a-dependent cell motility involves RhoA activation and is specifically regulated by dishevelled-2. *J Biol Chem* **280**, 777-86.
Erskine, L., Williams, S. E., Brose, K., Kidd, T., Rachel, R. A., Goodman, C. S., Tessier-Lavigne, M. and Mason, C. A. (2000). Retinal ganglion cell axon guidance in the mouse optic chiasm: expression and function of robos and slits. *J Neurosci* **20**, 4975-82.
Erter, C. E., Wilm, T. P., Basler, N., Wright, C. V. and Solnica-Krezel, L. (2001). Wnt8 is required in lateral mesendodermal precursors for neural posteriorization in vivo. *Development* **128**, 3571-83.
Espreafico, E. M., Cheney, R. E., Matteoli, M., Nascimento, A. A., De Camilli, P. V., Larson, R. E. and Mooseker, M. S. (1992). Primary structure and cellular localization of chicken brain myosin-V (p190), an unconventional myosin with calmodulin light chains. *J Cell Biol* **119**, 1541-57.
Fan, J., Mansfield, S. G., Redmond, T., Gordon-Weeks, P. R. and Raper, J. A. (1993). The organization of F-actin and microtubules in growth cones exposed to a brain-derived collapsing factor. *J Cell Biol* **121**, 867-78.
Fanto, M., Weber, U., Strutt, D. I. and Mlodzik, M. (2000). Nuclear signaling by Rac and Rho GTPases is required in the establishment of epithelial planar polarity in the Drosophila eye. *Curr Biol* **10**, 979-88.
Fass, J., Gehler, S., Sarmiere, P., Letourneau, P. and Bamburg, J. R. (2004). Regulating filopodial dynamics through actin-depolymerizing factor/cofilin. *Anat Sci Int* **79**, 173-83.
Fischer, M., Kaech, S., Knutti, D. and Matus, A. (1998). Rapid actin-based plasticity in dendritic spines. *Neuron* **20**, 847-54.
Forscher, P., Lin, C. H. and Thompson, C. (1992). Novel form of growth cone motility involving site-directed actin filament assembly. *Nature* **357**, 515-8.
Forscher, P. and Smith, S. J. (1988). Actions of cytochalasins on the organization of actin filaments and microtubules in a neuronal growth cone. *J Cell Biol* **107**, 1505-16.
Fournier, A. E., Nakamura, F., Kawamoto, S., Goshima, Y., Kalb, R. G. and Strittmatter, S. M. (2000). Semaphorin3A enhances endocytosis at sites of receptor-F-actin colocalization during growth cone collapse. *J Cell Biol* **149**, 411-22.
Fritsche, J., Reber, B. F., Schindelholz, B. and Bandtlow, C. E. (1999). Differential cytoskeletal changes during growth cone collapse in response to hSema III and thrombin. *Mol Cell Neurosci* **14**, 398-418.

Fukata, M., Watanabe, T., Noritake, J., Nakagawa, M., Yamaga, M., Kuroda, S., Matsuura, Y., Iwamatsu, A., Perez, F. and Kaibuchi, K. (2002a). Rac1 and Cdc42 capture microtubules through IQGAP1 and CLIP-170. *Cell* **109**, 873-85.

Fukata, Y., Itoh, T. J., Kimura, T., Menager, C., Nishimura, T., Shiromizu, T., Watanabe, H., Inagaki, N., Iwamatsu, A., Hotani, H. *et al.* (2002b). CRMP-2 binds to tubulin heterodimers to promote microtubule assembly. *Nat Cell Biol* **4**, 583-91.

Gallo, G. (1998). Involvement of microtubules in the regulation of neuronal growth cone morphologic remodeling. *J Neurobiol* **35**, 121-40.

Gallo, G. and Letourneau, P. C. (2000). Neurotrophins and the dynamic regulation of the neuronal cytoskeleton. *J Neurobiol* **44**, 159-73.

Gallo, G. and Letourneau, P. C. (1998). Localized sources of neurotrophins initiate axon collateral sprouting. *J Neurosci* **18**, 5403-14.

Gallo, G. and Pollack, E. D. (1997). Temporal regulation of growth cone lamellar protrusion and the influence of target tissue. *J Neurobiol* **33**, 929-44.

Gallo, G., Yee, H. F., Jr. and Letourneau, P. C. (2002). Actin turnover is required to prevent axon retraction driven by endogenous actomyosin contractility. *J Cell Biol* **158**, 1219-28.

Garcia-Castro, M. I., Marcelle, C. and Bronner-Fraser, M. (2002). Ectodermal Wnt function as a neural crest inducer. *Science* **297**, 848-51.

Gehler, S., Shaw, A. E., Sarmiere, P. D., Bamburg, J. R. and Letourneau, P. C. (2004). Brain-derived neurotrophic factor regulation of retinal growth cone filopodial dynamics is mediated through actin depolymerizing factor/cofilin. *J Neurosci* **24**, 10741-9.

George, S. E., Simokat, K., Hardin, J. and Chisholm, A. D. (1998). The VAB-1 Eph receptor tyrosine kinase functions in neural and epithelial morphogenesis in C. elegans. *Cell* **92**, 633-43.

Georgiou, M. and Tear, G. (2002). Commissureless is required both in commissural neurones and midline cells for axon guidance across the midline. *Development* **129**, 2947-56.

Gibney, J. and Zheng, J. Q. (2003). Cytoskeletal dynamics underlying collateral membrane protrusions induced by neurotrophins in cultured Xenopus embryonic neurons. *J Neurobiol* **54**, 393-405.

Glinka, A., Wu, W., Delius, H., Monaghan, A. P., Blumenstock, C. and Niehrs, C. (1998). Dickkopf-1 is a member of a new family of secreted proteins and functions in head induction. *Nature* **391**, 357-62.

Glinka, A., Wu, W., Onichtchouk, D., Blumenstock, C. and Niehrs, C. (1997). Head induction by simultaneous repression of Bmp and Wnt signalling in Xenopus. *Nature* **389**, 517-9.

Goldberg, D. J. and Burmeister, D. W. (1986). Stages in axon formation: observations of growth of Aplysia axons in culture using video-enhanced contrast-differential interference contrast microscopy. *J Cell Biol* **103**, 1921-31.

Goldberg, D. J., Foley, M. S., Tang, D. and Grabham, P. W. (2000). Recruitment of the Arp2/3 complex and mena for the stimulation of actin polymerization in growth cones by nerve growth factor. *J Neurosci Res* **60**, 458-67.

Gomes, E. R., Jani, S. and Gundersen, G. G. (2005). Nuclear movement regulated by Cdc42, MRCK, myosin, and actin flow establishes MTOC polarization in migrating cells. *Cell* **121**, 451-63.
Gomez, T. M. and Spitzer, N. C. (1999). In vivo regulation of axon extension and pathfinding by growth-cone calcium transients. *Nature* **397**, 350-5.
Goode, B. L., Drubin, D. G. and Barnes, G. (2000). Functional cooperation between the microtubule and actin cytoskeletons. *Curr Opin Cell Biol* **12**, 63-71.
Goold, R. G., Owen, R. and Gordon-Weeks, P. R. (1999). Glycogen synthase kinase 3beta phosphorylation of microtubule-associated protein 1B regulates the stability of microtubules in growth cones. *J Cell Sci* **112 (Pt 19)**, 3373-84.
Gordon-Weeks, P. R. (1991). Evidence for microtubule capture by filopodial actin filaments in growth cones. *Neuroreport* **2**, 573-6.
Goslin, K., Schreyer, D. J., Skene, J. H. and Banker, G. (1990). Changes in the distribution of GAP-43 during the development of neuronal polarity. *J Neurosci* **10**, 588-602.
Grabham, P. W., Reznik, B. and Goldberg, D. J. (2003). Microtubule and Rac 1-dependent F-actin in growth cones. *J Cell Sci* **116**, 3739-48.
Graef, I. A., Wang, F., Charron, F., Chen, L., Neilson, J., Tessier-Lavigne, M. and Crabtree, G. R. (2003). Neurotrophins and netrins require calcineurin/NFAT signaling to stimulate outgrowth of embryonic axons. *Cell* **113**, 657-70.
Guan, K. L. and Rao, Y. (2003). Signalling mechanisms mediating neuronal responses to guidance cues. *Nat Rev Neurosci* **4**, 941-56.
Gunhaga, L., Marklund, M., Sjodal, M., Hsieh, J. C., Jessell, T. M. and Edlund, T. (2003). Specification of dorsal telencephalic character by sequential Wnt and FGF signaling. *Nat Neurosci* **6**, 701-7.
Guthrie, S. (2004). Axon guidance: mice and men need Rig and Robo. *Curr Biol* **14**, R632-4.
Guthrie, S. (1997). Axon guidance: netrin receptors are revealed. *Curr Biol* **7**, R6-9.
Habas, R., Dawid, I. B. and He, X. (2003). Coactivation of Rac and Rho by Wnt/Frizzled signaling is required for vertebrate gastrulation. *Genes Dev* **17**, 295-309.
Hall, A. C., Lucas, F. R. and Salinas, P. C. (2000). Axonal remodeling and synaptic differentiation in the cerebellum is regulated by WNT-7a signaling. *Cell* **100**, 525-35.
Halloran, M. C. and Kalil, K. (1994). Dynamic behaviors of growth cones extending in the corpus callosum of living cortical brain slices observed with video microscopy. *J Neurosci* **14**, 2161-77.
Hao, J. C., Yu, T. W., Fujisawa, K., Culotti, J. G., Gengyo-Ando, K., Mitani, S., Moulder, G., Barstead, R., Tessier-Lavigne, M. and Bargmann, C. I. (2001). C. elegans slit acts in midline, dorsal-ventral, and anterior-posterior guidance via the SAX-3/Robo receptor. *Neuron* **32**, 25-38.
Harris, R. M. (1987). Axon collaterals in the thalamic reticular nucleus from thalamocortical neurons of the rat ventrobasal thalamus. *J Comp Neurol* **258**, 397-406.
Hasaka, T. P., Myers, K. A. and Baas, P. W. (2004). Role of actin filaments in the axonal transport of microtubules. *J Neurosci* **24**, 11291-301.
Hedgecock, E. M., Culotti, J. G. and Hall, D. H. (1990). The unc-5, unc-6, and unc-40 genes guide circumferential migrations of pioneer axons and mesodermal cells on the epidermis in C. elegans. *Neuron* **4**, 61-85.

Heisenberg, C. P., Tada, M., Rauch, G. J., Saude, L., Concha, M. L., Geisler, R., Stemple, D. L., Smith, J. C. and Wilson, S. W. (2000). Silberblick/Wnt11 mediates convergent extension movements during zebrafish gastrulation. *Nature* **405**, 76-81.

Hirabayashi, Y., Itoh, Y., Tabata, H., Nakajima, K., Akiyama, T., Masuyama, N. and Gotoh, Y. (2004). The Wnt/beta-catenin pathway directs neuronal differentiation of cortical neural precursor cells. *Development* **131**, 2791-801.

Holland, S. J., Gale, N. W., Mbamalu, G., Yancopoulos, G. D., Henkemeyer, M. and Pawson, T. (1996). Bidirectional signalling through the EPH-family receptor Nuk and its transmembrane ligands. *Nature* **383**, 722-5.

Holmberg, J., Clarke, D. L. and Frisen, J. (2000). Regulation of repulsion versus adhesion by different splice forms of an Eph receptor. *Nature* **408**, 203-6.

Hong, K., Hinck, L., Nishiyama, M., Poo, M. M., Tessier-Lavigne, M. and Stein, E. (1999). A ligand-gated association between cytoplasmic domains of UNC5 and DCC family receptors converts netrin-induced growth cone attraction to repulsion. *Cell* **97**, 927-41.

Hopker, V. H., Shewan, D., Tessier-Lavigne, M., Poo, M. and Holt, C. (1999). Growth-cone attraction to netrin-1 is converted to repulsion by laminin-1. *Nature* **401**, 69-73.

Houart, C., Caneparo, L., Heisenberg, C., Barth, K., Take-Uchi, M. and Wilson, S. (2002). Establishment of the telencephalon during gastrulation by local antagonism of Wnt signaling. *Neuron* **35**, 255-65.

Howard, J. and Hyman, A. A. (2003). Dynamics and mechanics of the microtubule plus end. *Nature* **422**, 753-8.

Hu, H., Marton, T. F. and Goodman, C. S. (2001). Plexin B mediates axon guidance in Drosophila by simultaneously inhibiting active Rac and enhancing RhoA signaling. *Neuron* **32**, 39-51.

Huelsken, J. and Birchmeier, W. (2001). New aspects of Wnt signaling pathways in higher vertebrates. *Curr Opin Genet Dev* **11**, 547-53.

Huynh-Do, U., Stein, E., Lane, A. A., Liu, H., Cerretti, D. P. and Daniel, T. O. (1999). Surface densities of ephrin-B1 determine EphB1-coupled activation of cell attachment through alphavbeta3 and alpha5beta1 integrins. *Embo J* **18**, 2165-73.

Hynes, R. O. (1992). Integrins: versatility, modulation, and signaling in cell adhesion. *Cell* **69**, 11-25.

Ikeya, M., Lee, S. M., Johnson, J. E., McMahon, A. P. and Takada, S. (1997). Wnt signalling required for expansion of neural crest and CNS progenitors. *Nature* **389**, 966-70.

Imondi, R., Wideman, C. and Kaprielian, Z. (2000). Complementary expression of transmembrane ephrins and their receptors in the mouse spinal cord: a possible role in constraining the orientation of longitudinally projecting axons. *Development* **127**, 1397-410.

Inagaki, N., Chihara, K., Arimura, N., Menager, C., Kawano, Y., Matsuo, N., Nishimura, T., Amano, M. and Kaibuchi, K. (2001). CRMP-2 induces axons in cultured hippocampal neurons. *Nat Neurosci* **4**, 781-2.

Inoue, A. and Sanes, J. R. (1997). Lamina-specific connectivity in the brain: regulation by N-cadherin, neurotrophins, and glycoconjugates. *Science* **276**, 1428-31.

Irie, F. and Yamaguchi, Y. (2004). EPHB receptor signaling in dendritic spine development. *Front Biosci* **9**, 1365-73.
Irving, C., Malhas, A., Guthrie, S. and Mason, I. (2002). Establishing the trochlear motor axon trajectory: role of the isthmic organiser and Fgf8. *Development* **129**, 5389-98.
Iwai, Y., Usui, T., Hirano, S., Steward, R., Takeichi, M. and Uemura, T. (1997). Axon patterning requires DN-cadherin, a novel neuronal adhesion receptor, in the Drosophila embryonic CNS. *Neuron* **19**, 77-89.
Javaherian, A. and Cline, H. T. (2005). Coordinated motor neuron axon growth and neuromuscular synaptogenesis are promoted by CPG15 in vivo. *Neuron* **45**, 505-12.
Jay, D. G. (2000). The clutch hypothesis revisited: ascribing the roles of actin-associated proteins in filopodial protrusion in the nerve growth cone. *J Neurobiol* **44**, 114-25.
Jin, Z. and Strittmatter, S. M. (1997). Rac1 mediates collapsin-1-induced growth cone collapse. *J Neurosci* **17**, 6256-63.
Jones, S. B., Lu, H. Y. and Lu, Q. (2004). Abl tyrosine kinase promotes dendrogenesis by inducing actin cytoskeletal rearrangements in cooperation with Rho family small GTPases in hippocampal neurons. *J Neurosci* **24**, 8510-21.
Jones, S. E. and Jomary, C. (2002). Secreted Frizzled-related proteins: searching for relationships and patterns. *Bioessays* **24**, 811-20.
Jurney, W. M., Gallo, G., Letourneau, P. C. and McLoon, S. C. (2002). Rac1-mediated endocytosis during ephrin-A2- and semaphorin 3A-induced growth cone collapse. *J Neurosci* **22**, 6019-28.
Kabir, N., Schaefer, A. W., Nakhost, A., Sossin, W. S. and Forscher, P. (2001). Protein kinase C activation promotes microtubule advance in neuronal growth cones by increasing average microtubule growth lifetimes. *J Cell Biol* **152**, 1033-44.
Kalil, K. and Dent, E. W. (2004). Hot +TIPS: guidance cues signal directly to microtubules. *Neuron* **42**, 877-9.
Kalil, K. and Skene, J. H. (1986). Elevated synthesis of an axonally transported protein correlates with axon outgrowth in normal and injured pyramidal tracts. *J Neurosci* **6**, 2563-70.
Kalil, K., Szebenyi, G. and Dent, E. W. (2000). Common mechanisms underlying growth cone guidance and axon branching. *J Neurobiol* **44**, 145-58.
Katanaev, V. L., Ponzielli, R., Semeriva, M. and Tomlinson, A. (2005). Trimeric G protein-dependent frizzled signaling in Drosophila. *Cell* **120**, 111-22.
Keleman, K. and Dickson, B. J. (2001). Short- and long-range repulsion by the Drosophila Unc5 netrin receptor. *Neuron* **32**, 605-17.
Keleman, K., Rajagopalan, S., Cleppien, D., Teis, D., Paiha, K., Huber, L. A., Technau, G. M. and Dickson, B. J. (2002). Comm sorts robo to control axon guidance at the Drosophila midline. *Cell* **110**, 415-27.
Keleman, K., Ribeiro, C. and Dickson, B. J. (2005). Comm function in commissural axon guidance: cell-autonomous sorting of Robo in vivo. *Nat Neurosci* **8**, 156-63.
Kennedy, T. E., Serafini, T., de la Torre, J. R. and Tessier-Lavigne, M. (1994). Netrins are diffusible chemotropic factors for commissural axons in the embryonic spinal cord. *Cell* **78**, 425-35.

Kidd, T., Bland, K. S. and Goodman, C. S. (1999). Slit is the midline repellent for the robo receptor in Drosophila. *Cell* **96**, 785-94.
Kidd, T., Brose, K., Mitchell, K. J., Fetter, R. D., Tessier-Lavigne, M., Goodman, C. S. and Tear, G. (1998). Roundabout controls axon crossing of the CNS midline and defines a novel subfamily of evolutionarily conserved guidance receptors. *Cell* **92**, 205-15.
Kiecker, C. and Niehrs, C. (2001). A morphogen gradient of Wnt/beta-catenin signalling regulates anteroposterior neural patterning in Xenopus. *Development* **128**, 4189-201.
Kishida, S., Yamamoto, H. and Kikuchi, A. (2004). Wnt-3a and Dvl induce neurite retraction by activating Rho-associated kinase. *Mol Cell Biol* **24**, 4487-501.
Kitajewski, J., Mason, J. O. and Varmus, H. E. (1992). Interaction of Wnt-1 proteins with the binding protein BiP. *Mol Cell Biol* **12**, 784-90.
Kleiman, R., Banker, G. and Steward, O. (1994). Development of subcellular mRNA compartmentation in hippocampal neurons in culture. *J Neurosci* **14**, 1130-40.
Klein, P. S. and Melton, D. A. (1996). A molecular mechanism for the effect of lithium on development. *Proc Natl Acad Sci U S A* **93**, 8455-9.
Kleitman, N., Wood, P. and Bunge, R.P. (1991). Tissue culture methods for the study of myelination. In Banker, G. and Goslin, K.: "Culturing Nerve Cells": The MIT Press, Cambridge, Massachussets.
Klingensmith, J. and Nusse, R. (1994). Signaling by wingless in Drosophila. *Dev Biol* **166**, 396-414.
Knoll, B., Zarbalis, K., Wurst, W. and Drescher, U. (2001). A role for the EphA family in the topographic targeting of vomeronasal axons. *Development* **128**, 895-906.
Kolodkin, A. L., Matthes, D. J. and Goodman, C. S. (1993). The semaphorin genes encode a family of transmembrane and secreted growth cone guidance molecules. *Cell* **75**, 1389-99.
Kolodkin, A. L., Matthes, D. J., O'Connor, T. P., Patel, N. H., Admon, A., Bentley, D. and Goodman, C. S. (1992). Fasciclin IV: sequence, expression, and function during growth cone guidance in the grasshopper embryo. *Neuron* **9**, 831-45.
Krendel, M., Zenke, F. T. and Bokoch, G. M. (2002). Nucleotide exchange factor GEF-H1 mediates cross-talk between microtubules and the actin cytoskeleton. *Nat Cell Biol* **4**, 294-301.
Krylova, O., Herreros, J., Cleverley, K. E., Ehler, E., Henriquez, J. P., Hughes, S. M. and Salinas, P. C. (2002). WNT-3, expressed by motoneurons, regulates terminal arborization of neurotrophin-3-responsive spinal sensory neurons. *Neuron* **35**, 1043-56.
Krylova, O., Messenger, M. J. and Salinas, P. C. (2000). Dishevelled-1 regulates microtubule stability: a new function mediated by glycogen synthase kinase-3beta. *J Cell Biol* **151**, 83-94.
Kuhl, M., Sheldahl, L. C., Park, M., Miller, J. R. and Moon, R. T. (2000). The Wnt/Ca2+ pathway: a new vertebrate Wnt signaling pathway takes shape. *Trends Genet* **16**, 279-83.
Kullander, K., Mather, N. K., Diella, F., Dottori, M., Boyd, A. W. and Klein, R. (2001). Kinase-dependent and kinase-independent functions of EphA4 receptors in major axon tract formation in vivo. *Neuron* **29**, 73-84.

Lalli, G., Gschmeissner, S. and Schiavo, G. (2003). Myosin Va and microtubule-based motors are required for fast axonal retrograde transport of tetanus toxin in motor neurons. *J Cell Sci* **116**, 4639-50.

Lanier, L. M., Gates, M. A., Witke, W., Menzies, A. S., Wehman, A. M., Macklis, J. D., Kwiatkowski, D., Soriano, P. and Gertler, F. B. (1999). Mena is required for neurulation and commissure formation. *Neuron* **22**, 313-25.

Lawson, S. N., Harper, A. A., Harper, E. I., Garson, J. A. and Anderton, B. H. (1984). A monoclonal antibody against neurofilament protein specifically labels a subpopulation of rat sensory neurones. *J Comp Neurol* **228**, 263-72.

Lebrand, C., Dent, E. W., Strasser, G. A., Lanier, L. M., Krause, M., Svitkina, T. M., Borisy, G. G. and Gertler, F. B. (2004). Critical role of Ena/VASP proteins for filopodia formation in neurons and in function downstream of netrin-1. *Neuron* **42**, 37-49.

Lee, H., Engel, U., Rusch, J., Scherrer, S., Sheard, K. and Van Vactor, D. (2004). The microtubule plus end tracking protein Orbit/MAST/CLASP acts downstream of the tyrosine kinase Abl in mediating axon guidance. *Neuron* **42**, 913-26.

Lee, H. Y., Kleber, M., Hari, L., Brault, V., Suter, U., Taketo, M. M., Kemler, R. and Sommer, L. (2004). Instructive role of Wnt/beta-catenin in sensory fate specification in neural crest stem cells. *Science* **303**, 1020-3.

Lee, S., Harris, K. L., Whitington, P. M. and Kolodziej, P. A. (2000a). short stop is allelic to kakapo, and encodes rod-like cytoskeletal-associated proteins required for axon extension. *J Neurosci* **20**, 1096-108.

Lee, S. and Kolodziej, P. A. (2002). Short Stop provides an essential link between F-actin and microtubules during axon extension. *Development* **129**, 1195-204.

Lee, S. M., Tole, S., Grove, E. and McMahon, A. P. (2000b). A local Wnt-3a signal is required for development of the mammalian hippocampus. *Development* **127**, 457-67.

Letourneau, P. C. (1983). Differences in the organization of actin in the growth cones compared with the neurites of cultured neurons from chick embryos. *J Cell Biol* **97**, 963-73.

Letourneau, P. C. and Shattuck, T. A. (1989). Distribution and possible interactions of actin-associated proteins and cell adhesion molecules of nerve growth cones. *Development* **105**, 505-19.

Leyns, L., Bouwmeester, T., Kim, S. H., Piccolo, S. and De Robertis, E. M. (1997). Frzb-1 is a secreted antagonist of Wnt signaling expressed in the Spemann organizer. *Cell* **88**, 747-56.

Lijam, N., Paylor, R., McDonald, M. P., Crawley, J. N., Deng, C. X., Herrup, K., Stevens, K. E., Maccaferri, G., McBain, C. J., Sussman, D. J. *et al.* (1997). Social interaction and sensorimotor gating abnormalities in mice lacking Dvl1. *Cell* **90**, 895-905.

Lin, C. H., Espreafico, E. M., Mooseker, M. S. and Forscher, P. (1996). Myosin drives retrograde F-actin flow in neuronal growth cones. *Neuron* **16**, 769-82.

Lin, C. H. and Forscher, P. (1995). Growth cone advance is inversely proportional to retrograde F-actin flow. *Neuron* **14**, 763-71.

Lin, C. H., Thompson, C. A. and Forscher, P. (1994a). Cytoskeletal reorganization underlying growth cone motility. *Curr Opin Neurobiol* **4**, 640-7.

Lin, D. M., Fetter, R. D., Kopczynski, C., Grenningloh, G. and Goodman, C. S. (1994b). Genetic analysis of Fasciclin II in Drosophila: defasciculation, refasciculation, and altered fasciculation. *Neuron* **13**, 1055-69.
Lin, W. and Szaro, B. G. (1995). Neurofilaments help maintain normal morphologies and support elongation of neurites in Xenopus laevis cultured embryonic spinal cord neurons. *J Neurosci* **15**, 8331-44.
Lin, X. and Perrimon, N. (2000). Role of heparan sulfate proteoglycans in cell-cell signaling in Drosophila. *Matrix Biol* **19**, 303-7.
Lu, W., Yamamoto, V., Ortega, B. and Baltimore, D. (2004). Mammalian Ryk is a Wnt coreceptor required for stimulation of neurite outgrowth. *Cell* **119**, 97-108.
Lucas, F. R., Goold, R. G., Gordon-Weeks, P. R. and Salinas, P. C. (1998). Inhibition of Gsk-3beta leading to the loss of phosphorylated MAP-1B is an early event in axonal remodelling induced by WNT-7a or lithium. *J Cell Sci* **111 (Pt 10)**, 1351-61.
Lucas, F. R. and Salinas, P. C. (1997). WNT-7a induces axonal remodeling and increases synapsin I levels in cerebellar neurons. *Dev Biol* **192**, 31-44.
Luduena, R. F. (1998). Multiple forms of tubulin: different gene products and covalent modifications. *Int Rev Cytol* **178**, 207-75.
Luo, L. (2002). Actin cytoskeleton regulation in neuronal morphogenesis and structural plasticity. *Annu Rev Cell Dev Biol* **18**, 601-35.
Luo, L. (2000). Rho GTPases in neuronal morphogenesis. *Nat Rev Neurosci* **1**, 173-80.
Luo, Y., Raible, D. and Raper, J. A. (1993). Collapsin: a protein in brain that induces the collapse and paralysis of neuronal growth cones. *Cell* **75**, 217-27.
Luo, Z. G., Wang, Q., Zhou, J. Z., Wang, J., Luo, Z., Liu, M., He, X., Wynshaw-Boris, A., Xiong, W. C., Lu, B. *et al.* (2002). Regulation of AChR clustering by Dishevelled interacting with MuSK and PAK1. *Neuron* **35**, 489-505.
Lyuksyutova, A. I., Lu, C. C., Milanesio, N., King, L. A., Guo, N., Wang, Y., Nathans, J., Tessier-Lavigne, M. and Zou, Y. (2003). Anterior-posterior guidance of commissural axons by Wnt-frizzled signaling. *Science* **302**, 1984-8.
Mack, T. G., Koester, M. P. and Pollerberg, G. E. (2000). The microtubule-associated protein MAP1B is involved in local stabilization of turning growth cones. *Mol Cell Neurosci* **15**, 51-65.
Mallavarapu, A. and Mitchison, T. (1999). Regulated actin cytoskeleton assembly at filopodium tips controls their extension and retraction. *J Cell Biol* **146**, 1097-106.
Manser, E., Leung, T., Salihuddin, H., Zhao, Z. S. and Lim, L. (1994). A brain serine/threonine protein kinase activated by Cdc42 and Rac1. *Nature* **367**, 40-6.
Mao, B., Wu, W., Davidson, G., Marhold, J., Li, M., Mechler, B. M., Delius, H., Hoppe, D., Stannek, P., Walter, C. *et al.* (2002). Kremen proteins are Dickkopf receptors that regulate Wnt/beta-catenin signalling. *Nature* **417**, 664-7.
McNally, F. J. and Vale, R. D. (1993). Identification of katanin, an ATPase that severs and disassembles stable microtubules. *Cell* **75**, 419-29.
Meng, Y., Zhang, Y., Tregoubov, V., Janus, C., Cruz, L., Jackson, M., Lu, W. Y., MacDonald, J. F., Wang, J. Y., Falls, D. L. *et al.* (2002). Abnormal spine morphology and enhanced LTP in LIMK-1 knockout mice. *Neuron* **35**, 121-33.
Messersmith, E. K., Leonardo, E. D., Shatz, C. J., Tessier-Lavigne, M., Goodman, C. S. and Kolodkin, A. L. (1995). Semaphorin III can function as a selective chemorepellent to pattern sensory projections in the spinal cord. *Neuron* **14**, 949-59.

Miller, J. R., Hocking, A. M., Brown, J. D. and Moon, R. T. (1999). Mechanism and function of signal transduction by the Wnt/beta-catenin and Wnt/Ca2+ pathways. *Oncogene* **18**, 7860-72.

Ming, G. L., Song, H. J., Berninger, B., Holt, C. E., Tessier-Lavigne, M. and Poo, M. M. (1997). cAMP-dependent growth cone guidance by netrin-1. *Neuron* **19**, 1225-35.

Mitchison, T. and Kirschner, M. (1988). Cytoskeletal dynamics and nerve growth. *Neuron* **1**, 761-72.

Mlodzik, M. (2000). Spiny legs and prickled bodies: new insights and complexities in planar polarity establishment. *Bioessays* **22**, 311-5.

Morales, M., Colicos, M. A. and Goda, Y. (2000). Actin-dependent regulation of neurotransmitter release at central synapses. *Neuron* **27**, 539-50.

Mu, X., Silos-Santiago, I., Carroll, S. L. and Snider, W. D. (1993). Neurotrophin receptor genes are expressed in distinct patterns in developing dorsal root ganglia. *J Neurosci* **13**, 4029-41.

Mukhopadhyay, M., Shtrom, S., Rodriguez-Esteban, C., Chen, L., Tsukui, T., Gomer, L., Dorward, D. W., Glinka, A., Grinberg, A., Huang, S. P. *et al.* (2001). Dickkopf1 is required for embryonic head induction and limb morphogenesis in the mouse. *Dev Cell* **1**, 423-34.

Muroyama, Y., Fujihara, M., Ikeya, M., Kondoh, H. and Takada, S. (2002). Wnt signaling plays an essential role in neuronal specification of the dorsal spinal cord. *Genes Dev* **16**, 548-53.

Myat, A., Henry, P., McCabe, V., Flintoft, L., Rotin, D. and Tear, G. (2002). Drosophila Nedd4, a ubiquitin ligase, is recruited by Commissureless to control cell surface levels of the roundabout receptor. *Neuron* **35**, 447-59.

Nakagawa, H., Koyama, K., Murata, Y., Morito, M., Akiyama, T. and Nakamura, Y. (2000). EB3, a novel member of the EB1 family preferentially expressed in the central nervous system, binds to a CNS-specific APC homologue. *Oncogene* **19**, 210-6.

Nakagawa, S., Takada, S., Takada, R. and Takeichi, M. (2003). Identification of the laminar-inducing factor: Wnt-signal from the anterior rim induces correct laminar formation of the neural retina in vitro. *Dev Biol* **260**, 414-25.

Nakamura, M., Zhou, X. Z. and Lu, K. P. (2001). Critical role for the EB1 and APC interaction in the regulation of microtubule polymerization. *Curr Biol* **11**, 1062-7.

Nakamura, T., Hamada, F., Ishidate, T., Anai, K., Kawahara, K., Toyoshima, K. and Akiyama, T. (1998). Axin, an inhibitor of the Wnt signalling pathway, interacts with beta-catenin, Gsk-3beta and APC and reduces the beta-catenin level. *Genes Cells* **3**, 395-403.

Niclou, S. P., Jia, L. and Raper, J. A. (2000). Slit2 is a repellent for retinal ganglion cell axons. *J Neurosci* **20**, 4962-74.

Niell, C. M., Meyer, M. P. and Smith, S. J. (2004). In vivo imaging of synapse formation on a growing dendritic arbor. *Nat Neurosci* **7**, 254-60.

Nobes, C. D. and Hall, A. (1995). Rho, rac, and cdc42 GTPases regulate the assembly of multimolecular focal complexes associated with actin stress fibers, lamellipodia, and filopodia. *Cell* **81**, 53-62.

Nusse, R. (2003). Wnts and Hedgehogs: lipid-modified proteins and similarities in signaling mechanisms at the cell surface. *Development* **130**, 5297-305.

Nusse, R. and Varmus, H. E. (1982). Many tumors induced by the mouse mammary tumor virus contain a provirus integrated in the same region of the host genome. *Cell* **31**, 99-109.

Nusslein-Volhard, C. and Wieschaus, E. (1980). Mutations affecting segment number and polarity in Drosophila. *Nature* **287**, 795-801.

Nuydens, R., Van Den Kieboom, G., Nolten, C., Verhulst, C., Van Osta, P., Spittaels, K., Van den Haute, C., De Feyter, E., Geerts, H. and Van Leuven, F. (2002). Coexpression of Gsk-3beta corrects phenotypic aberrations of dorsal root ganglion cells, cultured from adult transgenic mice overexpressing human protein tau. *Neurobiol Dis* **9**, 38-48.

Okamoto, K., Nagai, T., Miyawaki, A. and Hayashi, Y. (2004). Rapid and persistent modulation of actin dynamics regulates postsynaptic reorganization underlying bidirectional plasticity. *Nat Neurosci* **7**, 1104-12.

Osterfield, M., Kirschner, M. W. and Flanagan, J. G. (2003). Graded positional information: interpretation for both fate and guidance. *Cell* **113**, 425-8.

Owen, R. and Gordon-Weeks, P. R. (2003). Inhibition of glycogen synthase kinase 3beta in sensory neurons in culture alters filopodia dynamics and microtubule distribution in growth cones. *Mol Cell Neurosci* **23**, 626-37.

Ozaki, S. and Snider, W. D. (1997). Initial trajectories of sensory axons toward laminar targets in the developing mouse spinal cord. *J Comp Neurol* **380**, 215-29.

Packard, M., Koo, E. S., Gorczyca, M., Sharpe, J., Cumberledge, S. and Budnik, V. (2002). The Drosophila Wnt, wingless, provides an essential signal for pre- and postsynaptic differentiation. *Cell* **111**, 319-30.

Paglini, G., Pigino, G., Kunda, P., Morfini, G., Maccioni, R., Quiroga, S., Ferreira, A. and Caceres, A. (1998). Evidence for the participation of the neuron-specific CDK5 activator P35 during laminin-enhanced axonal growth. *J Neurosci* **18**, 9858-69.

Palazzo, A. F., Cook, T. A., Alberts, A. S. and Gundersen, G. G. (2001). mDia mediates Rho-regulated formation and orientation of stable microtubules. *Nat Cell Biol* **3**, 723-9.

Papkoff, J., Rubinfeld, B., Schryver, B. and Polakis, P. (1996). Wnt-1 regulates free pools of catenins and stabilizes APC-catenin complexes. *Mol Cell Biol* **16**, 2128-34.

Papkoff, J. and Schryver, B. (1990). Secreted int-1 protein is associated with the cell surface. *Mol Cell Biol* **10**, 2723-30.

Parr, B. A. and McMahon, A. P. (1995). Dorsalizing signal Wnt-7a required for normal polarity of D-V and A-P axes of mouse limb. *Nature* **374**, 350-3.

Parr, B. A., Shea, M. J., Vassileva, G. and McMahon, A. P. (1993). Mouse Wnt genes exhibit discrete domains of expression in the early embryonic CNS and limb buds. *Development* **119**, 247-61.

Parsons, J. T., Martin, K. H., Slack, J. K., Taylor, J. M. and Weed, S. A. (2000). Focal adhesion kinase: a regulator of focal adhesion dynamics and cell movement. *Oncogene* **19**, 5606-13.

Pasterkamp, R. J. and Kolodkin, A. L. (2003). Semaphorin junction: making tracks toward neural connectivity. *Curr Opin Neurobiol* **13**, 79-89.

Pedrotti, B., Ulloa, L., Avila, J. and Islam, K. (1996). Characterization of microtubule-associated protein MAP1B: phosphorylation state, light chains, and binding to microtubules. *Biochemistry* **35**, 3016-23.

Perry, R. P. and Kelley, D. E. (1970). Inhibition of RNA synthesis by actinomycin D: characteristic dose-response of different RNA species. *J Cell Physiol* **76**, 127-39.
Pfenninger, K. H., Laurino, L., Peretti, D., Wang, X., Rosso, S., Morfini, G., Caceres, A. and Quiroga, S. (2003). Regulation of membrane expansion at the nerve growth cone. *J Cell Sci* **116**, 1209-17.
Pinson, K. I., Brennan, J., Monkley, S., Avery, B. J. and Skarnes, W. C. (2000). An LDL-receptor-related protein mediates Wnt signalling in mice. *Nature* **407**, 535-8.
Plump, A. S., Erskine, L., Sabatier, C., Brose, K., Epstein, C. J., Goodman, C. S., Mason, C. A. and Tessier-Lavigne, M. (2002). Slit1 and Slit2 cooperate to prevent premature midline crossing of retinal axons in the mouse visual system. *Neuron* **33**, 219-32.
Pollard, T. D. and Beltzner, C. C. (2002). Structure and function of the Arp2/3 complex. *Curr Opin Struct Biol* **12**, 768-74.
Pollard, T. D. and Borisy, G. G. (2003). Cellular motility driven by assembly and disassembly of actin filaments. *Cell* **112**, 453-65.
Powell, S. K. and Kleinman, H. K. (1997). Neuronal laminins and their cellular receptors. *Int J Biochem Cell Biol* **29**, 401-14.
Raper, J. A. (2000). Semaphorins and their receptors in vertebrates and invertebrates. *Curr Opin Neurobiol* **10**, 88-94.
Rashid, T., Banerjee, M. and Nikolic, M. (2001). Phosphorylation of Pak1 by the p35/Cdk5 kinase affects neuronal morphology. *J Biol Chem* **276**, 49043-52.
Reilein, A. and Nelson, W. J. (2005). APC is a component of an organizing template for cortical microtubule networks. *Nat Cell Biol* **7**, 463-73.
Rijsewijk, F., Schuermann, M., Wagenaar, E., Parren, P., Weigel, D. and Nusse, R. (1987). The Drosophila homolog of the mouse mammary oncogene int-1 is identical to the segment polarity gene wingless. *Cell* **50**, 649-57.
Riley, B. B., Chiang, M. Y., Storch, E. M., Heck, R., Buckles, G. R. and Lekven, A. C. (2004). Rhombomere boundaries are Wnt signaling centers that regulate metameric patterning in the zebrafish hindbrain. *Dev Dyn* **231**, 278-91.
Ringstedt, T., Braisted, J. E., Brose, K., Kidd, T., Goodman, C., Tessier-Lavigne, M. and O'Leary, D. D. (2000). Slit inhibition of retinal axon growth and its role in retinal axon pathfinding and innervation patterns in the diencephalon. *J Neurosci* **20**, 4983-91.
Rochlin, M. W., Dailey, M. E. and Bridgman, P. C. (1999). Polymerizing microtubules activate site-directed F-actin assembly in nerve growth cones. *Mol Biol Cell* **10**, 2309-27.
Rochlin, M. W., Wickline, K. M. and Bridgman, P. C. (1996). Microtubule stability decreases axon elongation but not axoplasm production. *J Neurosci* **16**, 3236-46.
Roelink, H. and Nusse, R. (1991). Expression of two members of the Wnt family during mouse development--restricted temporal and spatial patterns in the developing neural tube. *Genes Dev* **5**, 381-8.
Roos, J., Hummel, T., Ng, N., Klambt, C. and Davis, G. W. (2000). Drosophila Futsch regulates synaptic microtubule organization and is necessary for synaptic growth. *Neuron* **26**, 371-82.
Roper, K., Gregory, S. L. and Brown, N. H. (2002). The 'spectraplakins': cytoskeletal giants with characteristics of both spectrin and plakin families. *J Cell Sci* **115**, 4215-25.

Rosso, S. B., Sussman, D., Wynshaw-Boris, A. and Salinas, P. C. (2005). Wnt signaling through Dishevelled, Rac and JNK regulates dendritic development. *Nat Neurosci* **8**, 34-42.

Rothbacher, U., Laurent, M. N., Deardorff, M. A., Klein, P. S., Cho, K. W. and Fraser, S. E. (2000). Dishevelled phosphorylation, subcellular localization and multimerization regulate its role in early embryogenesis. *Embo J* **19**, 1010-22.

Ruiz-Canada, C., Ashley, J., Moeckel-Cole, S., Drier, E., Yin, J. and Budnik, V. (2004). New synaptic bouton formation is disrupted by misregulation of microtubule stability in aPKC mutants. *Neuron* **42**, 567-80.

Ruthazer, E. S., Akerman, C. J. and Cline, H. T. (2003). Control of axon branch dynamics by correlated activity in vivo. *Science* **301**, 66-70.

Ruthel, G. and Hollenbeck, P. J. (2000). Growth cones are not required for initial establishment of polarity or differential axon branch growth in cultured hippocampal neurons. *J Neurosci* **20**, 2266-74.

Sabatier, C., Plump, A. S., Le, M., Brose, K., Tamada, A., Murakami, F., Lee, E. Y. and Tessier-Lavigne, M. (2004). The divergent Robo family protein rig-1/Robo3 is a negative regulator of slit responsiveness required for midline crossing by commissural axons. *Cell* **117**, 157-69.

Sakaba, T. and Neher, E. (2003). Involvement of actin polymerization in vesicle recruitment at the calyx of Held synapse. *J Neurosci* **23**, 837-46.

Salinas, P. C., Fletcher, C., Copeland, N. G., Jenkins, N. A. and Nusse, R. (1994). Maintenance of Wnt-3 expression in Purkinje cells of the mouse cerebellum depends on interactions with granule cells. *Development* **120**, 1277-86.

Salinas, P. C. and Price, S. R. (2005). Cadherins and catenins in synapse development. *Curr Opin Neurobiol* **15**, 73-80.

Saneyoshi, T., Kume, S., Amasaki, Y. and Mikoshiba, K. (2002). The Wnt/calcium pathway activates NF-AT and promotes ventral cell fate in Xenopus embryos. *Nature* **417**, 295-9.

Sankaranarayanan, S., Atluri, P. P. and Ryan, T. A. (2003). Actin has a molecular scaffolding, not propulsive, role in presynaptic function. *Nat Neurosci* **6**, 127-35.

Sasaki, Y., Cheng, C., Uchida, Y., Nakajima, O., Ohshima, T., Yagi, T., Taniguchi, M., Nakayama, T., Kishida, R., Kudo, Y. *et al.* (2002). Fyn and Cdk5 mediate semaphorin-3A signaling, which is involved in regulation of dendrite orientation in cerebral cortex. *Neuron* **35**, 907-20.

Schachner, M. (1991). Neural recognition molecules and their influence on cellular functions. In Letourneau PC, Kater SB and Macagno ER: "The Nerve Growth Cone": Raven Press, New York.

Schaefer, A. W., Kabir, N. and Forscher, P. (2002). Filopodia and actin arcs guide the assembly and transport of two populations of microtubules with unique dynamic parameters in neuronal growth cones. *J Cell Biol* **158**, 139-52.

Sharp DJ, Rogers GC and Scholey JM. (2000). Roles of motor proteins in building microtubule-based structures: a basic principle of cellular design. *Biochim Biophys Acta* **1496**, 128-41.

Schwarz, P. M., Liggins, J. R. and Luduena, R. F. (1998). Beta-tubulin isotypes purified from bovine brain have different relative stabilities. *Biochemistry* **37**, 4687-92.

Semaphorin Nomenclature Committee (1999). Unified nomenclature for the semaphorins/collapsins. *Cell* **97**, 551-552.
Serafini, T. (1997). An old friend in a new home: cadherins at the synapse. *Trends Neurosci* **20**, 322-3.
Serafini, T., Kennedy, T. E., Galko, M. J., Mirzayan, C., Jessell, T. M. and Tessier-Lavigne, M. (1994). The netrins define a family of axon outgrowth-promoting proteins homologous to C. elegans UNC-6. *Cell* **78**, 409-24.
Shamah, S. M., Lin, M. Z., Goldberg, J. L., Estrach, S., Sahin, M., Hu, L., Bazalakova, M., Neve, R. L., Corfas, G., Debant, A. *et al.* (2001). EphA receptors regulate growth cone dynamics through the novel guanine nucleotide exchange factor ephexin. *Cell* **105**, 233-44.
Sharma, K. and Frank, E. (1998). Sensory axons are guided by local cues in the developing dorsal spinal cord. *Development* **125**, 635-43.
Shekarabi, M. and Kennedy, T. E. (2002). The netrin-1 receptor DCC promotes filopodia formation and cell spreading by activating Cdc42 and Rac1. *Mol Cell Neurosci* **19**, 1-17.
Sheldahl, L. C., Slusarski, D. C., Pandur, P., Miller, J. R., Kuhl, M. and Moon, R. T. (2003). Dishevelled activates Ca2+ flux, PKC, and CamKII in vertebrate embryos. *J Cell Biol* **161**, 769-77.
Shibamoto, S., Higano, K., Takada, R., Ito, F., Takeichi, M. and Takada, S. (1998). Cytoskeletal reorganization by soluble Wnt-3a protein signalling. *Genes Cells* **3**, 659-70.
Shimogori, T., VanSant, J., Paik, E. and Grove, E. A. (2004). Members of the Wnt, Fz, and Frp gene families expressed in postnatal mouse cerebral cortex. *J Comp Neurol* **473**, 496-510.
Shupliakov, O., Bloom, O., Gustafsson, J. S., Kjaerulff, O., Low, P., Tomilin, N., Pieribone, V. A., Greengard, P. and Brodin, L. (2002). Impaired recycling of synaptic vesicles after acute perturbation of the presynaptic actin cytoskeleton. *Proc Natl Acad Sci U S A* **99**, 14476-81.
Simpson, J. H., Kidd, T., Bland, K. S. and Goodman, C. S. (2000). Short-range and long-range guidance by slit and its Robo receptors. Robo and Robo2 play distinct roles in midline guidance. *Neuron* **28**, 753-66.
Slusarski, D. C., Corces, V. G. and Moon, R. T. (1997). Interaction of Wnt and a Frizzled homologue triggers G-protein-linked phosphatidylinositol signalling. *Nature* **390**, 410-3.
Snider, W. D. and Wright, D. E. (1996). Neurotrophins cause a new sensation. *Neuron* **16**, 229-32.
Spector, I., Shochet, N. R., Blasberger, D. and Kashman, Y. (1989). Latrunculins--novel marine macrolides that disrupt microfilament organization and affect cell growth: I. Comparison with cytochalasin D. *Cell Motil Cytoskeleton* **13**, 127-44.
Sperry, R. (1963). Chemoaffinity in the orderly growth of nerve fibre patterns and connections. *PNAS*, 703-710.
Stafford, P., Brown, J. and Langford, G. M. (2000). Interaction of actin- and microtubule-based motors in squid axoplasm probed with antibodies to myosin V and kinesin. *Biol Bull* **199**, 203-5.

Star, E. N., Kwiatkowski, D. J. and Murthy, V. N. (2002). Rapid turnover of actin in dendritic spines and its regulation by activity. *Nat Neurosci* **5**, 239-46.
Stark, K., Vainio, S., Vassileva, G. and McMahon, A. P. (1994). Epithelial transformation of metanephric mesenchyme in the developing kidney regulated by Wnt-4. *Nature* **372**, 679-83.
Stein, E. and Tessier-Lavigne, M. (2001). Hierarchical organization of guidance receptors: silencing of netrin attraction by slit through a Robo/DCC receptor complex. *Science* **291**, 1928-38.
Stepanova, T., Slemmer, J., Hoogenraad, C. C., Lansbergen, G., Dortland, B., De Zeeuw, C. I., Grosveld, F., van Cappellen, G., Akhmanova, A. and Galjart, N. (2003). Visualization of microtubule growth in cultured neurons via the use of EB3-GFP (end-binding protein 3-green fluorescent protein). *J Neurosci* **23**, 2655-64.
Strasser, G. A., Rahim, N. A., VanderWaal, K. E., Gertler, F. B. and Lanier, L. M. (2004). Arp2/3 is a negative regulator of growth cone translocation. *Neuron* **43**, 81-94.
Strutt, D. I., Weber, U. and Mlodzik, M. (1997). The role of RhoA in tissue polarity and Frizzled signalling. *Nature* **387**, 292-5.
Su, L. K., Burrell, M., Hill, D. E., Gyuris, J., Brent, R., Wiltshire, R., Trent, J., Vogelstein, B. and Kinzler, K. W. (1995). APC binds to the novel protein EB1. *Cancer Res* **55**, 2972-7.
Suh, L. H., Oster, S. F., Soehrman, S. S., Grenningloh, G. and Sretavan, D. W. (2004). L1/Laminin modulation of growth cone response to EphB triggers growth pauses and regulates the microtubule destabilizing protein SCG10. *J Neurosci* **24**, 1976-86.
Suter, D. M., Errante, L. D., Belotserkovsky, V. and Forscher, P. (1998). The Ig superfamily cell adhesion molecule, apCAM, mediates growth cone steering by substrate-cytoskeletal coupling. *J Cell Biol* **141**, 227-40.
Suter, D. M. and Forscher, P. (2000). Substrate-cytoskeletal coupling as a mechanism for the regulation of growth cone motility and guidance. *J Neurobiol* **44**, 97-113.
Suter, D. M., Schaefer, A. W. and Forscher, P. (2004). Microtubule dynamics are necessary for SRC family kinase-dependent growth cone steering. *Curr Biol* **14**, 1194-9.
Svitkina, T. M., Verkhovsky, A. B. and Borisy, G. G. (1995). Improved procedures for electron microscopic visualization of the cytoskeleton of cultured cells. *J Struct Biol* **115**, 290-303.
Szebenyi, G., Callaway, J. L., Dent, E. W. and Kalil, K. (1998). Interstitial branches develop from active regions of the axon demarcated by the primary growth cone during pausing behaviors. *J Neurosci* **18**, 7930-40.
Szebenyi, G., Dent, E. W., Callaway, J. L., Seys, C., Lueth, H. and Kalil, K. (2001). Fibroblast growth factor-2 promotes axon branching of cortical neurons by influencing morphology and behavior of the primary growth cone. *J Neurosci* **21**, 3932-41.
Tabb, J. S., Molyneaux, B. J., Cohen, D. L., Kuznetsov, S. A. and Langford, G. M. (1998). Transport of ER vesicles on actin filaments in neurons by myosin V. *J Cell Sci* **111 (Pt 21)**, 3221-34.
Takahashi, T., Fournier, A., Nakamura, F., Wang, L. H., Murakami, Y., Kalb, R. G., Fujisawa, H. and Strittmatter, S. M. (1999). Plexin-neuropilin-1 complexes form functional semaphorin-3A receptors. *Cell* **99**, 59-69.

Tamagnone, L., Artigiani, S., Chen, H., He, Z., Ming, G. I., Song, H., Chedotal, A., Winberg, M. L., Goodman, C. S., Poo, M. *et al.* (1999). Plexins are a large family of receptors for transmembrane, secreted, and GPI-anchored semaphorins in vertebrates. *Cell* **99**, 71-80.

Tamagnone, L. and Comoglio, P. M. (2000). Signalling by semaphorin receptors: cell guidance and beyond. *Trends Cell Biol* **10**, 377-83.

Tamai, K., Semenov, M., Kato, Y., Spokony, R., Liu, C., Katsuyama, Y., Hess, F., Saint-Jeannet, J. P. and He, X. (2000). LDL-receptor-related proteins in Wnt signal transduction. *Nature* **407**, 530-5.

Tanaka, E., Ho, T. and Kirschner, M. W. (1995). The role of microtubule dynamics in growth cone motility and axonal growth. *J Cell Biol* **128**, 139-55.

Tanaka, E. M. and Kirschner, M. W. (1991). Microtubule behavior in the growth cones of living neurons during axon elongation. *J Cell Biol* **115**, 345-63.

Tanaka, J., Kira, M. and Sobue, K. (1993). Gelsolin is localized in neuronal growth cones. *Brain Res Dev Brain Res* **76**, 268-71.

Tang, F., Dent, E. W. and Kalil, K. (2003). Spontaneous calcium transients in developing cortical neurons regulate axon outgrowth. *J Neurosci* **23**, 927-36.

Tao, W., Pennica, D., Xu, L., Kalejta, R. F. and Levine, A. J. (2001). Wrch-1, a novel member of the Rho gene family that is regulated by Wnt-1. *Genes Dev* **15**, 1796-807.

Tear, G., Harris, R., Sutaria, S., Kilomanski, K., Goodman, C. S. and Seeger, M. A. (1996). commissureless controls growth cone guidance across the CNS midline in Drosophila and encodes a novel membrane protein. *Neuron* **16**, 501-14.

Tennyson, V. M. (1970). The fine structure of the axon and growth cone of the dorsal root neuroblast of the rabbit embryo. *J Cell Biol* **44**, 62-79.

Tessier-Lavigne, M., Placzek, M., Lumsden, A. G., Dodd, J. and Jessell, T. M. (1988). Chemotropic guidance of developing axons in the mammalian central nervous system. *Nature* **336**, 775-8.

Togashi, H., Abe, K., Mizoguchi, A., Takaoka, K., Chisaka, O. and Takeichi, M. (2002). Cadherin regulates dendritic spine morphogenesis. *Neuron* **35**, 77-89.

Torres, M. A. and Nelson, W. J. (2000). Colocalization and redistribution of dishevelled and actin during Wnt-induced mesenchymal morphogenesis. *J Cell Biol* **149**, 1433-42.

Tosney, K. W. and Wessells, N. K. (1983). Neuronal motility: the ultrastructure of veils and microspikes correlates with their motile activities. *J Cell Sci* **61**, 389-411.

Trousse, F., Marti, E., Gruss, P., Torres, M. and Bovolenta, P. (2001). Control of retinal ganglion cell axon growth: a new role for Sonic hedgehog. *Development* **128**, 3927-36.

Tsui, H. T., Lankford, K. L., Ris, H. and Klein, W. L. (1984). Novel organization of microtubules in cultured central nervous system neurons: formation of hairpin loops at ends of maturing neurites. *J Neurosci* **4**, 3002-13.

Umemori, H., Linhoff, M. W., Ornitz, D. M. and Sanes, J. R. (2004). FGF22 and its close relatives are presynaptic organizing molecules in the mammalian brain. *Cell* **118**, 257-70.

Uren, A., Reichsman, F., Anest, V., Taylor, W. G., Muraiso, K., Bottaro, D. P., Cumberledge, S. and Rubin, J. S. (2000). Secreted frizzled-related protein-1 binds

directly to Wingless and is a biphasic modulator of Wnt signaling. *J Biol Chem* **275**, 4374-82.

Varnum-Finney, B. and Reichardt, L. F. (1994). Vinculin-deficient PC12 cell lines extend unstable lamellipodia and filopodia and have a reduced rate of neurite outgrowth. *J Cell Biol* **127**, 1071-84.

Veeman, M. T., Slusarski, D. C., Kaykas, A., Louie, S. H. and Moon, R. T. (2003). Zebrafish prickle, a modulator of noncanonical Wnt/Fz signaling, regulates gastrulation movements. *Curr Biol* **13**, 680-5.

Wadsworth, W. G., Bhatt, H. and Hedgecock, E. M. (1996). Neuroglia and pioneer neurons express UNC-6 to provide global and local netrin cues for guiding migrations in C. elegans. *Neuron* **16**, 35-46.

Wagner, U., Utton, M., Gallo, J. M. and Miller, C. C. (1996). Cellular phosphorylation of tau by Gsk-3 beta influences tau binding to microtubules and microtubule organisation. *J Cell Sci* **109 (Pt 6)**, 1537-43.

Wang, K. H., Brose, K., Arnott, D., Kidd, T., Goodman, C. S., Henzel, W. and Tessier-Lavigne, M. (1999). Biochemical purification of a mammalian slit protein as a positive regulator of sensory axon elongation and branching. *Cell* **96**, 771-84.

Wang, X. H., Zheng, J. Q. and Poo, M. M. (1996). Effects of cytochalasin treatment on short-term synaptic plasticity at developing neuromuscular junctions in frogs. *J Physiol* **491 (Pt 1)**, 187-95.

Wang, Y. L. (1985). Exchange of actin subunits at the leading edge of living fibroblasts: possible role of treadmilling. *J Cell Biol* **101**, 597-602.

Watanabe, T., Wang, S., Noritake, J., Sato, K., Fukata, M., Takefuji, M., Nakagawa, M., Izumi, N., Akiyama, T. and Kaibuchi, K. (2004). Interaction with IQGAP1 links APC to Rac1, Cdc42, and actin filaments during cell polarization and migration. *Dev Cell* **7**, 871-83.

Waterman-Storer, C. M., Desai, A., Bulinski, J. C. and Salmon, E. D. (1998). Fluorescent speckle microscopy, a method to visualize the dynamics of protein assemblies in living cells. *Curr Biol* **8**, 1227-30.

Waterman-Storer, C. M., Worthylake, R. A., Liu, B. P., Burridge, K. and Salmon, E. D. (1999). Microtubule growth activates Rac1 to promote lamellipodial protrusion in fibroblasts. *Nat Cell Biol* **1**, 45-50.

Weiss, P. (1941). Nerve patterns: The mechanics of nerve growth. *Growth (Suppl)*, 163-203.

Westphal, M., Jungbluth, A., Heidecker, M., Muhlbauer, B., Heizer, C., Schwartz, J. M., Marriott, G. and Gerisch, G. (1997). Microfilament dynamics during cell movement and chemotaxis monitored using a GFP-actin fusion protein. *Curr Biol* **7**, 176-83.

Wharton, K. A., Jr. (2003). Runnin' with the Dvl: proteins that associate with Dsh/Dvl and their significance to Wnt signal transduction. *Dev Biol* **253**, 1-17.

Wilkinson, D. G. (2001). Multiple roles of EPH receptors and ephrins in neural development. *Nat Rev Neurosci* **2**, 155-64.

Willert, K., Brown, J. D., Danenberg, E., Duncan, A. W., Weissman, I. L., Reya, T., Yates, J. R., 3rd and Nusse, R. (2003). Wnt proteins are lipid-modified and can act as stem cell growth factors. *Nature* **423**, 448-52.

Winter, C. G., Wang, B., Ballew, A., Royou, A., Karess, R., Axelrod, J. D. and Luo, L. (2001). Drosophila Rho-associated kinase (Drok) links Frizzled-mediated planar cell polarity signaling to the actin cytoskeleton. *Cell* **105**, 81-91.
Wodarz, A. and Nusse, R. (1998). Mechanisms of Wnt signaling in development. *Annu Rev Cell Dev Biol* **14**, 59-88.
Wong, G. T., Gavin, B. J. and McMahon, A. P. (1994). Differential transformation of mammary epithelial cells by Wnt genes. *Mol Cell Biol* **14**, 6278-86.
Wong, H. C., Bourdelas, A., Krauss, A., Lee, H. J., Shao, Y., Wu, D., Mlodzik, M., Shi, D. L. and Zheng, J. (2003). Direct binding of the PDZ domain of Dishevelled to a conserved internal sequence in the C-terminal region of Frizzled. *Mol Cell* **12**, 1251-60.
Wood, W. and Martin, P. (2002). Structures in focus--filopodia. *Int J Biochem Cell Biol* **34**, 726-30.
Wu, C. H. and Nusse, R. (2002). Ligand receptor interactions in the Wnt signaling pathway in Drosophila. *J Biol Chem* **277**, 41762-9.
Wulf, E., Deboben, A., Bautz, F. A., Faulstich, H. and Wieland, T. (1979). Fluorescent phallotoxin, a tool for the visualization of cellular actin. *Proc Natl Acad Sci U S A* **76**, 4498-502.
Yamada, K. M., Spooner, B. S. and Wessells, N. K. (1971). Ultrastructure and function of growth cones and axons of cultured nerve cells. *J Cell Biol* **49**, 614-35.
Yamada, K. M., Spooner, B. S. and Wessells, N. K. (1970). Axon growth: roles of microfilaments and microtubules. *Proc Natl Acad Sci U S A* **66**, 1206-12.
Yamaguchi, T. P., Bradley, A., McMahon, A. P. and Jones, S. (1999). A Wnt5a pathway underlies outgrowth of multiple structures in the vertebrate embryo. *Development* **126**, 1211-23.
Yanagawa, S., van Leeuwen, F., Wodarz, A., Klingensmith, J. and Nusse, R. (1995). The dishevelled protein is modified by wingless signaling in Drosophila. *Genes Dev* **9**, 1087-97.
Yang-Snyder, J., Miller, J. R., Brown, J. D., Lai, C. J. and Moon, R. T. (1996). A frizzled homolog functions in a vertebrate Wnt signaling pathway. *Curr Biol* **6**, 1302-6.
Yoshikawa, S., McKinnon, R. D., Kokel, M. and Thomas, J. B. (2003). Wnt-mediated axon guidance via the Drosophila Derailed receptor. *Nature* **422**, 583-8.
Yoshikawa, S. and Thomas, J. B. (2004). Secreted cell signaling molecules in axon guidance. *Curr Opin Neurobiol* **14**, 45-50.
Yoshimura, T., Kawano, Y., Arimura, N., Kawabata, S., Kikuchi, A. and Kaibuchi, K. (2005). Gsk-3beta regulates phosphorylation of CRMP-2 and neuronal polarity. *Cell* **120**, 137-49.
Yu, H. H., Araj, H. H., Ralls, S. A. and Kolodkin, A. L. (1998). The transmembrane Semaphorin Sema I is required in Drosophila for embryonic motor and CNS axon guidance. *Neuron* **20**, 207-20.
Yu, W., Ahmad, F. J. and Baas, P. W. (1994). Microtubule fragmentation and partitioning in the axon during collateral branch formation. *J Neurosci* **14**, 5872-84.
Yu, W., Ling, C. and Baas, P. W. (2001). Microtubule reconfiguration during axogenesis. *J Neurocytol* **30**, 861-75.
Yuste, R. and Bonhoeffer, T. (2004). Genesis of dendritic spines: insights from ultrastructural and imaging studies. *Nat Rev Neurosci* **5**, 24-34.

Zallen, J. A., Yi, B. A. and Bargmann, C. I. (1998). The conserved immunoglobulin superfamily member SAX-3/Robo directs multiple aspects of axon guidance in C. elegans. *Cell* **92**, 217-27.

Zhang, H. L., Singer, R. H. and Bassell, G. J. (1999). Neurotrophin regulation of beta-actin mRNA and protein localization within growth cones. *J Cell Biol* **147**, 59-70.

Zhang, L., Schmidt, R. E., Yan, Q. and Snider, W. D. (1994). NGF and NT-3 have differing effects on the growth of dorsal root axons in developing mammalian spinal cord. *J Neurosci* **14**, 5187-201.

Zhang, W. and Benson, D. L. (2001). Stages of synapse development defined by dependence on F-actin. *J Neurosci* **21**, 5169-81.

Zhang, X. and Poo, M. M. (2002). Localized synaptic potentiation by BDNF requires local protein synthesis in the developing axon. *Neuron* **36**, 675-88.

Zhang, X. F., Schaefer, A. W., Burnette, D. T., Schoonderwoert, V. T. and Forscher, P. (2003). Rho-dependent contractile responses in the neuronal growth cone are independent of classical peripheral retrograde actin flow. *Neuron* **40**, 931-44.

Zheng, J. Q., Wan, J. J. and Poo, M. M. (1996). Essential role of filopodia in chemotropic turning of nerve growth cone induced by a glutamate gradient. *J Neurosci* **16**, 1140-9.

Zhou, F. Q. and Cohan, C. S. (2004). How actin filaments and microtubules steer growth cones to their targets. *J Neurobiol* **58**, 84-91.

Zhou, F. Q. and Cohan, C. S. (2001). Growth cone collapse through coincident loss of actin bundles and leading edge actin without actin depolymerization. *J Cell Biol* **153**, 1071-84.

Zhou, F. Q., Waterman-Storer, C. M. and Cohan, C. S. (2002). Focal loss of actin bundles causes microtubule redistribution and growth cone turning. *J Cell Biol* **157**, 839-49.

Zhou, F. Q., Zhou, J., Dedhar, S., Wu, Y. H. and Snider, W. D. (2004). NGF-induced axon growth is mediated by localized inactivation of Gsk-3beta and functions of the microtubule plus end binding protein APC. *Neuron* **42**, 897-912.

Zou, Y., Stoeckli, E., Chen, H. and Tessier-Lavigne, M. (2000). Squeezing axons out of the gray matter: a role for slit and semaphorin proteins from midline and ventral spinal cord. *Cell* **102**, 363-75.

Zumbrunn, J., Kinoshita, K., Hyman, A. A. and Nathke, I. S. (2001). Binding of the adenomatous polyposis coli protein to microtubules increases microtubule stability and is regulated by GSK3 beta phosphorylation. *Curr Biol* **11**, 44-9.